Supporting Information for

Evidence for Simultaneous Dearomatization of Two Aromatic Rings Under Mild Conditions in Cu(I)-Catalyzed Direct Asymmetric Dearomatization of Pyridine

Michael W. Gribble Jr,* Richard Y. Liu,* and Stephen L. Buchwald

Department of Chemistry, Massachusetts Institute of Technology, Cambridge, MA 02139, USA

*Correspondence to: mwgribblejr@gmail.com, ryl@mit.edu

Table of Contents

1. General Experimental

1.1 General reagent information

Unless noted otherwise, reagents and starting materials were purchased from commercial vendors and used as supplied. Piperidines **22ab** and **22ag** were previously reported in reference 1. The (+)-(2*S*,5*S*) and (–)-(2*R*,5*R*) isomers of 1,2-bis(2,5-diphenylphospholano)ethane (i.e., Ph-BPE) were obtained from Namëna Chemicals. $Cu(OAc)_2$ was anhydrous and obtained from Alfa Aesar as a crystalline powder having 99.999% metals-basis purity. For mechanistic experiments, the greater solubility of this form of $Cu(OAc)_2$ compared to the amorphous powder is important for reproducibility in the duration required for catalyst activation, whereas preparative dearomatization reactions work well with either source. Dimethoxy(methyl)silane (DMMS, CAS #16881-77-9) was obtained from TCI America and stored in an N_2-atmosphere glovebox (henceforth referred to simply as a glovebox). See section 1.4 for a discussion of safety considerations involving this reagent. Styrene and 3-fluorostyrene were obtained from Aldrich and TCI, respectively, and degassed inside oven-dried Kontes Schlenk storage tubes fitted with HI-VAC valves (which seal with screw-in PTFE plugs) using three freeze-pump-thaw cycles on a dual manifold. A freeze-pump-thaw cycle was accomplished by freezing the styrene in liquid N_2 while the valve of the storage tube was closed, opening the tube to the dual manifold and applying vacuum until the internal pressure was ca. 20 mTorr, and then allowing the styrene to thaw after closing the valve. The degassed styrenes were transferred to a glovebox and stored in a –35 °C freezer in oven-dried 20 mL scintillation vials. *Meta*-fluorobenzaldehyde-α-^{13}C was prepared from 3-fluoro-1-iodobenzene and *N*,*N*-dimethylformamide-carbonyl-^{13}C using the procedure described in reference 2 for preparation of 3-chlorobenzlaldehyde-*d*; it had the expected NMR spectroscopic characteristics for 3-fluorobenzaldehyde, albeit with a very large (177.2 Hz) $^1J_{C,H}$ splitting. Pyridine (Aldrich) was anhydrous and stored in a SureSeal bottle in a glovebox. The kinetics model substrate (3-phenylpyridine) was obtained from Aldrich and used as received (**Experiments 1-7**) or obtained from Combi-blocks or TCI, distilled under high vacuum through a short-path distillation adapter (**Experiments 8-14** and **16-17**), and subsequently stored in a glovebox. Heterocyclic substrates **1f** and **1g** were prepared by Suzuki-Miyaura coupling of 3-pyridineboronic acid pinacol ester and the corresponding aryl bromides and exhibited extremely high purity as determined by ^{1}H NMR analysis. Tetrahydrofuran (THF) used in calorimetry or preparative experiments was obtained from J.T. Baker in CYCLE-TAINER® delivery kegs, purified by successive filtrations though packed columns of neutral alumina and CuO under Ar pressure, sparged with Ar for > 30 min, and then stored in a glovebox in an oven-dried glass bottle. Toluene (PhMe) and unstabilized diethyl ether (Et_2O) used as reaction solvents were obtained and purified similarly, but the sparging step was omitted, and these solvents were purified on demand, not stored. Anhydrous 1,4-dioxane used in calorimetry experiments was obtained from Aldrich in SureSeal bottles, vigorously sparged with dry Ar for ca. 1 h, and stored inside a glovebox. Ethyl acetate (EtOAc) used in chromatography eluents was HPLC grade (Aldrich HPLC plus, 99.9%, Aldrich catalog # 650528); EtOAc used in all other applications was ACS reagent grade (Aldrich, 99.5%). All NMR solvents were acquired from Cambridge Isotope Labs. C_6D_6 used for NMR analysis of 1,4-dihydropyridines (1,4-DHPs) was degassed using three freeze-pump-thaw cycles and then stored over activated 4 Å molecular sieves in an oven-dried glass bottle inside a glovebox. THF-d_8 was passively distilled from benzophenone ketyl into a Schlenk storage vessel using a vacuum-transfer manifold. This was accomplished by aging the THF (10-20 mL) for several days in the presence of benzophenone (ca. 200 mg) and finely

diced metallic sodium (ca. 2.0 g; rinsed 5X with hexanes) in a 100 mL Kontes Schlenk storage tube having a HI-VAC valve and a right-angled glass sidearm terminating in a female 14/20 ground-glass joint. Once the ketyl mixture had acquired a deep royal-purple color, the Schlenk flask was attached to one 14/20 male ground-glass joint on a solvent-transfer manifold (flame dried under high vacuum and itself directly attached to a 14/20 male ground-glass joint on a dual manifold). Another Schlenk storage tube of the same type (oven-dried) was attached to the other 14/20 male joint of the solvent-transfer manifold. The solvent-transfer manifold and receptacle tube were placed under high vacuum, and the valve of the receptacle tube was left open throughout the distillation. The ketyl mixture was subjected to three freeze-pump-thaw cycles and frozen a final time. The valve to the vessel containing the ketyl mixture was then opened, the valve connecting the vacuum transfer manifold to the dual manifold was closed, the receptacle Schlenk tube was cooled in liquid N_2, and the ketyl mixture was allowed to gradually thaw. The receptacle vessel, once all of the THF-d_8 had condensed inside it, was placed under a slight positive pressure of N_2, sealed, and stored inside a glovebox. All other NMR solvents were used as received. Flash chromatography was performed on wet-loaded, manually eluted silica columns using SiliCycle SiliaFlash® F60 silica gel (40–63 μm, 230–400 mesh, 60 Å pore diameter). Preparative TLC separations used Silicycle glass-backed extra-hard-layer plates (60 Å pore-diameter, 1.0-mm-thick silica layer, F-254 indicator, 20 x 20 cm).

1.2. Instrumentation and analytical methodology

Calorimetry experiments were performed using an Omnical Insight Parallel Reaction Calorimeter (Figure SI-1). The temperature of the calorimeter block was regulated using external constant-temperature oil-recirculating baths (Anova A-25 Refrigerated and Heating Circulator; Figure SI-2). The reaction temperature was measured at the calorimeter. Calorimetric data were processed according to the specific formulae in the attached representative Excel document; the general principles underlying this analysis are described in Section 2.1 below and reference 3. Proton, carbon, and fluorine NMR spectra recorded for routine characterization purposes were obtained on either a two-channel Bruker Avance-III HD Nanobay spectrometer equipped with a 5 mm liquid N_2-cooled Prodigy BBO cryoprobe and operating at 400.09 MHz, or a Bruker Avance Neo spectrometer equipped with a 5 mm BBFO SmartProbe and operating at 500.18 MHz. Mechanistic experiments were exclusively performed using the latter instrument. Chemical shifts of ^{1}H NMR signals are referenced to the indicated residual solvent peak ($CDCl_3$, $\delta = 7.26$; CD_2Cl_2, $\delta = 5.32$; benzene-d_6, $\delta = 7.16$; acetone-d_6, $\delta = 2.05$; THF-d_8 $\delta = 1.72$) and reported in ppm relative to tetramethylsilane. Carbon-13 chemical shifts are reported in ppm relative to the indicated solvent shifts at $\delta = 53.84$ (CD_2Cl_2) and 25.31 (THF-d_8) ppm. Phosphorus-31 and fluorine-19 chemical shifts are reported in ppm relative to phosphoric acid and $CFCl_3$, respectively, and determined as an automated part of the NMR experiment based on the known frequency relationship between the deuterium lock signal of THF-d_8 and the signals of the respective reference compounds. All ^{13}C and ^{31}P NMR spectra are proton-decoupled. Important acquisition parameters for non-routine NMR experiments are provided below with the relevant procedures. TLC analyses employed Silicycle SiliaPlate® glass-backed extra-hard-layer TLC plates (60 Å, 250 μm thickness, 20 x 20 cm, UV-254 indicator) and visualization with 254 nm light or I_2/SiO_2. Chiral supercritical fluid chromatography (SFC) was performed using a Waters Acquity UPC^2 system equipped with a CHIRALCEL OD-H column. Method details are included in section 9.2.

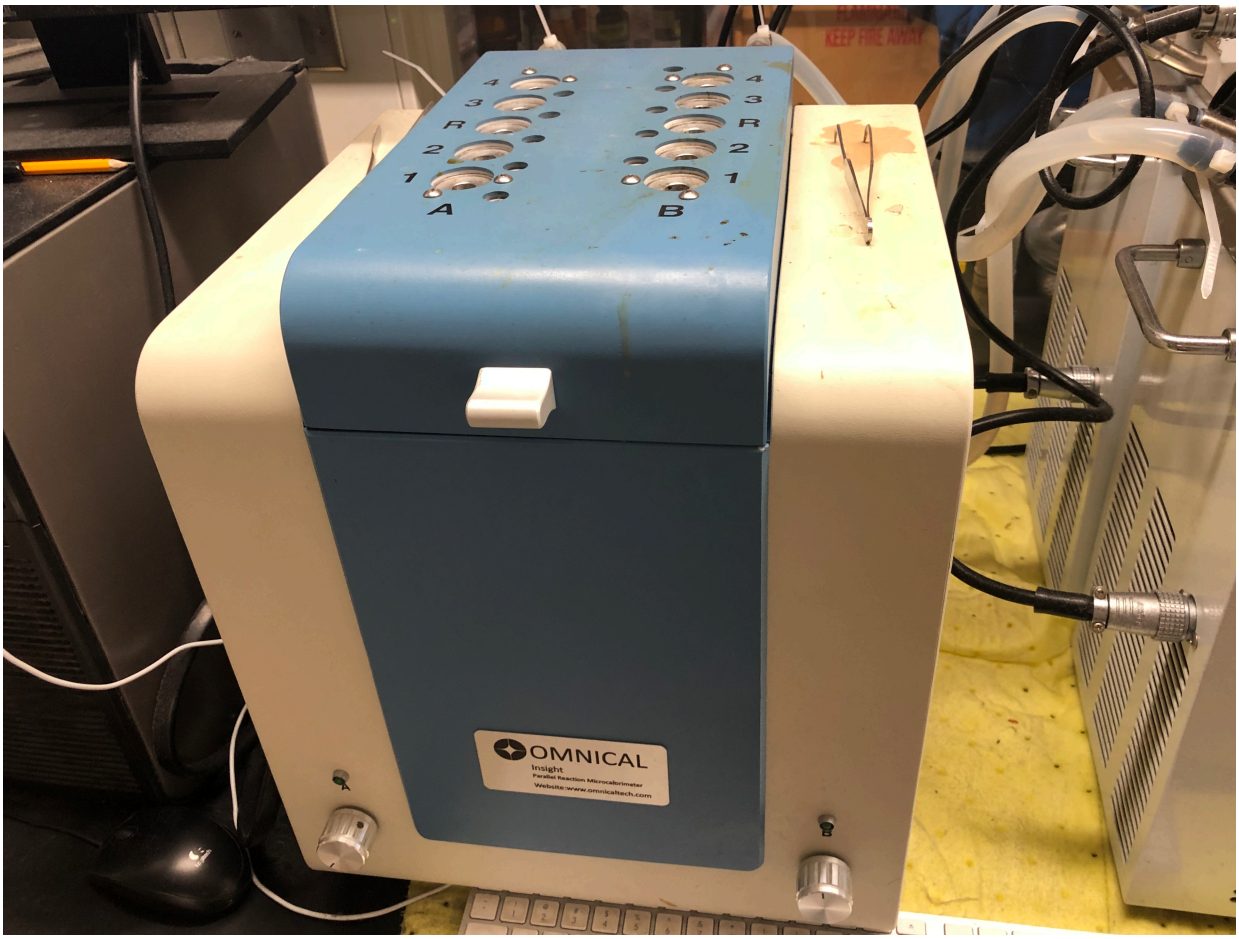

Figure SI-1. Omnical Insight Parallel Reaction Calorimeter used in kinetics experiments.

Figure SI-2. Anova constant-temperature oil-recirculating baths associated with the calorimeter.

1.3. Reaction apparatus

Phenethylcopper stock solutions and reference mixtures for calorimetry experiments were prepared inside the apparatus depicted in Figure SI-3. Stock solutions of heterocycles for either calorimetry or NMR experiments, as well as catalyst solutions used in NMR experiments, were prepared inside the apparatus shown in Figure SI-4. Calorimetric rate measurements commenced upon adding a heterocycle stock solution through an injection port on the upper lid of the calorimeter to a phenethylcopper stock solution using the type of syringe in Figure SI-5, A. Unless otherwise specified, liquid transfers performed during the preparation of solutions for calorimetry or NMR experiments used oven-dried cemented-needle Luer-tip gastight microsyringes of the type shown in

Figure SI-5, B. Preparative dearomatization experiments were performed inside oven-dried glass cultures tube, as in Figure SI-6. Isolation of crude 1,4-DHPs by concentration of dearomatization reaction mixtures (e.g., for NMR analysis or use in aerobic oxidation experiments) was performed on a dual manifold using the gas-adapter/connecting-adapter assembly in Figure SI-7. All mechanistic NMR experiments were performed inside oven-dried medium-wall J-Young-type NMR tubes ('low-pressure-vacuum tubes' in Wilmad terminology) sealed with screw-in PTFE pistons (Figure SI-8).

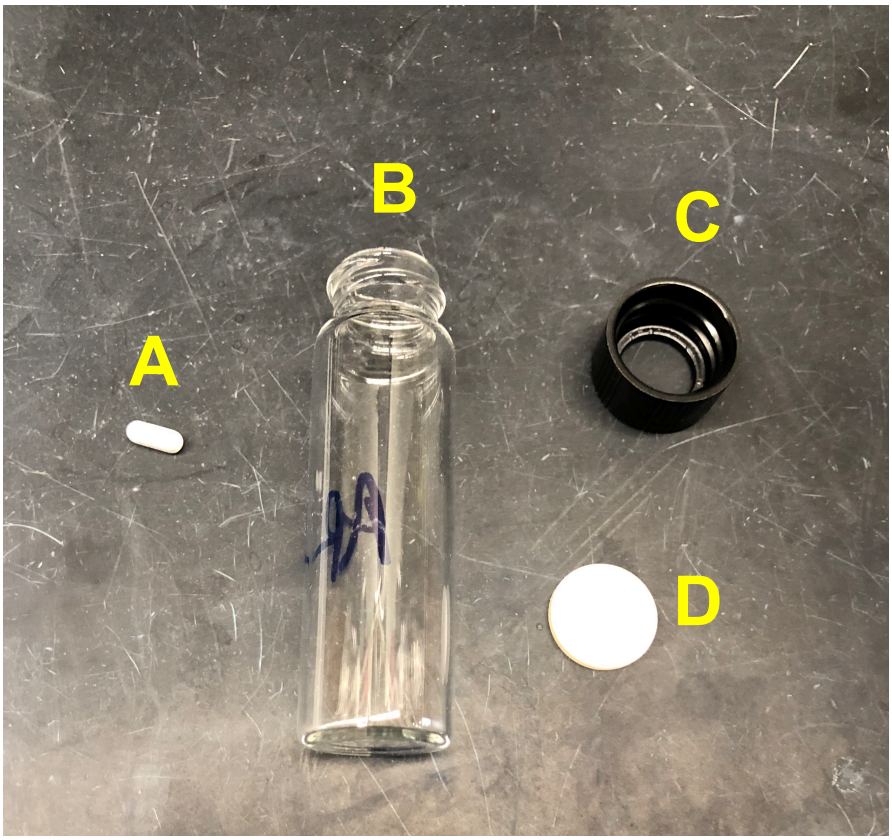

Figure SI-3. Apparatus for reactions conducted inside the calorimeter.
A. A small PTFE-coated magnetic stir bar
B. Kimble® 60942A-16 KIMAX® 16mL Clear Glass Sample Vial, O.D. x Height: 21 x 72 mm (part # 60942A 16). Referred to below as a calorimeter vial.
C. A size 18-400 mm screw-on open-top cap for use with PTFE/silicone septa. Kimble part # 73804-18400
D. A PTFE-lined silicone septum. Thermo Fisher scientific part # B7995-15.
The assembly of **C** and **D** is referred to below as a PTFE/silicone septum-cap.

A. A small PTFE-coated magnetic stir bar. For heterocycle stock solutions, this component is omitted.
B. VWR 1 dram borosilicate glass vial, O.D. x Height: 15 x 45 mm, Cap Size: 13-425 mm (VWR part # 66011-041). Referred to below as a one-dram vial.
C. A size 13-425 mm screw-on open-top cap for use with PTFE/silicone septa. Thermo Fisher scientific part # C4015-66.
D. A PTFE-lined silicone septum. Thermo Fisher scientific part # C4015-60.

Figure SI-4. Apparatus for preparation of stock solutions for calorimetry and NMR experiments.

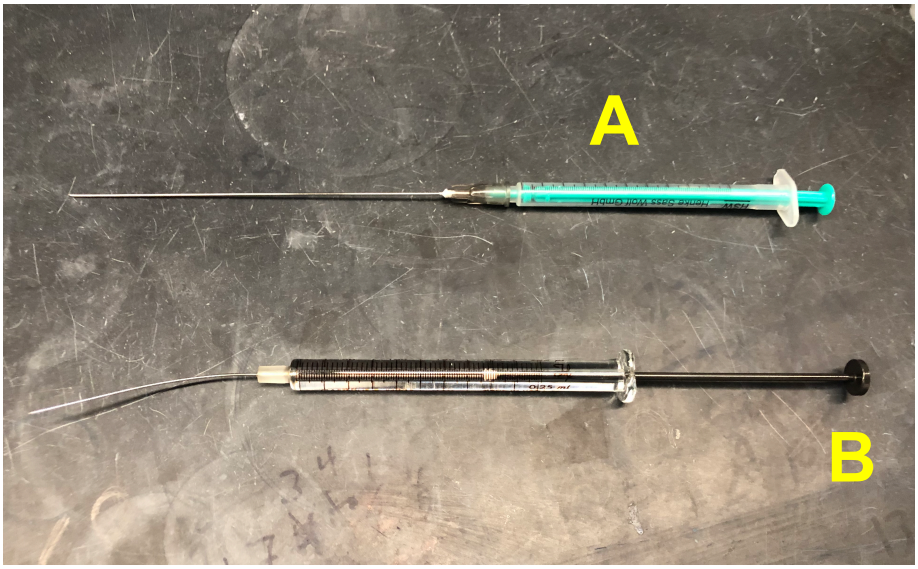

Figure SI-5. Syringes used in preparing reaction mixture for calorimetry and NMR experiments.
A. A Norm-Ject single-use Luer-tip 1.00 mL syringe (Ref # 4010-200V0) equipped with a 22-gauge, 4-inch Air-Tite hypodermic needle (Ref # 8300014471).
B. A Hamilton Luer-tip cemented-needle gastight microsyringe (250 μL size: Hamilton model 1725, part # 81175. 500 μL size: Hamilton model 1750, part # 81243).

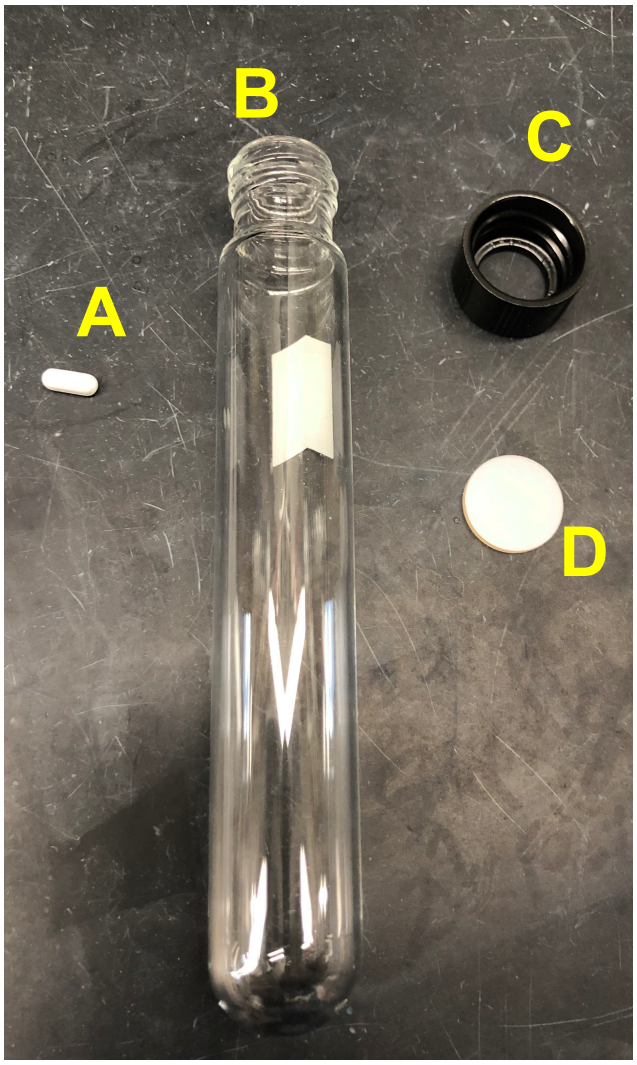

A. A small PTFE-coated magnetic stir bar.

B. Glass culture tube with threaded end (20 x 125 mm; Fisher scientific part # 14-959-35A. Referred to below as a culture tube.

C. A size 18-400 mm screw-on open-top cap for use with PTFE/silicone septa. Kimble part # 73804-18400.

D. A PTFE-lined silicone septum. Thermo Fisher scientific part # B7995-15.

Figure SI-6. Apparatus for preparative dearomatization experiments.

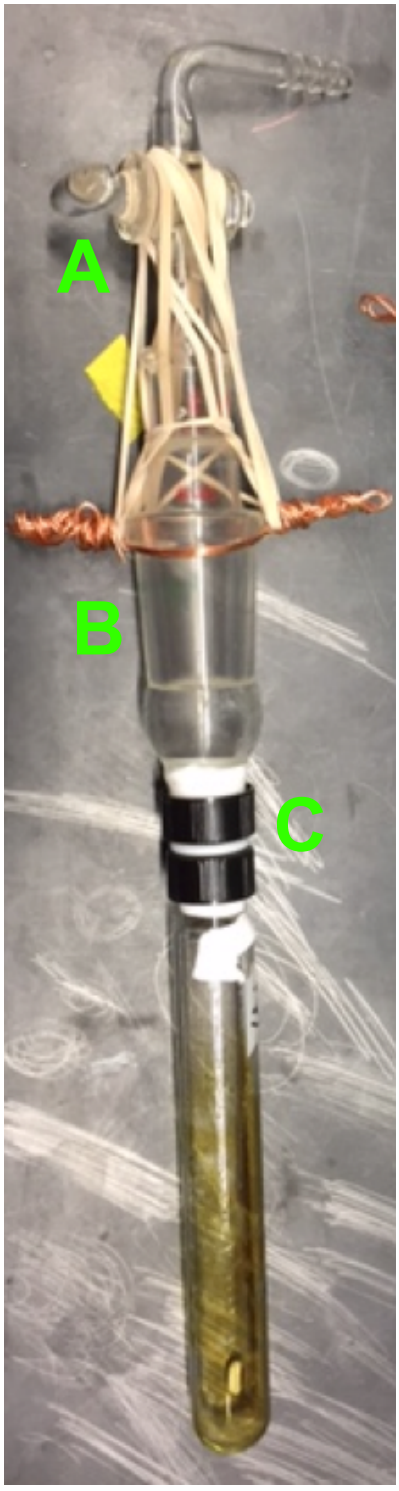

A. A gas-adapter with a greased ground-glass stopcock and ground-glass joint.

B + C. A connecting adapter (Chemglass part # CG-1318-10 and CG-1318-23).

The threaded parts of the connecting adapter and culture tube are wound with Teflon tape.

The rubber bands and copper wire hold the assembly together if pressurized internally on a manifold or placed under an external vacuum (e.g., in a glovebox antechamber).

Figure SI-7. Adapter assembly for concentrating dearomatization reaction mixtures on a dual manifold.

Wilmad 5 mm Medium Wall Precision Low Pressure/Vacuum NMR Sample Tube 7" L, 400 MHz, part # 524-LPV-7. Referred to below as a J-Young NMR tube. The cap is referred to as a PTFE piston.

Figure SI-8. J-Young-style NMR tube used in mechanistic spectroscopy experiments

Important safety note: When NMR samples are stored frozen in liquid N_2, the part of the tube that forms a seal with the piston must never be allowed to come near the cryogen, and the Dewar flask in which the tubes are stored must never be covered. Either of these circumstances can result in the seal with the piston being broken and liquid oxygen condensing inside the tube, which would create a serious explosion hazard. The level of cryogen in the Dewar should not surpass the meniscus of a typical (ca. 600 μL) sample by more than 1–2 cm. We recommend gently retightening the piston upon cooling the tube and ascertaining that the seal is intact prior to storing the tube in cryogen for more than a few minutes. Alternatively, one can use *i*PrOH/CO_2 as the cryogen, as dearomatization reactions generally do not proceed at –78 °C.

1.4. General safety considerations

All of the dearomatization reaction procedures involve addition of DMMS to mixtures of $Cu(OAc)_2$ and Ph-BPE in THF inside vessels that are sealed with PTFE/silicone septum-caps. This manipulation invariably results in some evolution of hydrogen and the potential for modest pressurization of the reaction vessel. The septa used here are designed to give way if the pressure inside the vessel exceeds a safe limit. This has never occurred in our experience, but the mixtures should nevertheless be prepared inside a contained environment, such as a glovebox.

Several vendors (TCI, Alfa Aesar) assign a GHS hazard code of H318 to DMMS,[4] indicating that it is a Category I serious eye-damage hazard (i.e., causes serious eye damage). Other vendors (Gelest, AK Scientific) assign DMMS a GHS hazard code of H319, indicating that it is a category II Eye Irritant. DMMS should be handled in a well-ventilated fumehood using proper precautions as outlined for the handling of hazardous materials in "Prudent Practices in the Laboratory."[5] In the general oxidation procedure, as well as in the procedure for characterizing crude 1,4-dihydropyridines (DHPs) by ^{1}H NMR, excess DMMS is evaporated using a vacuum manifold once the dearomatization has gone to completion. This operation must be performed inside a well-ventilated chemical fumehood using a vacuum manifold with two liquid-nitrogen-cooled traps in order to prevent release of DMMS into the atmosphere. After the oxidation step, the reaction mixture is stirred in the presence of saturated methanolic NH_4F inside a fumehood prior to other manipulations.

The medium-wall J-Young NMR tubes used in the procedures below are rated for maximum internal pressures of 100 psi – a value that we expect greatly exceeds the kinds of pressures that could conceivably be generated in a typical dearomatization experiment. Nevertheless, we recommend wearing protective eyewear at all times when manipulating reaction mixtures in sealed NMR tubes.

1.5. General technical considerations

1.5.i. *Protection of phenethylcopper and dearomatization reaction mixtures from light.*

Because alkylcopper complexes have been described in various sources as susceptible to decomposition caused by light, we have taken precautions throughout this work to limit the light exposure of solutions containing phenethylcopper complexes. Preparation of phenethylcopper solutions and dearomatization reaction mixtures was always performed in a glovebox with the lights turned off. Further, when phenethylcopper-containing mixtures were aged for extended periods, this was done with a sheet of aluminum foil protecting the mixture from light, with the exception of NMR samples stored frozen in liquid nitrogen, which should not be covered for safety reasons.

1.5.ii. *General techniques for manipulating solutions and liquid reagents in mechanistic experiments.*

Dearomatization reaction mixtures contain several volatile components, and we consider it important for quantitative reproducibility in mechanistic experiments to minimize loss of reagents due to evaporation and prevent passive concentration of stock solutions being stored for extended periods. In our experience, the marked effervescence that occurs during catalyst activation steps that use relatively large amounts of $Cu(OAc)_2$ can result in loss of volatile reaction components if the reaction vessel is not sealed, for example. In general, liquid reagents and solutions are transferred in the procedures below by injecting the liquid via syringe into the receptacle vessel through the septum of a PTFE/silicone septum-cap without a vent needle in place, and then quickly replacing the septum-cap with a new one shortly afterward. This operation can result in modest, transient pressurization of the vessel, but it has never caused a septum to fail in our experience. THF used as a reaction solvent or in the preparation of a calorimetry reference mixture was generally transferred using a disposable plastic 1.00 mL syringe (See Figure SI-5, A) that had been rinsed 3x with THF immediately prior to use. CuH and phenethylcopper solutions were transferred with an oven-dried gas tight syringe that had been rinsed 5x with small aliquots of the solution immediately prior to transfer. As catalyst transfers generally entailed some disturbance of the solution and required that the vessel containing it be left open for several minutes, the circulator in the glovebox was temporarily shut off throughout this manipulation in order to minimize gas flow over the sample. Heterocycle stock solutions were prepared in a glovebox by weighing the heterocycle into an oven-dried one-dram vial, sealing it with a PTFE/silicone septum cap, adding the desired quantity of solvent (THF or 1,4-dioxane) using an oven-dried glass microsyringe, replacing the septum-cap, and then manually agitating the mixture. Aliquots of stock solutions for injection into calorimetry reaction mixtures were obtained by using a disposable plastic 1.00 mL syringe (See Figure SI-5, A) to discharge a volume of N_2 slightly in excess of the desired injection volume into the stock solution

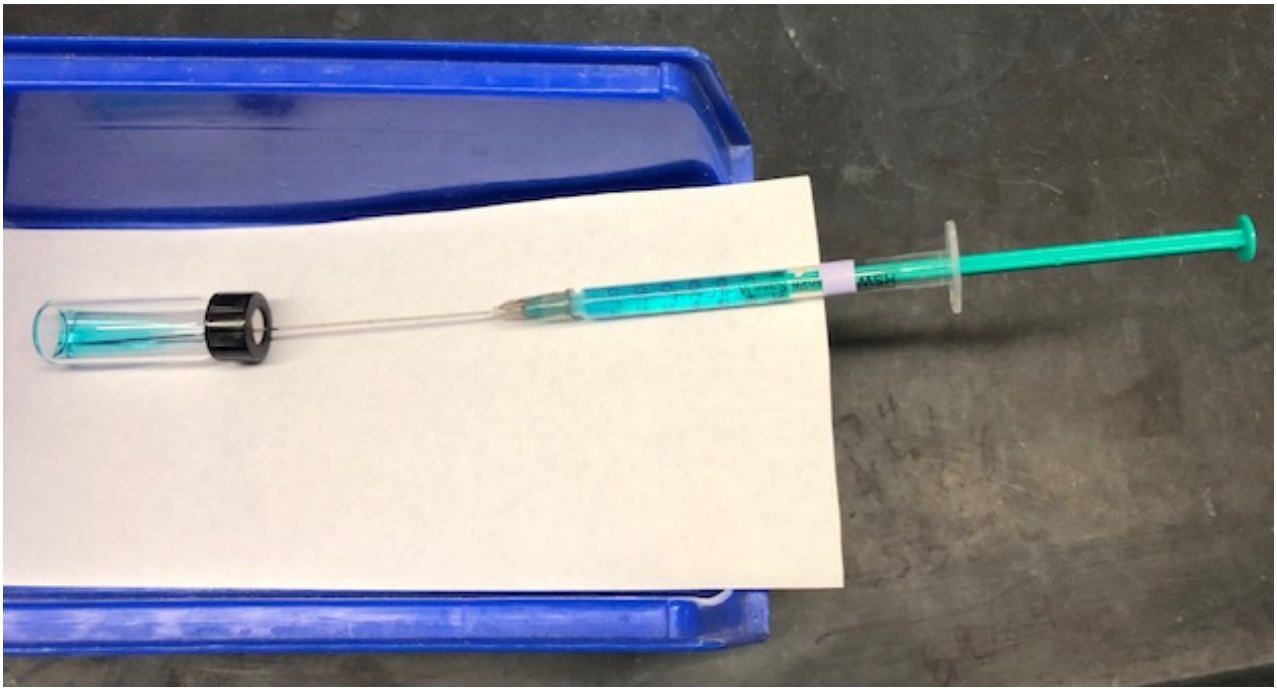

Figure SI-9. Manner of storage of heterocycle stock solutions pending injection into the calorimeter. Note that actual heterocycle stock solutions are not blue.

vial, withdrawing an equally excessive volume of stock solution, displacing all gas from the syringe, and then adjusting the plunger to the desired injection volume. The stock solutions were stored with the needle inserted through the septum and the tip of the needle resting in the liquid reservoir until immediately prior to the injection (Figure SI-9). The solutions were generally removed from the glovebox shortly before injection into the calorimeter.

1.5.iii. *Estimation of reaction mixture and stock solution compositions.*

In some instances, very precise quantitation of the concentration of a reactant in a solution or reaction mixture was important, and in those cases, which are noted below in the relevant procedures, the composition of the mixture was determined either via density measurements or by analyzing a known quantity of the mixture by ^{1}H NMR in the presence of an internal standard. However, in many cases other cases, extremely precise quantitation was not important. Unless otherwise specified, concentrations of individual reaction components in a final reaction mixture (in units of M) are estimated by assuming that the volumes of all liquid components are additive upon mixing, and that solid reaction components contribute 1 μl per mg to the total volume of the final mixture. Errors associated with the latter assumption are expected to be small given that solid reaction components are typically minor contributors to the total mass of a given reaction mixture.

2. Calorimetric Study of Reaction Kinetics

2.1. Determination of the kinetic order in copper for dearomatization of 3-phenylpyridine (1d) with 3-fluorostyrene (6h).

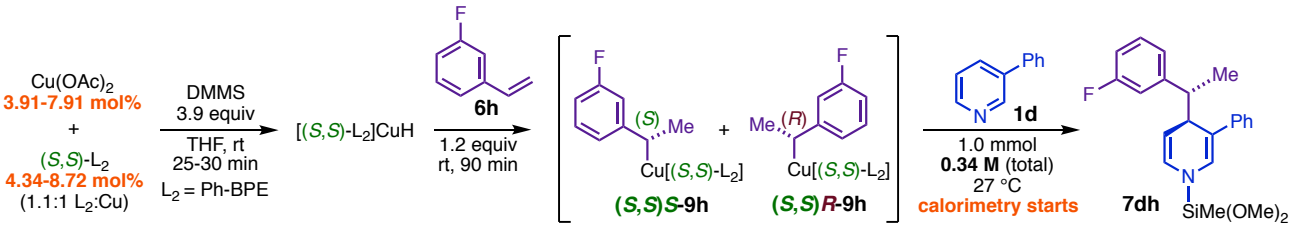

Procedure

Step one: Inside a glovebox, an oven-dried calorimeter vial was equipped with an oven-dried PTFE stir-bar and charged with $Cu(OAc)_2$ (14.5 mg, 79.8 μmol, 7.91 mol% based on **1d** in **Experiment 1**; 7.17 mg, 39.5 μmol, 3.91 mol% in **Experiment 2**) and (*S*,*S*)-Ph-BPE (44.6 mg, 88.0 μmol in **Experiment 1**; 22.0 mg, 44.0 μmol in **Experiment 2**; 1.10 L_2:Cu mol ratio in both). The vial was sealed with a PTFE/silicone septum-cap. The catalyst precursors were dissolved in THF (1.00 mL), and DMMS (490 μL, 3.98 mmol) was added immediately afterward. The interior walls of the vial were rinsed with an additional 0.300 mL THF. The resulting mixture was stirred at rt for 30 min, during which time all $Cu(OAc)_2$ dissolved and the color turned orange. The resulting activated catalyst solution was charged with 3-fluorostyrene (150 μL, 1.26 mmol) and stirred at rt for 30 min. A calorimeter reference mixture having approximately the same volume as the phenethylcopper solution was prepared inside an identical reaction vessel from 1.51 mL THF and 490 μL DMMS. The phenethylcopper solution and the reference solution were then inserted into the calorimeter block (pre-equilibrated at 26.7 °C) and stirred at ca. 1600 rpms until the heat flow curve returned to baseline.

Step two: A stock solution of the heterocycle was prepared inside the glovebox from 3-phenylpyridine (232.3 mg, 1.497 mmol) and 1.27 mL THF. A 1.00 mL plastic syringe (see Fig SI-5, A) was charged with 1.00 mL of the heterocycle stock solution. A second 1.00 mL syringe was charged with 1.00 mL of THF for injection into the reference mixture. The syringes were then removed from the glovebox in the state depicted in Figure SI-9. It was estimated that the 1.00 mL aliquot contained 1.009 mmol 3-phenylpyridine, and thus the heterocycle concentration at the start of dearomatization was ca. $[Het]_0 = 0.336$ M. The quantities of DMMS and 3-fluorostyrene present at the start of the dearomatization ($[DMMS]_0$ and $[3\text{-fluorostyrene}]_0$) were corrected for the quantities of those reagents consumed during formation of the phenethylcopper, which were assumed to be 2.00 equiv of DMMS and 0.75 equiv of 3-fluorostyrene for every 1.00 equiv of $Cu(OAc)_2$. This yielded estimates of $[DMMS]_0 = 1.27$ M (3.85 equiv) and $[3\text{-fluorostyrene}]_0 = 0.400$ M (1.19 equiv) in **Experiment 1,** and $[DMMS]_0 = 1.30$ M (3.87 equiv) and $[3\text{-fluorostyrene}]_0 = 0.410$ M (1.22 equiv) in **Experiment 2**, based on the final reaction volume of 3.00 mL. Modest discrepancies in the DMMS and 3-fluorostyene concentrations between the two experiments were inconsequential because it was shown (see section 2.2) that the reaction has kinetic orders of zero in both.

Step three: After the phenethylcopper mixture had been aged at rt for a total of 90 min, calorimetric measurement of the reaction rate was begun. The 1.00 mL aliquot of heterocycle stock solution and the 1.00 mL aliquot of THF were injected, respectively, into the phenethylcopper and reference mixture vials through the injection ports of the calorimeter, as close to simultaneously as possible. Care was taken not to physically disturb the vials, which results in heatflow artifacts; thus, each vial was immobilized with the aid of a metal spatula (lowered through the injection port and in contact with the outer plastic shell of the septum cap) when the needles were being inserted or removed through the septa. The heatflow was recorded until the heat curve for the reaction mixture reattained a stable baseline value, and the heat of reaction (ΔH_{rxn}) was determined by integrating the curve, starting from the time of injection (t_0), along the axis coinciding with the terminal baseline. Although in general the total heatflow is not required to be exclusively due to the enthalpy of the process of interest, we have reproducibly found that dearomatization of **1d** with **6h** is quantitative, clean, and highly regio- and diastereo-selective, and consequently equating the total heatflow with ΔH_{rxn} is appropriate in this case.

The data were processed according to the formulas contained within the representative Excel file included with the SI. The mathematical analysis underlying these calculations comes from reference 3. In general, the instantaneous reaction rate is proportional to the instantaneous heatflow and given by

$$rate_t = \frac{q_t}{\Delta H_{rxn} \bullet V} \qquad \text{(eq 1)},$$

where q_t is the heatflow (recorded in mW during the calorimetry experiment) at time t, V is the reaction volume, and ΔH_{rxn} is the heat of reaction determined above. The fractional conversion (X_t) at time t is given by

$$X_t = \frac{\int_{t_0}^{t} q_t dt}{\int_{t_o}^{t_f} q_t dt} \qquad \text{(eq 2)},$$

where t_f is the time at which the heatflow returns to baseline. For the purpose of calculating fractional conversions in this work, the two integrals in eq 2 were approximated as Riemann sums as in the included Excel file. The heatflow values used in those calculations were baseline-corrected by subtracting from each absolute heatflow data point an estimated baseline value obtained by averaging all of the heatflow data points within a segment of the terminal baseline. The fractional conversion and starting heterocycle concentration ($[\text{Het}]_0$) were used to associate the reaction rate at time *t* to the concentration of heterocycle at time t, thus:

$$[\text{Het}]_t = [\text{Het}]_0(1 - X_t) \qquad \text{(eq 3)}.$$

The initial part of the heat curve is not directly illustrative of the reaction kinetics and has been omitted for clarity in the text and below, although a complete curve is provided in the attached Excel file.

Experiment 1: 7.91 mol% $Cu(OAc)_2$, [Cu] = 26.6 mM. $\Delta H_{rxn} = 33.8$ kcal/mol, effective first-order rate constant (obtained by linear regression) $k_{eff} = 5.48 \cdot 10^{-2}$ $(Ms)^{-1}$ ($R^2 = 0.9993$)

Experiment 2: 3.95 mol% $Cu(OAc)_2$, [Cu] = 13.2 mM. $\Delta H_{rxn} = 34.0$ kcal/mol, $k_{eff} = 5.34 \cdot 10^{-2}$ $(Ms)^{-1}$ ($R^2 = 0.9995$)

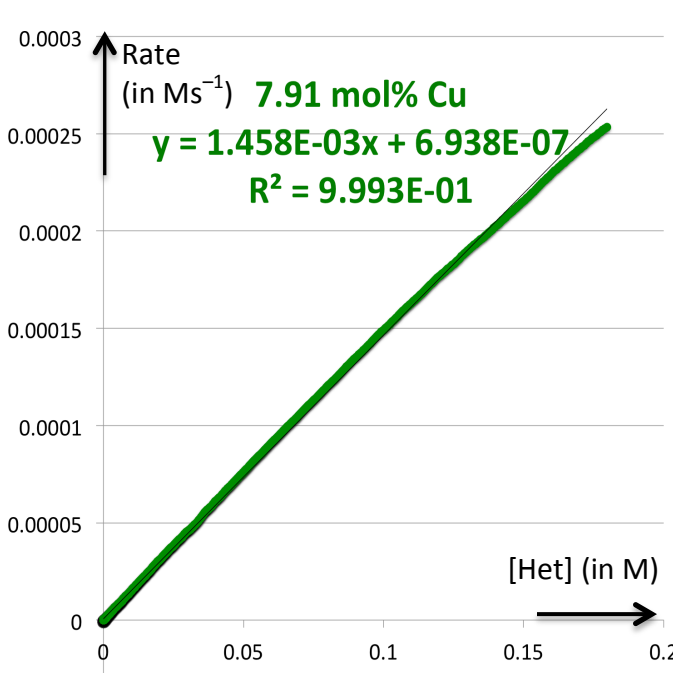

Figure SI-10: Reaction rate plotted versus [Het] for Experiment 1.

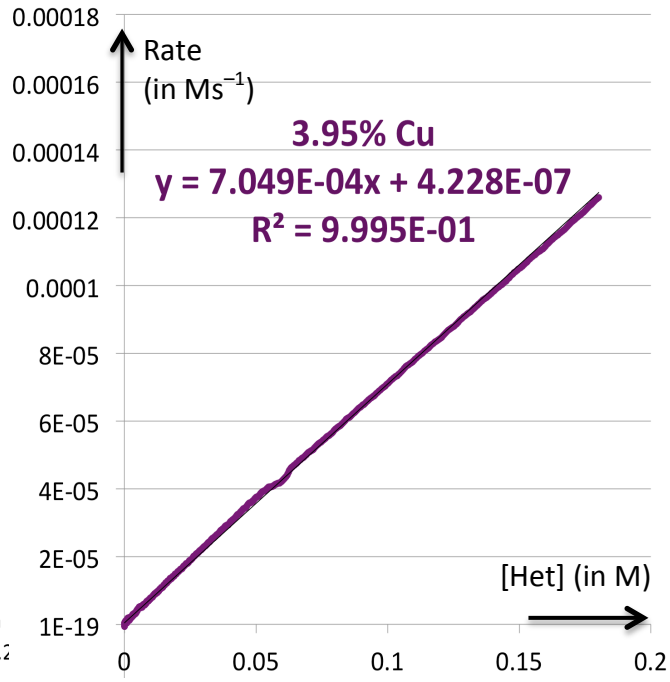

Figure SI-11: Reaction rate plotted versus [Het] for Experiment 2.

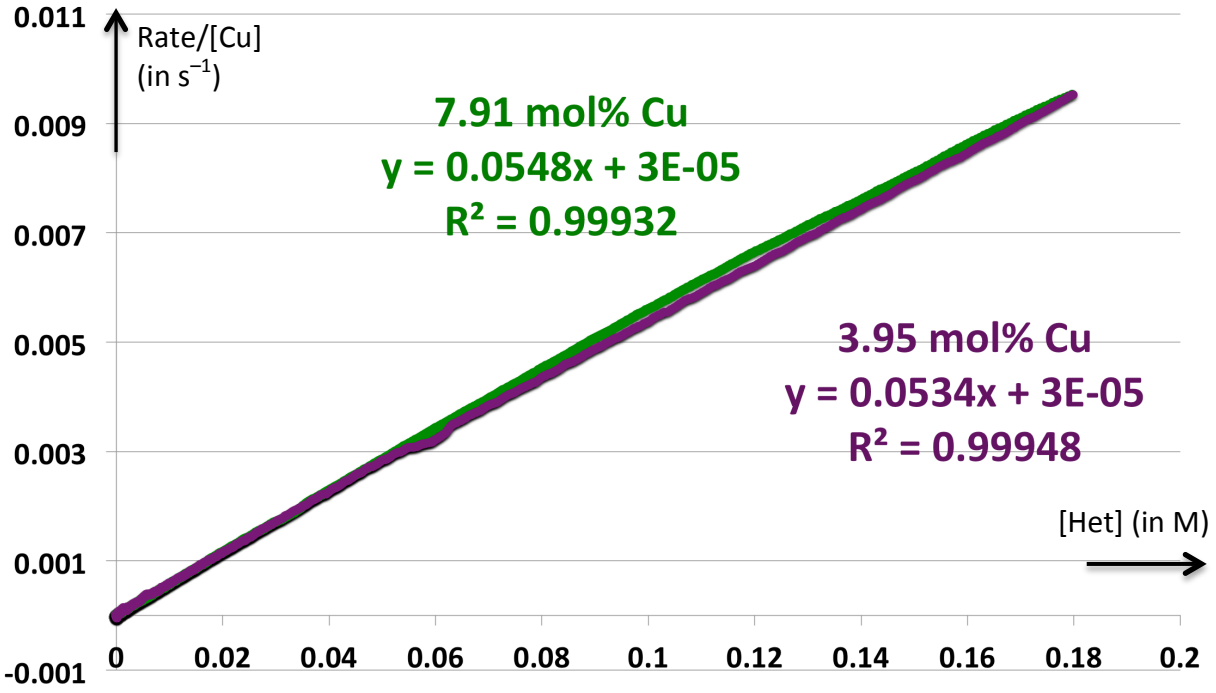

Figure SI-12: Rate/[Cu] plotted versus [Het] for Experiments 1 and 2. The reaction is first-order in Cu.

The near perfect overlay of the curves obtained when ($rate_t$/[Cu]) is plotted as a function of $[\text{Het}]_t$ for the two different reaction mixtures (Figure SI-12) indicates that the rate law is first-order in copper. (Division of a rate law by $[\text{Cu}]^{\mathbf{n}}$ yields a function with no dependence on [Cu] only if the rate has an order of **n** in copper.)

This finding was confirmed in a separate pair of experiments of similar design (see Figure SI-13).

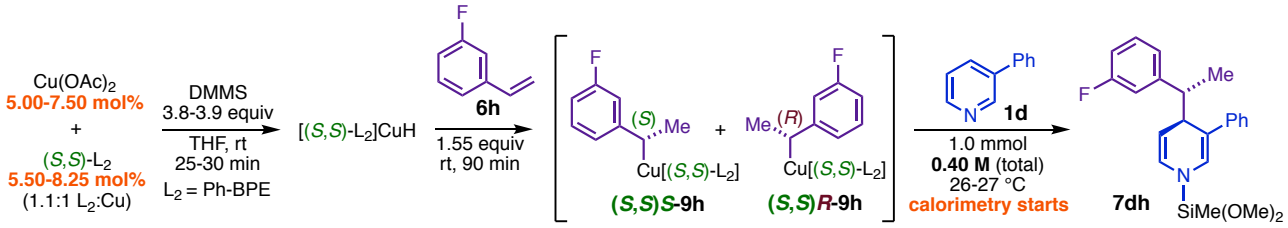

Experiment 3: 5.00 mol% $Cu(OAc)_2$, [Cu] = 20.0 mM. $\Delta H_{rxn} = 34.8$ kcal/mol, $k_{\text{eff}} = 5.91 \cdot 10^{-2}$ $(\text{Ms})^{-1}$ ($R^2 = 0.9997$).

$[\text{Het}]_0 = 0.400$ M, $[\text{DMMS}]_0 = 1.55$ M (3.88 equiv), $[\text{3-fluorostyrene}]_0 = 0.624$ M (1.56 equiv), 1.10:1 (*S*,*S*)-Ph-BPE:Cu, T = 26.3–26.8 °C.

Experiment 4: 7.50 mol% $Cu(OAc)_2$, [Cu] = 30.0 mM (1.50x that in **Experiment 3**). $\Delta H_{rxn} = 33.9$ kcal/mol, $k_{\text{eff}} = 5.99 \cdot 10^{-2}$ $(\text{Ms})^{-1}$ ($R^2 = 0.9985$)

$[\text{Het}]_0 = 0.400$ M, $[\text{DMMS}]_0 = 1.53$ M (3.83 equiv), $[\text{3-fluorostyrene}]_0 = 0.616$ M (1.54 equiv), 1.10:1 (*S*,*S*)-Ph-BPE:Cu, T = 26.0–26.5 °C.

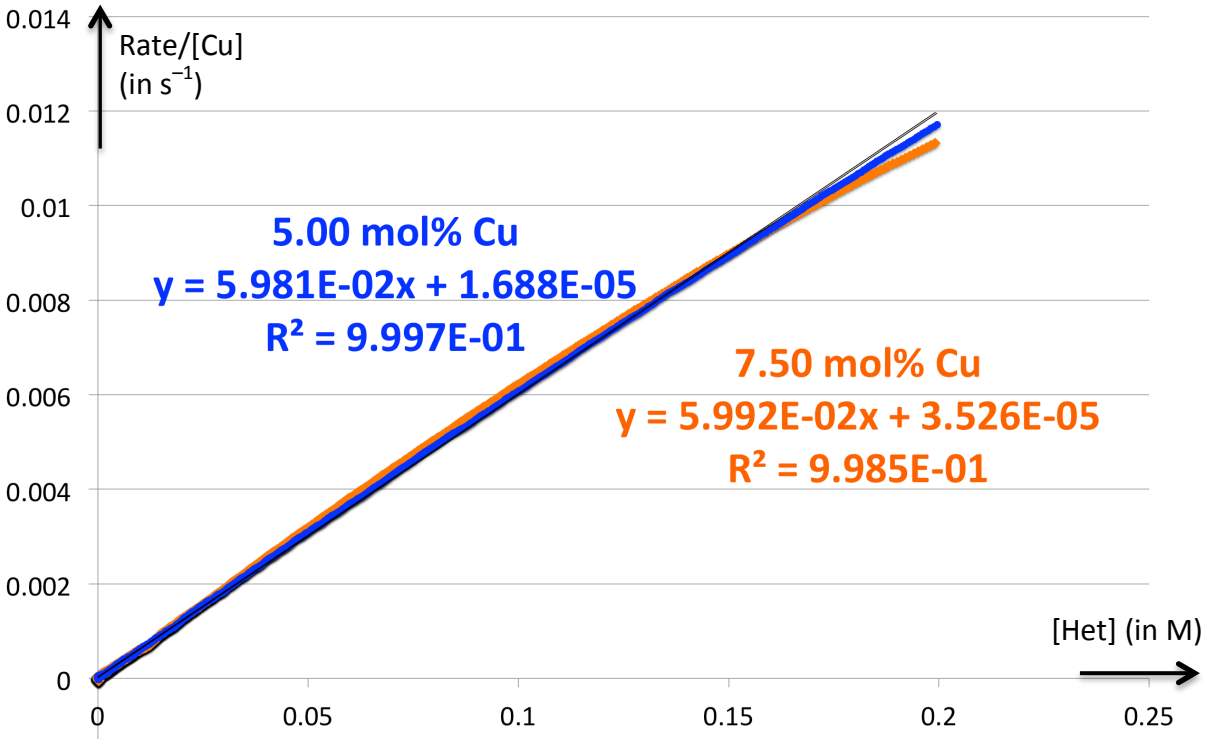

Figure SI-13: Rate/[Cu] plotted versus [Het] for Experiments 3 and 4

2.2. Determination of kinetics orders in DMMS, 3-fluorostyrene(6h), and heterocycle in the dearomatization of 3-phenylpyridine (1d).

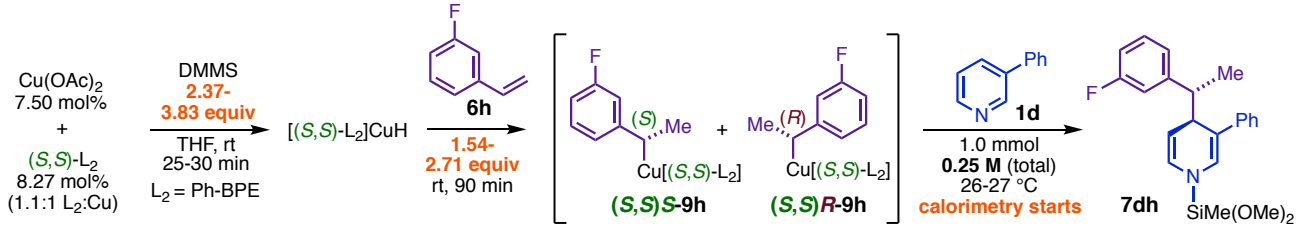

Procedure. Higher dilution than that in experiments 1–4 was employed here in order to permit significant variation in [DMMS] and [3-fluorostyrene] without markedly impacting medium properties. The phenethylcopper mixtures were generated in the same manner as above, but were instead composed of 13.65 mg $Cu(OAc)_2$ (75.15 μmol, 7.515 mol%), 41.88 mg (*S*,*S*)-Ph-BPE (82.67 μmol, 1.1:1 ratio relative to Cu), DMMS (490 μL, 3.98 mmol in **Experiments 5 and 7**; 310 μL, 2.52 mmol in **Experiment 6**), 3-fluorostyrene (190 μL, 1.59 mmol in **Experiments 5 and 6**; 330 μL 2.77 mmol in **Experiment 7**), and sufficient THF to give a final phenethylcopper solution having a total volume of 3.40 mL. The activated CuH solutions were aged at rt for 30 min prior to 3-fluorostyrene addition, and the phenethylcopper mixtures were aged for a total of 90 min at rt in the dark prior to the start of rate measurements performed as in section 2.1. The reference mixtures were composed of (3.40 – N) mL THF and N mL DMMS, where N mL is the volume of silane specified for a given experiment. At the initiation of rate measurement, the reference mixture was charged with 600 μL of THF, and the reaction mixture was charged with 600 μL of a heterocycle stock solution composed of 232.8 mg 3-phenylpyridine and 690 μL of THF. Such solutions had measured density = 0.940

mg/mL, from which it was calculated that the reaction mixtures received 1.00 mmol 3-Ph-pyridine (1.00 equiv). Upon addition of heterocycle, all reaction mixtures were 4.00 mL in volume ($[Het]_0$ = 0.250 M). Amounts of DMMS and 3-fluorostyrene provided below are corrected for the approximate quantities consumed during phenethylcopper formation.

Experiment 5: $[DMMS]_0$ = 0.957 M (3.83 equiv), $[3\text{-fluorostyrene}]_0$ = 0.385 M (1.54 equiv). ΔH_{rxn} = 34.4 kcal/mol, k_{eff} = $5.38 \cdot 10^{-2}$ $(Ms)^{-1}$ (R^2 = 0.9997)

Experiment 6: $[DMMS]_0$ = 0.592 M (2.37 equiv), $[3\text{-fluorostyrene}]_0$ = 0.385 M (1.54 equiv). ΔH_{rxn} = 34.2 kcal/mol, k_{eff} = $5.29 \cdot 10^{-2}$ $(Ms)^{-1}$ (R^2 = 0.9993)

Experiment 7: $[DMMS]_0$ = 0.957 M (3.83 equiv), $[3\text{-fluorostyrene}]_0$ = 0.677 M (2.71 equiv). ΔH_{rxn} = 34.0 kcal/mol, k_{eff} = $5.60 \cdot 10^{-2}$ $(Ms)^{-1}$ (R^2 = 0.9999)

Overlay of plots of $rate_t$ versus $[Het]_t$ for the three reactions (Figure SI-14 and 15) showed that the reaction rate exhibits negligible dependence on [3-fluorostyrene] and [DMMS].

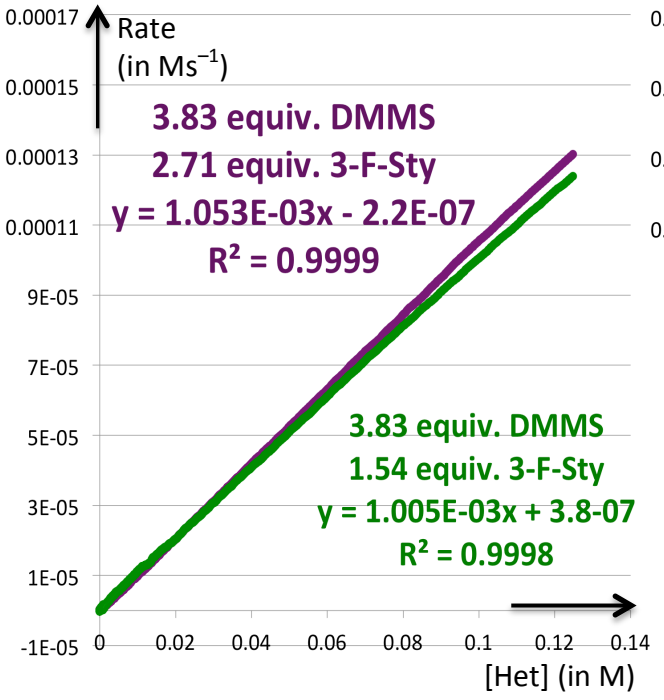

Figure SI-14: Overlaid rate curves plotted versus [Het] for Experiments 5 and 7.

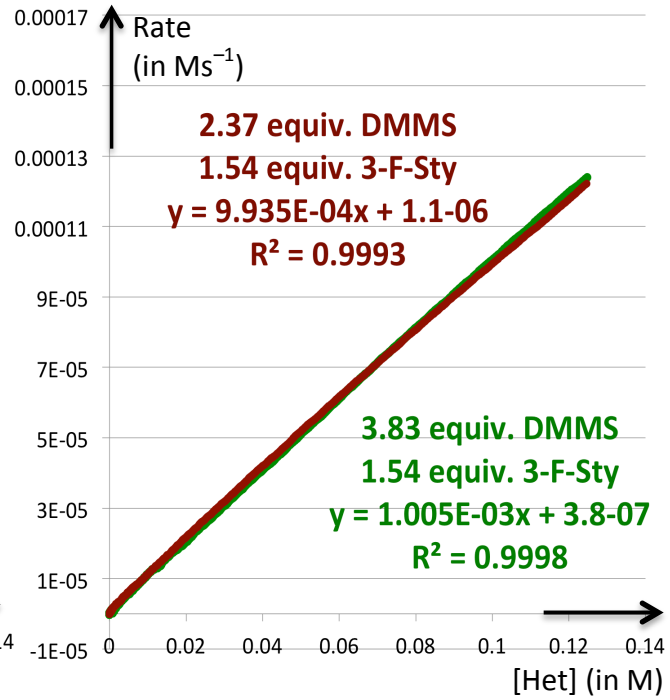

Figure SI-15: Overlaid rate curves plotted versus [Het] for Experiments 5 and 6.

A separate pair of experiments confirmed this finding. It is evident from the linearity of the plots in Figure SI-14 and SI-15 that the reaction is first-order in one reactant and zero order in the others. If the reaction were first-order in DMMS, then the effect on rate of simultaneously varying $[DMMS]_0$ and $[3\text{-fluorostyrene}]_0$ (holding all else the same) would be the same as if only $[DMMS]_0$ were varied. The same argument, *mutatis mutandis*, would apply if the reaction were instead first-order in 3-fluorostyrene. Thus, if one varies both $[DMMS]_0$ and $[3\text{-fluorostyrene}]_0$, the rate of reaction will be unchanged only if there are kinetics orders of zero in both. Plots of $rate_t$ versus $[Het]_t$ for

Experiments 8 and **9** (Figure SI-16) show that the rates are indeed the same in this case (reaction parameters not specified below are the same as in **Experiments 5–7**).

Experiment 8: $[DMMS]_0 = 0.592$ M (2.37 equiv), $[3\text{-fluorostyrene}]_0 = 0.677$ M (2.71 equiv). $\Delta H_{rxn} = 34.2$ kcal/mol, $k_{eff} = 4.65 \cdot 10^{-2}$ $(Ms)^{-1}$ ($R^2 = 0.9994$)

Experiment 9: $[DMMS]_0 = 0.957$ M (3.83 equiv), $[3\text{-fluorostyrene}]_0 = 0.385$ M (1.54 equiv). $\Delta H_{rxn} = 34.0$ kcal/mol, $k_{eff} = 4.59 \cdot 10^{-2}$ $(Ms)^{-1}$ ($R^2 = 0.9994$)

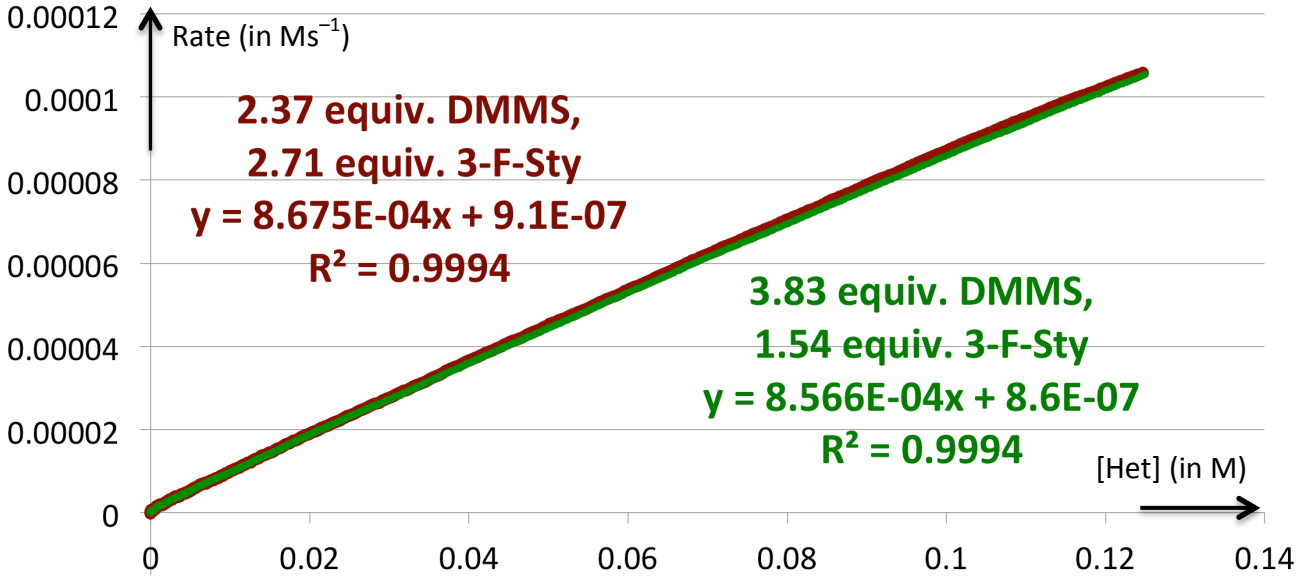

Figure SI-16: Overlaid rate curves plotted versus [Het] for Experiments 8 and 9. The reaction has kinetic orders of zero in DMMS and 3-fluorostyrene.

2.3. Kinetic dependence on the Cu:Ph-BPE ratio.

Procedure. Experiments 10–12 below were executed in the same manner as **Experiments 5–9** and with the same reactant and copper concentrations as **Experiment 8**. However, different amounts of phosphine were employed during preparation of the phenethylcopper. The volumes of THF used in preparing the phenethylcopper solutions were adjusted such that all had approximately the same final volume.

Experiment 10: 1.10:1 (*R*,*R*)-Ph-BPE:Cu. $\Delta H_{rxn} = 33.6$ kcal/mol, $k_{eff} = 4.84 \cdot 10^{-2}$ $(Ms)^{-1}$ ($R^2 = 0.9999$)

Experiment 11: 1.54:1 (*R*,*R*)-Ph-BPE:Cu. $\Delta H_{rxn} = 32.6$ kcal/mol, $k_{eff} = 5.54 \cdot 10^{-2}$ $(Ms)^{-1}$ ($R^2 = 0.9999$)

Experiment 12: 3.23:1 (*R*,*R*)-Ph-BPE:Cu. $\Delta H_{rxn} = 32.9$ kcal/mol, $k_{eff} = 5.29 \cdot 10^{-2}$ $(Ms)^{-1}$ ($R^2 = 0.9999$)

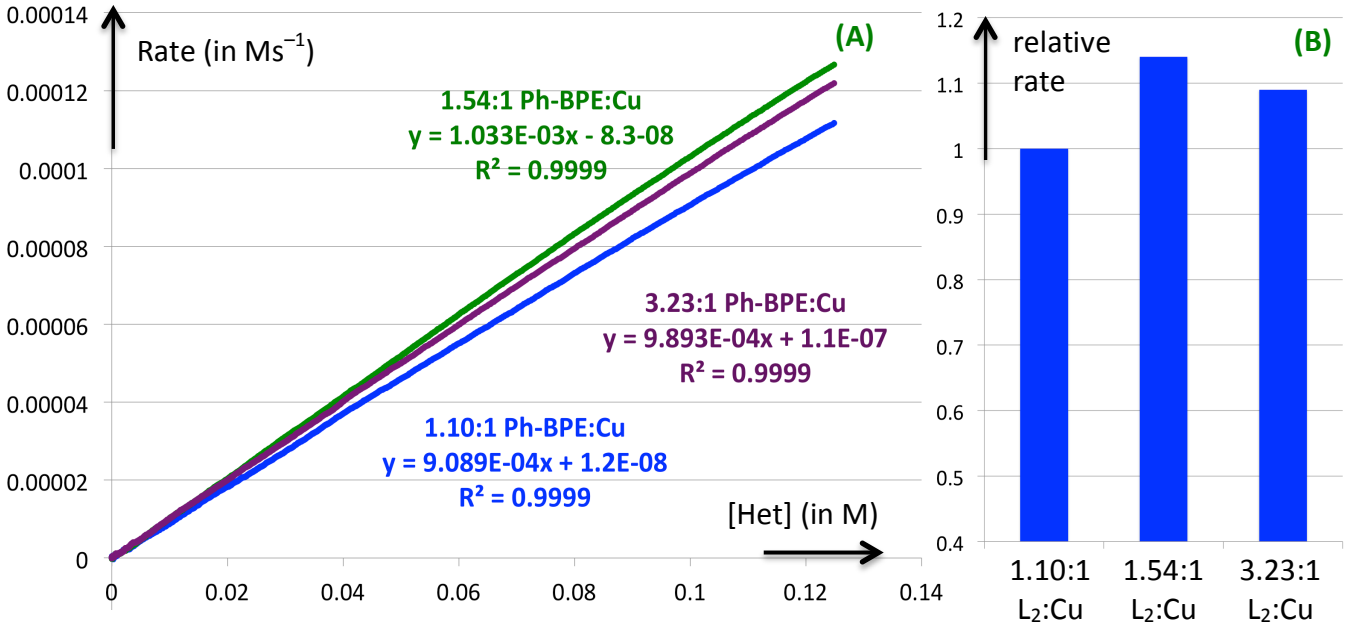

Figure SI-17: (A) overlaid rate curves plotted versus [Het] for Experiments 10–12, (B) relative rates.

The slight non-linear rate enhancement observed with higher ligand loadings (Figure SI-17) is plausibly the result of improved catalyst stability and consistent with similar effects seen in several other CuH-catalyzed reactions, including cases in which the excess phosphine is supplied as a species (e.g., Ph_3P) that is not expected to enter directly into the catalytic cycle. We have noted that preparation of dearomatization reaction mixtures with L_2:Cu ratios below 1.1:1 results in rapid catalyst decomposition as evinced by darkening of the solution and deposition of a Cu(0) mirror. This occurs much more slowly when higher ligand loadings (e.g., 1.4:1) are employed. In these calorimetry experiments, some potential for catalyst decomposition exists during the activation and hydrocupration steps, but decomposition does not appear to be significant on the timescale of the catalytic reaction once begun. Many mechanistic experiments in this work use L_2:Cu ratios close to 1.1:1 because these most closely emulate the conditions used in typical preparative experiments. However, higher loadings have been employed in various experiments when enhanced rate or prolonged catalyst stability were seen as important.

2.4. Study of heterocycle substituent effects on the rate of dearomatization with 3-fluorostyrene (6h).

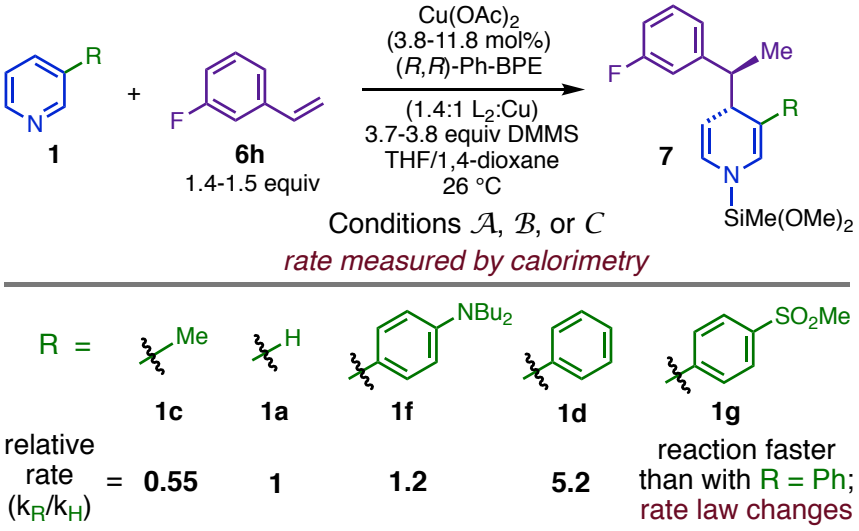

Relative rates for different heterocycles spanned a large enough range that it was necessary to use different sets of conditions for slow- and fast-reacting substrates in order to get high-quality calorimetry data in all cases (i.e., by increasing the catalyst loading or concentration as needed with slow-reacting substrates). In order to facilitate comparison between runs conducted under two different sets of conditions, one of the substrates was run under both sets: thus, e.g., the rate for 3-methylpyridine (determined using conditions **C**) could be compared to the rate for 3-phenylpyridine (determined using conditions **B**) by comparing the rate constant for 3-methylpyridine to the rate constant for pyridine (both determined using conditions **C**) and comparing the rate constant for pyridine to the rate constant for 3-phenylpyridine (both determined using conditions **B**). Differences between rate constants in these examples are primarily reflective of differences in the difficulty of the turnover-limiting step (TLS), which is not expected to be significantly affected by varying reaction parameters within the ranges employed here.

All conditions used 1.4-1.5 equiv 3-fluorostyrene, 3.7-3.8 equiv DMMS, and an (*R*,*R*)-Ph-BPE:Cu ratio of 1.4:1. The important parameters varied between conditions were:

Conditions A. 4.0% catalyst loading, $[\text{Het}]_0 = 0.13$ M
Conditions B. 12% catalyst loading, $[\text{Het}]_0 = 0.13$ M
Conditions C. 12% catalyst loading, $[\text{Het}]_0 = 0.36$ M

The substituents used in this study were selected in part due to their minimal liability to engage in intermolecular interactions that could confound the interpretation of relative rates. For example, whereas some substituents are theoretically capable of coordinating to Cu, the polar functional groups in this study – a dialkylaniline (**1f**) and an arylsulfone (**1g**) – are not expected to be competent dative ligands for $L_2Cu(I)$ species in general and are far less lewis-basic than pyridine in particular. We considered the possibility of C3-arenes engaging in π-complexation interactions, but our *in silico* models give us no reason to believe that these are important in the major pathways under consideration. We cannot discount the possibility of π-complexation occuring in an unknown third mechanistic possibility, but such effects should nevertheless be significantly controlled for in this study, given that the reactivity trend (rate increasing with increasing anion-stabilizing ability of the heterocycle) is evident within the set of C3-aryl-heterocycles. While steric interactions with C3 groups are possible, it is clear (compare **1a** to **1d**) that there must be a greater countervailing electronic effect, and the position of substituents on the C3-arenes (i.e., in **1f** and **1g**) places them too far away for significant new steric interactions with other reaction partners.

Representative Procedure: Determination of relative rates for **3-phenylpyridine** and **3-(*para*-*N*,*N*-dibutylaminophenyl)pyridine** (**Conditions B, Experiment 13**).

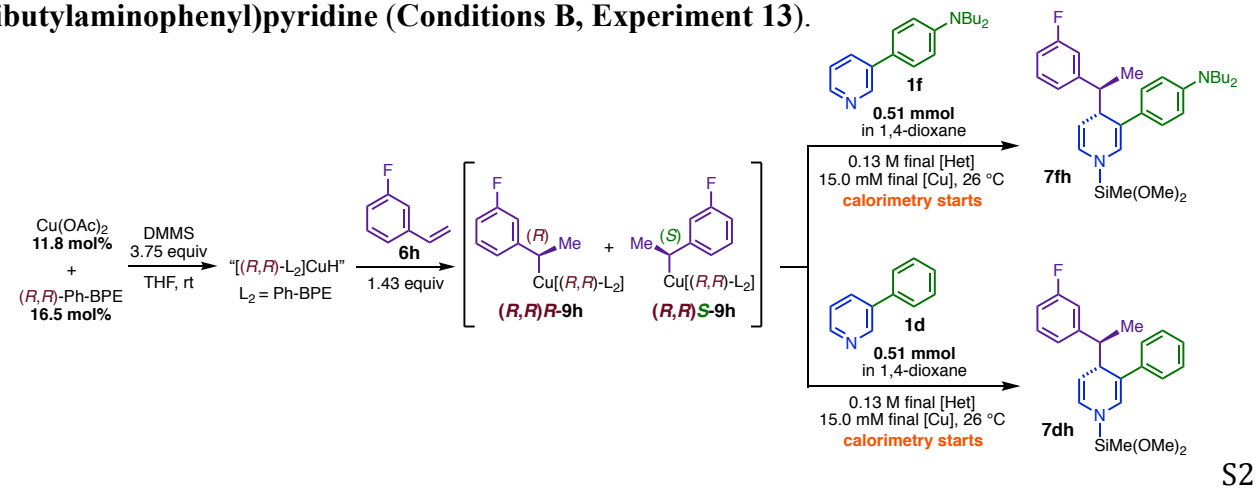

Step one: Inside a glovebox, an oven-dried calorimeter vial containing an oven-dried PTFE stir-bar was charged with $Cu(OAc)_2$ (27.2 mg, 150 μmol, 99.99% metals-basis purity) and (*R*,*R*)-Ph-BPE (106.5 mg, 210 μmol; 1.4:1 L_2:Cu). The vial was sealed with a PTFE/silicone septum-cap. The catalyst precursors were dissolved in THF (3.52 mL), and DMMS (620 μL, 5.04 mmol) was added immediately afterward. The resulting mixture was stirred at rt for 27 min, during which time all $Cu(OAc)_2$ dissolved and the color turned orange. This activated catalyst solution was charged with 3-fluorostyrene (230 μL, 1.93 mmol) and stirred at rt for 78 min.

Step two: The phenethylcopper solution generated above was partitioned into separate aliquots for use in the dearomatization experiments with the different heterocycles. First, the phenethylcopper solution was diluted with an additional 3.00 mL anhydrous THF, and then an oven-dried glass microsyringe was used to charge each of two new oven-dried calorimetry vials (which contained PTFE stir bars and had been equipped with PTFE/silicone septum-caps) with a 3.00 mL aliquot of the phenethylcopper solution. The volume of the phenethylcopper stock solution prior to partitioning was estimated at 7.50 mL, giving catalyst and reactant quantities for each 3.00 mL aliquot of 60.0 μmol $Cu(OAc)_2$, 84.1 μmol (*R*,*R*)-Ph-BPE, 1.90 mmol DMMS, and 0.725 mmol 3-fluorostyrene; the latter two values have been corrected for the approximate amounts consumed by the phenethylcopper formation step. Two identical reference mixtures were prepared from 2.75 mL of dry THF and 250 μL DMMS in the same type of reaction vessel described above. The phenethylcopper mixtures and reference mixtures were transferred to the calorimeter block (pre-equilibrated to 26.0 °C) and stirred at ca. 1600 rpms until the heatflow curve reattained a stable baseline.

Step three: Stock solutions of the heterocycles were prepared according to the procedure described in Section 1.5.ii. using 1,4-dioxane as the solvent. The stock solution of 3-Ph-pyridine (**1d**) was composed of 105.3 mg of the heterocycle and 1.25 mL 1,4-dioxane. The stock solution of 3-(*para*-*N*,*N*-dibutylaminophenyl)pyridine (**1f**) was prepared from 205.27 mg of heterocycle and 1.25 mL of 1,4-dioxane. Two 1.00 mL disposable plastic syringes were charged with 1.00 mL aliquots of the **1d** and **1f** stock solutions, respectively. Two other 1.00 mL syringes were charged with 1.00 mL aliquots of 1,4-dioxane in the same manner.

Step four: After the phenethylcopper solutions had been aged at rt for a total of 4 h, calorimetric rate measurements were commenced upon charging each reaction mixture and its reference mixture, respectively, with a 1.00 mL aliquot of the indicated heterocycle stock solution, and a 1.00 mL aliquot of 1,4-dioxane, giving approximate total volumes of 4.00 mL for each mixture. **Experiments 14**, **16**, and **17** similarly employed 1.00 mL injections volumes, whereas experiment **15** (**Conditions *C***) employed 0.700 mL injection volumes.

Step five: Once the injections were complete, the syringes were removed from the calorimeter vials, rinsed with acetone (5x) and water (10x) and then calibrated by using them to dispense nominally 1.00 mL aliquots of water into a tared vial and recording the mass. Measurements were taken for five aliquots using a given syringe and the results were averaged. The temperature of the water was measured, and its density at that temperature was used to estimate the true volume delivered to the reaction mixture. The **1d** solution had a measured density of 1.036 g/mL; from this value and the corrected volume of the syringe it was determined that 0.508 mmol (1.00 equiv) of the heterocycle had been delivered to the reaction mixture. It was similarly determined that

0.506 mmol (1.00 equiv) of **1f** had been delivered to the comparator reaction (**1f** stock solution density ρ = 1.029 g/mL). Relative stoichiometric values were 11.8 mol% Cu (both reactions), 1.43 equiv 3-fluorostyrene (both reactions), and 3.74 (relative to **1d**)–3.75 (relative to **1f**) equiv DMMS. Modest discrepancies in [DMMS] are inconsequential to the reaction rate for all heterocycles except 3-(*para*-mesylphenyl)pyridine (**1g**).

The stock solution of pyridine (**1a**) used in **Experiment 14** (ρ = 1.027 g/mL) was composed of 103.0 mg **1a** and 2.50 mL 1,4-dioxane, and that used in **Experiment 15** (ρ = 1.020 g/mL) was composed of 319.4 mg **1a** and 2.50 mL 1,4-dioxane. The stock solution of 3-methylpyridine (**1c**) used in **Experiment 15** (ρ = 1.017 g/mL) was composed of 386.1 mg **1e** and 2.50 mL 1,4-dioxane. The stock solution of 3-(*para*-mesylphenyl)pyridine (**1g**) used in **Experiment 16-17** (ρ = 1.060 g/mL) was composed of 165.7 mg **1g** and 1.25 mL 1,4-dioxane.

Experiment 13 (Conditions $\mathcal{B}$; described above):

3-phenylpyridine (**1d**):

$[Het]_0$ = 0.127 M, [Cu] = 15.0 mM (11.8 mol%), $[DMMS]_0$ = 0.474 M (3.74 equiv), $[3\text{-fluorostyrene}]_0$ = 0.181 M (1.43 equiv), $\Delta H_{rxn} = 32.1\ kcal/mol$, k_{eff} = 5.19•10^{-2} $(Ms)^{-1}$ (R^2 = 0.9997)

3-(*para*-*N*,*N*-dibutylaminophenyl)pyridine (**1f**):

$[Het]_0$ = 0.126 M, [Cu] = 15.0 mM (11.8 mol%), $[DMMS]_0$ = 0.474 M (3.75 equiv), $[3\text{-fluorostyrene}]_0$ = 0.181 M (1.43 equiv), $\Delta H_{rxn} = 32.6\ kcal/mol$, $\Delta H_{rxn} = 32.1\ kcal/mol$, k_{eff} = 1.16•10^{-2} $(Ms)^{-1}$ (R^2 = 0.9997)

relative rate (k_{Ph}/k_{Bu_2NPh}) = 4.47

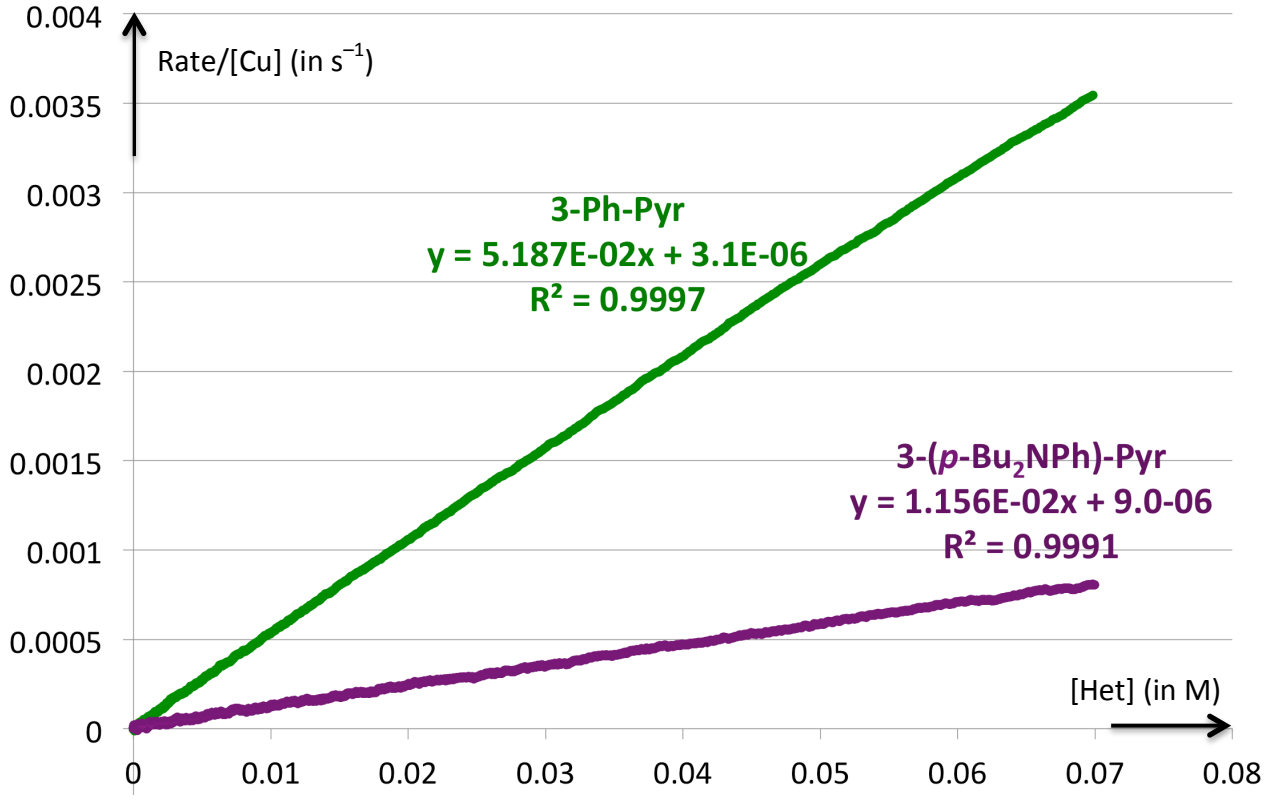

Figure SI-18: Overlaid rate curves plotted versus [Het] for Experiment 13.

Experiment 14 (Conditions $\mathcal{B}$):

Pyridine (**1a**):

$[Het]_0$ = 0.126 M, [Cu] = 14.9 mM (11.8 mol%), $[DMMS]_0$ = 0.474 M (3.76 equiv), $[3\text{-fluorostyrene}]_0$ = 0.181 M (1.43 equiv), $\Delta H_{rxn} = 36.3\ kcal/mol$, $k_{eff} = 8.75 \cdot 10^{-3}\ (Ms)^{-1}$ (R^2 = 0.9997)

3-phenylpyridine (**1d**):

$[Het]_0$ = 0.126 M, [Cu] = 14.9 mM (11.8 mol%), $[DMMS]_0$ = 0.474 M (3.75 equiv), $[3\text{-fluorostyrene}]_0$ = 0.181 M (1.43 equiv), $\Delta H_{rxn} = 37.2\ kcal/mol$, $k_{eff} = 4.53 \cdot 10^{-2}\ (Ms)^{-1}$ (R^2 = 0.9997)

relative rate (k_{Ph}/k_H) = 5.17

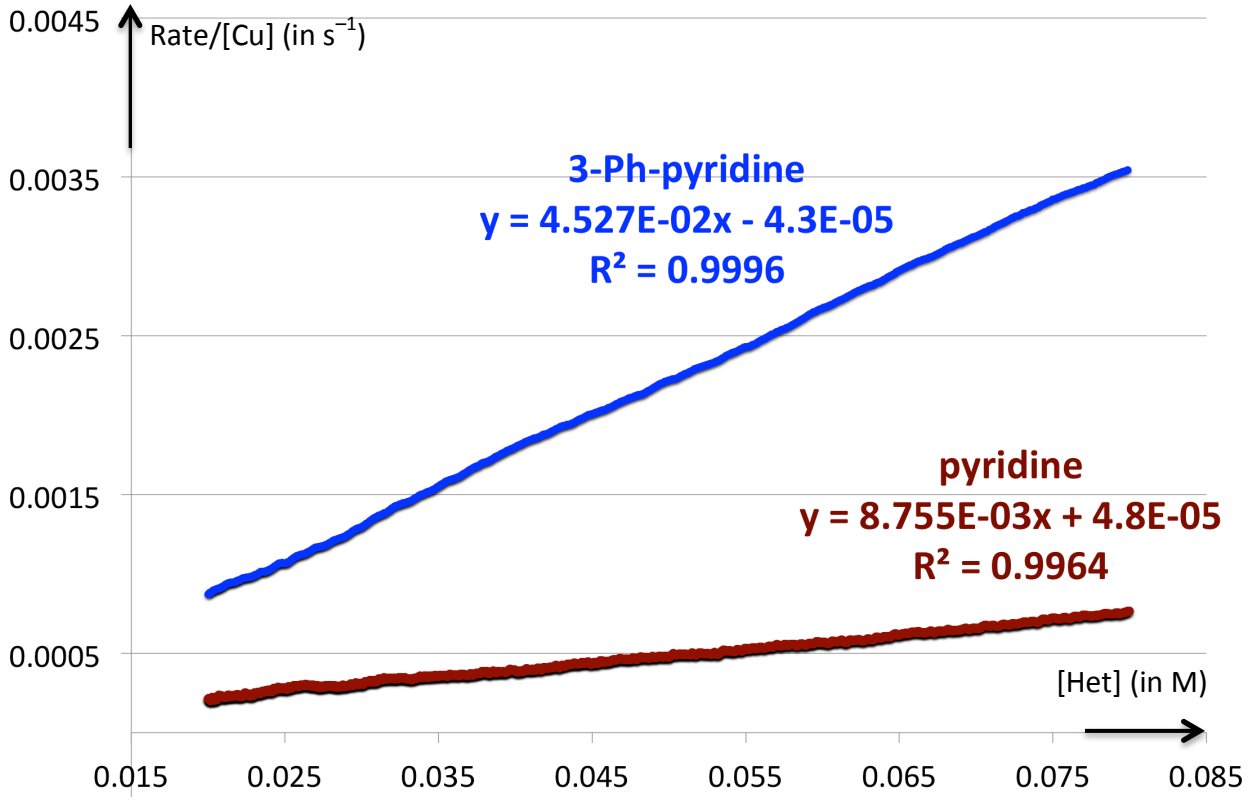

Figure SI-19: Overlaid rate curves plotted versus [Het] for Experiment 14.

Experiment 15 (Conditions $\mathcal{C}$):

Pyridine (**1a**):

$[Het]_0$ = 0.360 M, [Cu] = 42.5 mM (11.8 mol%), $[DMMS]_0$ = 1.35 M (3.74 equiv), $[3\text{-fluorostyrene}]_0$ = 0.515 M (1.43 equiv), $\Delta H_{rxn} = 34.7\ kcal/mol$, $k_{eff} = 1.05 \cdot 10^{-2}\ (Ms)^{-1}$ (R^2 = 0.9998)

3-Methylpyridine (**1c**):

$[Het]_0$ = 0.360 M, [Cu] = 42.5 mM (11.8 mol%), $[DMMS]_0$ = 1.35 M (3.74 equiv), $[3\text{-fluorostyrene}]_0$ = 0.515 M (1.43 equiv), $\Delta H_{rxn} = 34.3\ kcal/mol$, $k_{eff} = 5.74 \cdot 10^{-3}$ $(Ms)^{-1}$ (R^2 = 0.9998)

relative rate (k_H/k_{Me}) = 1.83

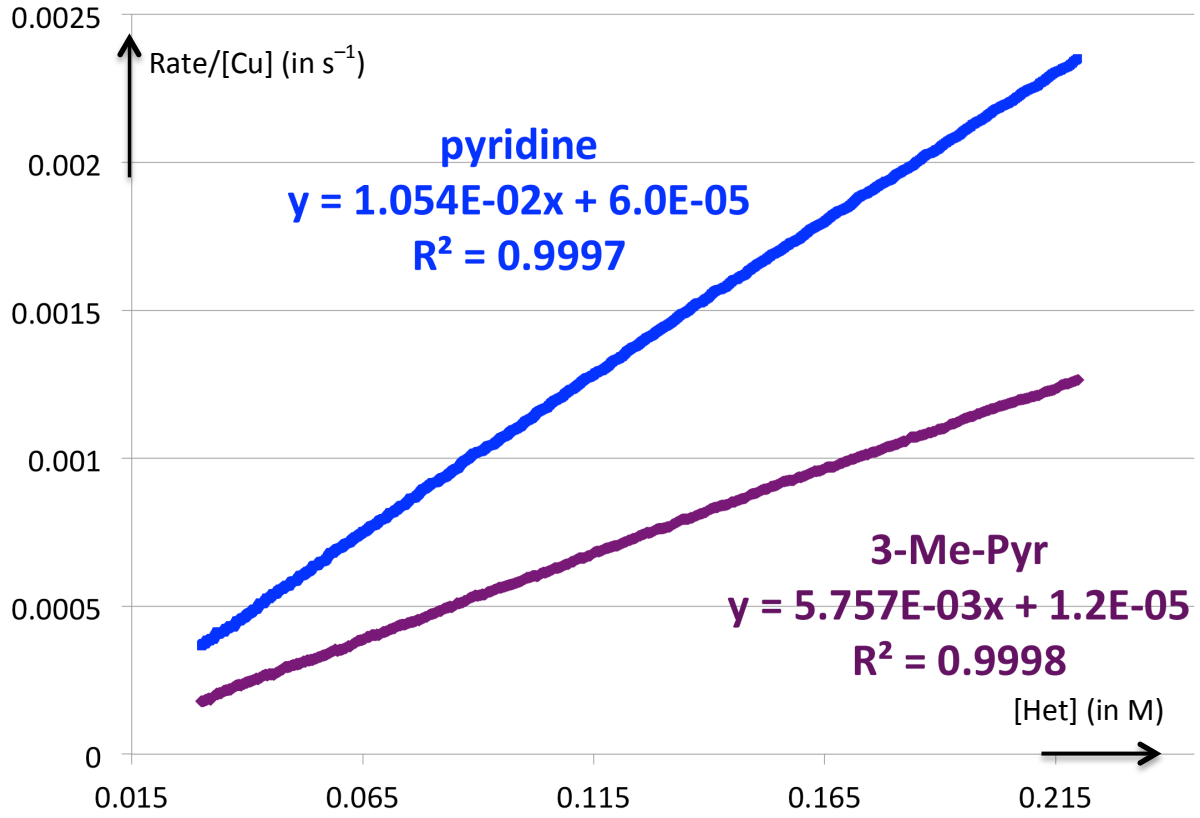

Figure SI-20: Overlaid rate curves plotted versus [Het] for Experiment 15.

Experiment 16 (Conditions $\mathcal{A}$):

3-phenylpyridine (**1d**):

$[Het]_0$ = 0.127 M, [Cu] = 4.98 mM (3.91 mol%), $[DMMS]_0$ = 0.493 M (3.87 equiv), $[3\text{-fluorostyrene}]_0$ = 0.188 M (1.47 equiv), $\Delta H_{rxn} = 31.2\ kcal/mol$, $k_{eff} = 5.37 \cdot 10^{-2}$ $(Ms)^{-1}$ (R^2 = 0.9996)

3-(*para*-mesylphenyl)pyridine (**1g**):

$[Het]_0$ = 0.130 M, [Cu] = 4.98 mM (3.82 mol%), $[DMMS]_0$ = 0.493 M (3.78 equiv), $[3\text{-fluorostyrene}]_0$ = 0.188 M (1.44 equiv), $\Delta H_{rxn} = 33.9\ kcal/mol$. The reaction of this substate does not exhibit simple first-order kinetics because its turnover-limiting step is different from that of the examples above (see Section 4). The reaction is, however, faster than that of 3-phenylpyridine (see Figure SI-21 and SI-22). The increased reaction rate for **1g** was more pronounced at higher concentration (**Experiment 17**, Figure SI-22). **Experiments 18–21**

show that the larger rate disparity in **Experiment 17** is specifically due to the increased silane loading; the reaction of **1g** is accelerated by increasing [DMMS], whereas that of **1d** is unaffected.

Experiment 17:

3-phenylpyridine (**1d**):

$[Het]_0 = 0.169$ M, [Cu] = 0.0199 mM (11.8 mol%), $[DMMS]_0 = 0.627$ M (3.71 equiv), $[3\text{-fluorostyrene}]_0 = 0.238$ M (1.41 equiv), $\Delta H_{rxn} = 33.0\ kcal/mol$, $k_{eff} = 4.79 \cdot 10^{-2}\ (Ms)^{-1}$ ($R^2 = 0.9998$)

3-(*para*-mesylphenyl)pyridine (**1g**):

$[Het]_0 = 0.174$ M, [Cu] = 0.0199 mM (11.4 mol%), $[DMMS]_0 = 0.627$ M (3.61 equiv), $[3\text{-fluorostyrene}]_0 = 0.238$ M (1.37 equiv), $\Delta H_{rxn} = 34.3\ kcal/mol$.

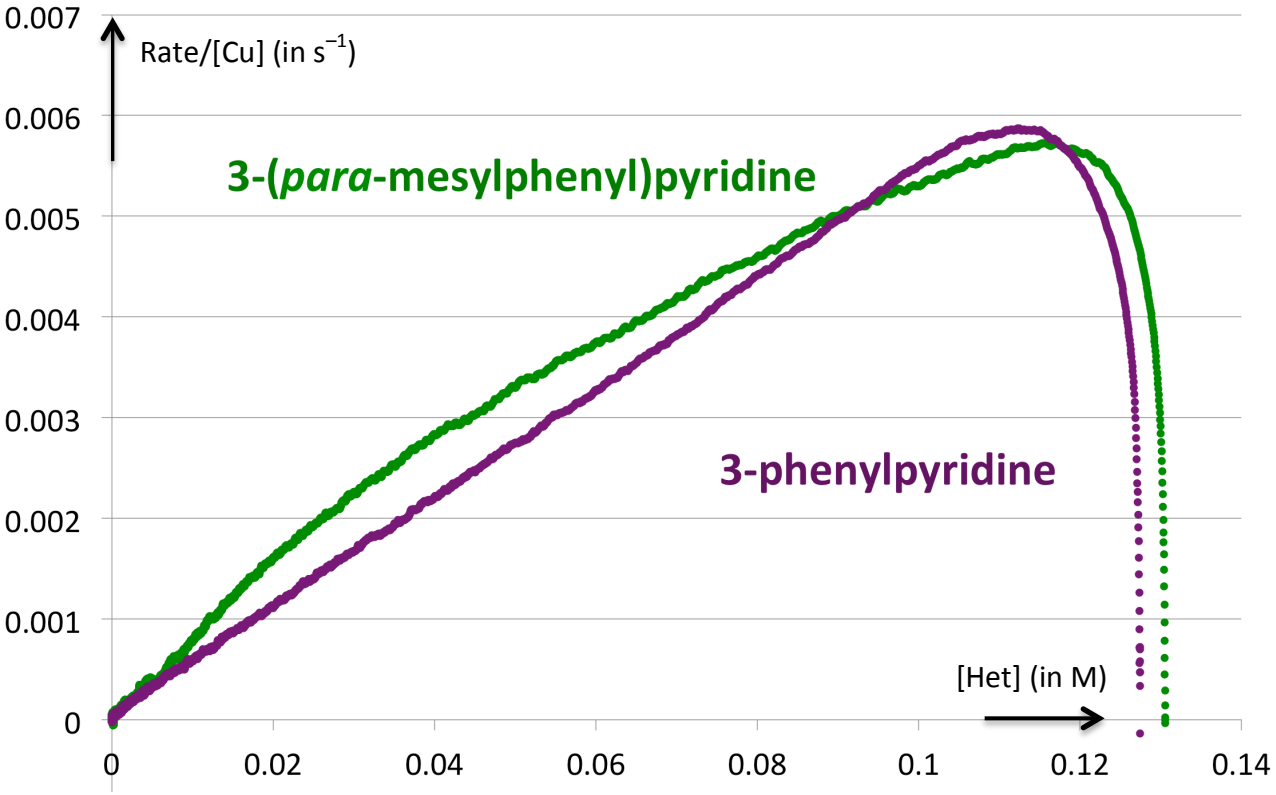

Figure SI-21: Overlaid rate curves plotted versus [Het] for Experiment 16.

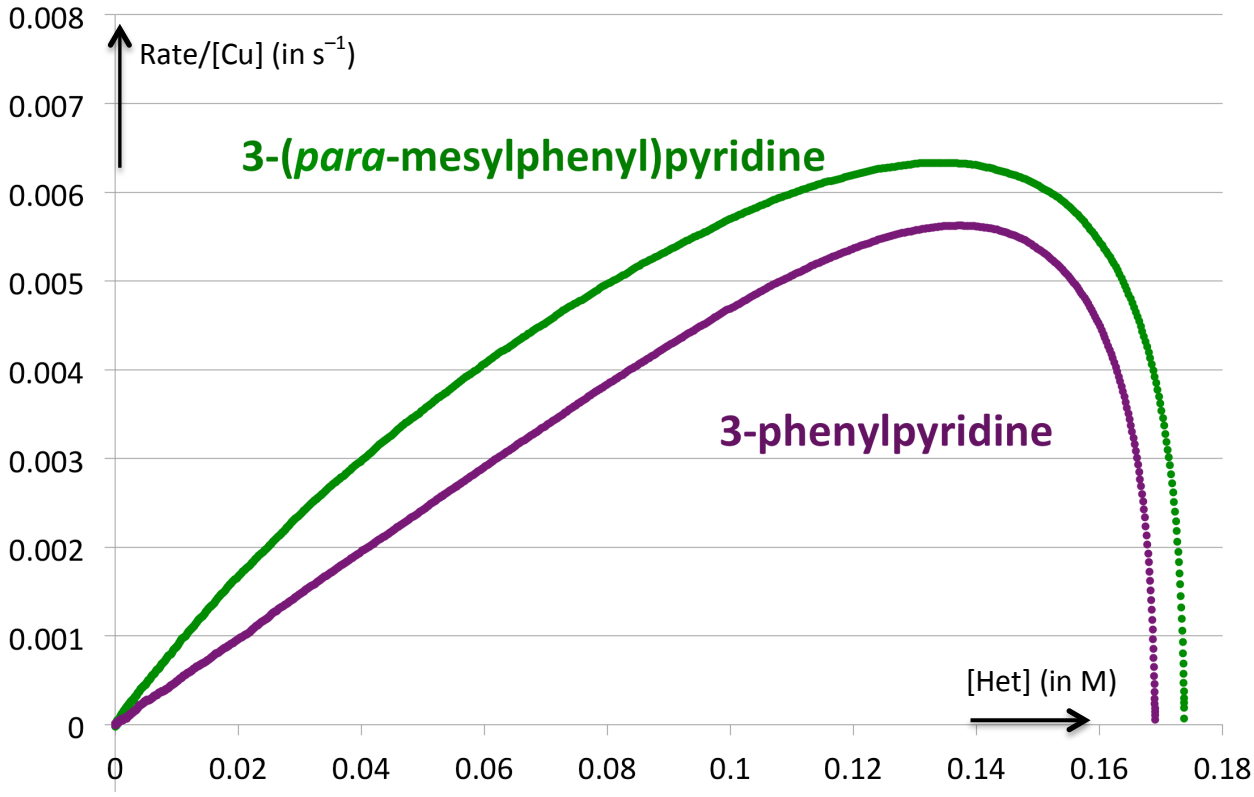

Figure SI-22: Overlaid rate curves plotted versus [Het] for Experiment 17.

2.5. Study of the kinetic dependence on [DMMS] and [3-fluorostyrene] in the dearomatization of 3-(*para*-mesylphenyl)pyridine (1g) with 3-fluorostyrene (6h) (Experiments 18-21).

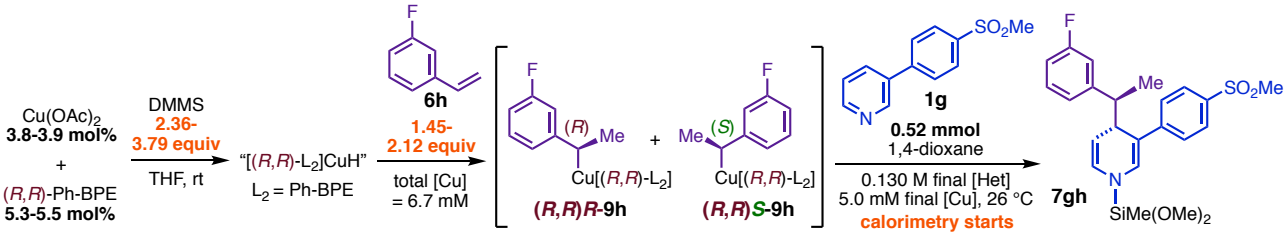

In order to minimize potential differences in rate due to catalyst formation occurring under different conditions, the phenethylcopper mixtures in all examples were prepared using the same stoichiometry, and the quantity of DMMS was subsequently adjusted as indicated shortly before the reaction mixtures were transferred to the calorimeter.

Procedure. Step one: Inside a glovebox, an oven-dried calorimeter vial containing an oven-dried PTFE stir bar was charged with $Cu(OAc)_2$ (9.08 mg, 50 μmol) and (*R*,*R*)-Ph-BPE (35.5 mg, 70.1 μmol; 1.4:1 L_2:Cu). The vial was sealed with a PTFE/silicone septum-cap. The catalyst precursors were dissolved in THF (3.84 mL), and DMMS (390 μL, 3.17 mmol) was added immediately afterward. The resulting mixture was stirred at rt for 20–25 min, during which time all $Cu(OAc)_2$ dissolved and the color turned orange. This activated catalyst solution was charged with 3-fluorostyrene (230 μL, 1.93 mmol) and stirred at rt for 145–155 min.

Step two: The phenethylcopper solution was partitioned into separate aliquots. An oven-dried glass microsyringe was used to charge each of two new oven-dried calorimetry vials (both of which were equipped with PTFE stir bars and PTFE/silicone septum-caps) with 1.80 mL aliquots of the phenethylcopper solution. Each of the 1.80 mL aliquots constituted 40% of the total initial volume of stock solution, from which it was estimated that each reaction mixture received 20 μmol Cu, 1.23 mmol DMMS, and 0.755 mmol 3-fluorostyrene (the latter two quantities are corrected for the approximate amounts consumed during phenethylcopper formation).

Step three: One of the phenethylcopper mixtures was diluted at this time with 1.20 mL THF, giving a mixture with volume = 3.00 mL containing 2.36 equiv DMMS and 1.45 equiv 3-fluorostyrene relative to **1g**. The second phenethylcopper mixture was diluted with 1.11 mL THF and 92 μL DMMS), giving a mixture with volume = 3.00 mL containing 3.81 equiv DMMS and 1.45 equiv 3-fluorostyrene relative to **1g.** The reference mixture was prepared from 250 μL DMMS and 2.75 mL THF. The three mixtures were transferred to the calorimeter block (pre-equilibrated at 26 °C) and stirred at ca. 1600 rpms until the heatflow returned to baseline.

Step four: The heterocycle stock solution had the same composition as those used in **Experiments 16–17** in Section 2.4. Once the phenethylcopper solutions had been aged at rt for a total of 5 h, calorimetric rate measurements were commenced upon charging each reaction mixture with a 1.00 mL aliquot of the 3-(*p*-MsPh)pyridine stock solution and charging the reference mixture with a 1.00 mL aliquot of 1,4-dioxane. Once the injections were complete, the syringes were removed from the calorimeter vials and calibrated in the manner described in Step 5 in Section 2.4.

In **Experiments 20–21** below, the phenethylcopper solution was generated as above, but using 3.72 mL rather than 3.84 mL of THF. Additional DMMS (125 μL) was added immediately before the solution was partitioned. One reaction mixture was further diluted with 1.20 mL THF, giving a mixture with volume = 3.00 mL containing 3.12 equiv DMMS and 1.44 equiv 3-fluorostyrene. The second phenethylcopper mixture was diluted with 1.16 mL and 40 μL 3-fluorostyrene, giving a mixture with volume = 3.00 mL containing 3.17 equiv DMMS and 2.12 equiv 3-fluorostyrene.

Experiment 18: $[Het]_0$ = 0.130 M, [Cu] = 5.03 mM (3.87 mol%; 1.4:1 Ph-BPE:Cu), $[DMMS]_0$ = 0.307 M (**2.36 equiv**), $[3\text{-fluorostyrene}]_0$ = 0.188 M (**1.45 equiv**), $\Delta H_{rxn} = 34.6\ kcal/mol$

Experiment 19: $[Het]_0$ = 0.130 M, [Cu] = 4.96 mM (3.82 mol%; 1.4:1 Ph-BPE:Cu), $[DMMS]_0$ = 0.494 M (**3.79 equiv**), $[3\text{-fluorostyrene}]_0$ = 0.188 M (**1.45 equiv**), $\Delta H_{rxn} = 33.5\ kcal/mol$

Experiment 20: $[Het]_0$ = 0.130 M, [Cu] = 5.01 mM (3.85 mol%; 1.4:1 Ph-BPE:Cu), $[DMMS]_0$ = 0.406 M (**3.12 equiv**), $[3\text{-fluorostyrene}]_0$ = 0.188 M (**1.45 equiv**), $\Delta H_{rxn} = 35.3\ kcal/mol$

Experiment 21: $[Het]_0$ = 0.129 M, [Cu] = 5.03 mM (3.90 mol%; 1.4:1 Ph-BPE:Cu), $[DMMS]_0$ = 0.307 M (**3.17 equiv**), $[3\text{-fluorostyrene}]_0$ = 0.273 M (**2.12 equiv**), $\Delta H_{rxn} = 36.0\ kcal/mol$

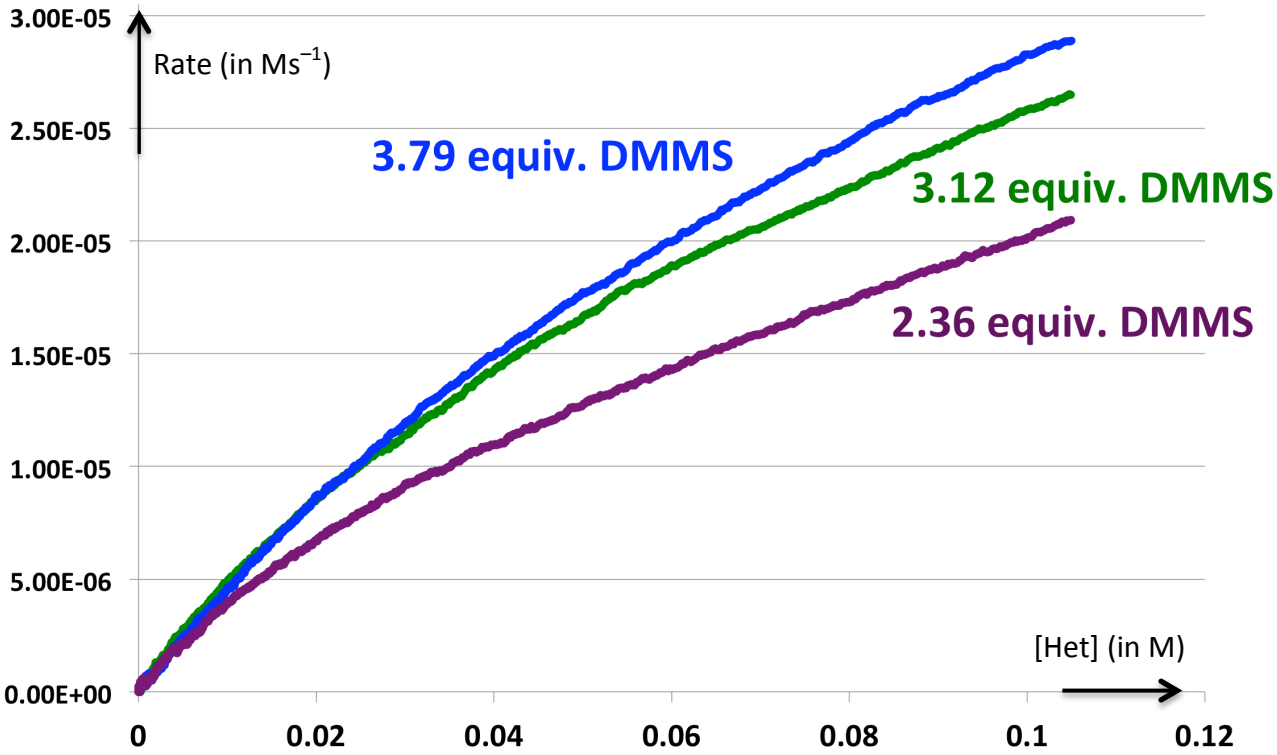

Figure SI-23: Overlaid rate curves plotted versus [Het] for Experiments 18–20. The reaction exhibits a kinetic dependence on [DMMS].

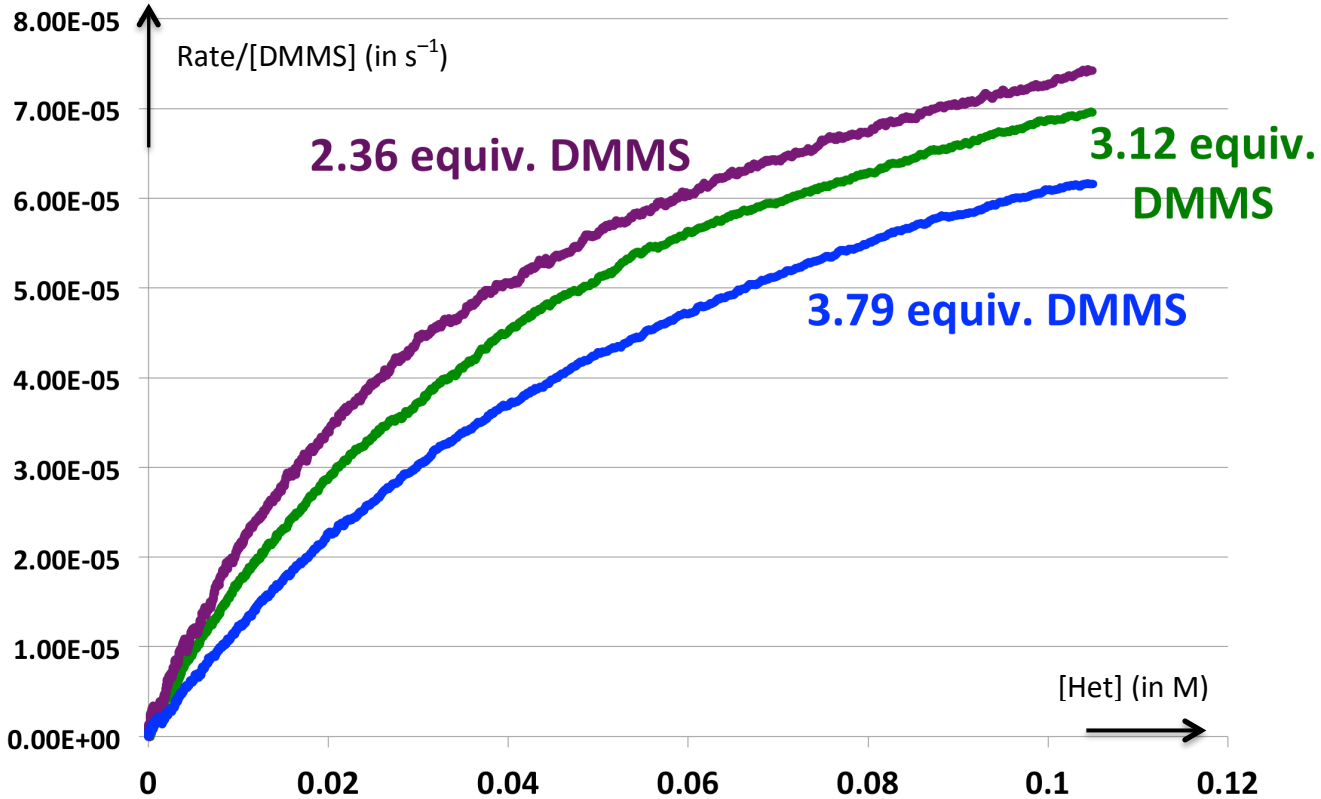

Figure SI-24: Overlaid rate curves plotted versus [Het] for Experiments 18–20. The kinetic dependence on [DMMS] is less than first order (curves for reactions with higher [DMMS] appear lower on the graphs).

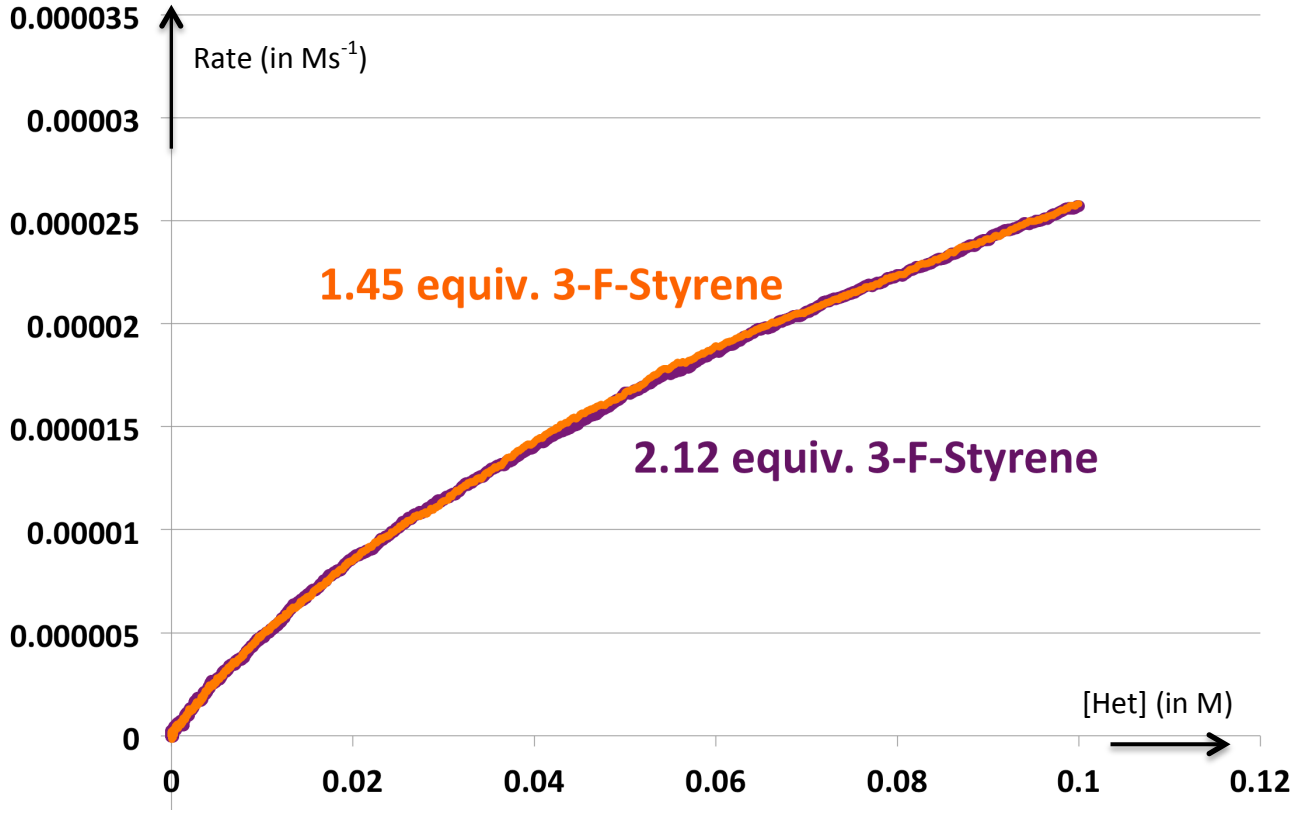

Figure SI-25: Overlaid rate curves plotted versus [Het] for Experiments 20–21. There is no kinetic dependence on [3-fluorostyrene].

3. Derivation of the Double-dearomatization Rate Equation for Unactivated Heterocycles.

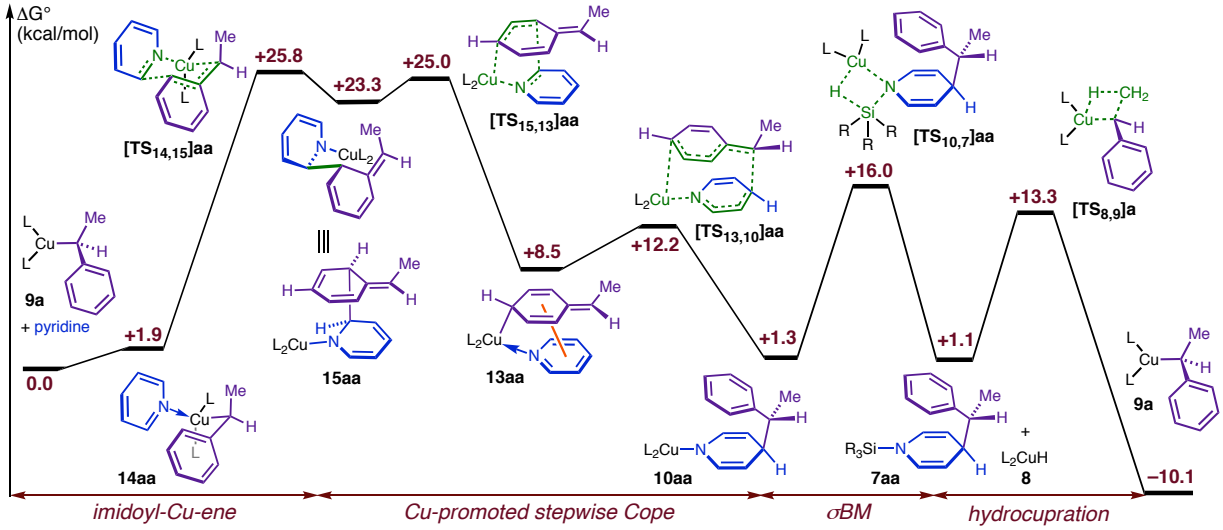

Figure SI-26: Computed PES for dearomatization of pyridine with styrene via the doubly dearomative pathway

Scheme SI-1: Simplified catalytic cycle for theoretical kinetics analysis

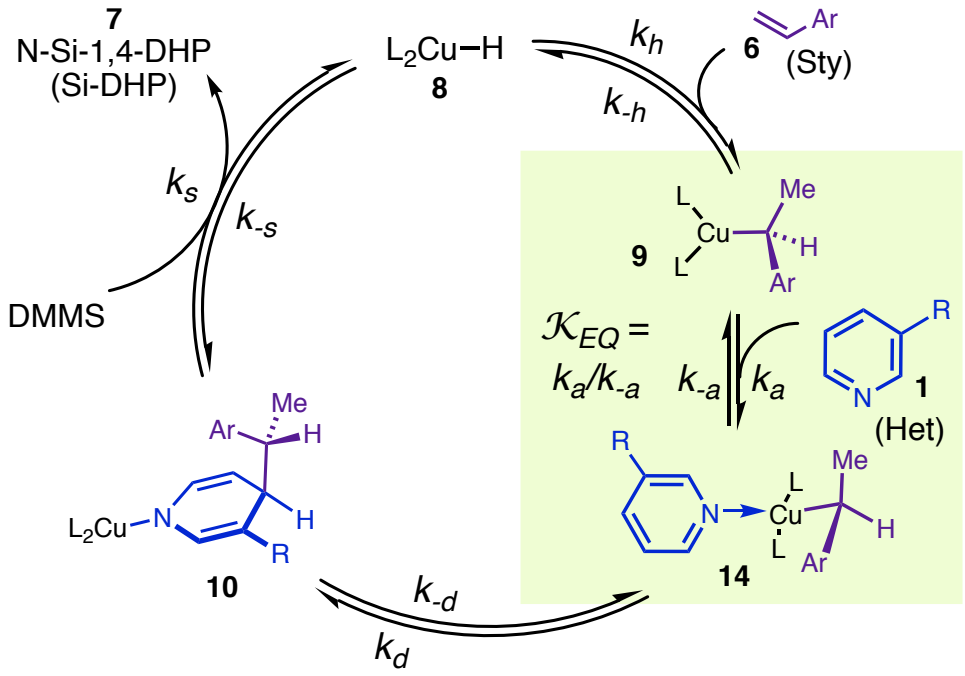

Under steady-state conditions, the general rate law for the cycle in Scheme SI-1 (derived using "Christiansen mathematics" – see reference 6 and references therein for description of the procedure) is

$$rate = \frac{(\lambda_h\lambda_d\lambda_s - \lambda_{-h}\lambda_{-d}\lambda_{-s})[\mathrm{Cu}]_A}{\sum \mathcal{M}} \qquad \text{(eq 4)},$$

where $[\mathrm{Cu}]_A$ ($\propto [\mathrm{Cu}]$) is the total concentration of active Cu species, $\sum \mathcal{M}$ indicates the sum of the elements in the matrix

$$\mathcal{M} = \begin{bmatrix} \lambda_d\lambda_s & \lambda_{-h}\lambda_s & \lambda_{-h}\lambda_{-d} \\ \lambda_s\lambda_h & \lambda_{-d}\lambda_h & \lambda_{-d}\lambda_{-s} \\ \lambda_h\lambda_d & \lambda_{-s}\lambda_d & \lambda_{-s}\lambda_{-h} \end{bmatrix}$$

First row associated with **8**

Second row associated with **9** + **14**

Third row associated with **10**

(eq 5),

and the effective first-order rate constants are

$\lambda_h = k_h[\mathrm{Sty}]$, $\lambda_{-h} = k_{-h}/(1 + \mathcal{K}_{EQ}[\mathrm{Het}])$, $\lambda_d = (k_d\mathcal{K}_{EQ}[\mathrm{Het}])/(1 + \mathcal{K}_{EQ}[\mathrm{Het}])$, $\lambda_{-d} = k_{-d}$, $\lambda_s = k_s[\mathrm{DMMS}]$, and $\lambda_{-s} = k_{-s}[\mathrm{Si\text{-}DHP}]$.

In long form,

$$\mathcal{M} = \begin{bmatrix} \frac{k_d k_s \mathcal{K}_{EQ}[\mathrm{Het}][\mathrm{DMMS}]}{1+\mathcal{K}_{EQ}[\mathrm{Het}]} & \frac{k_{-h}k_s[\mathrm{DMMS}]}{1+\mathcal{K}_{EQ}[\mathrm{Het}]} & \frac{k_{-h}k_{-d}}{1+\mathcal{K}_{EQ}[\mathrm{Het}]} \\ k_h k_s[\mathrm{Sty}][\mathrm{DMMS}] & k_h k_{-d}[\mathrm{Sty}] & k_{-d}k_{-s}[\mathrm{Si\text{-}DHP}] \\ \frac{k_h k_d \mathcal{K}_{EQ}[\mathrm{Sty}][\mathrm{Het}]}{1+\mathcal{K}_{EQ}[\mathrm{Het}]} & \frac{k_d k_{-s} \mathcal{K}_{EQ}[\mathrm{Het}][\mathrm{Si\text{-}DHP}]}{1+\mathcal{K}_{EQ}[\mathrm{Het}]} & \frac{k_{-h}k_{-s}[\mathrm{Si\text{-}DHP}]}{1+\mathcal{K}_{EQ}[\mathrm{Het}]} \end{bmatrix} \qquad \text{(eq 6)}.$$

Because the reaction is irreversible, $\lambda_{-h}\lambda_{-d}\lambda_{-s} \sim 0$,

and

$$rate = \frac{\lambda_h\lambda_d\lambda_s[\mathrm{Cu}]_A}{\sum \mathcal{M}} = \frac{k_h k_d k_s \mathcal{K}_{EQ}[\mathrm{Sty}][\mathrm{Het}][\mathrm{DMMS}][\mathrm{Cu}]_A}{(1+\mathcal{K}_{EQ}[\mathrm{Het}])\cdot \sum \mathcal{M}} \qquad \text{(eq 7)}.$$

The sum of elements in a given row of $\mathcal{M}$ is proportional to the fraction of active catalyst present as the species associated with that row (see eq 5). The PES in Figure SI-26 implies that **9** should be the only significant catalyst species present during dearomatization, i.e., be the MACS (most abundant catalyst species), and we have found spectroscopically that this prediction is correct (see Section 5). Consequently, all elements in the first and third rows of $\mathcal{M}$ must be negligible. Further, the PES implies that dearomative isomerization must be the TLS, which is equivalent to requiring that k_d and k_{-d} be sufficiently small that all elements containing them are also negligible. Applying these conditions eliminates all matrix elements except for $k_h k_s[\mathrm{Sty}][\mathrm{DMMS}]$, thus:

$$\mathcal{M} = \begin{bmatrix} 0 & 0 & 0 \\ k_h k_s[\text{Sty}][\text{DMMS}] & 0 & 0 \\ 0 & 0 & 0 \end{bmatrix} \qquad \text{(eq 8)},$$

in which case

$$rate = \frac{k_d \mathcal{K}_{EQ}[\text{Het}][\text{Cu}]_A}{1+\mathcal{K}_{EQ}[\text{Het}]} \qquad \text{(eq 9)}.$$

In qualitative terms, sigma-bond metathesis (σBM) and hydrocupration occur after the TLS and are not kinetically relevant. $\mathcal{K}_{EQ}$[Het] is the pseudoequilibrium ratio [**14**]/[**9**], and the PES implies that this must have value << 1. Thus, (1 + $\mathcal{K}_{EQ}$[Het]) ~ 1, and one obtains

$$rate = k_d \mathrm{K}_{EQ}[\text{Het}][\text{Cu}]_A = k_{eff}[\text{Het}][\text{Cu}] \qquad \text{(eq 10)},$$

in agreement with experiment. The non-linear dependence of rate on L_2:Cu means that the rate law would be more complex if [Ph-BPE] were explicitly included in it. Presumably, the phosphine dependence arises because $[\text{Cu}]_A$ is a function of both [Cu] and L_2:Cu for the reasons discussed in Section 2.3. However, for kinetics experiments conducted at fixed L_2:Cu ratios, the empirical rate law has the simple form in eq 10.

It is possible to deduce the rate law in an interesting way using the fluctuating dr of phenethylcopper **9** observed during enantioselective catalysis (see Figure SI-39 and the accompanying discussion in section 5.2.i below), which implies that the rate constants for β-hydride elimination (k_{-h}) and dearomative isomerization (k_d) must be comparable, with dearomatization being faster under typical conditions. Thus if k_d and k_{-d} are treated as negligible due to dearomatization being turnover-limiting, then k_{-h} must also be negligible. These three constraints eliminate all matrix elements except for $\lambda_s\lambda_h = k_h k_s$[DMMS][Sty], yielding eq 8.

4. Mechanistic Implications of the Saturation Kinetics Observed in the Dearomatization of 3-(*Para*-mesylphenyl)pyridine (1g).

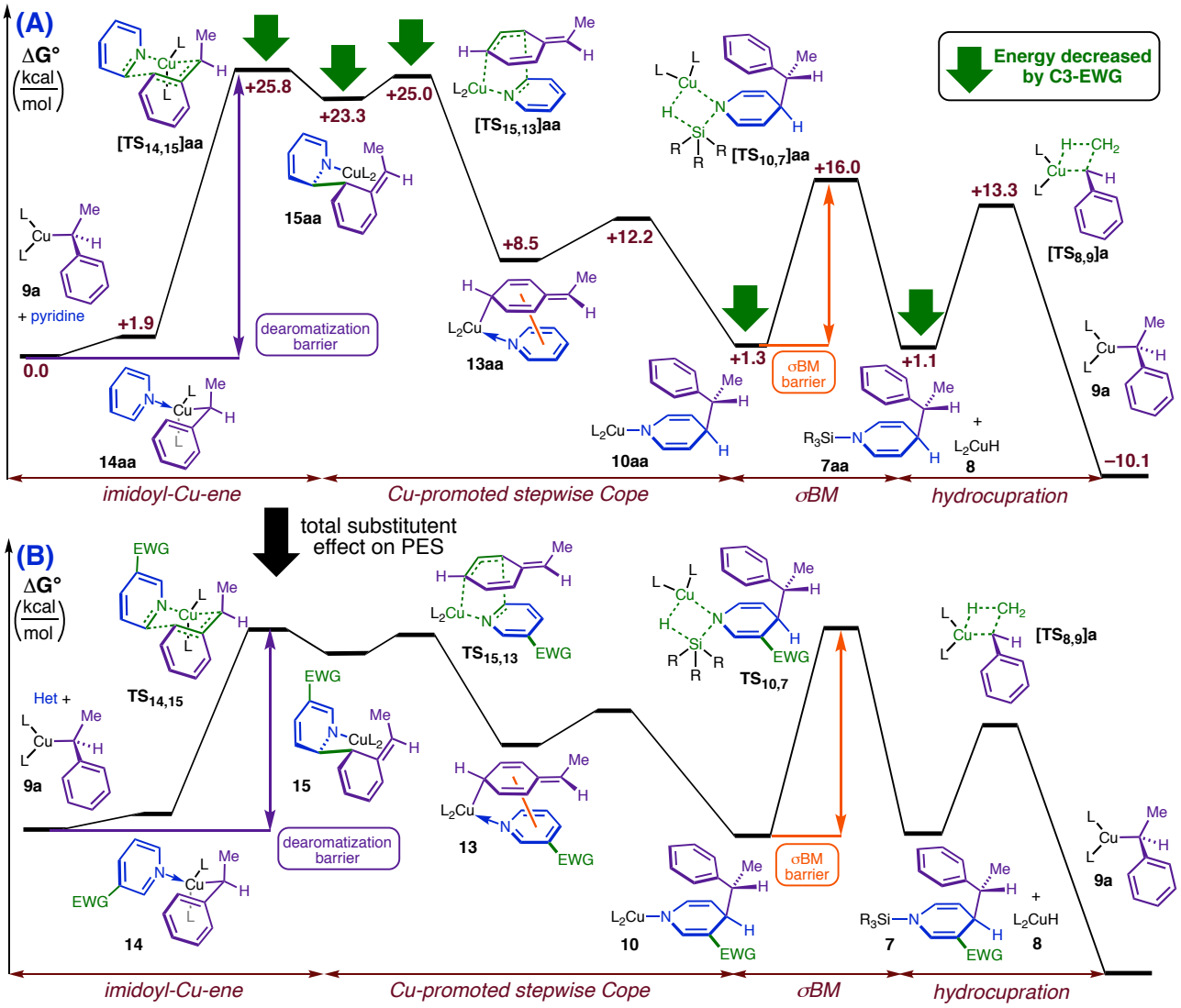

Figure SI-27: (A) Expected perturbations for an anion-stabilizing C3 substituent on the energies of individual catalytic intermediates; (B) Modified energy surface for the substituted heterocycle.

The influence of strongly activating heterocycle substituents on the form of the rate law is informative for several reasons, and very electron-deficient heterocycles make up one of the most important substrates classes for the asymmetric dearomatization. One can apply chemical reasoning to the prediction of how anion-stabilizing C3 substituents should affect the energies of individual structures in the double-dearomatization PES (Figure SI-27, A) and formulate readily testable predictions about how the kinetics and catalyst resting state should change. In addition, the fact that strongly activating C3 substituents change the rate law provides an opportunity to use reaction kinetics to obtain empirical information about catalytic steps and intermediates that occur after dearomative isomerization and are thus not kinetically relevant for substrates like **1a** and **1d**.

Because the doubly dearomative imidoyl ene (**14aa** → **15aa**; see Figure SI-27, A) and the ene leading from **13aa** to **15aa** (Figure SI-27, A) both have nucleophilic addition character, anion-stabilizing C3 groups must lower the barriers to both of those steps (i.e., decrease the energies of $\mathbf{TS_{14,15}}$ and $\mathbf{TS_{15,13}}$ relative to **9**). Such groups must also lower the energy of the doubly dearomatized intermediate **15**, in which a fully developed metalloenamine functional group is present. The overall effect of these changes is to lower the rate-controlling barrier to the dearomative isomerization process (**9** → **10** in Scheme SI-1), increasing k_d. However, our group's earlier study on substituent effects[7] on the rate of σBM by Cu-carboxylate species showed that that transformation is markedly slowed by groups that attenuate the nucleophilicity of the carboxylate ligand, and we expect similar deceleration to occur here with substituents that attenuate the nucleophilicity of **10**. This implies an increase in the energy of σBM transition state $\mathbf{TS_{10,7}}$ relative to **10** and a decrease in k_s. If the opposing effects on dearomative isomerization and σBM are sufficiently large, then their respective barriers should become comparable in magnitude, making the σBM step kinetically relevant. If this occurs, however, the catalyst resting state is also expected to change. Because metalloenamine **10aa** is predicted to be very close in energy to phenethylcopper **9a** in the absence of a substituent, the double dearomatization PES indicates that even modest additional stabilization should render **10** isoenergetic with or potentially more stable than **9**. Consequently, if the barrier to σBM becomes comparable to or greater than the barrier to dearomative isomerization, then the previously unobserved intermediate **10** must become a major component of the catalyst resting state. In agreement with experiment (see Section 2.5), the hydrocupration step should remain kinetically irrelevant: this step cannot exhibit a (heterocycle) substituent effect, and its barrier is already significantly below that of σBM when no substituent is present. Figure SI-27, B, provides a qualitative predicted PES reflecting all of these changes for a heterocycle bearing a strongly activating C3 substituent.

These considerations are straightforwardly applied to prediction of a new rate law for activated heterocycles using the mathematical analysis in Section 3. If k_d and k_s are permitted to be comparable in magnitude, then matrix elements containing k_d cannot be assumed to be negligible. The effect of a substituent on k_{-d} (the rate constant for reverse-dearomative-isomerization, i.e., **10** → **9** in Scheme SI-1) is difficult to predict on first principles, but its value could be increased if the substituent lowers the rate-controlling barrier to dearomative isomerization more than it stabilizes **10**. Consequently, we allow, but do not require, matrix elements containing factors of $k_{-d}$to be non-negligible. One major simplifying assumption does apply, however. Because the hydrocupration step is expected to be kinetically irrelevant, all matrix elements that do not contain a factor of [Sty] must be negligible, as required for cancellation of the factor of [Sty] in the numerator of eq. 7. This condition eliminates all matrix elements except for $\lambda_s\lambda_h$, $\lambda_{-d}\lambda_h$, and $\lambda_h\lambda_d$, and consequently $\mathcal{M}$ becomes

$$\mathcal{M} = \begin{bmatrix} 0 & 0 & 0 \\ k_h k_s[\text{Sty}][\text{DMMS}] & k_h k_{-d}[\text{Sty}] & 0 \\ \frac{k_h k_d \mathcal{K}_{EQ}[\text{Sty}][\text{Het}]}{1+\mathcal{K}_{EQ}[\text{Het}]} & 0 & 0 \end{bmatrix} \quad \text{(eq 11)},$$

giving the rate equation

$$rate = \left(\frac{1}{1 + \mathcal{K}_{EQ}[\text{Het}]}\right) \frac{\mathcal{K}_{EQ} k_d k_s[\text{Het}][\text{DMMS}][\text{Cu}]_A}{\left(\frac{\mathcal{K}_{EQ} k_d[\text{Het}]}{1 + \mathcal{K}_{EQ}[\text{Het}]}\right) + k_s[\text{DMMS}] + k_{-d}} \quad \text{(eq 12)}.$$

It is noteworthy that the third row of $\mathcal{M}$, whose sum is proportional to the fraction of catalyst present as **10**, now contains a non-negligible element. In agreement with our qualitative analysis, this directly implies that **10** must become a significant component of the resting state.

Our failure to observe **14** with various styrenes and heterocycles suggests that the association equilibrium (**1**+ **9** ⇌ **14**) is generally unfavorable, and it is implausible that an EWG substituent on **1** would alter this. Empirically, we have found no evidence for appreciable formation of **14** in the resting state for dearomatization of activated substrate **1g**. Consequently, we still require that (1 + $\mathcal{K}_{EQ}$[Het]) ~ 1. Thus, one obtains

$$rate = \frac{\mathcal{K}_{EQ} k_d k_s[\text{Het}][\text{DMMS}][\text{Cu}]_A}{\mathcal{K}_{EQ} k_d[\text{Het}] + k_s[\text{DMMS}] + k_{-d}} = \frac{k_D k_s[\text{Het}][\text{DMMS}][\text{Cu}]_A}{k_D[\text{Het}] + k_s[\text{DMMS}] + k_{-d}} \quad \text{(eq 13)},$$

defining $k_D := \mathcal{K}_{EQ} k_d$.

Consequently, one can write

$$\frac{[\text{DMMS}][\text{Het}][\text{Cu}]_A}{rate} = \frac{k_D[\text{Het}] + k_s[\text{DMMS}] + k_{-d}}{k_D k_s} \quad \text{(eq 14)}.$$

But because [DMMS] is linearly related to [Het] over the course of the reaction as [DMMS] = [Het] + $(\chi - 1)[\text{Het}]_0$, where χ is the fold-excess of DMMS used in a given reaction, and $[\text{Het}]_0$ is the initial heterocycle concentration, this becomes, after rearrangement:

$$\frac{[\text{DMMS}][\text{Het}][\text{Cu}]_A}{rate} = \left(\frac{k_D + k_s}{k_D k_s}\right)[\text{Het}] + \left(\frac{(\chi-1)[\text{Het}]_0}{k_D} + \frac{k_{-d}}{k_D k_s}\right) \quad \text{(eq 15)}.$$

Eq 15 provides a convenient graphical way to diagnose whether the kinetics of a given dearomative reaction obey eq 13, and, if so, to estimate the individual rate constants for the kinetically relevant steps. It is clear that if the rate obeys eq 13, then plots of $([\text{DMMS}][\text{Het}][\text{Cu}]/rate)$ using actual rate and concentration data must be linear functions of [Het] having slope $\boldsymbol{N} \cong (k_D + k_s)/k_D k_s$. Further, the Y-intercepts of those lines must constitute a linear function of $(\chi - 1)[\text{Het}]_0$ having slope $\boldsymbol{n} \cong 1/k_D$:

$$\text{Y}(\chi, [\text{Het}]_0) \cong \left(\frac{1}{k_D}\right)(\chi - 1)[\text{Het}]_0 + \frac{k_{-d}}{k_D k_s} \qquad \text{(eq 16).}$$

Implication also goes in the other direction. Given respective kinetic orders of zero and one for [Sty] and $[\text{Cu}]_\text{A}$, if plots of $([\text{DMMS}][\text{Het}][\text{Cu}]/rate)$ using actual rate and concentration data are found to be linear functions of [Het], then the reaction *must* obey a saturation rate law like eq 13. Taking the inverse of the rate law (i.e, forming $1/rate$) transposes the numerator and denominator of the original rate expression. With the exception of trivial examples like $rate = k[\text{Het}][\text{Cu}]_A$ and $rate = k[\text{DMMS}][\text{Cu}]_A$ (which are themselves just limiting cases of eq 13), multiplying $(1/rate)$ by $[\text{DMMS}][\text{Het}][\text{Cu}]_A$ can only yield a simple linear function of [Het] if two conditions are met. First, the denominator of $rate$ must be a linear function of [Het]. Second, multiplying $(1/rate)$ by $[\text{DMMS}][\text{Het}][\text{Cu}]_A$ must have the effect of cancelling all of the concentration factors that were in the numerator of $rate$, and this can only occur if [DMMS] and [Het] both appear with exponents of one in the numerator of $rate$. Thus, if the plots are linear in [Het], it is established that the rate law has the form

$$rate = \frac{k_1[\text{Het}][\text{DMMS}][\text{Cu}]_A}{k_2[\text{Het}] + k_3} \qquad \text{(eq 17).}$$

Eq 13 is an instance of eq 17 given that [DMMS] is a linear function of [Het] throughout a given reaction, as noted above. Graphically determined linear parameters then indicate whether [DMMS], [Het], or both appear with non-negligible coefficients in the denominator of the true rate expression. For example, if the true rate law were

$$rate = \frac{k_D k_s[\text{Het}][\text{DMMS}][\text{Cu}]_A}{k_D[\text{Het}] + k_{-d}} \qquad \text{(eq 18),}$$

which corresponds to the limiting case of eq 13 in which $k_s \sim 0$, then

$$\frac{[\text{DMMS}][\text{Het}][\text{Cu}]_A}{rate} = \frac{k_D[\text{Het}] + k_{-d}}{k_D k_s} \qquad \text{(eq 19).}$$

Consequently, the Y intercepts of the plots will exhibit no dependence on $(\chi - 1)[\text{Het}]_0$. On the other hand, if the true rate law were

$$rate = \frac{k_D k_s[\text{Het}][\text{DMMS}][\text{Cu}]_A}{k_s[\text{DMMS}] + k_{-d}} \qquad \text{(eq 20),}$$

which corresponds to the limiting case of eq 13 in which $k_D \sim 0$, then one would obtain

$$\frac{[\text{DMMS}][\text{Het}][\text{Cu}]_A}{rate} = \frac{k_s\{[\text{Het}] + (\chi - 1)[\text{Het}]_0\} + k_{-d}}{k_D k_s}$$

$$= \left(\frac{1}{k_D}\right)[\text{Het}] + \left(\frac{(\chi - 1)[\text{Het}]_0}{k_D} + \frac{k_{-d}}{k_D k_s}\right) \qquad \text{(eq 21)}.$$

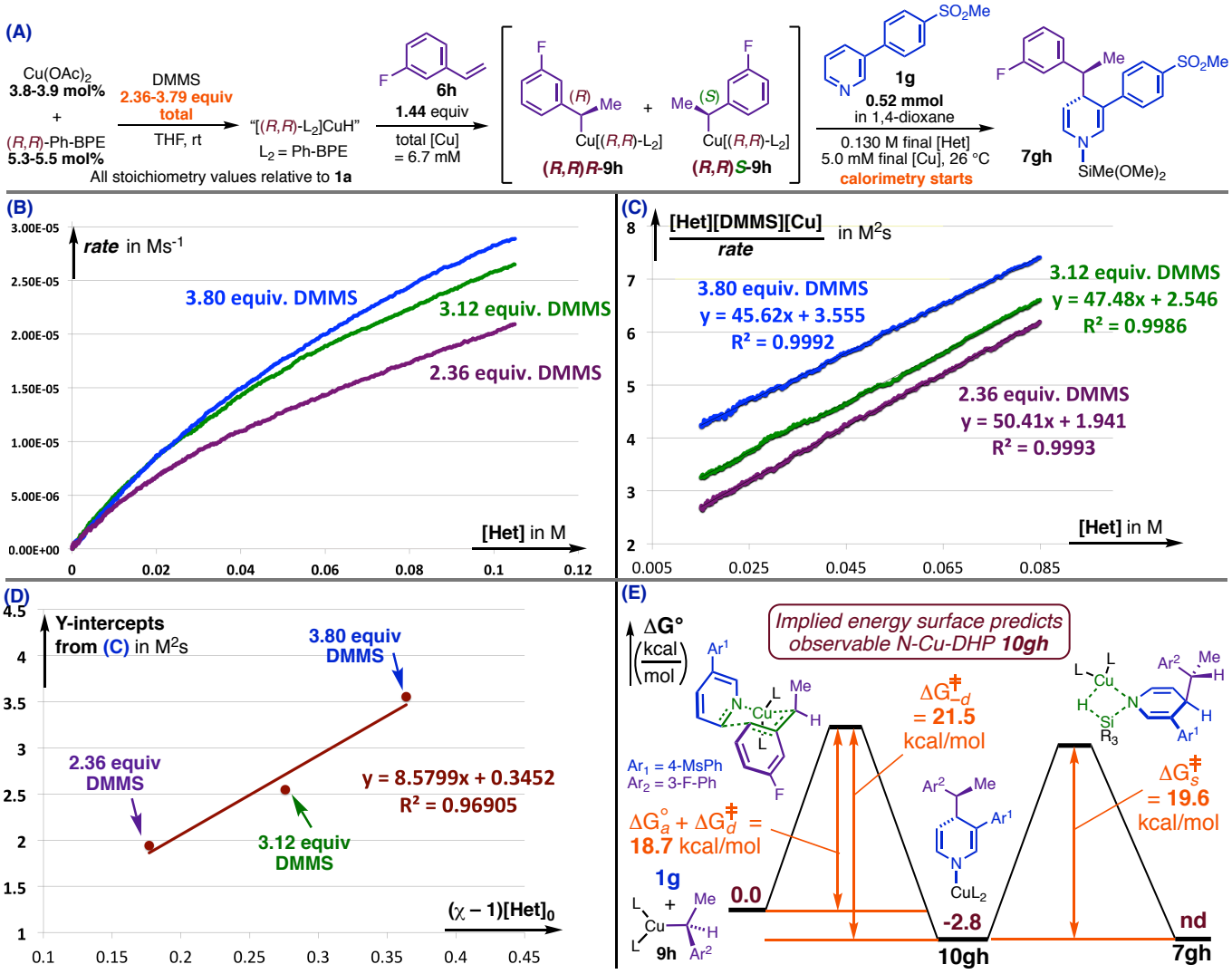

Figure SI-28: Analysis of saturation kinetics observed in dearomatization of 1g yields an approximate energy surface for kinetically relevant steps and empirically predicts observable intermediate 10gh.

In this scenario, the slope of the line obtained upon plotting the Y-intercepts versus $(\chi - 1)[\text{Het}]_0$ will be identical to the slope of the line obtained upon plotting $([\text{DMMS}][\text{Het}][\text{Cu}]/rate)$ versus [Het] (i.e., $\boldsymbol{n} = \boldsymbol{N} = 1/k_D$).

Thus, if the plots of $[\mathrm{DMMS}][\mathrm{Het}][\mathrm{Cu}]/rate$ yield a linear function of [Het] whose Y-intercepts are a (non-constant) linear function of $(\chi - 1)[\mathrm{Het}]_0$ having slope $\boldsymbol{n \neq N}$, then [Het] and [DMMS] must both appear with non-negligible coefficients in the denominator of the true rate law (see eq 13), and indeed one can then calculate what those coefficients must be.

It is clear from the plots in Figure SI-28, C, that for the reaction of **1g** with **6h**, the expression $([\mathrm{DMMS}][\mathrm{Het}][\mathrm{Cu}])/rate$ is a linear function of [Het]. Further, the slopes of those lines are similar (average 47.8 Ms; treating all slopes as resulting from identical measurements would yield standard deviation 1.88 (n = 5)) as required by eq 15. The Y-intercepts of the lines in Figure SI-28, C, show a pronounced monotonic dependence on $(\chi - 1)[\mathrm{Het}]_0$, as required by eq 15 and inconsistent with eq 19. The slope of the line obtained by regression (Figure SI-28, D) of the Y-intercepts, $\boldsymbol{n}$ (8.58 Ms), is very different from the average slope $\boldsymbol{N}$ of the plots of $([\mathrm{DMMS}][\mathrm{Het}][\mathrm{Cu}])/rate$, which is incompatible with eq 21 but in agreement with eq 15. Consequently, we conclude that the true rate law for dearomatization of **1d** with **6h** is an instance of eq. 13 in which k_D and k_s are both non-negligible, in agreement with the predictions of our mechanistic model.

Equating linear parameters from the plots in Figure SI-28, C and D, with individual rate constants by way of eq 15 requires information about the relationship between [Cu] (the total concentration of Cu) and $[\mathrm{Cu}]_\mathrm{A}$. Our prior kinetics and spectroscopic studies (*vide infra*) suggest that active copper species should make up the majority of Cu, be proportional to [Cu] over the course of the reaction, and exhibit a proportionality constant largely unaffected by modest variation in the conditions. The spectroscopy experiments in Section 5.2.v support the view that this should be true for dearomatization of **1g** in particular. For simplicity, we use here the approximation that $[\mathrm{Cu}]_\mathrm{A} = [\mathrm{Cu}]$, although it can be expected that this will result in each of the individual rate constants being modestly underestimated.

From equation 15, it is clear that $k_D = (1/\boldsymbol{n})$, and k_S can thus be determined from the relationship:

$$\boldsymbol{N} = \frac{k_D + k_S}{k_D k_S} = \frac{\left(\frac{1}{n}\right) + k_S}{\left(\frac{1}{n}\right) k_S} = \frac{1 + n k_S}{k_S} \qquad \text{(eq 22)},$$

which implies that

$$k_S = \frac{1}{\boldsymbol{N} - \boldsymbol{n}} \qquad \text{(eq 23)}.$$

Defining $\boldsymbol{q}$ to be the Y-intercept of the plot in Figure SI-28, D, eq 15 implies that

$$k_{-d} = q k_D k_S = \frac{q}{\boldsymbol{n}(\boldsymbol{N} - \boldsymbol{n})} \qquad \text{(eq 24)}.$$

Solving these equations using the linear parameters in Figures SI-28, C and D, yields

k_D = 0.117 $\mathrm{M^{-1}s^{-1}}$, k_S = 0.0255 $\mathrm{M^{-1}s^{-1}}$, and k_{-d} = 1.02•$10^{-3}\mathrm{s^{-1}}$

Relating these rate constants to $\Delta G^{\ddagger}$ values for the associated processes by way of the Eyring equation (eq 25) gives the energy landscape in Figure SI-28, E.

$$k = \frac{k_B T}{h} e^{\frac{-\Delta G^{\ddagger}}{RT}} \qquad \text{(eq 25)}$$

Thus, our empirical analysis of the reaction kinetics for **1g** yields approximate energy values for kinetically relevant steps that are in excellent agreement with the qualitative predictions of the double-dearomatization PES; in particular, they imply that the barriers to dearomatization and σBM have indeed become very similar, with the former being somewhat lower. This corroborates the view that the anion-stabilizing group at C3 alters the rate law by facilitating an otherwise turnover-limiting nucleophilic addition event (i.e., the doubly dearomative imidoyl-Cu-ene). Consistent with our qualitative and mathematical analyses, these empirically estimated rate constants also indicate that N-Cu-1,4-DHP **10gh** should be a major component of the resting state during the dearomatization of **1g** with **6h**.

In support of the robustness of these conclusions, it is worth noting that, because $k_D = 1/\boldsymbol{n}$, $k_s = 1/(\boldsymbol{N} - \boldsymbol{n})$, and $\boldsymbol{N} >> \boldsymbol{n}$, it is not necessary to know $\boldsymbol{n}$ with extremely high precision in order to conclude that $k_D > k_s$ (i.e., that the barrier to dearomative isomerization starting from **9** is lower than the barrier to σBM). In order for the converse to obtain, the true value of $\boldsymbol{n}$ would need to be greater than our estimate by an unreasonably large margin (a factor of about 250%). The estimated value of k_{-d} (obtained from the intercept in Figure SI-28, D) is pertinent to the *empirical* prediction that **10gh** should be observable: provided that $k_D > k_s$, the converse (unobservable **10gh**) could only be true if $k_{-d} > k_D$, which would make **10gh** unstable relative to **9h**. In an equation, that would require

$$k_D - k_{-d} = \frac{\boldsymbol{N} - (\boldsymbol{q} + \boldsymbol{n})}{\boldsymbol{n}(\boldsymbol{N} - \boldsymbol{n})} < 0 \qquad \text{(eq 26).}$$

Our estimates for $\boldsymbol{q}$ and $\boldsymbol{n}$ are both much smaller than $\boldsymbol{N}$ (in particular, $\boldsymbol{q} << \boldsymbol{n} << \boldsymbol{N}$), and thus eq 26 could only be fulfilled if one or both of those estimates were in extraordinarily large disagreement with the true values of $\boldsymbol{n}$ and $\boldsymbol{q}$. In section 5.2.v, we show that **10gh** is indeed a major component of the resting state during dearomatization of **1g** with **6h**, and, further, that the proportion of Cu present as **10gh** during dearomatization varies over the course of the reaction in exactly the manner expected if dearomative isomerization and σBM have comparable barriers, as in the approximate energy landscape in Figure SI-28, E.

5. NMR Spectroscopy of Catalyst Species

5.1. Observation of α-phenethylcopper complexes (9a) derived from styrene (6a) in the absence of heterocycle.

5.1.i. Hydrocupration of styrene-α-^{13}C with enantiomerically pure (S,S)-Ph-BPE

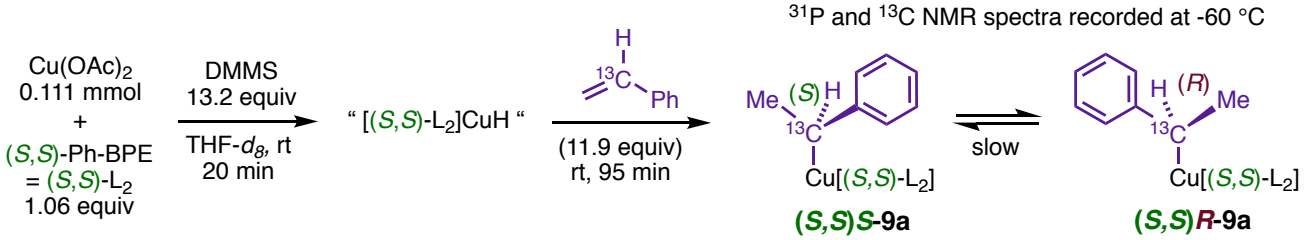

Procedure. Inside a glovebox, an oven-dried one-dram vial was charged with $Cu(OAc)_2$ (20.2 mg, 0.111 mmol) and (*S*,*S*)-Ph-BPE (59.8 mg, 0.118 mmol; 1.06:1 L_2:Cu). The vial was equipped with an oven-dried PTFE stir bar and sealed with a PTFE/silicone septum-cap. The solids were dissolved in THF-d_8 (500 μL), and DMMS (180 μL, 1.46 mmol) was added immediately afterward. The mixture was stirred at rt for 20 min, during which time all $Cu(OAc)_2$ dissolved and the color turned orange.

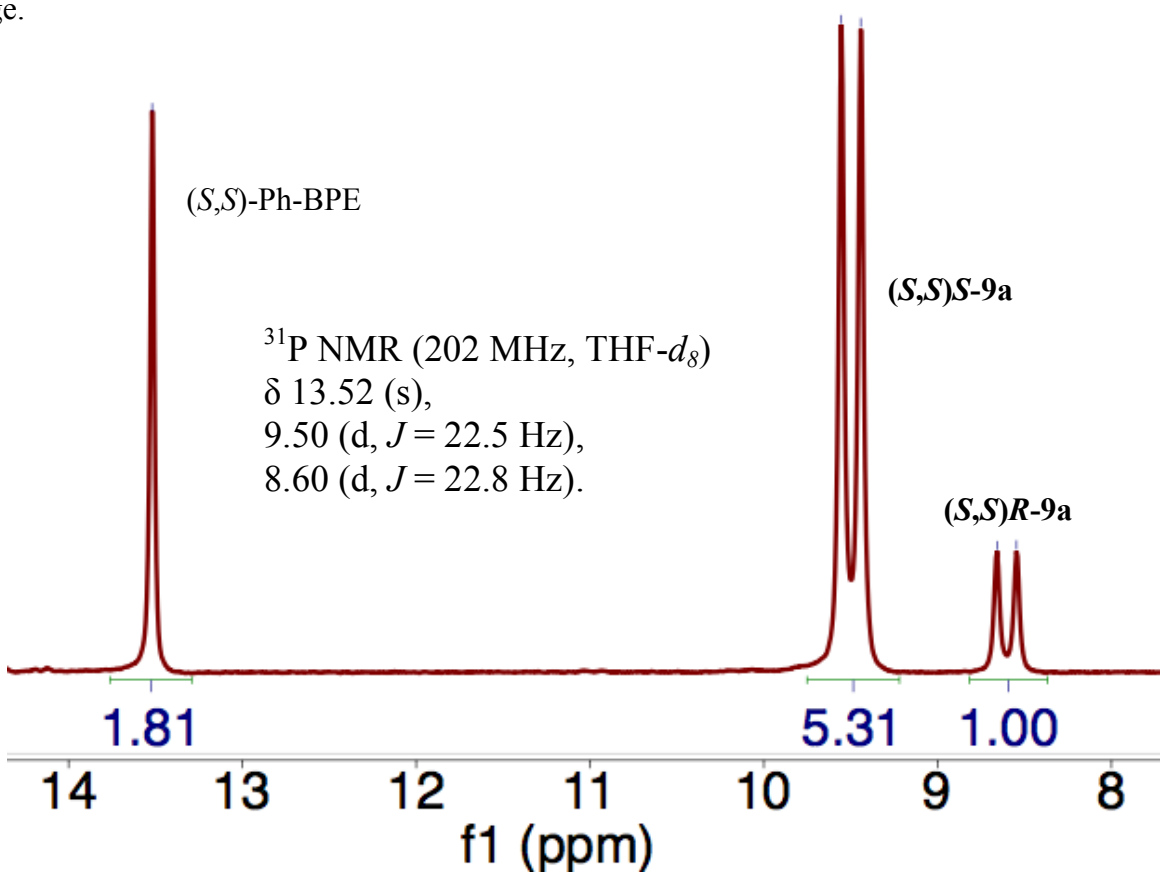

Figure SI-29: Excerpted ^{31}P NMR spectrum of phenethylcopper 9a-α-^{13}C

Styrene-α-^{13}C (150 μL, 1.31 mmol) was added via syringe, and the resulting mixture was transferred to an oven-dried medium-wall J-Young NMR tube using an oven-dried glass pipet. The NMR tube was sealed with a PTFE piston and allowed to stand at rt for ten minutes before being immersed in a slurry of ^{i}PrOH/CO_2. While the mixture was at –78 °C, the probe of a Bruker 501 NMR spectrometer was cooled to –30 °C. Once the probe temperature stabilized, the NMR tube was removed from the cryogen, wiped dry, and injected into the spectrometer. Preliminary ^{31}P NMR analysis indicated that the hydrocupration reaction was incomplete at this time, and the tube was ejected from the spectrometer and aged at rt for a total of 85 minutes while the spectrometer probe was cooled to –60 °C. Proton-decoupled ^{31}P and ^{13}C NMR spectra were then recorded. The ^{31}P NMR resonance of (*S*,*S*)-Ph-BPE appeared as a singlet at 13.5 ppm, whereas the ^{31}P resonances of the major and minor phenethylcopper diastereomers appeared as doublets in a ratio of 5.31:1 at δ 9.50 and 8.60 ppm, respectively, with $^{2}J_{P,C}$ values of 22.5 Hz (major) and 22.8 Hz (minor) (Figure SI-29). Comparing the summed integrals for the phenethylcopper resonances to the total ^{31}P integral indicated that ca. 67% of total phosphorus was present as **(*S*,*S*)*S*-9a** + **(*S*,*S*)*R*-9a**; based on the Ph-BPE:Cu ratio of 1.06:1, this implies that approximately 71% of Cu was present as phenethylcopper. Subsequent hydrocupration experiments (*vide infra*) performed using ^{31}P acquisition parameter sets optimized for quantitative accuracy (i.e., by suppressing NOE enhancements) similarly indicated high conversion to phenethylcopper. The ^{13}C NMR resonances of **(*S*,*S*)*S*-9a** and **(*S*,*S*)*R*-9a** appeared as triplets at δ 33.1 (minor) and 31.3 (major) ppm in a 5.32:1 ratio (virtually the same as the ratio of the ^{31}P doublets). Each triplet had a $^{2}J_{C,P}$ value nearly identical to the doublet coupling of the corresponding ^{31}P signal (22.8 Hz, major; 23.2 Hz, minor) (Figure SI-30).

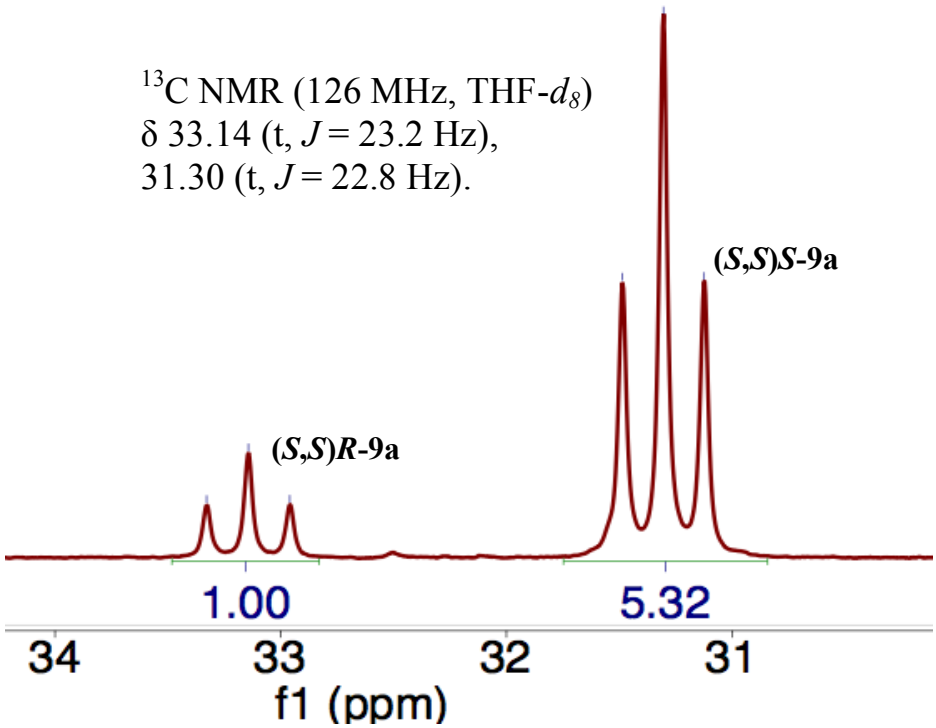

Figure SI-30: Excerpted ^{13}C NMR spectrum of phenethylcopper 9a-α-^{13}C

Based on Hartwig's work (reference 22 in the article), the phenethylcopper is expected to be a monometallic structure having formula L_2CuR. The spectroscopic properties of **9** observed here and in the following experiments are in excellent agreement with that assignment. The spectroscopic properties of **9** are also inconsistent with dimeric or otherwise polynuclear formulations of varying plausibility. The signal pattern and fine structures for **9** are incompatible with formulas such as $L_2Cu(\mu\text{-}R_2)CuL_2$ and $L_2RCuLLCuRL_2$. The % Cu present as **9** after hydrocupration (see, e.g., Section 5.2.iv below) rules out hypothetical polynuclear structures in which an NMR-silent second Cu center is present. Our efforts to identify viable dimers computationally were notably unfruitful; the most stable candidate we found, which corresponds to the conjectural macrocyclic structure **42**, was predicted to be very unfavorable (+10.9 kcal/mol) relative to the monomer. Further, contrary to the speciation we observe here and in sections 5.1.ii and 5.1.iii, a dimer like **42** would exist in three rather than two diastereomeric forms, and that number would increase to five in the presence of racemic ligand, three of which would contain chemically non-equivalent ^{31}P or ^{13}C nuclei.

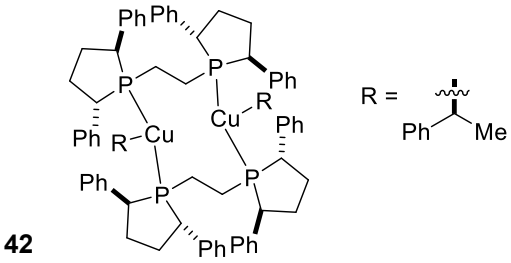

42

5.1.ii. Monitoring epimerization and the effect of temperature on ^{31}P speciation in the hydrocupration of styrene

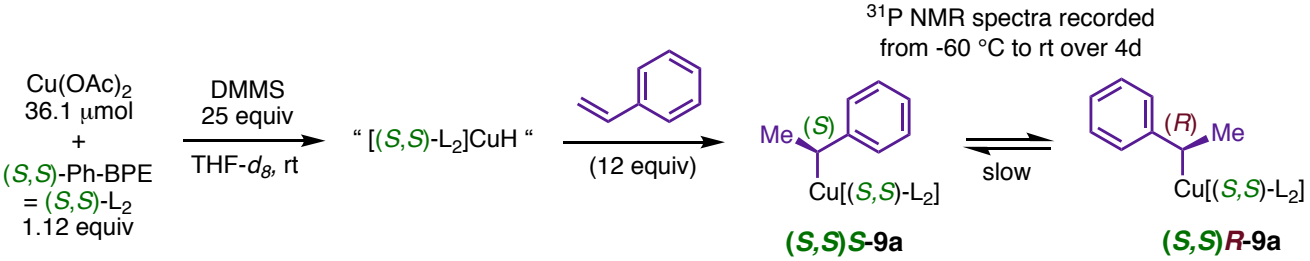

General Note. This and all subsequent spectroscopy experiments, except for that in Section 5.2.v., employed ^{31}P NMR acquisition parameters that had been optimized for quantitative accuracy. In particular, the decoupler pulse occurring before the acquisition pulse in a typical ^{31}P CPD parameter set was removed, suppressing NOE enhancements of the ^{31}P integrals. The spectra were acquired using 11 ppm as the center of the spectral window and employed d1 = 5.0 s, which appeared sufficiently long to minimize integration artifacts due to incomplete relaxation between pulses; acquiring spectra with still longer d1 values did not result in significant changes in integral ratios.

Procedure. Inside a glovebox, an oven-dried one-dram vial was charged with $Cu(OAc)_2$ (6.56 mg, 36.1 μmol) and (*S*,*S*)-Ph-BPE (20.5 mg, 40.5 μmol; 1.12:1 L_2:Cu). The vial was equipped with an oven-dried PTFE stir bar and sealed with a PTFE/silicone septum-cap. The solids were dissolved in

THF-d_8 (380 μL), and DMMS (110 μL, 0.894 mmol) was added immediately afterward. The mixture was stirred at rt for 15 min, during which time all $Cu(OAc)_2$ dissolved and the color turned orange. This activated catalyst solution was rapidly transferred to an oven-dried medium-wall J-Young NMR tube using an oven-dried glass pipet. The NMR tube was sealed with a PTFE piston, removed from the glovebox, and aged at rt for 30 minutes.

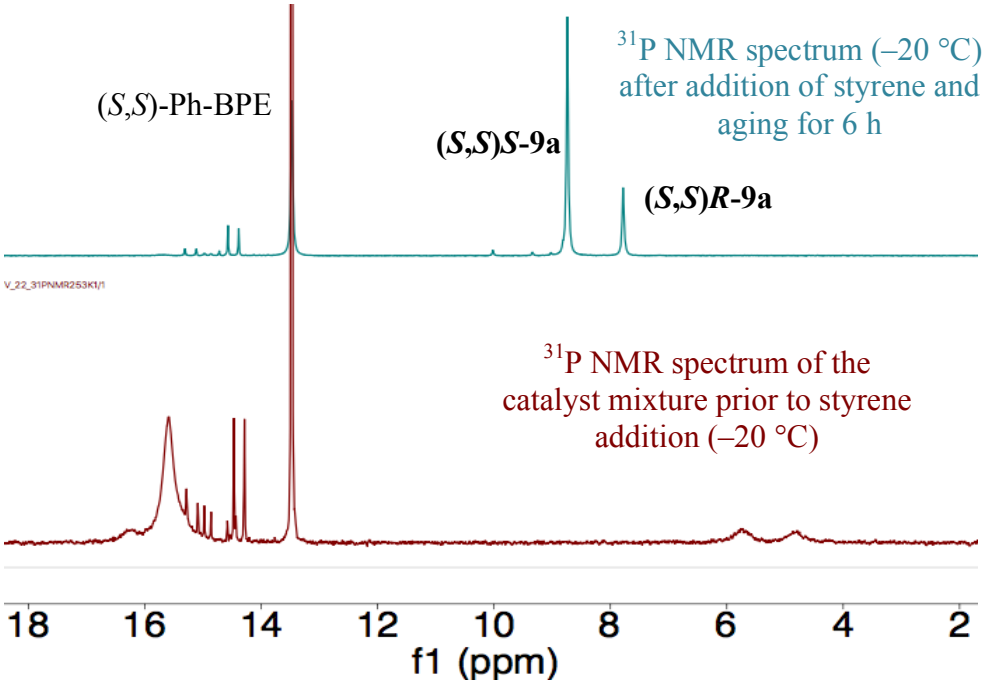

Figure SI-31: ^{31}P NMR spectra before and after addition of styrene.

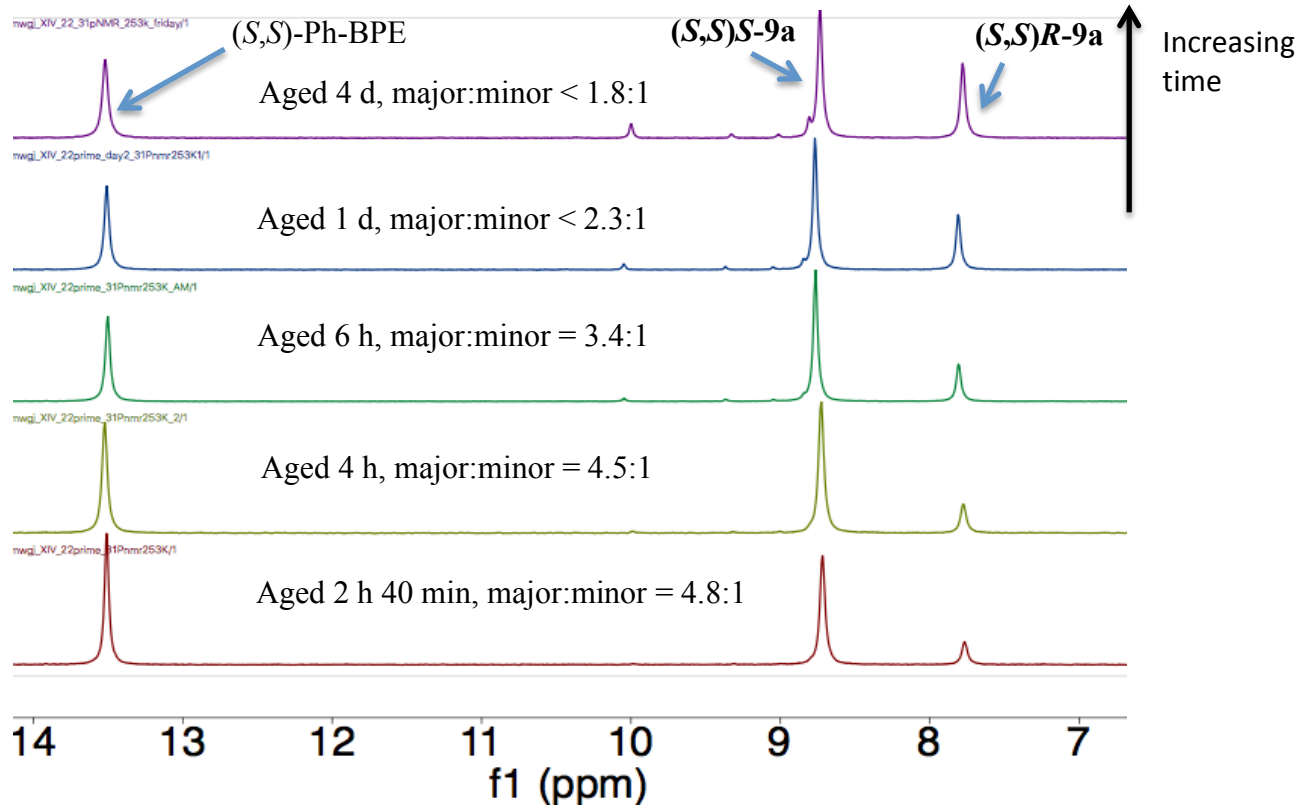

Figure SI-32: Time-lapsed ^{31}P NMR plot showing conversion of (*S*,*S*)*S*-9a into (*S*,*S*)*R*-9a

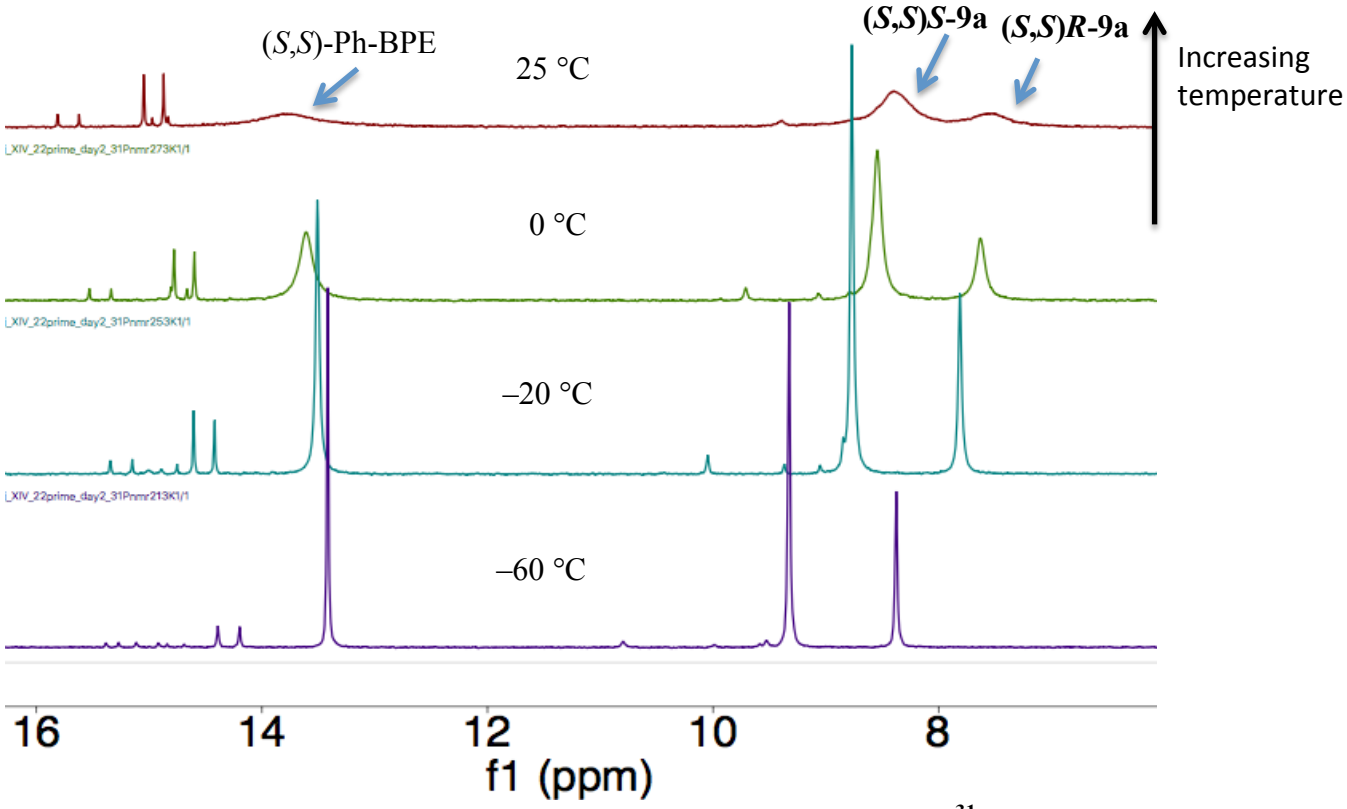

Figure SI-33: Increased T does not alter the distribution of observable ^{31}P-containing species but increases the rate of chemical exchange (broadening of the ^{31}P-signals).

The tube was injected into a Bruker 501 NMR spectrometer, and ^{31}P and ^{1}H NMR spectra were recorded at rt. The probe was cooled to –20 °C, and a second ^{31}P NMR spectrum was recorded. The tube was ejected from the spectrometer, returned to the glovebox, and charged with styrene (50 μL, 0.435 mmol). The tube was resealed and upended several times until the contents were homogenized. The mixture was periodically analyzed over the course of five days by ^{31}P NMR spectroscopy with the probe cooled to –20 °C. Representative ^{31}P NMR spectra before and after the addition of styrene are shown in Figure SI-31. The mixture was maintained at rt on the first day and stored in a 4 °C refrigerator between analyses on subsequent days. The (*S,S*)*S*:(*S,S*)*R* ratio steadily decreased over this period (Figure SI-32), although an equilibrium constant for the epimerization process could not be determined due to simultaneous decomposition and the appearance of interfering signals. On the second day of analyses, a set of ^{31}P spectra were recorded at several temperatures over the span of about an hour (Figure SI-33); this plot shows that the ^{31}P speciation does not change appreciably as the temperature is increased to 25 °C (a typical dearomatization reaction temperature); however, the signals associated with Ph-BPE and the phenethylcoppers broaden markedly due to chemical exchange.

5.1.iii. Hydrocupration of styrene-a-^{13}C with 1:1 (R,R)-Ph-BPE:(S,S)-Ph-BPE. Observation of static phenethylcopper dr and confirmation of chemical exchange by saturation-transfer.

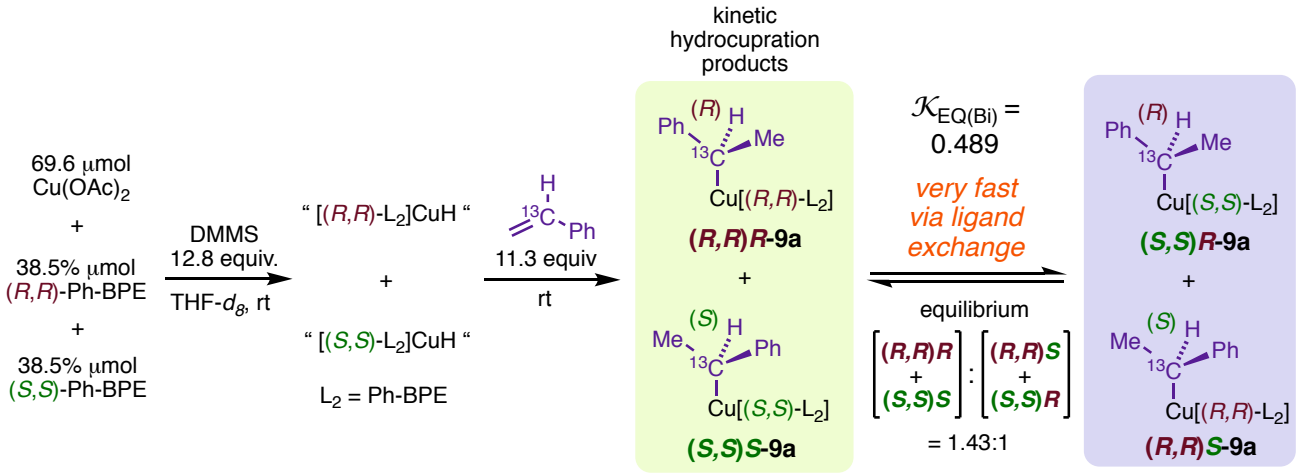

General Note. The fact that the species assigned as **(*S,S*)*S*-9a** is converted into the species assigned as **(*S,S*)*R*-9a** in a reaction that slows over time does not rigorously establish that these are equilibrating diastereomers, although the similarity of their diagnostic NMR resonances does confirm that they are both α-phenethylcoppers. Here we demonstrate that a modification in reaction parameters that is expected to induce rapid attainment of equilibrium between diastereomeric α-phenethylcopper complexes indeed results in rapid attainment of equilibrium between the species assigned as **(*S,S*)*S*-9a** and **(*S,S*)*R*-9a**, further supporting their assignment as a diastereomer pair.

Due to the principle of microscopic reversibility, the expected pathway for unimolecular equilibration of **(*S,S*)*S*-9a** and **(*S,S*)*R*-9a** is β-hydride elimination/reinsertion (Scheme SI-2), and a considerable body of evidence indicates that this process should not be rapid. However, a saturation transfer experiment (*vide infra*) demonstrated that the species assigned as **(*S,S*)*S*-9a** and **(*S,S*)*R*-9a** both exchange bound with free ligand on the NMR timescale at temperatures as low as –30 °C. Scheme SI-3 shows that the sum of two heterochiral ligand-exchange reactions (related to one

another as mirror images) is a rapid diastereomer interconversion reaction that is catalyzed by free racemic ligand. Thus, whereas diastereomer interconversion by changing the configuration at Cα is slow, diastereomer interconversion by changing the configuration of the ancillary ligand should be rapid, and if hydrocupration of styrene is conducted with racemic Ph-BPE, the species assigned as **(*S,S*)*S*-9a** and **(*S,S*)*R*-9a** (and their respective enantiomers) should be formed in their equilibrium ratio relatively early. Figure SI-34 shows that this is the case.

Scheme SI-2: Unimolecular diastereomer interconversion by epimerization of the C*α* stereocenter is slow.

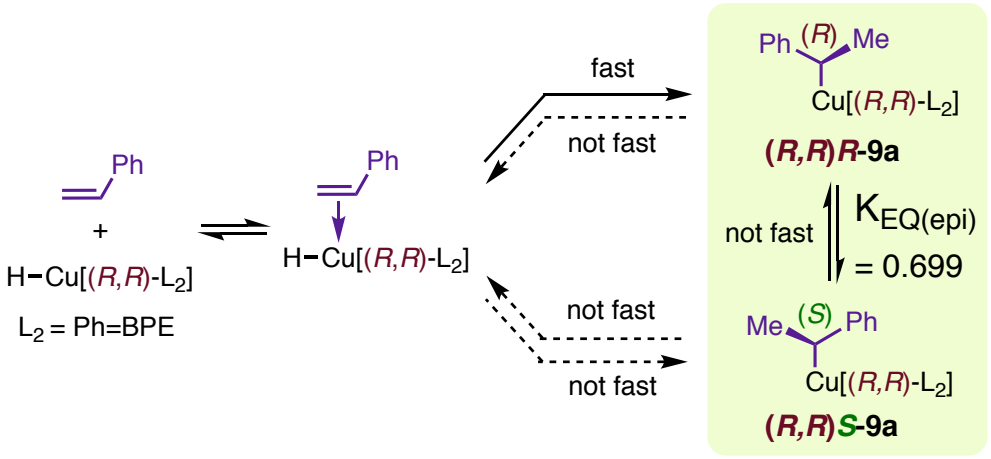

Scheme SI-3: Bimolecular diastereomer interconversion by heterochiral ligand exchange is very fast.

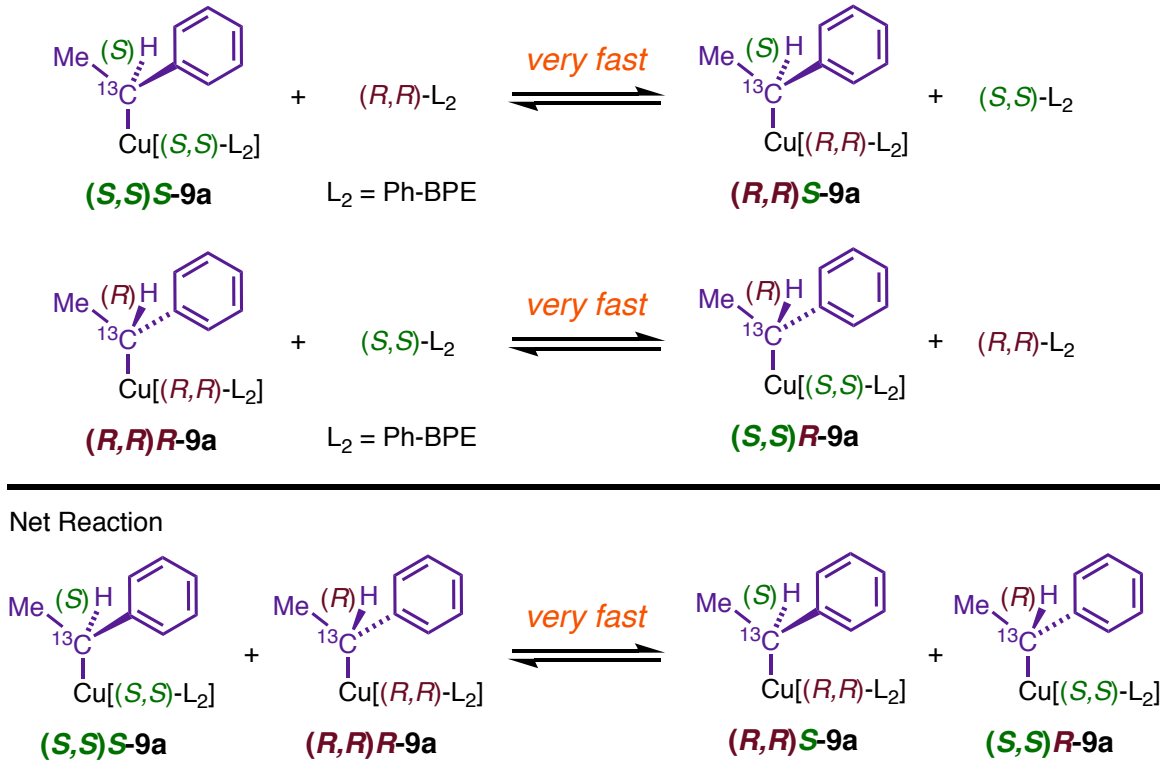

Procedure. Inside a glovebox, an oven-dried one-dram vial was charged with $Cu(OAc)_2$ (12.6 mg, 69.6 μmol), (*S*,*S*)-Ph-BPE (19.5 mg, 38.5 μmol), and (*R*,*R*)-Ph-BPE (19.5 mg, 38.5 μmol; 1.11 L_2:Cu ratio). The vial was equipped with an oven-dried PTFE stir-bar and sealed with a PTFE/silicone septum-cap. The solids were dissolved in THF-d_8 (310 μL), and DMMS (110 μL, 0.894 mmol) was added immediately afterward. The mixture was stirred at rt for 10 min, during which time all $Cu(OAc)_2$ dissolved and the color turned orange. Styrene-α-^{13}C (90 μL, 0.786 mmol) was added via microsyringe, and the resulting mixture was transferred to an oven-dried medium-wall J-Young NMR tube using an oven-dried glass pipet. The mixture was aged at rt for 90 min and then frozen in liquid N_2 pending analysis. Phosphorus-31 NMR spectra were periodically recorded at –30 °C over three days, maintaining the tube in a 4 °C refrigerator between analyses. The plot in Figure SI-34 shows that the initial dr of 1.42:1 was unchanged in subsequent spectra, indicating that diastereomeric equilibrium had been attained by the time of the first analysis. After six days, the tube was transferred to a –35 °C glovebox freezer pending a saturation-transfer ^{31}P NMR experiment conducted in a probe cooled to –30 °C 10 days after the sample was first prepared. In this experiment (Figure SI-35), saturation of the Ph-BPE resonance (accomplished by applying a 2s-long 0.5 mW saturation pulse at 13.50 ppm in channel f3 between the relaxation delay and acquisition pulse) markedly suppressed the resonances of the major and minor phenethylcoppers, which confirms that the hydrocupration products are in chemical exchange with free ligand (and one another) on the NMR timescale.

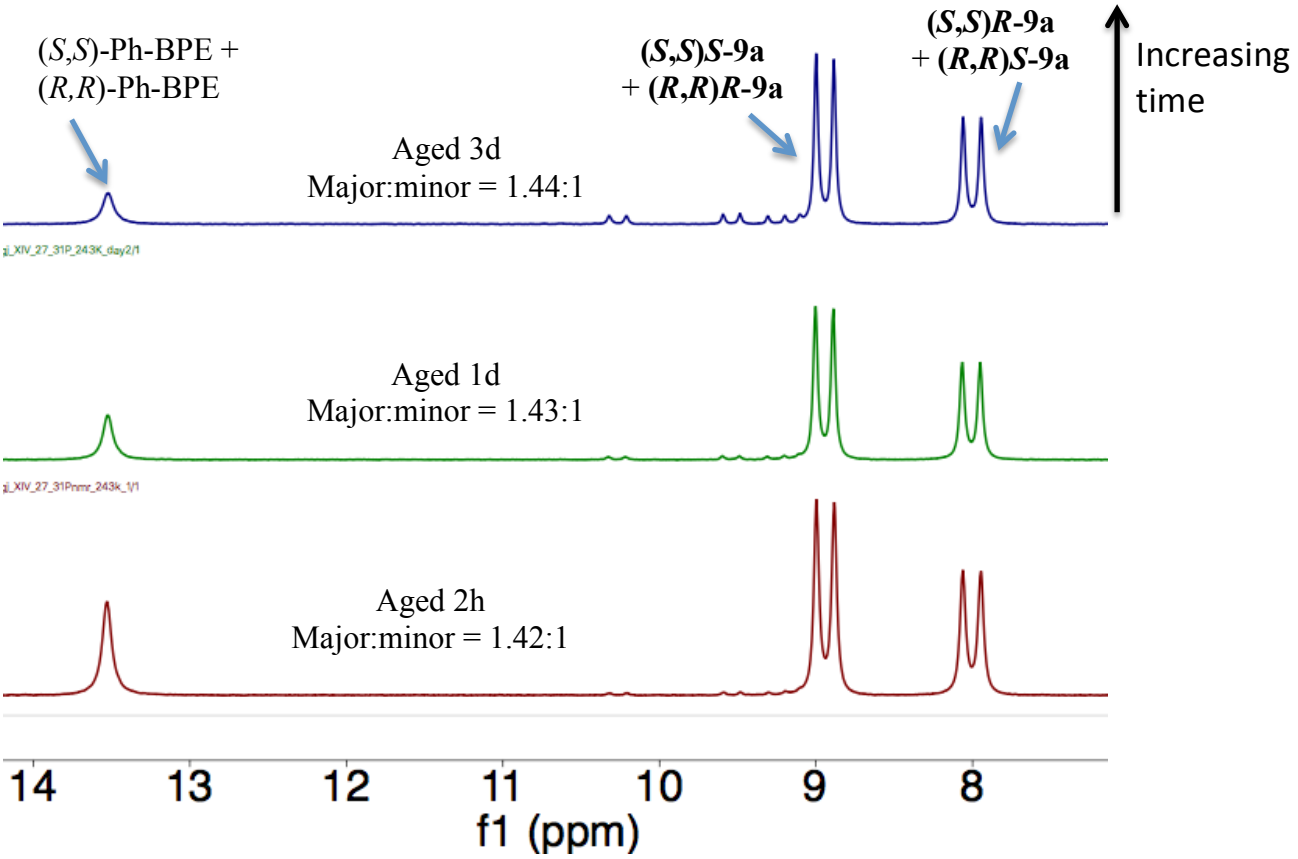

Figure SI-34: The phenethylcopper dr is invariant with time in the presence of racemic Ph-BPE.

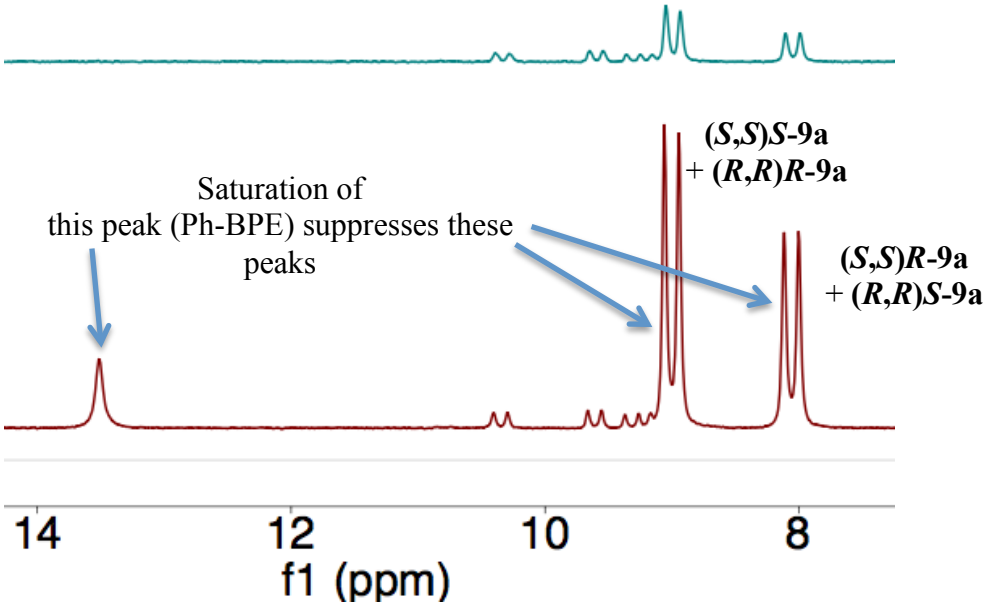

Figure SI-35: Observation of saturation transfer from Ph-BPE to both diastereomers of the phenethylcopper.

The equilibrium constant for the heterochiral ligand exchange pathway in the presence of racemic Ph-BPE is trivially calculated from the equilibrium dr of 1.43:1, thus:

$$\mathcal{K}_{EQ(Bi)} = \frac{[(R,R)S][(S,S)R]}{[(R,R)R][(S,S)S]} = \frac{[(R,R)S]^2}{[(R,R)R]^2} = (0.699)^2 = 0.489 \qquad \text{(eq 27)}.$$

This result also enables calculation of the equilibrium constant for unimolecular interconversion of ***(R,R)R*-9a** with ***(R,R)S*-9a** via epimerization.

It is clear that the free energy change for the heterochiral ligand exchange is

$$\Delta G_{Bi}{}^{o} = \Delta G_{(R,R)S}{}^{o} + \Delta G_{(S,S)R}{}^{o} - \Delta G_{(R,R)R}{}^{o} - \Delta G_{(S,S)S}{}^{o} \qquad \text{(eq 28)}.$$

But because enantiomeric compounds are isoenergetic, this becomes:

$$\Delta G_{Bi}{}^{o} = 2\Delta G_{(R,R)S}{}^{o} - 2\Delta G_{(R,R)R}{}^{o} = 2\Delta G_{epi}{}^{o} \qquad \text{(eq 29)},$$

where $\Delta G_{epi}{}^{o}$ is the free energy change associated with the unimolecular equilibration pathway. Consequently

$$-RTln\left(K_{EQ(epi)}\right) = -\left(\frac{RT}{2}\right) ln\left(K_{EQ(bi)}\right) \qquad \text{(eq 30)},$$

which implies that

$$K_{EQ(epi)} = \left(K_{EQ(bi)}\right)^{\frac{1}{2}} = 0.699 \qquad \text{(eq 31).}$$

If the ligand ee is between 0 and 100, the steady-state phenethylcopper dr will differ from 1.43:1 when dearomative catalysis occurs under conditions that continuously regenerate **(*R,R*)*R*-9a** and **(*S,S*)*S*-9a** with high kinetic selectivity in the hydrocupration step. The approximate steady-state ratio can be predicted by considering the idealized case of heterochiral ligand exchange occurring in a population of **(*R,R*)*R*-9a** and **(*S,S*)*S*-9a** diastereomers that have been generated with perfect kinetic selectivity, i.e., with (*R,R*)*R*:(*S,S*)*S* = ϕ:(1 – ϕ), where ϕ is the mol fraction of Ph-BPE supplied as the (*R,R*) enantiomer, and with **(*R,R*)*S*-9a** and **(*S,S*)*R*-9a** being initially absent. Because heterochiral ligand exchange converts **(*R,R*)*R*-9a** and **(*S,S*)*S*-9a** into **(*R,R*)*S*-9a** and **(*S,S*)*R*-9a** with 1:1 stoichiometry, one can frame the equilibration process thus:

	Major		minor	
	(*R,R*)*R*-9a	(*S,S*)*S*-9a	(*R,R*)*S*-9a	(*S,S*)*R*-9a
Initial	ϕ	$(1-\phi)$	0	0
Change	$-\psi$	$-\psi$	$+\psi$	$+\psi$
Equilibrium	$(\phi-\psi)$	$(1-\phi-\psi)$	$+\psi$	$+\psi$

Consequently

$$\mathcal{K}_{EQ(Bi)} = \frac{\psi^2}{(\phi-\psi)(1-\phi-\psi)} \qquad \text{(eq 32),}$$

and, upon rearrangement, one obtains

$$\left(1-\frac{1}{\mathcal{K}_{EQ(Bi)}}\right)\psi^2 - \psi = \phi^2 - \phi \qquad \text{(eq 33),}$$

where 2ψ is the steady-state mol fraction of phenethylcopper present as the minor diastereomer.

In section 5.2.ii. below, we take advantage of the ability to generate dearomatization reaction mixtures having different phenethylcopper diastereomeric compositions to show that both diastereomers of the phenethylcopper undergo dearomative addition, and to compare their selectivity properties in that step.

5.2. Observation of catalyst species present during catalytic dearomatization reactions.

5.2.i. In situ observation of the catalyst resting state during dearomatization of 3-phenylpyridine (1d) with styrene (6a) and quantitation of the phenethylcopper dr as a function of heterocycle conversion.

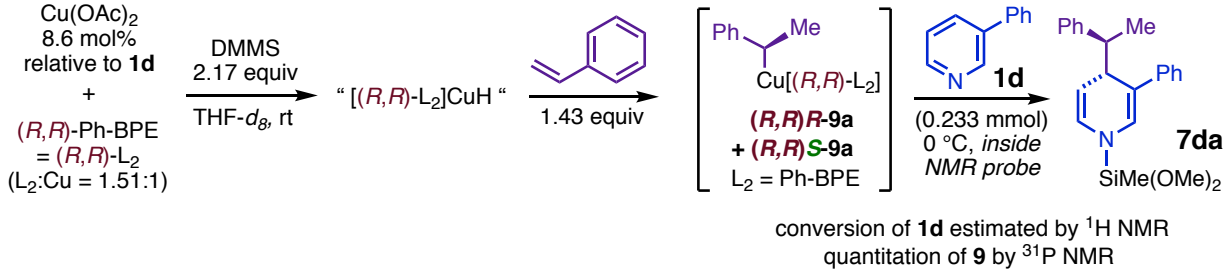

conversion of **1d** estimated by ^{1}H NMR
quantitation of **9** by ^{31}P NMR

Procedure. Inside a glovebox, an oven-dried calorimeter vial was charged with $Cu(OAc)_2$ (40.85 mg, 0.2249 mmol) and (*R*,*R*)-Ph-BPE (171.8 mg, 0.3391 mmol, 1.51 L_2:Cu ratio). The vial was equipped with an oven-dried PTFE stir-bar and sealed with a PTFE-silicone septum-cap. The solids were dissolved with 1.66 mL THF-d_8, and DMMS (700 μL, 5.69 mmol) was added immediately afterward. The resulting mixture was stirred at rt for 10 min, during which time the solids dissolved and the color turned yellow. The mixture was charged with styrene (430 μL, 3.74 mmol) and stirred at rt for 5 h before being further diluted with 1.50 mL THF-d_8. A 400 μL aliquot of this phenethylcopper stock solution was transferred to an oven-dried medium-wall J-Young NMR tube using an oven-dried glass microsyringe. The NMR tube was sealed with a PTFE piston, removed from the glovebox, and maintained in an ice-water bath in a darkened fumehood for 2 h. It was estimated that this aliquot of the phenethylcopper stock solution contained 3.63 mg $Cu(OAc)_2$ (20.0 μmol, 8.6 mol% relative to **1d**), 15.3 mg (*R*,*R*)-Ph-BPE (30.1 μmol), 0.506 mmol DMMS (2.17 equiv relative to **1d**), and 0.332 mmol styrene (1.43 equiv relative to **1d**).

A stock solution of the heterocycle was prepared from 3-phenylpyridine (310.4 mg, 2.00 mmol) and 720 μL THF-d_8 inside the glovebox. A 225 μL aliquot of this solution was withdrawn using an oven-dried glass microsyringe and injected by into an oven-dried one-dram glass vial containing 15.1 mg 1,3,5-trimethoxybenzene (TMB, the NMR internal standard). The NMR tube was returned to the glovebox and charged with a 125 μL aliquot of the solution containing **1d** + TMB, sealed, removed from the glovebox, and frozen in liquid N_2 pending NMR analyses. It was estimated that 0.233 mmol of **1d** had been delivered to the reaction mixture, giving $[Het]_0$ = 0.44 M.

The probe of a Bruker 501 NMR spectrometer was cooled to –20 °C, and the reaction mixture was thawed and injected into the spectrometer. Phosphorus-31 (32 scans, Figure SI-36) and proton (6 scans, d1 = 24s, Figure SI-37) NMR spectra were recorded, and the probe temperature was increased to 273 K, whereupon the dearomatization reaction began to occur at an appreciable rate. Proton (6 scans, d1 = 24s) and phosphorus-31 NMR spectra (96–128 scans) were then recorded alternately over the course of 8 h. The conversion of **1d** at a given timepoint was estimated from the ^{1}H NMR spectrum. Because the dearomatization is very clean and high-yielding, estimates based on comparison of the integrals of **1d** to those of the internal standard were very similar to estimates

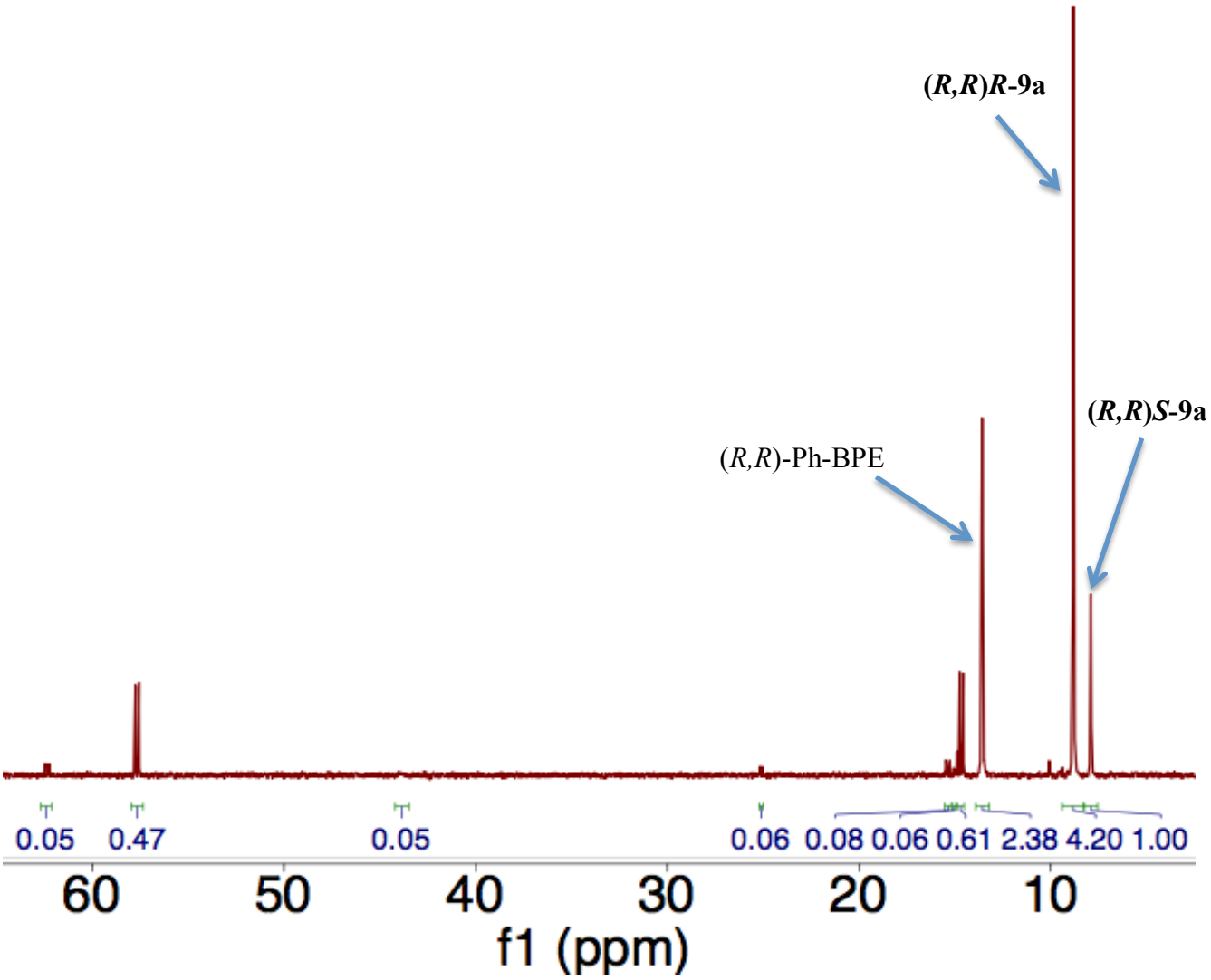

Figure SI-36: Complete ^{31}P NMR spectrum of dearomatization reaction mixtures at ca. 4% conversion of 1d (20 °C).

based on comparison of the integrals of **1d** to those of the product, **7dh**. Estimates of the latter type are employed in this and subsequent studies involving dearomatizations of 3-aryl-pyridines. The extent of conversion of **1d** corresponding to a given ^{31}P NMR timepoint was estimated as the midpoint between the conversion values determined for the immediately preceding and succeeding ^{1}H NMR spectra. For each ^{31}P NMR analysis, the dr of **9a** was estimated as the ratio of the integrals for the major and minor diastereomers. The fraction of Cu present as ***(R,R)R*-9a** + ***(R,R)S*-9a** was estimated from the fraction of the total ^{31}P integral made up by the integrals of ***(R,R)R*-9a** + ***(R,R)S*-9a**. Figure SI-37 provides a time-lapsed plot of representative ^{1}H NMR spectra collected during the reaction with diagnostic resonances for **1d** and **7da** indicated. Figure SI-38 provides a time-lapsed plot of excerpted ^{31}P NMR spectra showing the resonances of Ph-BPE and ***(R,R)R*-9a** + ***(R,R)S*-9a**. The estimated proportion of Cu present as **9a** is plotted in Figure SI-39, i, as a function of the reaction progress. The fact that the proportion of Cu present as **9a** is high and virtually unchanged during the reaction indicates that it is the MACS.

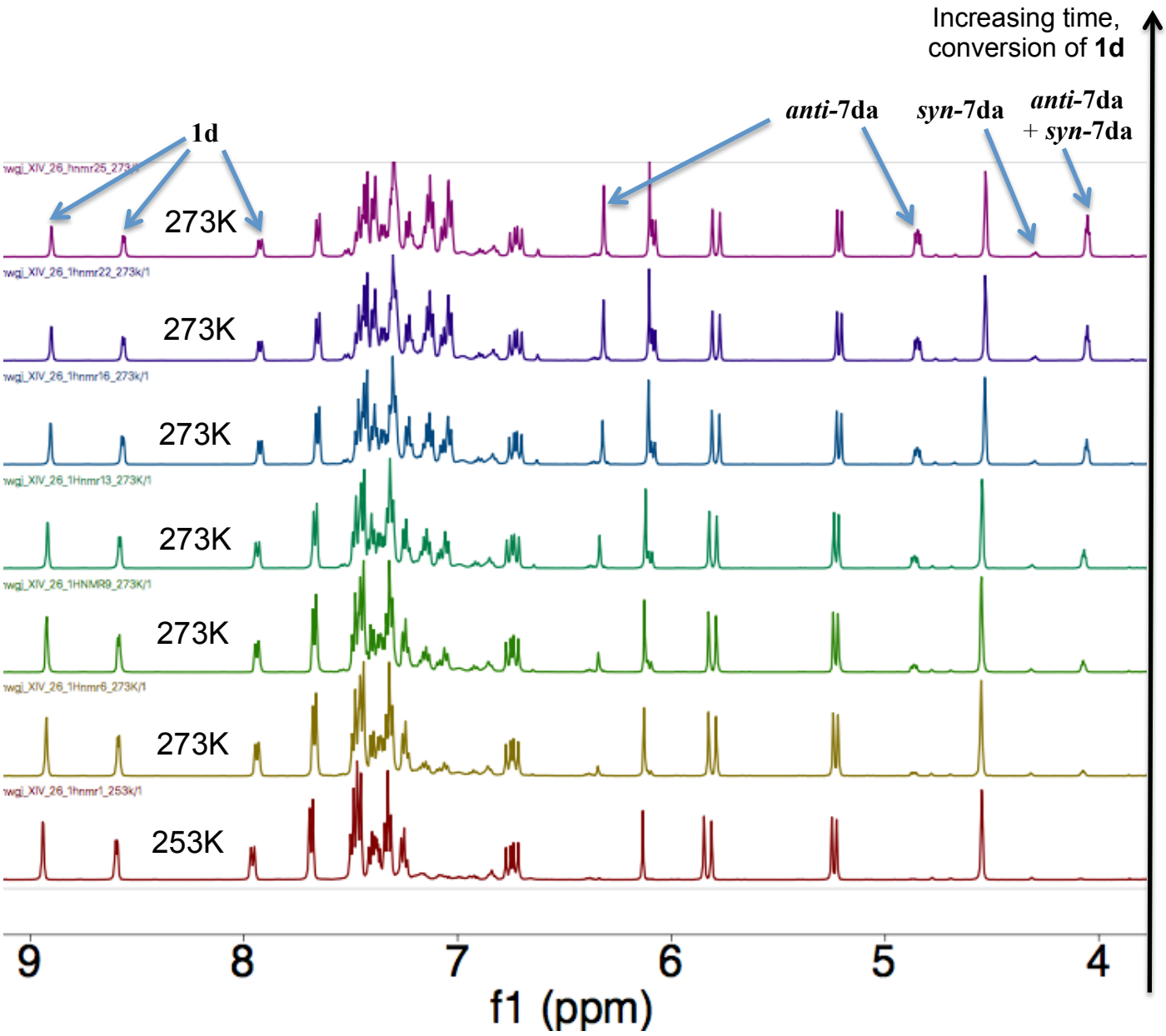

Figure SI-37: Time-lapsed plot of representative ^{1}H NMR spectra from dearomatization of 1d with 6a.

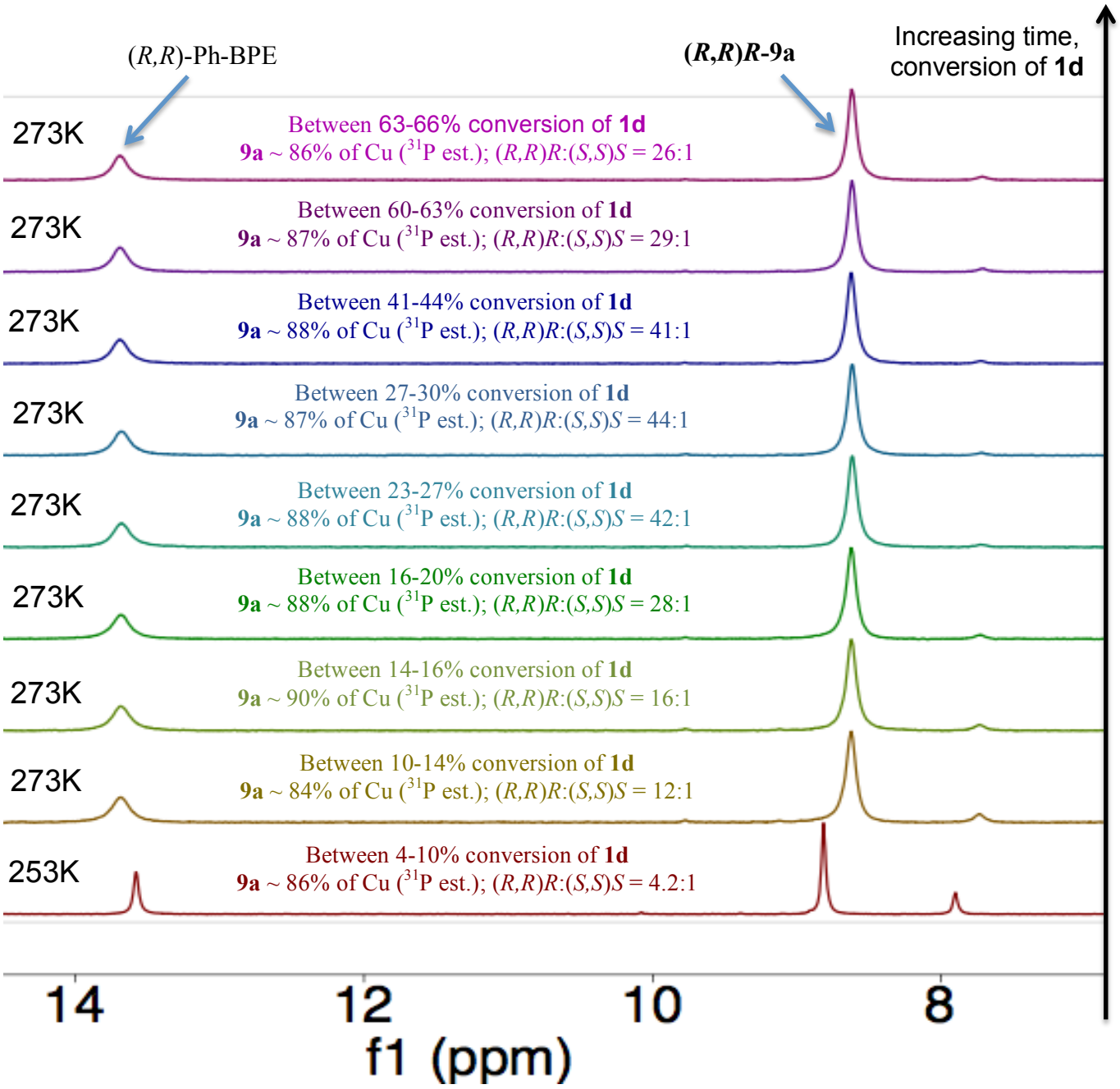

Figure SI-38: Time-lapsed plot of representative ^{31}P NMR spectra from dearomatization of 1d with 6a.

The phenethylcopper dr is plotted as a function of heterocycle conversion in Figure SI-39, ii. The dr of the phenethylcopper present at the outset of catalysis is low (ca. 4:1 (*R,R*)*R*:(*R,R*)*S*) due to extended aging of the catalyst in the absence of heterocycle: during this period (represented by the leftmost box in Scheme SI-4) the mixture progresses toward diastereomeric equilibrium via the slow β-hydride-elimination/reinsertion pathway. Over the first ca. 30% conversion of the

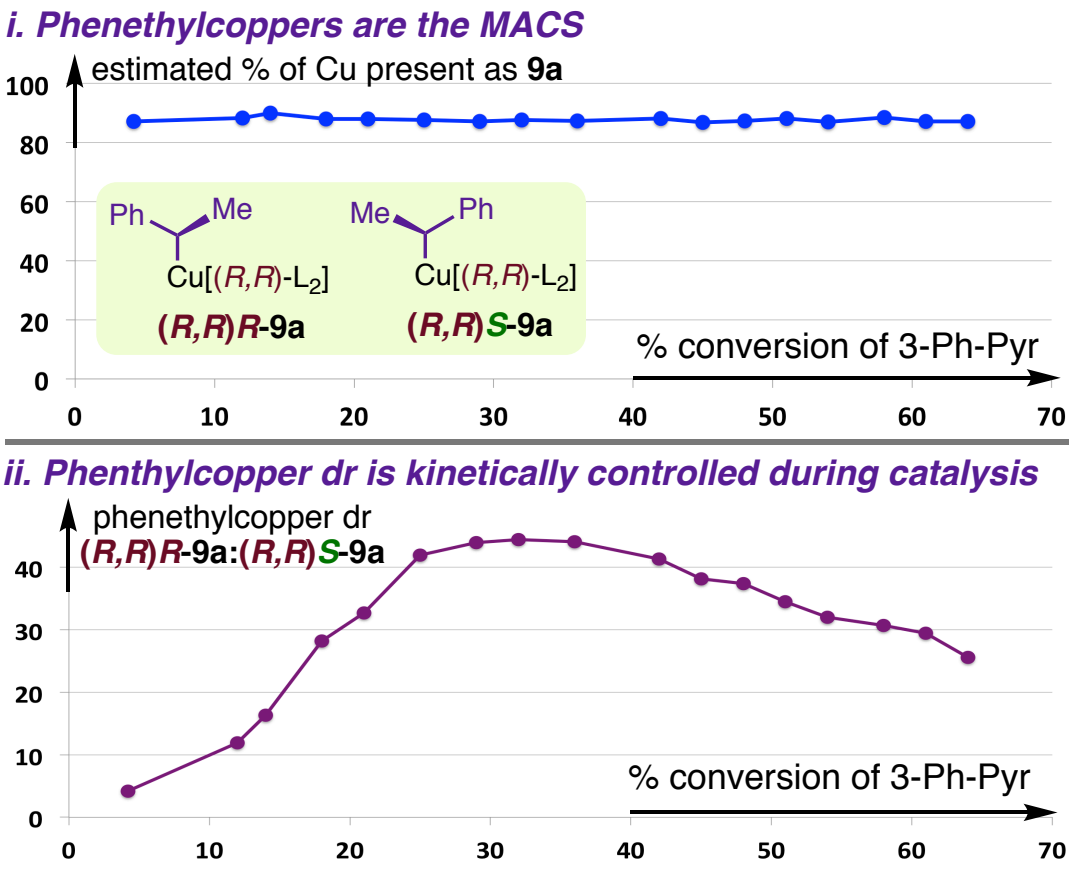

Figure SI-39: Composition of the catalyst resting state during dearomatization of 1d with 6a using ^{31}P-NMR-based estimates.

heterocycle, the phenethylcopper dr increases to a maximum of 45:1 before gradually declining again at higher conversion values. Since the initial increase constitutes a drastic shift away from the direction of equilibrium, it is clear that the phenethylcopper dr is kinetically controlled during catalysis. Scheme SI-4 illustrates the mechanistic basis for this phenomenon. All of the phenethylcopper present when the heterocycle is added is consumed by the dearomative addition step. The experiments in Section 5.2.ii. show that this is because **(*R,R*)*R*-9a** and **(*R,R*)*S*-9a** both directly react with **1d**. Turnover starting from either **(*R,R*)*R*-9a** or **(*R,R*)*S*-9a** regenerates stereochemically pure [(*R,R*)-Ph-BPE]CuH, which has a strong kinetic bias for hydrocupration to give **(*R,R*)*R*-9a**. When the heterocycle concentration is relatively high, recycling of the regenerated **(*R,R*)*R*-9a** via subsequent catalytic turnovers is evidently faster than epimerization via β-hydride-elimination/reinsertion, resulting in spontaneous diastereoconvergence in the population of **9a** and maintenance of a high (*R,R*)*R*:(*R,R*)*S* ratio throughout much of the reaction. Whereas epimerization of **9a** is a first-order approach to equilibrium, it is evident that the dearomative step that consumes

(*R,R*)*R*-9a has higher molecularity, and our kinetics experiments have independently shown that this is due to kinetic dependence on [**1d**] in particular. As conversion increases, the concentration of **1d** decreases, and the bimolecular step that is responsible for ultimate recycling of **9a** slows accordingly, whereas the rate of epimerization of recycled **9a** is unaffected by changes in [**1d**]. Consequently, the extent of epimerization evident in the resting state increases as the reaction approaches completion. This can be understood in probabilistic terms: the likelihood that a given molecule of **(*R,R*)*R*-9a** will undergo epimerization before being recycled increases as the average lifetime of **9a** increases, leading to an increasingly large proportion of **(*R,R*)*S*-9a** in the resting state. Intuitively, the catalytic dearomatization can be viewed as interrupting the phenethylcopper's approach to equilibrium to an extent that directly depends on the rate at which the dearomatization is occurring.

Scheme SI-4: Mechanistic basis for kinetic control of phenethylcopper dr during dearomatization with 100% (*R,R*)-Ph-BPE

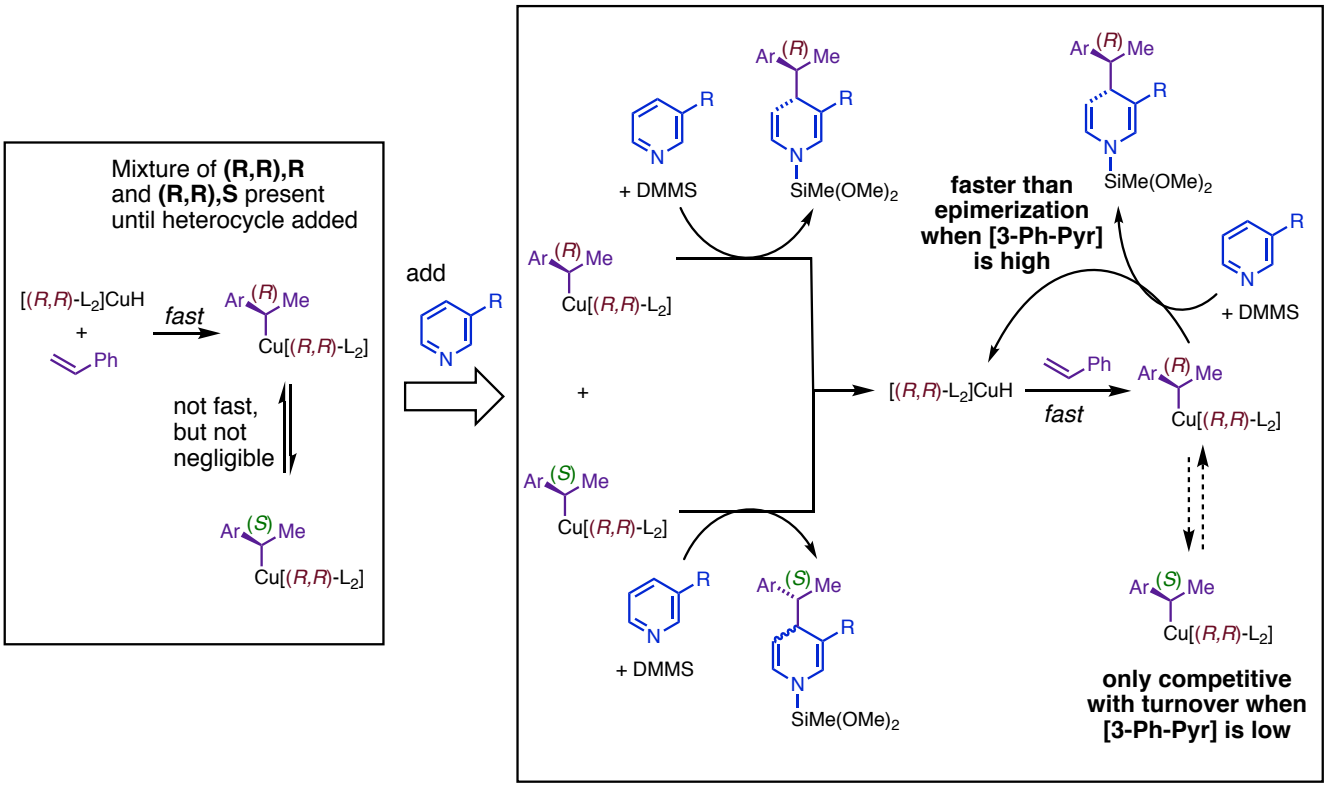

Mechanistic ramifications of the resting state stereochemical dynamics enabled us to demonstrate that the invertive nucleophilic approach trajectory that operates in Cu-catalyzed phenethylation of imines and the 1,4-dearomatization of pyridinium by phenethylboronates is not operative in the dearomatization (Scheme SI-5), disproving an early bimetallic transition state model we formulated by analogy to those reactions (see article text). Given that the major phenethylcopper and the major enantiomer of **7** have the same configuration at C*α*, the latter could only be formed by invertive approach if the phenethylcopper diastereomers equilibrate and the dearomative addition favors invertive reaction of the minor diastereomer, **(*R,R*)*S*-9a**. However, we find that the majority of 1,4-DHP generated in Cu-catalyzed dearomatization is formed by direct reaction of the major phenethylcopper, implying that the dearomative addition step is itself stereoretentive (Scheme SI-5). First, in the following pair of experiments, we show that both diastereomers of **9a** undergo

dearomative addition to **1d**, but only ***(R,R)R*-9a** exhibits a high preference for generating the *anti*-1,4-DHP **7da**. Because the catalytic dearomatization also exhibits high *anti*-selectivity under typical conditions, this provides further evidence that reaction via the minor phenethylcopper is not normally the predominant contributor to product formation.

Scheme SI-5: Enantiodetermination in the catalytic dearomatization.

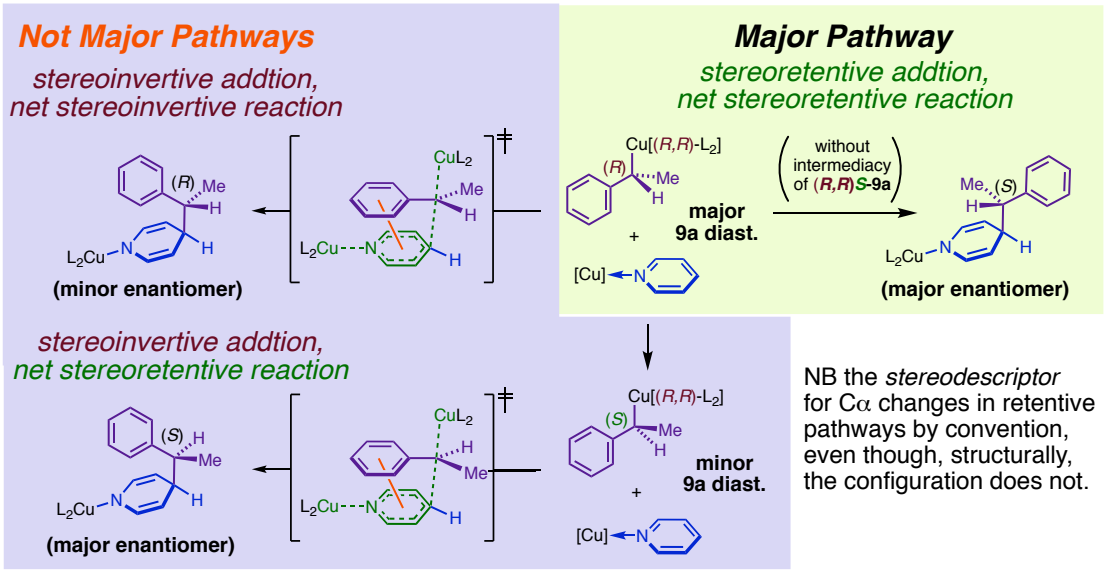

5.2.ii. Correlation of the dr of 1,4-DHP 7da with the dr of phenethylcopper 9a

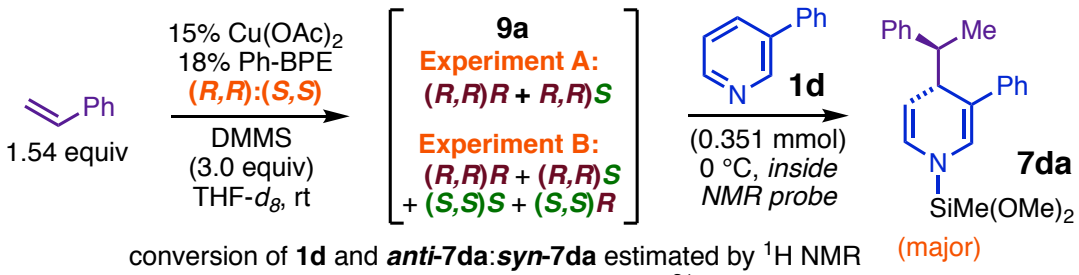

conversion of **1d** and ***anti*-7da**:***syn*-7da** estimated by ^{1}H NMR
quantitation of ***(R,R)R*-9a**:***(R,R)S*-9a** by ^{31}P NMR

Experiment	er of Ph-BPE	phenethylcopper (9a) dr	(*anti*:*syn*) of 7da
A	100:0	dynamic but very high **(16:1 - 42:1)** throughout most of reaction	**9.1:1**
B	70:30	constant at **1.80:1** (avg. of 8)	**3.7:1**

General Note. This experiment involves two dearomatization reactions that were identical except for the enantiomeric composition of the Ph-BPE. **Experiment A** uses enantiomerically pure (*R,R*)-Ph-BPE, and the catalyst resting state during dearomatization exhibited the same fluctuation that we observed in Section 5.2.i. Throughout most of the reaction (20%–85% conversion of **1d**), the minor diastereomer was a trace resting state component. **Experiment B** used 7.0:3.0 (*R,R*):(*S,S*)-Ph-BPE and gave a resting state with low steady-state dr for the reasons described in Section 5.1.iii.:

interconversion of phenethylcopper diastereomers via ligand exchange is much faster than dearomatization at all concentrations of **1d**. The observed phenethylcopper dr was constant at 1.80:1 **[(*R,R*)*R*-9a + (*S,S*)*S*-9a]**:**[(*R,R*)*S*-9a + (*S,S*)*R*-9a]** (average) throughout the reaction, in agreement with the mechanistic model in 5.3.iii. Using $\mathcal{K}_{EQ} = 0.489$ and setting $\phi = 0.7$ in eq 31 yields the quadratic equation

$$1.045\psi^2 + \psi - 0.21 = 0 \qquad \text{(eq 32).}$$

Solving this equation leads to a predicted equilibrium dr of 1.84:1.

Procedure. Inside a glovebox, two oven-dried glass one-dram vials were charged with $Cu(OAc)_2$ (10.7 mg, 58.9 μmol). One of the vials (used in **Experiment A**) was charged with (*R,R*)-Ph-PBE (35.9 mg, 70.9 μmol; L_2:Cu = 1.20), while the other (used in **Experiment B**) received a mixture of (*R,R*)- and (*S,S*)-Ph-BPE in a 7.0:3.0 ratio (36.0 mg total, 71.0 μmol; L_2:Cu = 1.21:1). Each vial was equipped with a small oven-dried PTFE stir-bar, sealed with a PTFE/silicone septum-cap, and charged with THF-d_8 (190 μL). DMMS (145 μL, 125 mg, 1.18 mmol) was added to each mixture immediately afterward. The resulting mixtures were stirred at rt for 15 min, during which time all $Cu(OAc)_2$ dissolved and the color turned orange. Each mixture was charged with styrene (**6a**, 70.0 μL, 63.4 mg, 0.609 mmol) using an over-dried glass microsyringe and aged at rt for 2h. At this point, a 400 μL aliquot of the phenethylcopper solution for **Experiment A** was transferred to one oven-dried medium-wall J-Young NMR tube, and a 400 μL aliquot of the phenethylcopper solution for **Experiment B** was transferred to another. Both tubes were charged with 125 μL of a stock solution prepared from 3-phenylpyridine (217.5 mg, 1.40 mml) and 300 μL THF-d_8. Upon addition of the heterocycle, each tube was sealed with PTFE piston, upended several times to ensure homogeneity, removed from the glovebox, and frozen in liquid N_2 pending analysis. The probe of a Bruker 500 NMR spectrometer was stabilized at –30°C, and the reaction mixture used in **Experiment A** was removed from cryogen, briefly thawed at rt, and injected into the spectrometer. Proton and ^{31}P NMR spectra were recorded to afford an estimate of the (*R,R*)*R*:(*R,R*)*S* ratio near the start of the reaction (ca. 4% conversion of **1d**), and then the probe was warmed to 0 °C. Proton and ^{31}P NMR spectra were then recorded alternately over the course of 5 h, by which time the conversion of **1d** was found to be 81%. The reaction mixture used in **Experiment B** was subsequently thawed and analyzed in the same fashion. For each reaction mixture, the approximate fraction of total copper present as the *major* phenethylcopper **(*R,R*)*R*-9a** in **Experiment A** and {**(*R,R*)*R*-9a** + **(*S,S*)*S*-9a**} was calculated for each ^{31}P NMR time-point in the manner described in Sections 5.1.i and 5.2.i. These data are plotted as a function of the approximate conversion of **1d** at the time the spectrum was recorded, which was taken to be the midpoint between the conversions evident from the ^{1}H NMR spectra recorded immediately prior to and immediately after the ^{31}P NMR time-point in question.

The two reaction mixtures exhibited comparable, but not identical, approximate proportions of total Cu present as **9a** (Figure SI-40). However, despite exhibiting a resting state with a much lower dr (Figure SI-41) than that in **Experiment A** – and thus having an accordingly much lower fraction of total copper present as the major diastereomer (Figure SI-42) – the reaction mixture in **Experiment B** (7:3 (*R,R*):(*S,S*)-Ph-BPE) gave a rate of catalytic dearomatization comparable to that obtained with **Experiment A** (Figure SI-43). This implies that reaction via the minor diastereomer (present as **(*R,R*)S-9a** + **(*S*,S)*R*-9a** in **Experiment B**) is a major contributor to the total rate of reaction in **Experiment B**. However, the dr of product **7a** (determined at ca. 75% conversion) generated in **Experiment B** was substantially lower {3:7:1 (***anti*-7da**):(***syn*-7da**)} than when the minor

phenethylcopper was a trace component of the resting state {9.1:1 (***anti*-7da**):(***syn*-7da**) in **Experiment A**}. This demonstrates that, unlike **(*R,R*)*R*-9a**, **(*R,R*)*S*-9a** undergoes dearomatization with very poor *anti*-selectivity. The altered diastereoselectivity for dearomatization via the minor phenethylcopper has been present for every heterocycle substrate we have investigated, and in several cases the differences are extreme. For example, pyridazine undergoes dearomatization with dr > 28:1 in the presence of 100% (*R,R*)-Ph-BPE yet gives a dr close to 1:1 when dearomatization is conducted with 1:1 (*R,R*):(*S,S*)-Ph-BPE. It is plausible in such cases that **(*R,R*)*S*-9a** is actually selective for ***syn*-7**. The fact that the relative configuration of the catalyst can profoundly affect the diastereoselectivity of the addition step indicates that substrate-controlled interactions cannot account for diastereodetermination.

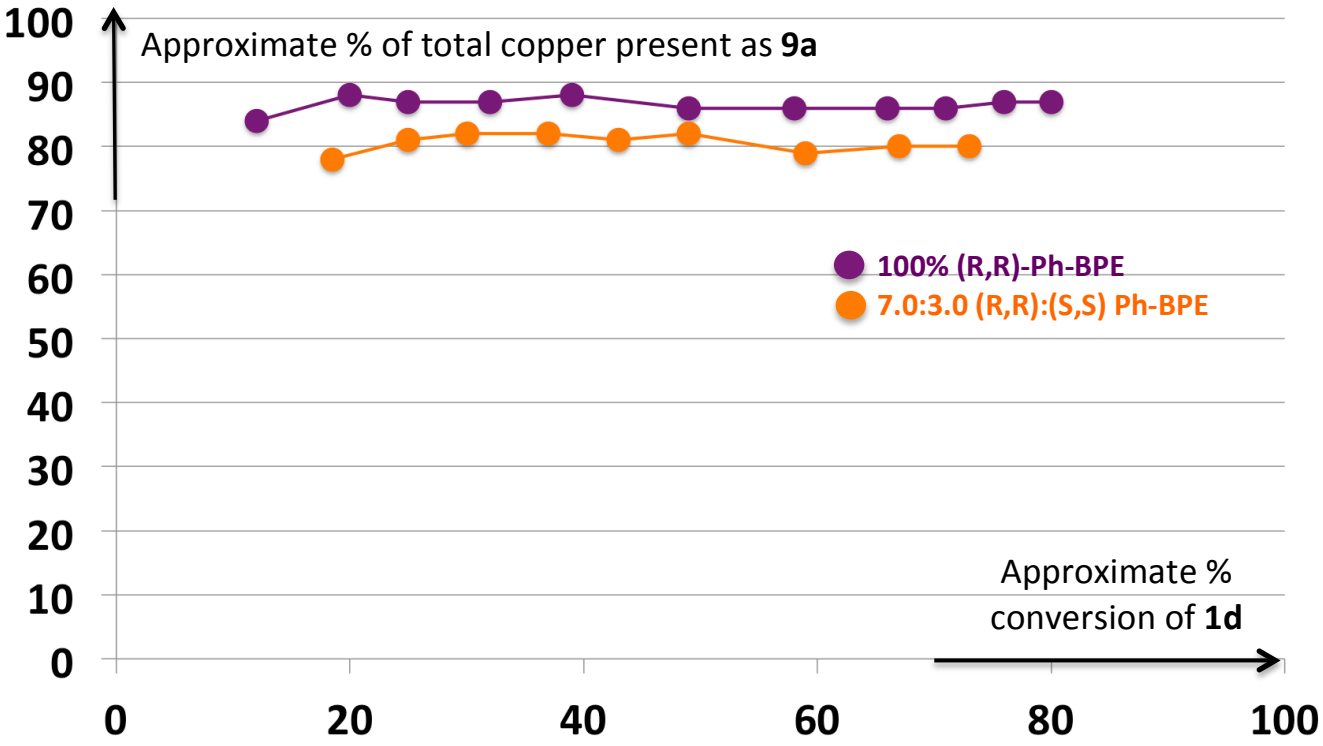

Figure SI-40: Composition of the catalyst resting state during dearomatization of 1d with 6a using ^{31}P-NMR-based estimates.

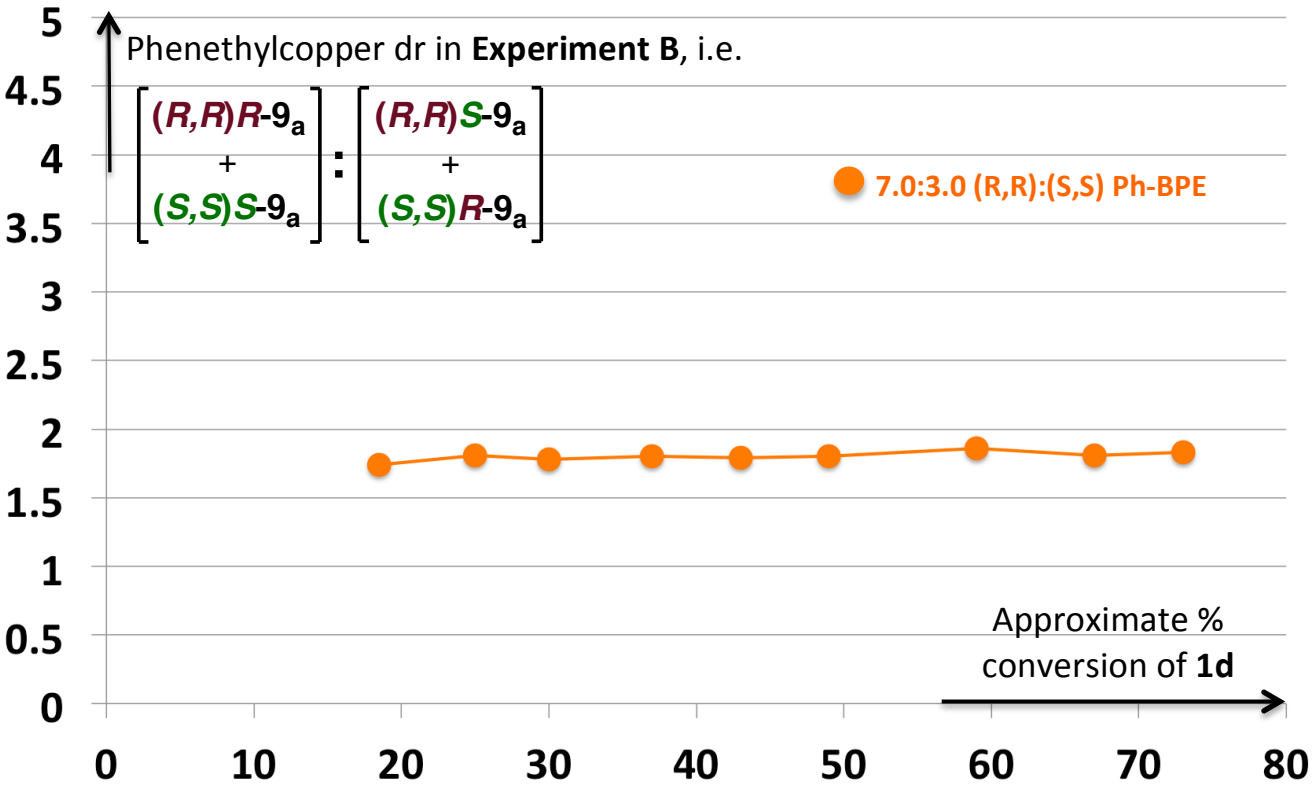

Figure SI-41: The phenethylcopper dr is constant and very low throughout dearomatization with 7.0:3.0 (*R*,*R*):(*S*,*S*)-Ph-BPE.

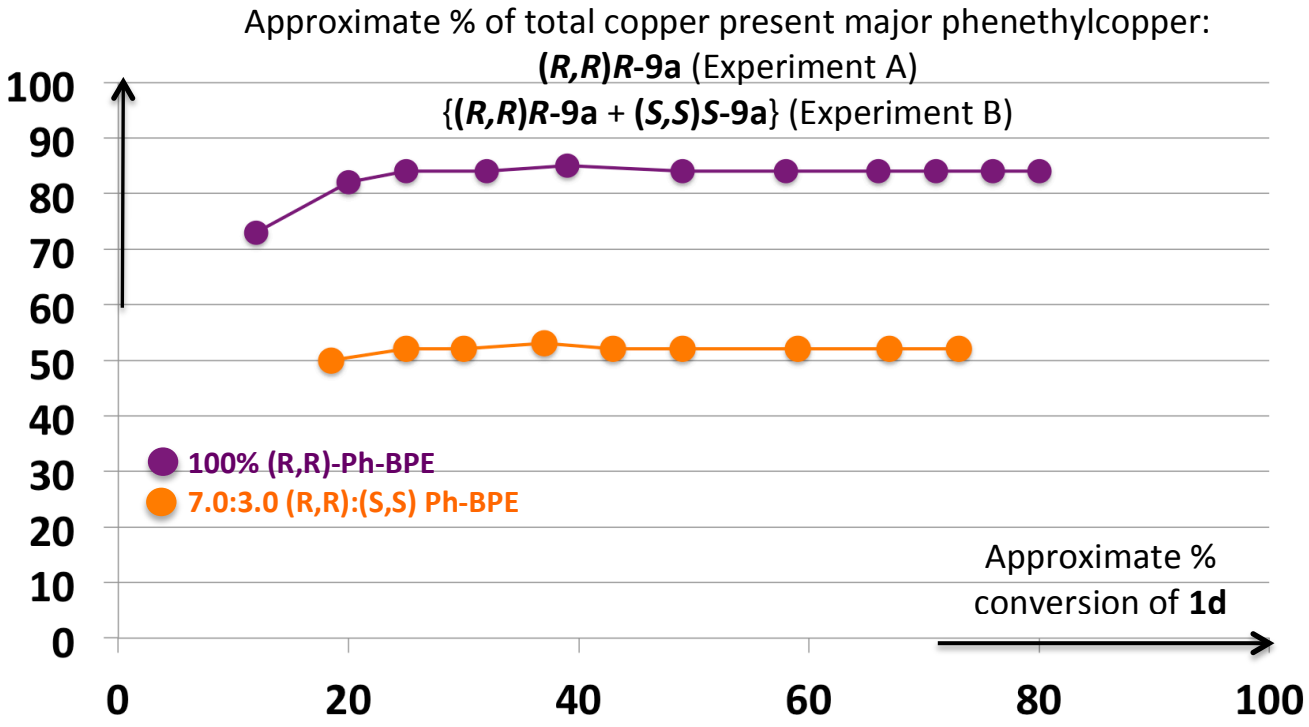

Figure SI-42: The proportion of Cu present as the major phenethylcopper is much lower with 7.0:3.0 (*R*,*R*):(*S*,*S*)-Ph-BPE than with 100% (*R*,*R*)-Ph-BPE.

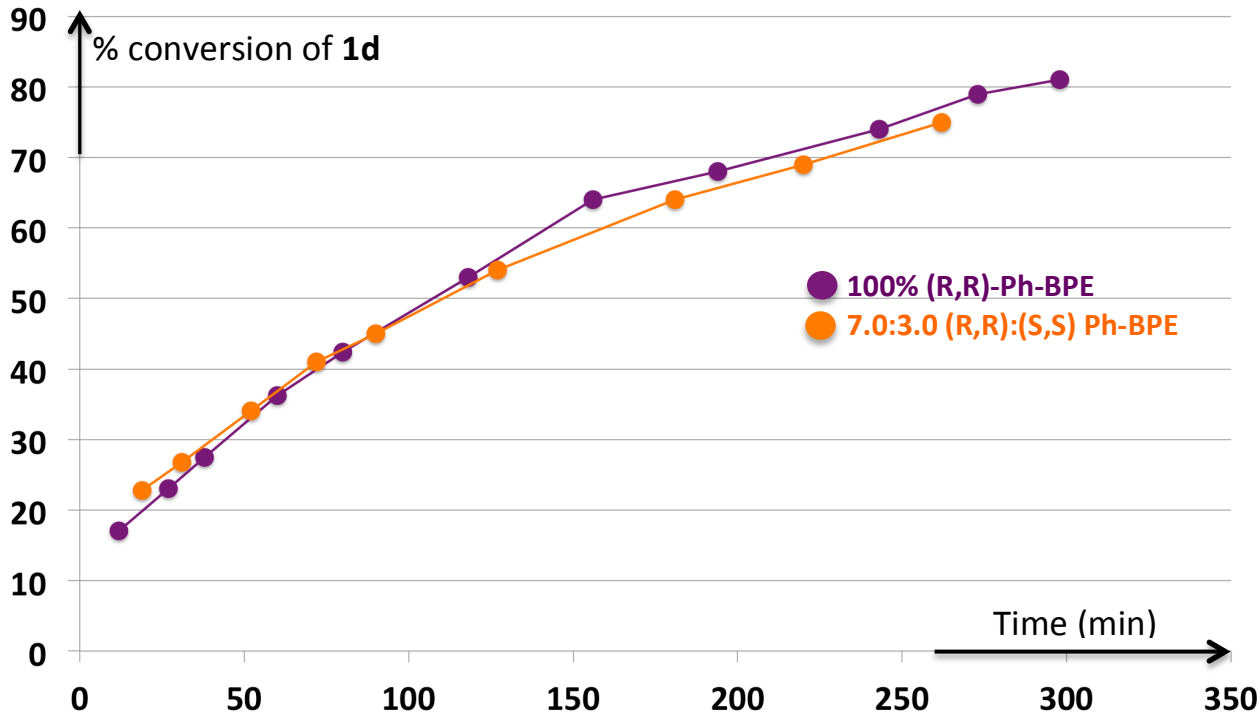

Figure SI-43: Reaction rates are very similar for both experiments.

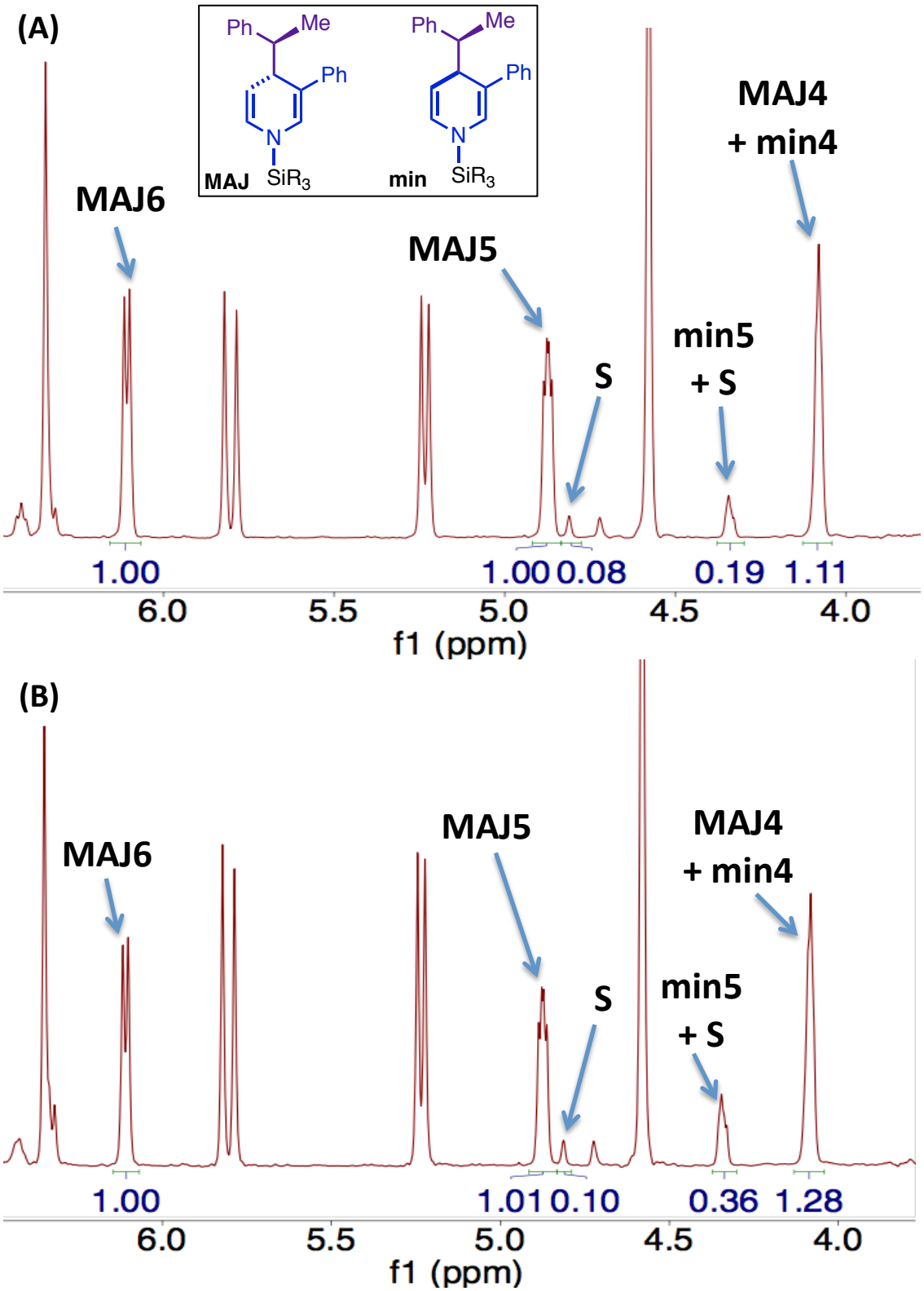

Figure SI-44: Estimation of the (anti):(syn) ratio for product 7da in reactions with (A) 100% (*R*,*R*)-Ph-BPE and (B) 7.0:3.0 (*R*,*R*):(*S*,*S*)-Ph-BPE.

The NMR data used in the dr calculations for the two reactions are shown in Figures SI-44, A and B. There are two well-resolved signals for the major diastereomer of ***anti*-7dh**: a doublet at δ 6.11 ppm (J = 7.9 Hz; MAJ6) corresponding to C6–H and a double-doublet at δ 4.87 (J = 7.9, 4.6 Hz; MAJ5) corresponding to C5–H. The C4–H protons of ***anti*-7dh** and ***syn*-7dh** coresonate as an apparent triplet at δ 4.08 (J = 4.1 Hz), and the C5–H signal of ***syn*-7dh** (min5) overlaps one of the satellites of the DMMS Si–H resonance at δ 4.34 ppm. One can calculate the integrals of signals for the minor diastereomer in several ways, e.g., as INT(MAJ4 + min4) – INT(MAJ5), INT(MAJ4 + min4) – INT(MAJ6), or INT(min5 + S) – INT(S), etc., where INT(x) denote the integral associated with signal x. The (***anti*-7dh**):(***syn*-7dh**) ratio can then be estimated as INT(MAJ):INT(min) for any given choice of major and minor signals. All give similar results: an (***anti*-7dh**):(***syn*-7dh**) ratio of 1.00:0.11 = 9.1 for the reaction run with 100% (R,R)-Ph-BPE, and an (***anti*-7dh**):(***syn*-7dh**) ratio in the range of 3.6:1–3.8:1 for the reaction conducted with 7.0:3.0 (*R,R*):(*S,S*)-Ph-BPE.

5.2.iii. Correlation of the er of 1,4-DHP 7dh with the proportion of total product formed via the minor phenethylcopper.

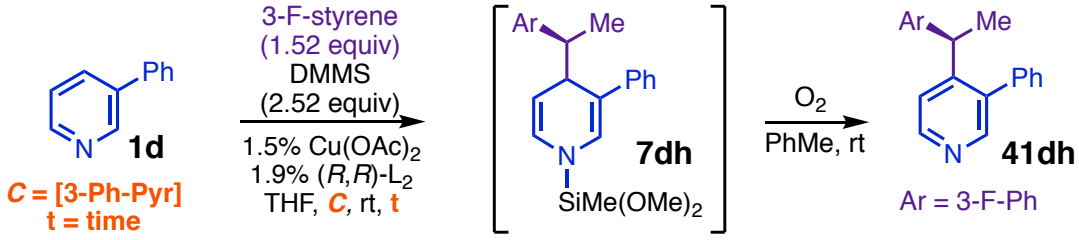

Exp.	C	t	NMR yield of 7dh	(*anti*:*syn*) of 7dh	er of 41dh
A	1.0 M	66 h	97	30:1	35:1
B	0.061 M	18 h	75	25:1	9.9:1
C	0.061 M	66 h	83	22:1	7.9:1

General Note. Having established that both diastereomers of **9** undergo dearomative addition to **1d**, it becomes possible to use the phenomenon of kinetically controlled catalyst dr to determine how the proportion of total reaction that occurs via the minor phenethylcopper influences the enantioselectivity of the catalytic reaction. If one conducts dearomatization at very low catalyst loading, then convergence of the mixture of ***(R,R)R*-9** and ***(R,R)S*-9** initially present to ***(R,R)R*-9** via catalytic recycling occurs while the catalytic reaction is still at very low conversion. In that case, terminating reactions at intermediate conversion strictly lowers the proportion of total product formed via the minor phenethylcopper relative to reactions run to high conversions. This is because aborting the reaction ensures that less of the total product (**7**) is generated during the phase of deteriorated catalyst dr that occurs late in the reaction. **Experiments B** and **C** in the table above show that premature termination of the reaction increases both the er and dr of **7dh**. Further, as described in Section 5.2.i., kinetic control of the catalyst dr during dearomatization with enantiomerically pure Ph-BPE arises because the dearomative addition step obeys a bimolecular rate law ($rate = k_{\text{eff}}[\mathbf{1d}][(\boldsymbol{R,R})\boldsymbol{R}\text{-}\mathbf{9h}]$), whereas epimerization is a first-order equilibration process for **9h** having $rate \sim k_{epi}\left[(\boldsymbol{R,R})\boldsymbol{R}\text{-}\mathbf{9h}\right]$ when the (*R,R*)*R*:(*R,R*)*S* ratio is very high (i.e., when the fractional distance from equilibrium is very large). It is easy to see that the selectivity factor for the two processes ($\xi = k_{\text{eff}}[\mathbf{1d}]$) must increase as the reaction concentration increases. **Experiments A** and **C** show that increasing the concentration – and thus favoring dearomative addition of ***(R,R)R*-9h** over epimerization – markedly increases the enantioselectivity (as determined after derivatization to

41dh). This outcome, and the dependence of the er on conversion, both show that reaction via **(*R,R*)*R*-9h** is responsible for the highly selective formation of **C*α*-(*S*)-*anti*-7dh** observed under typical conditions, proving that the dearomative addition step is itself stereoretentive

Procedure

Step One. Inside a glovebox, an oven-dried calorimetry vial was charged with $Cu(OAc)_2$ (6.35 mg, 35.0 μmol) and (*R,R*)-Ph-BPE (22.2 mg, 43.8 μmol), equipped with an oven-dried PTFE stir-bar, and sealed with a PTFE/silicone septum-cap. The solids were dissolved in THF (810 μL), and DMMS (720 μL, 6.85 mmol) was added immediately afterward. The mixture was stirred at rt for 15 min, during which time all of the $Cu(OAc)_2$ dissolved and the color turned orange. The solution was charged with 3-fluorostyrene (420 μL, 3.52 mmol) and stirred at rt for 50 min.

Step Two. A 330 µL aliquot of the phenethylcopper solution was transferred to an oven-dried one-dram vial that had been equipped with a small oven-dried PTFE stir-bar and sealed with a screw-on PTFE/silicone septum-cap. The vial was charged with 3-phenylpyridine (55.0 μL, 50.0 mg, 0.387 mmol), completing the preparation of reaction mixture **A**. Two oven-dried calorimetry vials that had been equipped with small PTFE-stir bars and sealed with PTFE/silicone septum-caps were each charged with a 330 μL aliquot of the phenethylcopper solution and then diluted with 6.00 mL THF. Each of these vials was subsequently charged with 3-phenylpyridine (55.0 μL, 50.0 mg, 0.387 mmol), completing the preparation of reaction mixtures **B** and **C**. The three reaction mixtures described above were stirred at rt inside the glovebox for the indicated duration.

Step Three: *NMR analysis of crude **7dh** from mixture **B** (C = 0.061M, t = 18 h) and ee determination of **41dh** after oxidation*. After 17 h, 1,3,5-trimethoxybenzene (25.6 mg, 0.152 mmol) was added as an internal standard to mixture **B**, which was then agitated to ensure homogeneity. A 3.4 mL aliquot of the mixture was transferred using a disposable 1.00 mL syringe to an oven-dried glass culture tube. The tube was equipped with the adapter assembly depicted in Figure SI-7, removed from the glovebox, and connected to a dual manifold with two liquid-N_2-cooled traps. The mixture was immersed in a ca. –35 °C CO_2/MeCN slurry for several minutes. The volatile reactants (DMMS and 3-fluorostyrene) were then stripped out of the mixture under high vacuum (18 h after addition of heterocycle), leading to termination of the reaction (NB, a dearomatization reaction under these conditions does not proceed at a meaningful rate at –35 °C). The resulting residue was further dried under high vacuum for 30 min, reintroduced into the glovebox, and dissolved in C_6D_6 (0.600 mL). The resulting solution was transferred to an oven-dried medium-wall J-young NMR tube, which was sealed with a PTFE piston. The mixture was analyzed by ^{1}H NMR spectroscopy (d1 = 24 s), and conversion to 1,4-DHP **7dh** was calculated as 75% by comparison of the integrals of diagnostic resonances of **7dh** to the integral of the internal standard peak. The NMR tube was returned to the glovebox and the sample was pipetted back into the culture tube, using 3.0 mL anhydrous, degassed toluene to complete the transfer. The tube was sealed with a new septum-cap, removed from the glovebox, and the headspace was purged with O_2 (g) with a vent needle in place. The mixture, which became an emerald-green solution, was then stirred under an atmosphere of O_2 at rt overnight. On the subsequent day, saturated NH_4F in MeOH (3.0 mL) was injected into the tube, and the resulting suspension was stirred at rt for 1 h, concentrated using a rotary evaporator, and filtered through a plug of silica gel, eluting with EtOAc. The filtrate was concentrated using a rotary evaporator to yield the crude C4-functionalized pyridine **41dh** as an oily residue, which was partially purified by preparative TLC using 1:4 acetone:hexanes as the eluent. The product band was stripped away from the plate with a razor blade, pulverized, extracted with EtOAc, and filtered

through a Chem-R-Us disposable plastic filter. The filtrate was concentrated to provide a sample of **41dh** for analysis of chiral purity (er = 9.9:1 for **41dh** isolated from mixture **B**) using the analytical method described in Section 9.2. This sample contained a significant quantity of **1d**, which is regenerating during the oxidation step and not efficiently separated during chromatography; however, the signal due to **1d** is well resolved by chiral SFC from those of the enantiomers of **41dh**.

Step Four: *NMR analysis of crude **7dh** from mixtures **A** (C = 1.0 M, t = 66 h) and **C** (C = 0.061M, t = 66 h) and isolation of **41dh** after oxidation.* After 66 h, mixtures **A** and **C** were concentrated on a vacuum manifold as described in Step Three, albeit without cooling in CO_2/MeCN in this case. The residues were processed in the manner described in Step Three to provide ^{1}H-NMR-based estimates for conversion to **7dh** (98% for mixture **A**, 83% for mixture **C**) and measurements of the chiral purity of **41dh** (35:1 er for mixture **A**, 7.9:1 er for mixture **C**).

5.2.iv. In situ observation of the catalyst resting state during dearomatization of 3-phenylpyridine with 3-fluorostyrene

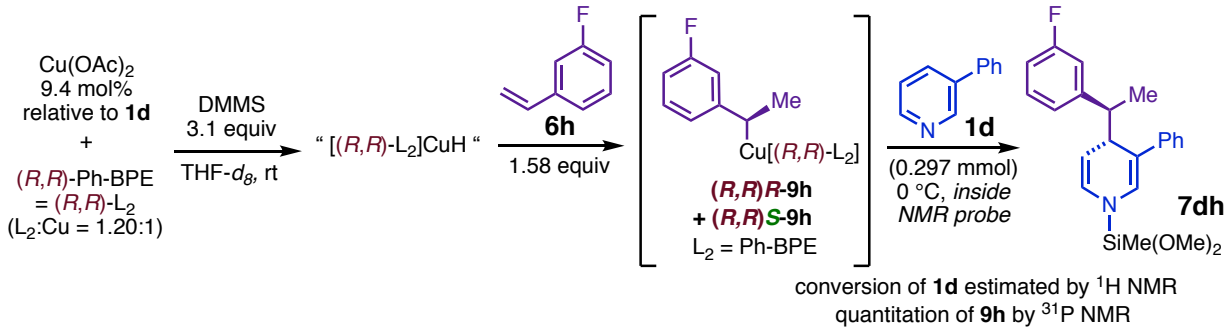

Procedure. Inside a glovebox, an oven-dried one-dram vial was charged with $Cu(OAc)_2$ (10.0 mg, 55.1 μmol) and (*R,R*)-Ph-BPE (33.5 mg, 66.1 μmol; 1.20 L_2:Cu ratio), equipped with an oven-dried PTFE stir-bar, and sealed with a PTFE-silicone septum-cap. The internal standard, *para*-fluoroanisole was added with a microsyringe and the quantity added was weighed (11.3 mg, 89.6 μmol). The resulting mixture was dissolved in THF-d_8 (600 μL), and DMMS (220 μL, 1.79 mmol) was added immediately afterward. The mixture was stirred at rt for 5 min, by which time the solution had become yellow in color. At this point, 3-fluorostyrene (110 μL, 0.923 mmol) was added, and the hydrocupration reaction mixture was stirred at rt for 1 h inside the glovebox. A 500 μL aliquot of the phenethylcopper solution was then transferred to an oven-dried medium-wall J-Young NMR tube, which was sealed with a PTFE piston and removed from the glovebox. The mixture was further aged at rt for 1 h and then frozen in liquid N_2 pending analysis. It was estimated that the 500 μL aliquot introduced into the NMR tube contained 28.0 μmol copper, 33.6 μmol (*R,R*)-Ph-BPE, 0.909 mmol DMMS, and 0.469 mmol 3-fluorostyrene.

The probe of a Bruker 501 NMR spectrometer was cooled to 0 °C, and the NMR sample was thawed and injected into the spectrometer. Fluorine-19 (16 scans, d1 = 20s, 01p = –121 ppm) and phosphorus-31 NMR spectra were recorded, the probe was cooled to –20 °C, and a second round of ^{19}F and ^{31}P NMR analyses were performed at this temperature using the same acquisition parameters.

The NMR sample was ejected from the probe, kept frozen in liquid N_2 during transport, briefly thawed, and returned to the glovebox. The tube was unsealed, charged with 75 μL of a solution prepared from 3-phenylpyridine (140.0 mg, 0.902 mmol) and THF-d_8 (100 μL), resealed, upended

several times, removed from the glovebox, and refrozen. It was estimated that 0.297 mmol 3-phenylpyridine had been added to the NMR tube, giving relative stoichiometry values of 9.4 mol% copper, 3.06 equiv DMMS, and 1.58 equiv 3-fluorostyrene. Copper and 4-fluoroanisole were present in a mol ratio of 0.615:1. The tube was briefly thawed and injected into the spectrometer probe, which had been maintained at –20 °C since the prior analyses. Proton, ^{19}F, and ^{31}P NMR spectra were periodically recorded until the reaction had reached ca. 50% conversion of **1d** as determined from ^{1}H NMR integrals. The probe of the spectrometer was then warmed to –10 °C and further rounds of analyses were performed using the same parameters as above until the conversion of **1d** was > 90%. Figure SI-45 provides a time-lapsed plot of representative ^{1}H NMR spectra acquired during the reaction, with diagnostic resonances for **1d** and ***anti*-7dh** indicated. Phosphorus-NMR-based estimates of total copper present as **(*R,R*)*R*-9h** + **(*R,R*)*S*-9h** were calculated as described in section 5.1.i and are included in the spectral plot in figure SI-46. Fluorine-NMR-based estimates of total copper present as phenethylcopper were calculated by comparing the integral of the ^{19}F NMR signals associated with **(*R,R*)*R*-9h** and **(*R,R*)*S*-9h** to the integral of the signal of internal 4-fluoroanisole and are included in the spectral plot in Figure SI-47. The latter two plots both indicate that **9h** was present as the major catalyst species throughout the reaction, and that its relative abundance was not markedly changed upon addition of heterocycle to the hydrocupration reaction mixture; neither shows the presence of any other major catalyst species.

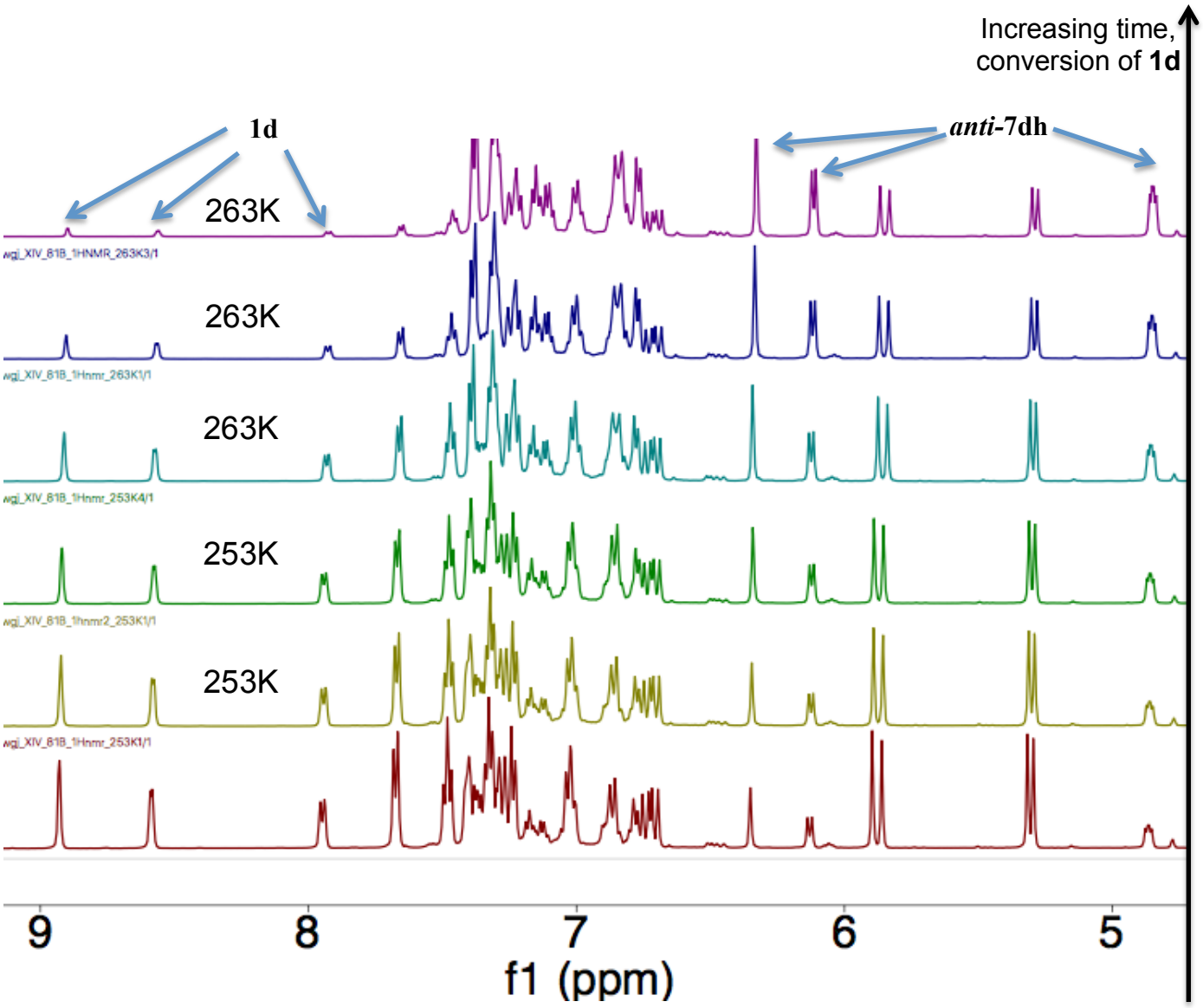

Figure SI-45: Time-lapsed plot of representative ^{1}H NMR spectra from dearomatization of 1d with 6h

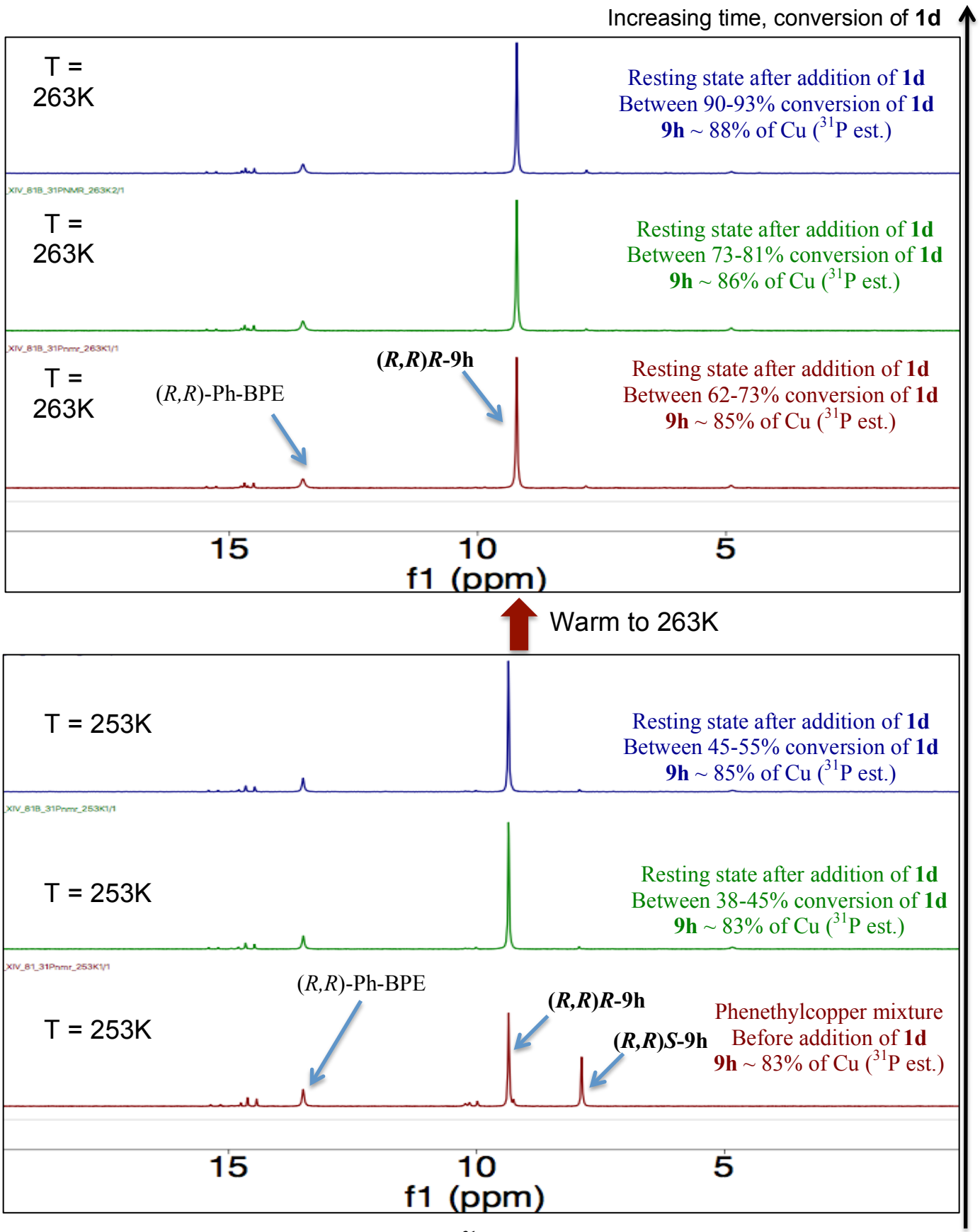

Figure SI-46: Time-lapsed plot of representative ^{31}P NMR spectra from dearomatization of 1d with 6h

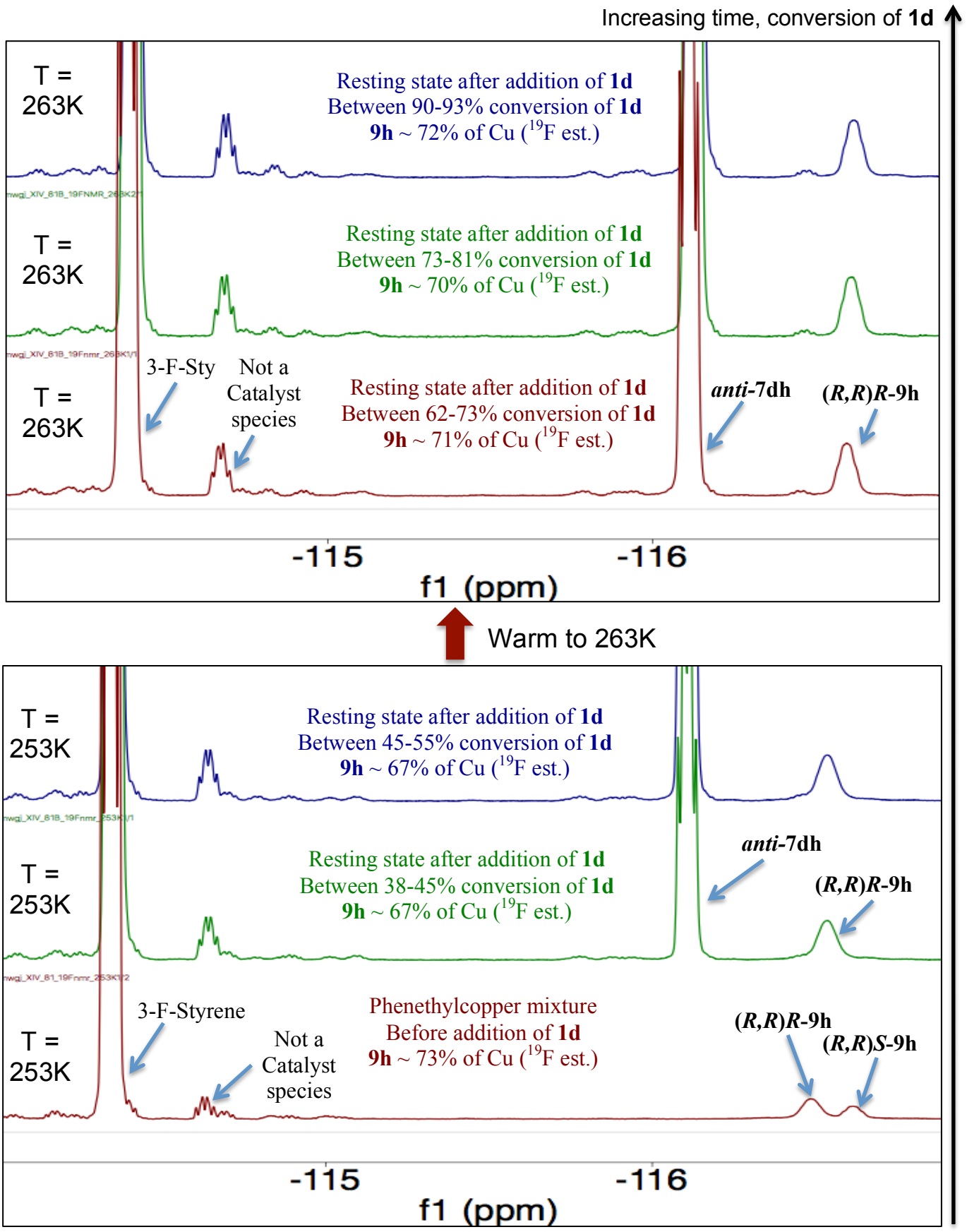

Figure SI-47: Time-lapsed plot of representative ^{31}P NMR spectra from dearomatization of 1d with 6h

5.2.v. Comparison of the resting state for dearomatization of 3-(para-mesylphenyl)pyridine to that of 3-phenylpyridine: Direct observation of N-cuprated-1,4-DHP catalytic intermediate 10gh

(a) Synthesis of 3-fluorostyrene-α-^{13}C (**6h-α-^{13}C**)

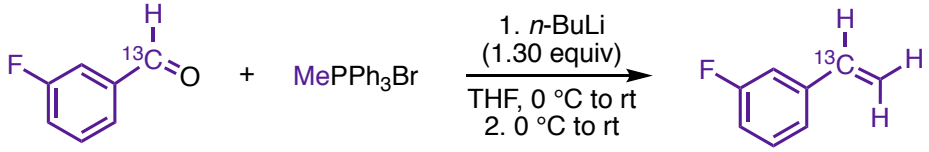

3.75 mmol
(added in step 2)

5.49 mmol
1.46 equiv

6h-α-^{13}C
2.24 mmol
60% yield

Procedure. An oven-dried 50 mL Schlenk tube containing a dry PTFE stir-bar was charged with methyltriphenylphosphonium bromide (1.96 g, 5.49 mmol, 1.46 equiv), sealed with a rubber septum, connected via the sidearm to a dual manifold, and placed under a N_2 atmosphere using three evacuation-backfill cycles. The phosphonium salt was suspended in 6.00 mL THF, and the resulting stirred mixture was cooled in an ice-water bath. *N*-butyllithium (2.60 M in hexanes, 1.88 mL, 4.89 mmol, 1.30 equiv) was added to the slurry dropwise, causing a color change to deep yellow-orange and the dissolution of most solids. The ylide solution was allowed to warm to rt over the course of 30 min and was then recooled in the ice-water bath. A solution of 3-fluorobenzaldehyde-α-^{13}C (469 mg, 3.75 mmol) in 1.00 mL THF was added dropwise to the reaction mixture, and two 500 μL aliquots of pentane were used to complete the transfer. Addition of the aldehyde resulted in copious precipitation and arrested stirring, and the mixture was warmed to rt, diluted with 4.00 mL additional THF, and briefly sonicated. Stirring at rt was resumed and continued for 1 h, 45 min. The reaction mixture was quenched by careful addition of saturated aqueous NH_4Cl and partitioned between Et_2O and saturated NH_4Cl. The aqueous layer was back-extracted 3x with Et_2O, and the combined organics were dried over Na_2SO_4, filtered, and stabilized with 0.2 mg of 4-*tert*-butylcatechol. The crude product was carefully concentrated with the aid of a rotary evaporator with ice chips in the bath using the minimal vacuum strength required for evaporation of most THF. The concentrated product solution was loaded onto a 40 g silica column and eluted with pentane. Product fractions devoid of polar impurities were combined in the presence of 0.4 mg of 4-*tert*-butylcatchol and carefully concentrated *in vacuo* as above. Finally, the sample was passively concentrated under open atmosphere until repeated weighings showed negligible further loss of mass, yielding the product as a pale-yellow oil weighing 276 mg (60% uncorrected yield). Analysis by NMR spectroscopy revealed very minor hydrocarbon impurities and the presence of a trace (ca. 1%) ^{19}F-containing impurity at δ -119.4 ppm (CD_2Cl_2). A 250 μL aliquot of this sample was transferred using a pipet to an oven-dried 10 mL Schlenk storage tube against N_2 pressure, and the tube was sealed with a screw-in PTFE plug and brought into a glovebox. The styrene was dissolved in THF-d_8 (500 μL), and the resulting solution was transferred with a 1.00 mL disposable plastic syringe to an oven-dried 20 mL scintillation vial. A 40 μL aliquot of this solution was injected into a solution of 17.3 mg of 2,6-dimethoxytoluene in THF-d_8, and analyzed by ^{1}H NMR to determine the concentration of the stock solution (found to be 2.21 M in **6h-α-^{13}C**). The stock solution was stored in the glovebox freezer at –35 °C in order to minimize decomposition. The product exhibited the expected NMR spectroscopic characteristics for 3-fluorostyrene, albeit with ^{13}C splitting of the olefinic resonances and the ^{19}F signal. ^{1}H NMR (400 MHz, CD_2Cl_2) δ 7.31 (td, J = 7.9, 6.0 Hz, 1H), 7.20 (ddt, J = 7.5, 4.7, 1.3 Hz, 1H), 7.13 (ddt, J = 10.3, 4.5, 2.1 Hz, 1H), 6.96 (td, J = 8.5, 2.7 Hz,

1H), 6.70 (ddd, J = 155.8, 17.6, 10.9 Hz, 1H; Cα–H), 5.78 (dd, J = 17.6, 3.1 Hz, 2H), 5.31 (d, J = 10.9 Hz, 1H). ^{13}C NMR (101 MHz, CD_2Cl_2) δ 136.14 (d, $^4J_{C,F}$ = 2.6 Hz; Cα). ^{19}F NMR (376 MHz, CD_2Cl_2) δ -114.45 (tdd, J = 8.7, 6.0, 2.6 Hz).

(b) NMR Experiments

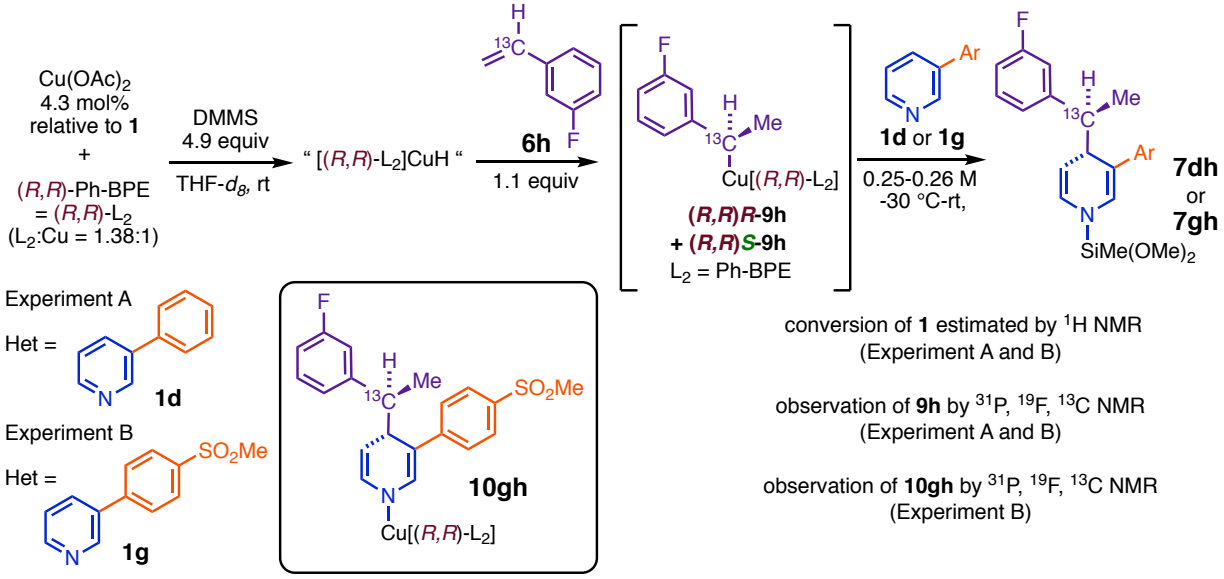

General Note. As described in Section 4, analysis of the double-dearomatization PES suggested that σBM should become kinetically relevant for **1g**, leading to **10gh** becoming an observable catalytic intermediate. The following two experiments involve characterization of the respective catalyst resting states for dearomatization of **1g** and **1d** with 3-fluorostyrene-α-^{13}C using ^{31}P, ^{13}C, and ^{19}F NMR spectroscopy. Due to the rapidity of the reaction of 3-fluorostyrene with **1g** and the small quantity of catalyst present, NMR spectra were recorded at (–30 °C), at which temperature the dearomatization reaction occurred at a negligible rate, in order to facilitate long acquisition times and attainment of high-quality data. The NMR sample was then allowed to warm to rt outside the spectrometer for brief intervals to permit incrementally increased conversion of **1g** before being reintroduced into the spectrometer and reanalyzed. We have previously confirmed, including in the dearomatization of **1d** with **6h**, that cooling the dearomatization reaction mixtures to temperatures below those required for efficient turnover does not result in a change in the distribution of observable Cu species relative to resting state observed during catalysis.

Procedure. Inside a glovebox, an oven-dried glass one-dram vial was charged with $Cu(OAc)_2$ (3.60 mg, 19.8 μmol), (*R,R*)-Ph-BPE (13.9 mg, 27.4 μmol; L_2:Cu = 1.38:1), and ca. 4 μL of 4-fluoroanisole (^{19}F NMR internal standard). The vial was equipped with an oven-dried PTFE stir-bar and sealed with a PTFE/silicone septum-cap. The solids were dissolved in THF-d_8 (275 μL), and DMMS (130 μL, 2.23 mmol) was added immediately afterward. The resulting mixture was stirred at rt for 10 min, during which time all $Cu(OAc)_2$ dissolved and the color turned yellow-orange. A 225 μL aliquot of a ca. 2.2 M solution of 3-fluorostyrene-α-^{13}C in THF-d_8 (0.495 mmol) was injected, and the resulting mixture was stirred at rt for 1 h. While the phenethylcopper mixture was being aged, solutions of **1d** (27.3 mg, 0.176 mmol + 400 μL THF-d_8) and **1g** (40.8 mg, 0.175 mmol + 400 μL THF-d_8) were prepared. Each heterocycle solution was transferred to its own oven-dried

medium-wall J-Young NMR tube using oven-dried glass pipets. Each tube was then charged with a 250 μL aliquot of the phenethylcopper stock solution and sealed with a PTFE piston. The NMR tubes were upended several times to ensure homogeneity, rapidly removed from the glovebox, and frozen in liquid N_2 pending analysis (about five minutes elapsed between addition of the phenethylcopper solution and freezing). The reaction mixture prepared from **1d** exhibited a yellow-orange color typical for dearomatization reaction mixtures, whereas the mixture prepared from **1g** took on a vivid salmon-pink color as soon as the heterocycle was exposed to phenethylcopper. It was estimated that each 250 μL aliquot of the phenethylcopper stock solution delivered 7.60 μmol Cu (4.3 mol%; all relative stoichiometry values are referenced to **1** and are the same for both experiments), 10.5 μmol (*R,R*)-Ph-BPE (6.0 mol%), 0.856 mmol DMMS (4.9 equiv), and 0.190 mmol 3-fluorostyrene- α-^{13}C (1.1 equiv). The approximate initial heterocycle concentrations were [**1d**]$_0$ ~ 0.26 M for **Experiment A** and [**1g**]$_0$ ~ 0.25 M for **Experiment B**.

Once the probe of the NMR spectrometer had been stabilized at –30 °C, the reaction mixture prepared from **1g** was removed from cryogen, briefly thawed, and then injected into the spectrometer. Proton, ^{13}C, ^{19}F, and ^{31}P NMR spectra were recorded, with only minor (11%) conversion to **7gh** being evident at this time. The mixture was warmed to rt for 10 min outside the probe and then reanalyzed in the same fashion, with ^{1}H NMR integrals indicating ca. 39% conversion of **1g**. The mixture was again warmed for 10 min outside the spectrometer and then subjected to reanalysis, with conversion of **1g** having increased to 60%. The reaction mixture was aged outside the spectrometer for 23 min and subjected to a final round of analyses performed when the reaction was at 88% conversion of **1d**; at this time-point, the (*anti*):(*syn*) ratio of **7gh** was estimated as dr = 8.3 from the ratio of integrals for the C5–H signals of the major and minor diastereomers. The vivid pink color noted at the beginning of the reaction progressively faded as the conversion increased, ultimately giving way to the yellow-orange color typical of dearomatization reaction mixtures. The reaction mixture prepared from 3-Ph-pyridine was subsequently thawed and analyzed by ^{1}H, ^{19}F, ^{13}C, and ^{31}P NMR spectroscopy under the same conditions.

The species assigned as intermediate **10gh** had clearly visible diagnostic ^{19}F (m, δ –118.0 ppm, 243 K), ^{13}C (s, δ 47.11 ppm), and ^{31}P NMR resonances (br. s, δ 11.5 ppm) indicative of a new CuL_2 complex containing an α-phenethyl group. It was a major component of the catalyst resting state during dearomatization of **1g** with **6h**, particularly at early reaction times. As the conversion increased, the diagnostic signals of this new species all simultaneously diminished, while those of phenethylcopper **9h**, initially present in a much lower amount than usual, simultaneously increased. (The fraction of total observable phosphorus present as **10gh** + **9h** was conserved throughout the reaction, see figure SI-48.) The singlet fine-structure of the ^{13}C NMR resonance of the new Cu complex indicates that the α-fluorophenethyl group cannot be bound to Cu, as this would result in coupling to the ^{31}P nuclei of Ph-BPE. The only chemically reasonable bonding partner for the Cα-C of the phenethyl unit is another carbon atom, and the only chemically reasonable contributor of this carbon atom is an equivalent of **1g**. Of course, the fact that **10gh** only forms in the presence of **1g** independently suggests that it results from reaction of the phenethylcopper with **1g**. The rate law of dearomatization of **1g** and the manner in which catalyst speciation changes throughout the reaction rule out hypothetical structures in which an equivalent of **7gh** (which contains a Cα-C4 bond) is coordinated to a copper complex (e.g., L_2CuH); the reaction in that case would show product-inhibition, and the amount of Cu present as the new complex would increase over time rather than decrease. Apart from the N-Cu-1,4-DHP intermediate, we are unable to formulate an alternative structure for a competent precursor to **7gh** that is comparably stable to the MACS and contains a

Cα–C-bound phenethyl unit and an equivalent of **1g** but not L_2CuH; on the other hand, the new species exhibits all of the properties expected for **10gh**, and we have accordingly assigned it as such.

The manner in which the distribution of catalyst species evolves during dearomatization of **1g** is consistent with dearomative isomerization and σBM steps having comparable activation barriers, as we calculated in our analysis of the reaction kinetics for this substrate (Section 4). As the reaction progresses, the proportional decrease in [**1g**] is much larger than that of [DMMS], because the latter is used in a significant excess (4.9 equiv); in our mechanistic model, this is expected to cause increasing accumulation of catalyst as **9h**, as is observed here. At very high conversion of **1g**, dearomative isomerization approaches the limit of being turnover-limiting, and **9h** resumes its role as the MACS. Although [**7gh**] and [3-fluorostyrene] change throughout the reaction in addition to [**1g**]:[DMMS], the kinetic irrelevance of hydrocupration and the lack of product-inhibition in the dearomatization of **1g** imply that variations in [**7gh**] and [3-fluorostyrene] are not capable of causing the changes in catalyst speciation observed in this experiment.

In the control reaction (Experiment A) with **1d**, observable signals attributable to the analogous N-Cu-1,4-DHP **10dh** were either negligible or absent when the resting state was analyzed by NMR, and the initial concentration of **9h** in that experiment was much higher. Experiment 5.2.iv. above established that **9h** is the MACS throughout the catalytic dearomatization of **1d**, implying that the dearomatization step in that example is more difficult than σBM by a sufficiently large margin that the resting state becomes insensitive to changes in reactant concentrations.

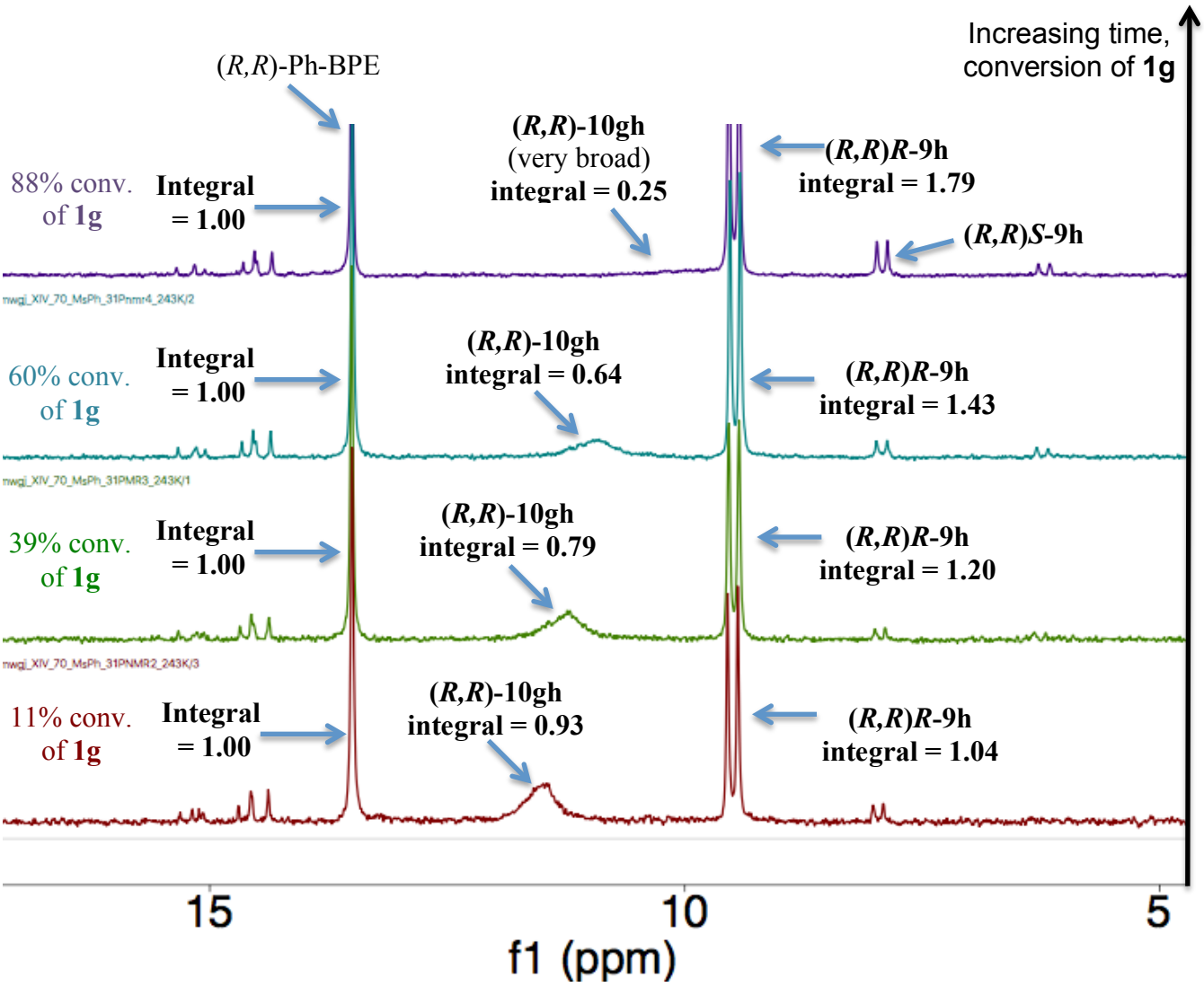

Figure SI-48: Time-lapsed plot of ^{31}P NMR plot showing changes in the catalyst resting state during dearomatization of 1g with 6h. The amount of Cu as 9 +10 is conserved, but [10] decreases and [9] increases as conversion of 1g increases.

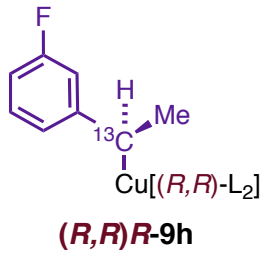

(*R,R*)*R*-9h

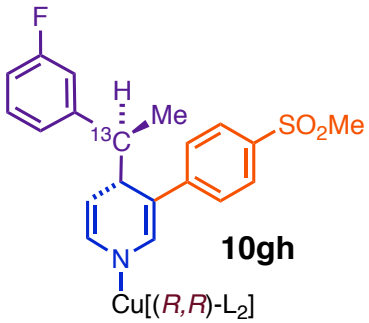

10gh

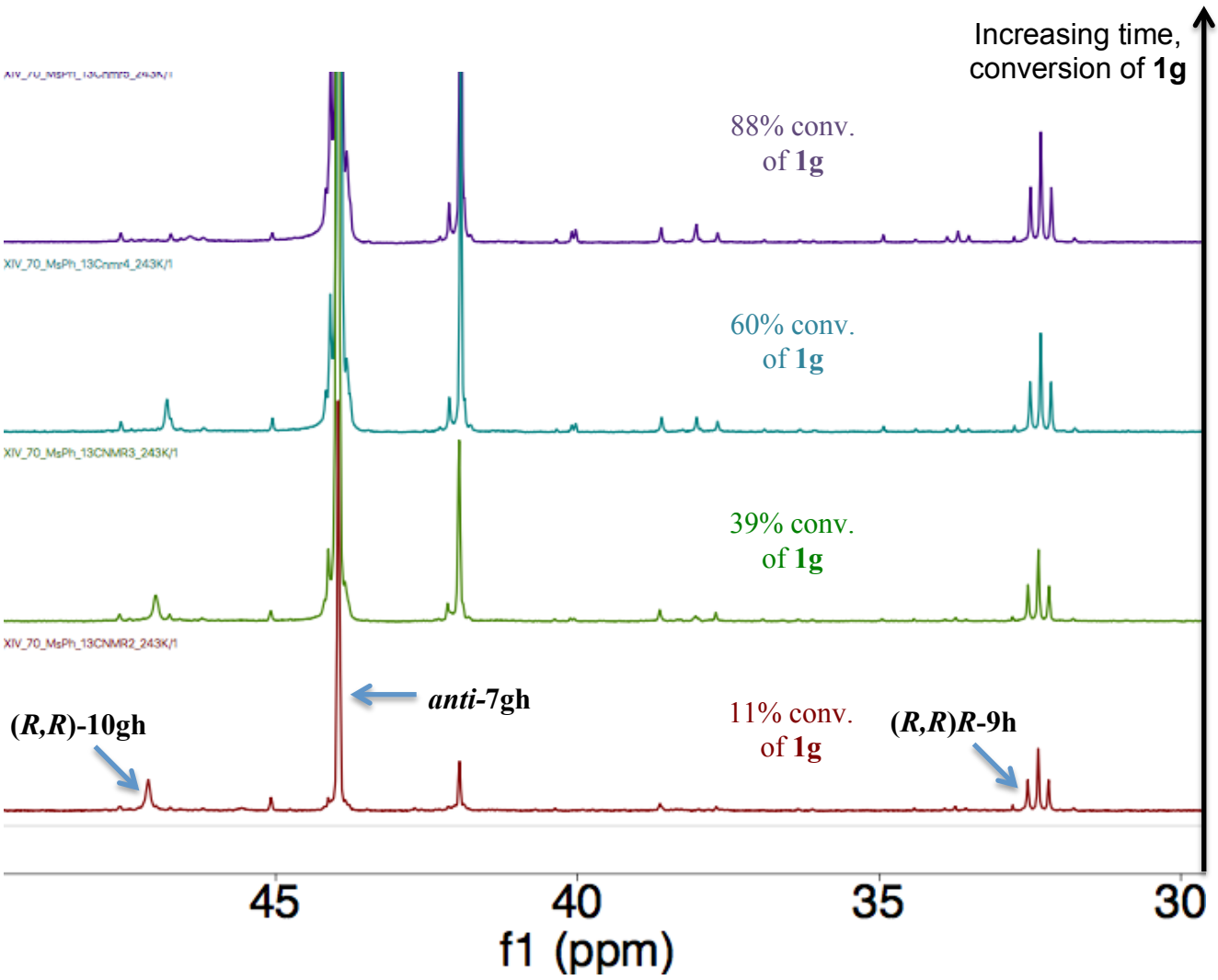

Figure SI-49: Time-lapsed ^{13}C NMR plot for dearomatization of 1g with 6h. The diagnostic signal for 10 is a singlet, indicating that it corresponds to a benzylic carbon bound to carbon rather than Cu. Like the ^{31}P diagnostic, this signal decays over the course of the reaction.

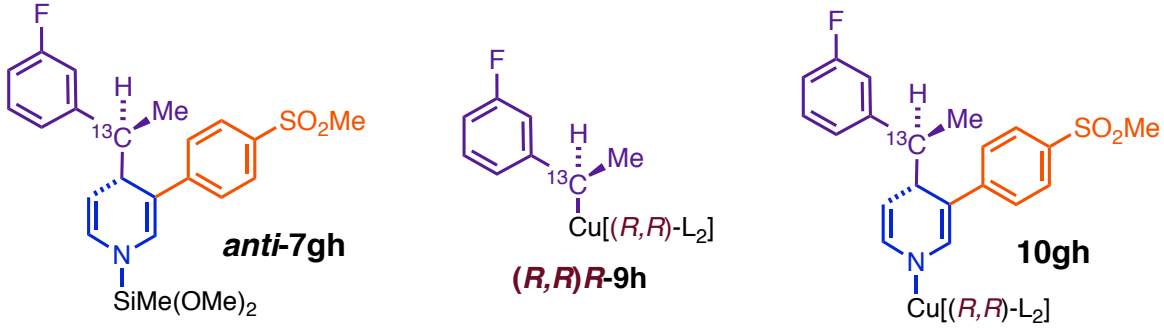

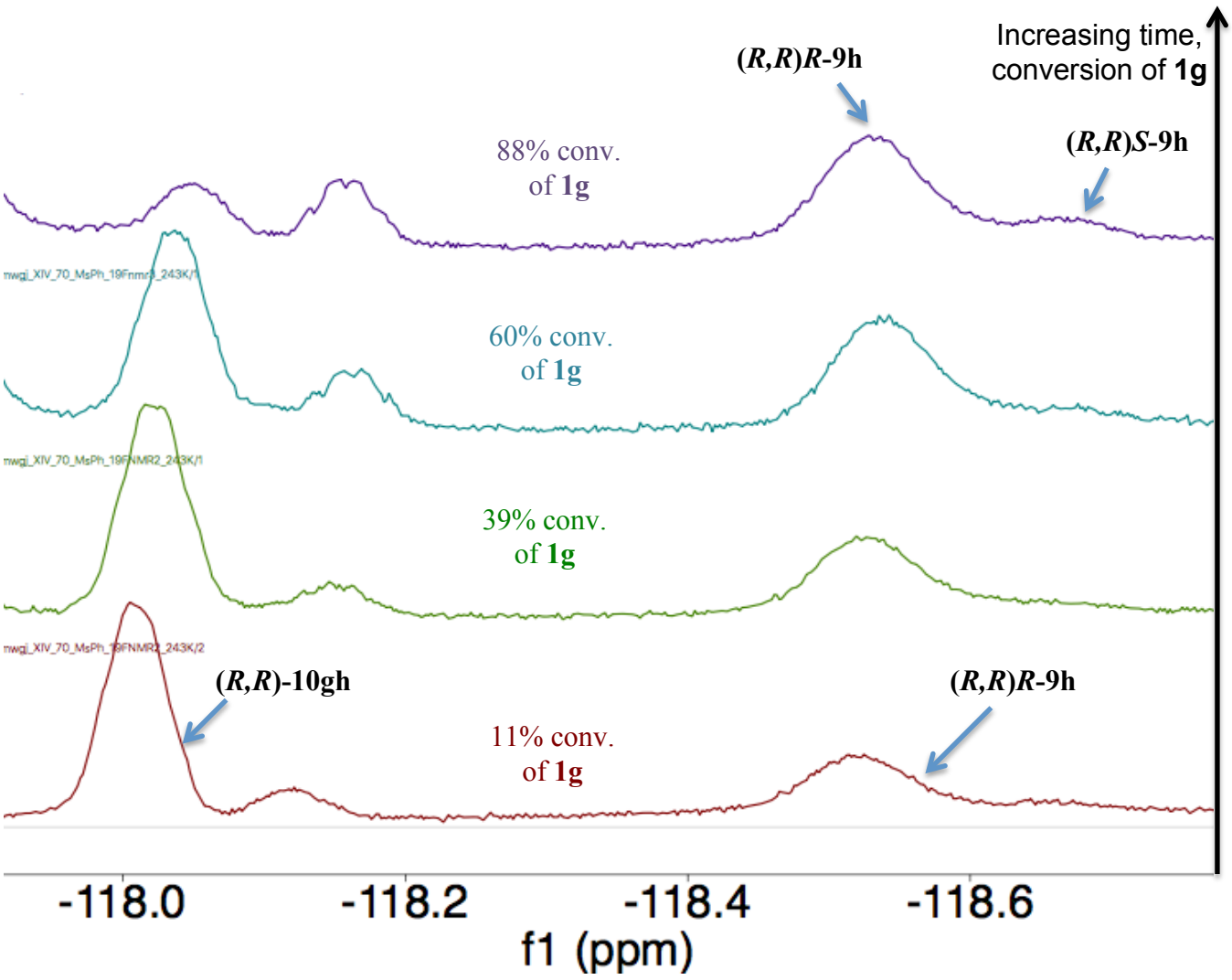

Figure SI-50: Time-lapsed ^{19}F NMR plot for dearomatization of 1g with 6h. The diagnostic resonance for 10gh decays throughout the reaction while that of 9h gets larger.

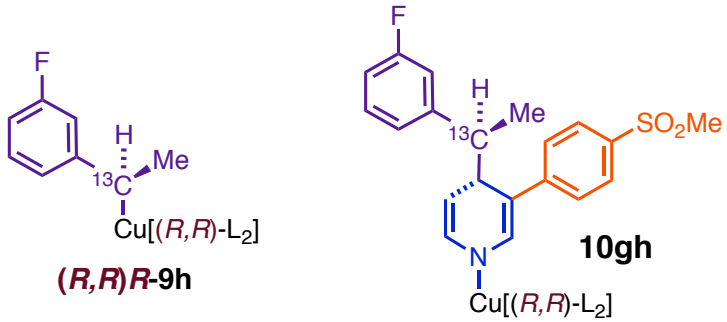

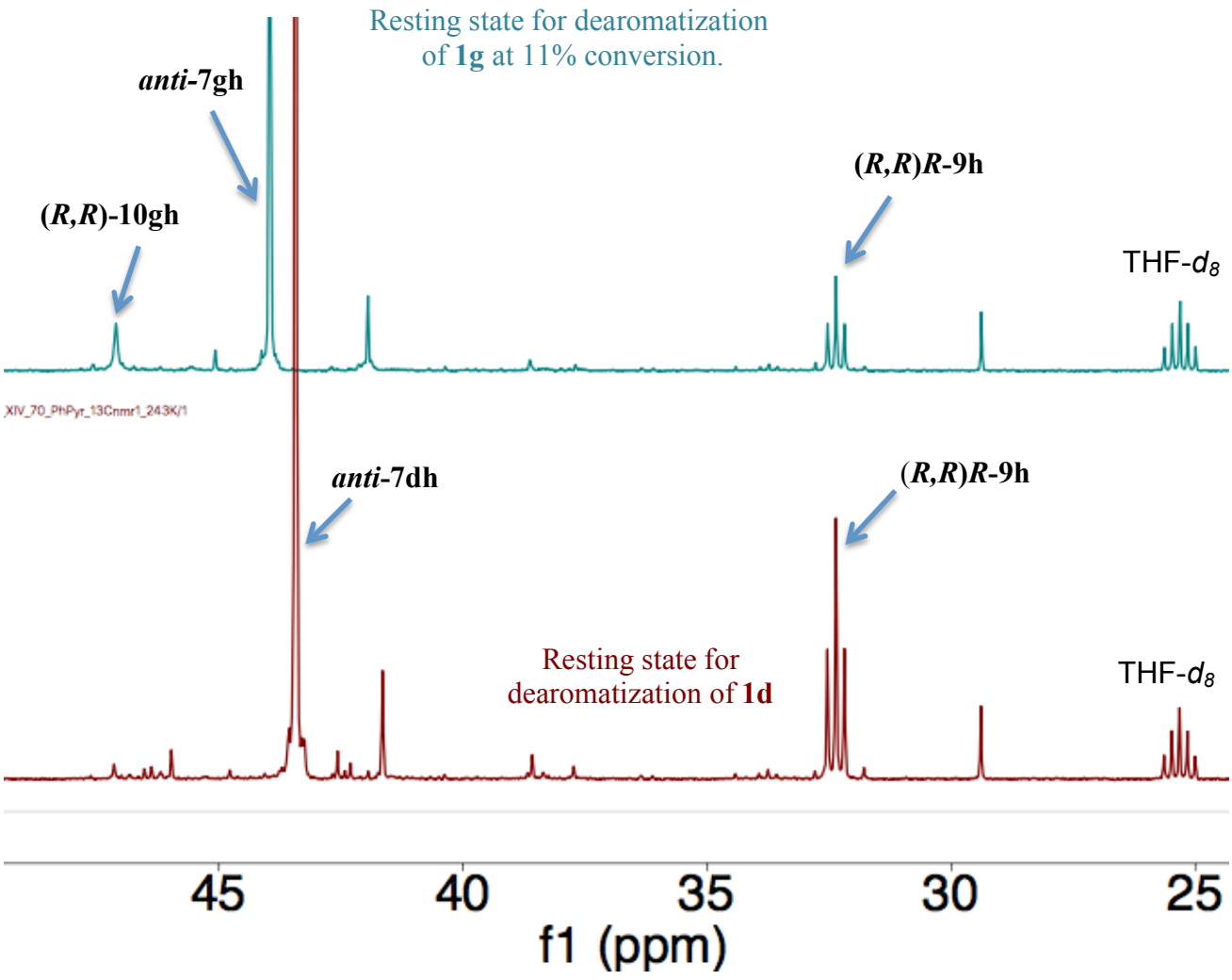

Figure SI-51: There is no significant ^{13}C NMR signal analogous to the diagnostic resonance for 10gh in the resting state during dearomatization of 1d with 6h.

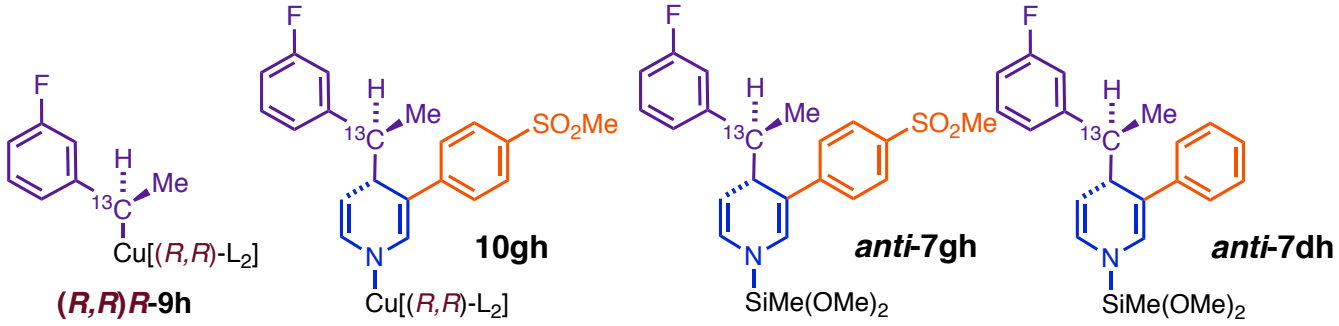

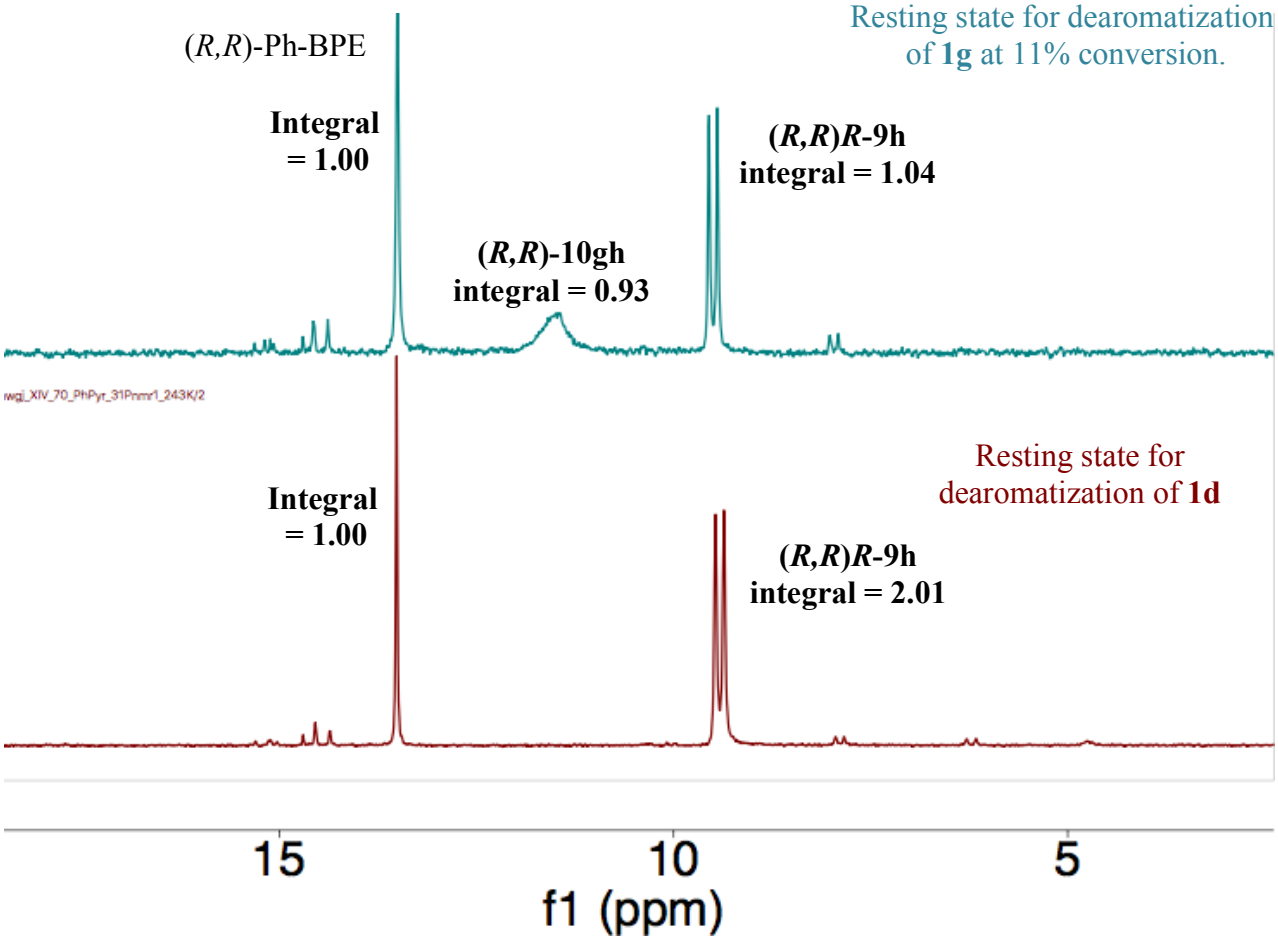

Figure SI-52: There is no significant ^{31}P NMR signal analogous to the diagnostic resonance for 10gh in the resting state during dearomatization of 1d with 6h.

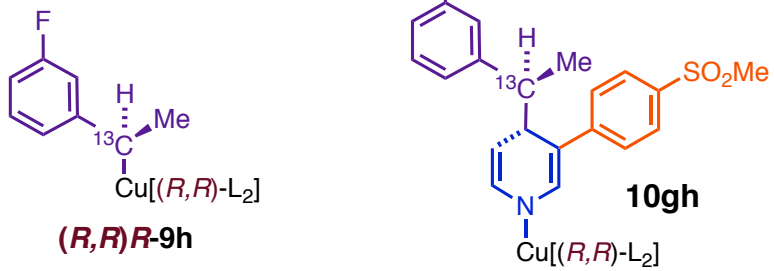

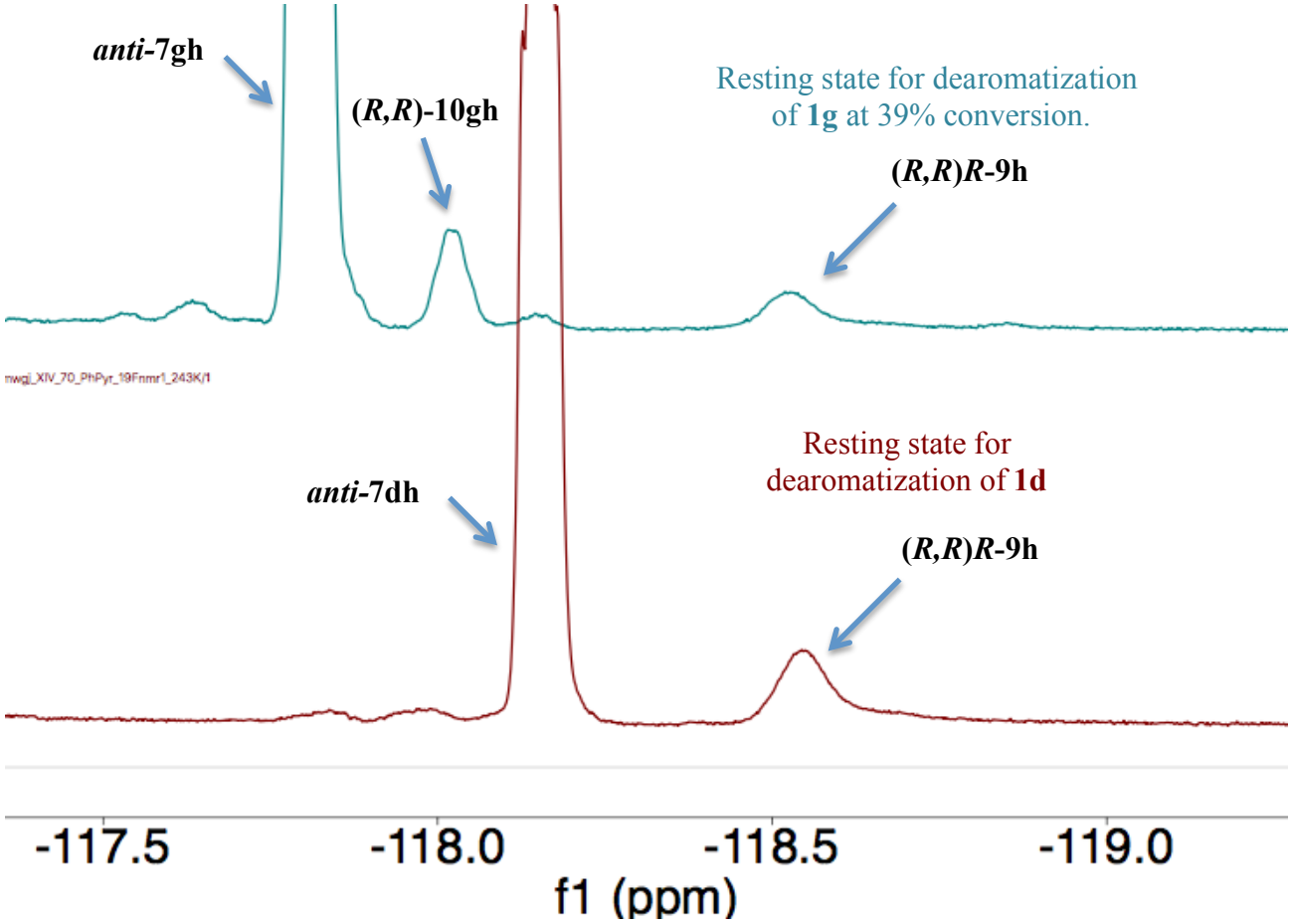

Figure SI-53: There is no significant ^{19}F NMR signal analogous to the diagnostic resonance for 10gh in the resting state during dearomatization of 1d with 6h.

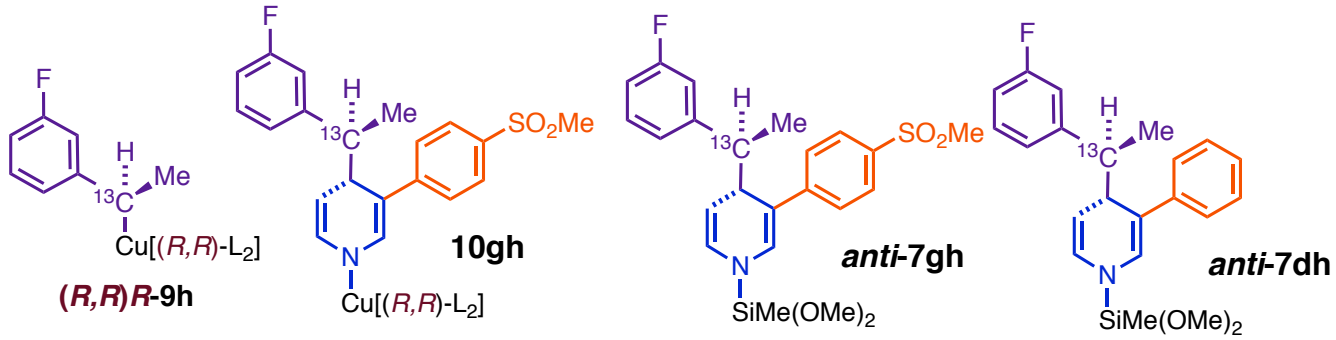

6. NMR-Monitoring of Catalytic Dearomatization Reactions. Study of the Effect of Heterocycle and Olefin Structure on Rate and Selectivity.

6.1. *In situ* ^{1}H-NMR monitoring of dearomatizations with vinyl arenes

6.1.i. Dearomatization of substituted pyridines with styrene.

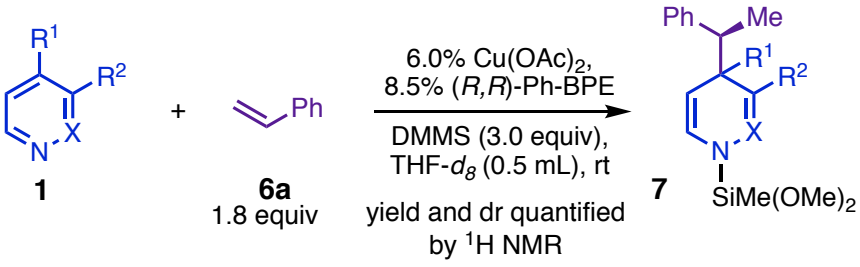

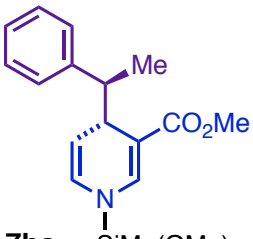

7ba
90% yield (3.5h)
92% yield (23.5h)
4.6:1 (*anti*):(*syn*)

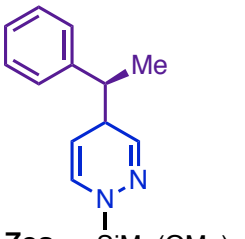

7ea
95% yield (4h)
>28:1 dr

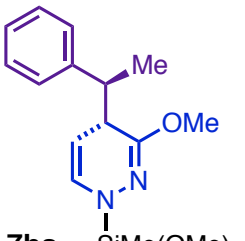

7ha
96% yield (4h)
>30:1 (*anti*):(*syn*)

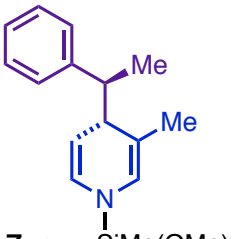

7ca
75% yield (7.5h)
98% yield (23.5h)
25:1 (*anti*):(*syn*)

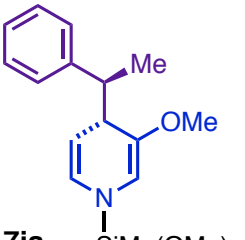

7ia
45% yield (8h)
78% yield (24h)
12:1 (*anti*):(*syn*)

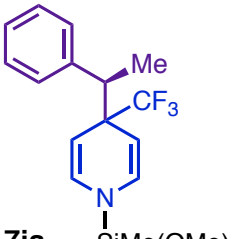

7ja
88% yield (3.5h)
95% yield (7h)

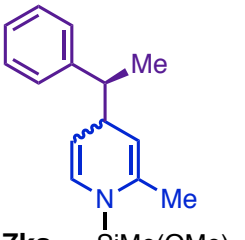

7ka
8% yield (7h)
20% yield (23.5h)
2:1 dr

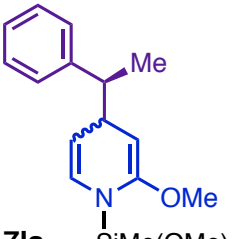

7la
2% yield (7h)
7% yield (23h)
2:1 dr

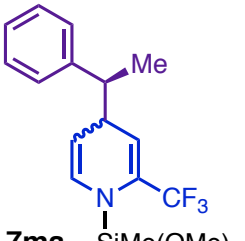

7ma
6% yield (7.5h)
12% yield (23.5h)
2:1 dr

Procedure. Inside a glovebox, an oven-dried one-dram vial was charged with $Cu(OAc)_2$ (18.0 mg, 99.1 μmol) and (*R,R*)-Ph-BPE (70.4 mg, 139 μmol; 1.40:1 L_2:Cu), equipped with a small oven-dried PTFE stir-bar, and sealed with a PTFE/silicone septum-cap. The solids were dissolved in THF-d_8 (1.92 mL), and DMMS (610 μL, 526 mg, 4.96 mmol) was added immediately afterward. The septum-cap was quickly replaced, and the resulting mixture was stirred at rt for 15 min, during which time all $Cu(OAc)_2$ dissolved and the color turned yellow-orange. Styrene (340 μL, 308 mg, 2.96 mmol) was added, and the resulting mixture was stirred at rt. Another oven-dried one-dram vial was charged with the indicated heterocycle (0.300 mmol; weighed) and a quantity of 2,6-dimethoxytoluene (the ^{1}H NMR internal standard) in the range of 0.13–0.16 mmol. This vial was sealed with a septum-cap. Once the phenethylcopper stock solution had been aged for 15 min, a 540 μL aliquot of it was transferred to the vial containing the heterocycle. It was estimated that the 540 μL aliquot contained 3.29 mg $Cu(OAc)_2$ (18.1 μmol, 6.0 mol%), 12.9 mg (*R,R*)-Ph-BPE (25.4 μmol), 112 μL DMMS (0.908 mmol, 3.03 equiv), and 62.0 μL styrene (0.542 mmol, 1.81 equiv). The resulting dearomatization reaction mixture was agitated several times to ensure homogeneity and then transferred to an oven-dried medium-wall J-Young NMR tube, which was then sealed with a PTFE piston and removed from the glovebox. Proton NMR spectra (8 scans, d1 = 24s) were recorded after 3–4 h,7–8 h, and 23–24 h. NMR yields of 1,4-DHP **7** were calculated by comparing the integrals of the diagnostic signals of **7** to the integral of the internal standard peak.

Pyridines bearing substituents at C3 yield easily assigned *anti*- and *syn*- diastereomers due to the presence of reliable, diastereomer-specific anisotropic interactions involving their diagnostic protons. See reference 1 for more detail. Diastereomers associated with 2-substituted 1,4-DHPs were easily identified but not readily assigned from their ^{1}H NMR spectra. The minor diastereomer of pyridazine could not be readily identified from NMR spectra of reaction mixtures generated using enantiomerically pure ligand because the level of diastereoselectivity was too high. However, given a reversal in diastereoselectivity observed for dearomative addition of the minor phenethylcopper to this heterocycle, we were able to prepare samples containing it in 1:1 ratio with the normally major 1,4-DHP diastereomer by conducting the dearomatization with 1:1 (*R,R*):(*S,S*) Ph-BPE.

Figure SI-54: Diagnostic ^{1}H NMR resonances for a representative C3-subsitutited 1,4-DHP (observed *in situ*).

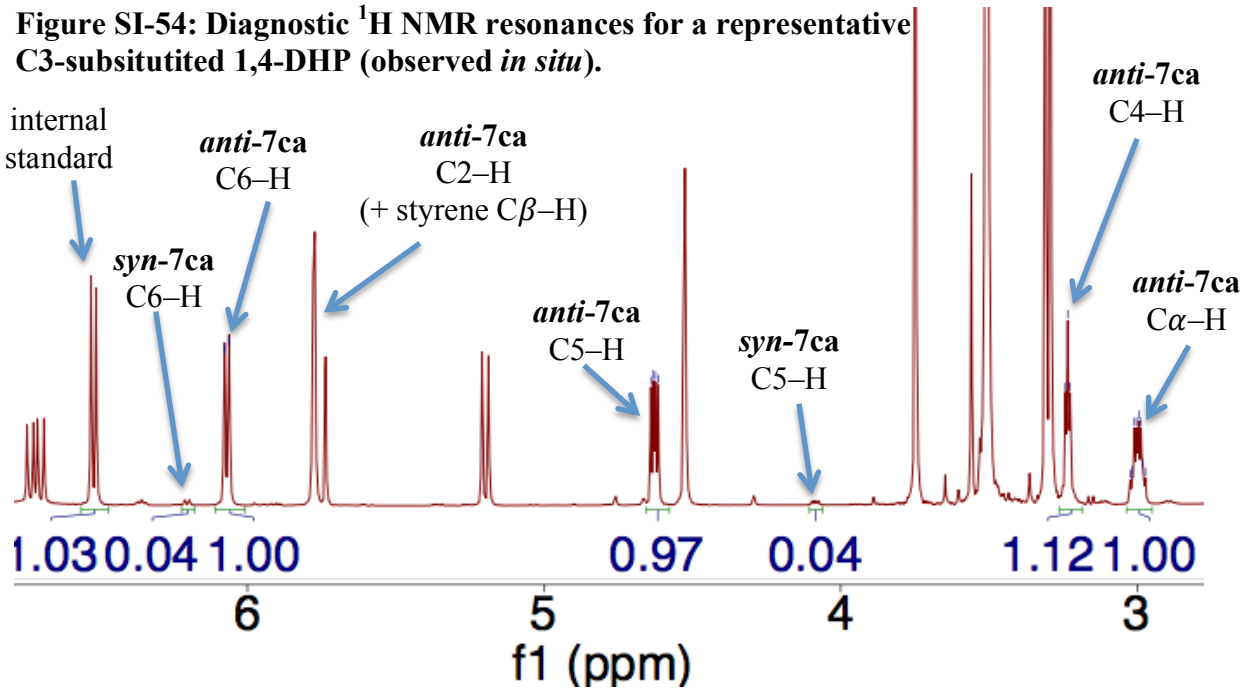

Methyl 1-(dimethoxy(methyl)silyl)-4-((S)-1-phenylethyl)-1,4-dihydropyridine-3-carboxylate (**7ba**)

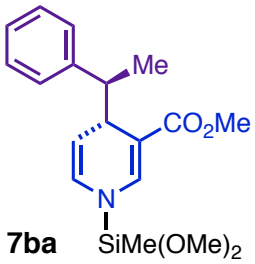

7ba

^{1}H NMR (500 MHz, THF-d_8):

Anti diastereomer

δ 6.01 (dd, J = 7.8, 1.2 Hz, 1H; C6–H), 4.93 (dd, J = 7.8, 5.1 Hz, 1H; C5–H), 3.09 (apparent qd, J = 7.3, 4.4 Hz, 1H; Cα–H), 1.27 (d, J = 7.3 Hz, 3H; Cα–CH_3).

Syn diastereomer

δ 6.23 (dd, J = 8.0, 1.2 Hz, 1H; C6–H), 4.47 (dd, J = 7.9, 4.8 Hz, 1H; C5–H), 3.19 (apparent dtd, J = 9.6, 7.0, 5.9, 3.7 Hz, 1H; Cα–H), 1.24 (d, J = 7.2 Hz, 3H; Cα–CH_3).

Conversion to **7ba**: 90% (3.5 h), 93% (7 h), 92% (23.5 h; no **1b** remaining).

(*Anti*):(*Syn*) = 4.6:1 (23.5 h)

(S)-1-(dimethoxy(methyl)silyl)-3-methyl-4-((S)-1-phenylethyl)-1,4-dihydropyridine (**7ca**)

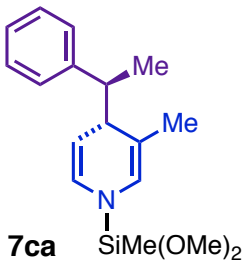

7ca

^{1}H NMR (500 MHz, THF-d_8):

Anti diastereomer

δ 6.07 (dd, J = 7.8, 1.2 Hz, 1H; C6–H), 4.63 (dd, J = 7.9, 4.4 Hz, 1H; C5–H), 3.24 (apparent t, J = 4.1 Hz, 1H; C4–H), 3.00 (qd, J = 7.2, 3.7 Hz, 1H; Cα–H), 1.29 (d, J = 7.3 Hz, 3H; Cα–CH_3).

Syn diastereomer

δ 6.21 (d, J = 8.0 Hz, 1H; C6–H), 4.09 (dd, J = 8.0, 4.1 Hz, 1H; C5–H).

Conversion to **7ca**: 51% (3.5 h), 75% (7 h), 98% (23.5 h, <1% **1c** remaining).

(*Anti*):(*Syn*) = 25:1 (23.5 h).

1-(dimethoxy(methyl)silyl)-4-((S)-1-phenylethyl)-1,4-dihydropyridazine (**7ea**)

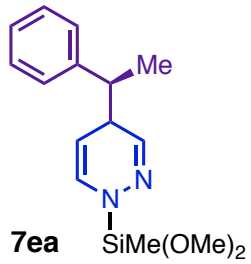

^{1}H NMR (500 MHz, THF-d_8):

Major diastereomer
δ 6.57 (apparent t, J = 2.6, 1H; C3–H), 6.38 (d, J = 8.4 Hz, 1H; C6–H), 4.38 (ddd, J = 8.0, 4.0, 2.7 Hz, 1H; C5–H), 3.09 (dt, J = 6.7, 3.5 Hz, 1H; C4–H), 2.75 (p, J = 7.0 Hz, 1H; Cα–H), 1.32 (d, J = 7.1 Hz, 3H; Cα–CH_3).

Minor diastereomer
δ 6.50–6.40 (m, C6–H and C3–H), 4.44–4.40 m; C5–H).

Conversion to **7ea**: 95% (4 h; no **1e** remaining).

dr > 28:1 (4 h; NB, the integrals of the diagnostic signals for the minor diastereomer are clearly inflated due to partial overlap with the much larger signals of the major diastereomer).

(S)-1-(dimethoxy(methyl)silyl)-3-methoxy-4-((S)-1-phenylethyl)-1,4-dihydropyridazine (**7ha**)

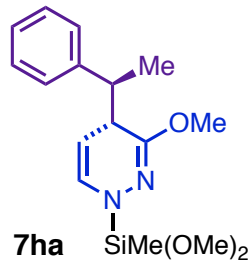

^{1}H NMR (500 MHz, THF-d_8):

Anti diastereomer
δ 6.34 (d, J = 7.8 Hz, 1H; C6–H), 4.54–4.51 (m, 1H; C5–H; overlaps DMMS Si–H signal), 3.36 (apparent t, J = 4.5 Hz, 1H; C4–H), 3.19 (qd, J = 7.2, 5.1 Hz, 1H; Cα–H) 1.27 (d, J = 7.3 Hz, 3H; Cα–CH_3).

Syn diastereomer
δ 4.12 (dd, J = 7.9, 4.0 Hz, 1H; C5–H).

Conversion to **7ea**: 96% (4 h; no **1h** remaining).

(*Anti*):(*Syn*) = >30:1 (4 h).

(S)-1-(dimethoxy(methyl)silyl)-3-methoxy-4-((S)-1-phenylethyl)-1,4-dihydropyridine (**7ia**)

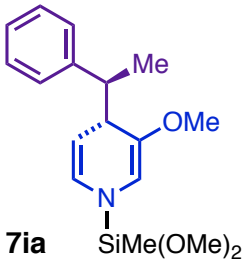

7ia

^{1}H NMR (500 MHz, THF-d_8):

Anti diastereomer
δ 6.01 (d, J = 7.8 Hz, 1H; C6–H), 5.47 (s, 1H; C2–H), 4.59 (dd, J = 7.9, 4.4 Hz, 1H; C5–H), 3.15 (qd, J = 7.3, 4.0 Hz, 1H; Cα–H), 1.27 (d, J = 7.4 Hz, 3H; Cα–CH_3).

Syn diastereomer
δ 6.18 (d, J = 7.9 Hz, 1H; C6–H), 4.15 (dd, J = 8.0, 4.0 Hz, 1H; C5–H).

Conversion to **7ia**: 27% (4 h), 45% (8 h), 78% (24 h, 9% **1i** remaining)

(*Anti*):(*Syn*) = 12:1 (24 h)

(R)-1-(dimethoxy(methyl)silyl)-4-(1-phenylethyl)-4-(trifluoromethyl)-1,4-dihydropyridine (**7ja**)

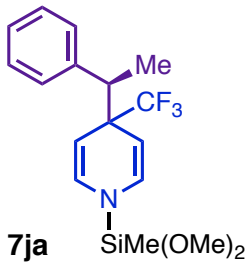

7ja

^{1}H NMR (500 MHz, THF-d_8) δ 6.41 (dd, J = 8.0, 1.4 Hz, 1H; C2/6–H), 6.29 (dd, J = 8.2, 1.4 Hz, 1H; C2/6–H), 4.61 (dd, J = 8.1, 2.9 Hz, 1H; C3/5–H), 4.45 (dd, J = 8.2, 2.9 Hz, 1H; C3/5–H), 2.98 (q, J = 7.2 Hz, 1H; Cα–H), 1.38 – 1.28 (m, 3H; Cα–CH_3).

Conversion to **7ja**: 88% (3.5 h), 95% (7 h; no **1j** remaining).

(S)-1-(dimethoxy(methyl)silyl)-2-methyl-4-(1-phenylethyl)-1,4-dihydropyridine (**7ka**)

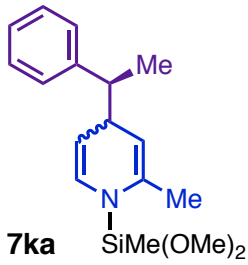

7ka

^{1}H NMR (500 MHz, THF-d_8):

Major diastereomer

δ 6.30 (dd, J = 8.1, 0.8 Hz, 1H; C6–H), 4.41 (ddd, J = 8.0, 3.9, 2.3 Hz, 1H; C5–H), 4.35 (ddd, J = 3.9, 2.5, 1.3 Hz, 1H; C3–H), 1.28 (d, J = 7.1 Hz, 3H; Cα–CH_3).

Minor diastereomer

δ 6.35 (d, J = 8.2 Hz, 1H; C6–H), 4.46 (ddd, J = 8.2, 4.0, 2.4 Hz, 1H; C5–H), 4.29 (ddd, J = 3.8, 2.4, 1.2 Hz, 1H; C3–H), 1.28 (d, J = 7.1 Hz, 3H; Cα–CH_3).

Conversion to **7ka**: 4% (3 h), 8% (7 h), 20% (23.5 h, 63% **1k** remaining)

dr = 2:1 (23.5 h)

(S)-1-(dimethoxy(methyl)silyl)-2-methoxy-4-(1-phenylethyl)-1,4-dihydropyridine (**7la**)

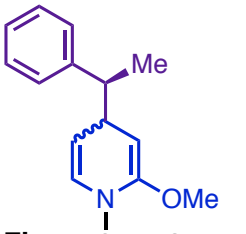

7la

^{1}H NMR (500 MHz, THF-d_8):

Major diastereomer

δ 6.25 (d, J = 8.0 Hz, 1H; C6–H), 4.43 – 4.37 (m, 1H; C5–H).

Minor diastereomer

δ 6.28 (d, J = 8.1 Hz, 1H; C6–H), 4.47 – 4.44 (m, 1H; C5–H).

Conversion to **7la**: 0% (3.5 h), 2% (8 h), 7% (23 h, 76% **1l** remaining)

dr = ca. 2:1 (23.5 h)

(S)-1-(dimethoxy(methyl)silyl)-4-(1-phenylethyl)-2-(trifluoromethyl)-1,4-dihydropyridine (**7ma**)

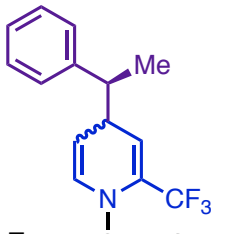

7ma

^{1}H NMR (500 MHz, THF-d_8):

Major diastereomer

δ 6.41 (d, J = 7.9 Hz, 1H; C6–H), 5.42 (d, J = 4.9 Hz, 1H; C3–H), 3.18 (apparent t, J = 5.1 Hz, 1H; C4–H), 2.74 (p, J = 7.0 Hz, 1H; Cα–H), 1.29 (dd, J = 7.1Hz, 3H; Cα–CH_3).

Minor diastereomer

δ 6.48 (d, J = 7.9 Hz, 1H; C6–H), 5.30 (d, J = 5.4 Hz, 1H; C3–H), 4.65 (ddd, J = 7.5, 3.9, 1.8 Hz, 1H; C5–H), 1.29 (dd, J = 7.1, 3H; Cα–CH_3).

Conversion to **7ma**: trace (3.5 h), 6% (7.5 h), 12% (23.5 h, 77% **1m** remaining)

dr = 2:1 (23.5 h)

6.1.ii. Dearomatization of pyridine with styrene and substituted styrenes

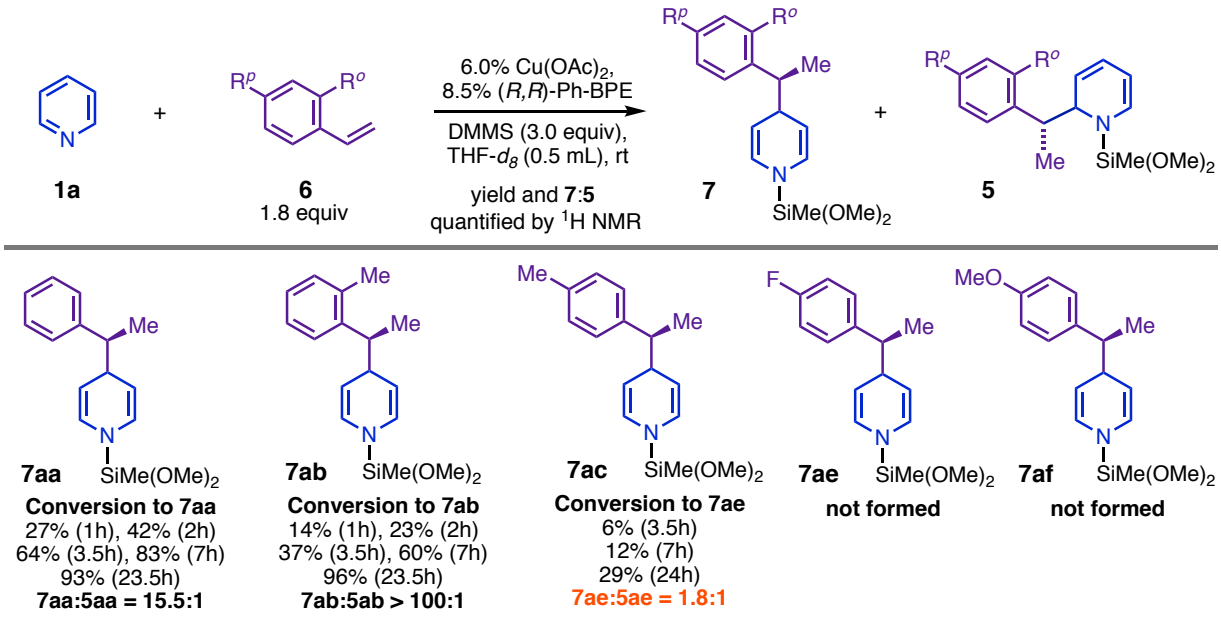

Procedure. Inside a glovebox, an oven-dried one-dram vial was charged with $Cu(OAc)_2$ (16.6 mg, 91.4 μmol) and (*R,R*)-Ph-BPE (64.7 mg, 128 μmol, 1.4:1 L_2:Cu), equipped with a small oven-dried PTFE stir-bar, and sealed with a PTFE/silicone septum-cap. The solids were dissolved in 1.00 mL THF-d_8, and DMMS (0.560 mL, 4.55 mmol) was added immediately afterward. The resulting mixture was stirred at rt for 15 min, during which time all $Cu(OAc)_2$ dissolved and the color turned yellow-orange. An oven-dried glass microsyringe was used to deliver a 330 μL aliquot of the phenethylcopper solution to another oven-dried one-dram vial that had been equipped with a PTFE stir-bar and sealed with a PTFE/silicone septum-cap. The indicated styrene (0.54 mmol) was added, and the resulting mixture was aged for 20–35 min before being charged with 200 μL of a solution prepared from pyridine (119.4 mg, 1.51 mmol, weighed), 2,6-dimethoxytoluene (113.8 mg, 0.748 mmol; NMR internal standard), and 750 μL THF-d_8. The resulting reaction mixture was then transferred to an oven-dried medium-wall J-Young NMR tube using an oven-dried glass pipet, and the tube was sealed with a PTFE piston. The mixture was removed from the glovebox and periodically monitored by ^{1}H NMR spectroscopy (ns = 8, d1= 24s), being maintained at rt between analyses. It was estimated that the phenethylcopper mixture generated upon addition of **6** contained 18.4 μmol $Cu(OAc)_2$ (6.0 mol%), 25.7 μmol (*R,R*)-Ph-BPE, 0.915 mmol DMMS (3.0 equiv), and 0.54 mmol **6** (1.76 equiv.). The 200 μL aliquot of heterocycle solution was estimated to have contained 0.306 mmol pyridine, giving $[Het]_0$ = ca. 0.51 M.

(S)-1-(dimethoxy(methyl)silyl)-4-(1-phenylethyl)-1,4-dihydropyridine and *1-(dimethoxy(methyl)silyl)-2-((R)-1-phenylethyl)-1,2-dihydropyridine* (**7aa** + **5aa**)

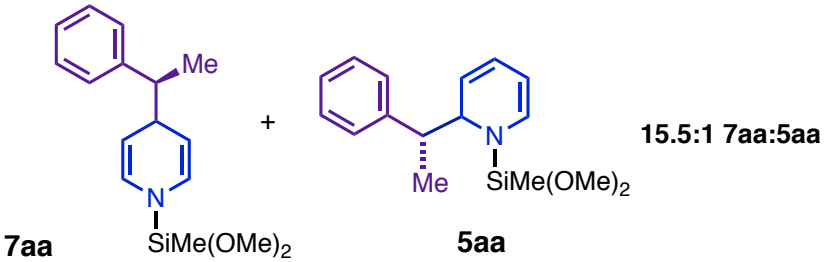

7aa **5aa**

^{1}H NMR (500 MHz, THF-d_8):

7aa

δ 6.13 (d, J = 8.1 Hz, 1H; C2/6–H), 6.09 (d, J = 8.1 Hz, 1H; C2/6–H), 4.43 (ddd, J = 8.1, 3.8, 2.5 Hz, 1H; C3/5–H), 4.39 (ddd, J = 8.1, 3.8, 2.5 Hz, 1H; C3/5–H), 3.27 – 3.22 (m, 1H; C4–H), 2.73 – 2.62 (m, 1H; Cα–H), 1.30 (d, J = 7.1 Hz, 3H; Cα–CH_3).

5aa

δ 6.23 (dd, J = 7.2, 1.1 Hz, 1H; C6–H), 6.03 – 5.97 (m, 1H; C4–H), 5.26 (ddt, J = 8.9, 5.9, 1.2 Hz, 1H; C3–H), 4.05 (ddd, J = 8.3, 5.9, 1.1 Hz, 1H; C2–H), 3.08 (p, J = 7.2 Hz, 1H; Cα–H). The multiplet associated with C5–H is visible but partly obscured by the styrene olefinic resonance at δ 5.20 ppm.

Conversion to **7aa**: 27% (1 h), 42% (2 h), 64% (3.5 h), 83% (7h), 93% (23.5 h).

Conversion to **5aa**: ca. 2% (1 h), 3% (2 h), 5% (3.5 h), 6% (7h), 6% (23.5 h).

(1,4):(1,2) = 15.5:1.

Figure SI-55: Diagnostic resonances for 7aa and the 1,2-regioisomer, 5aa

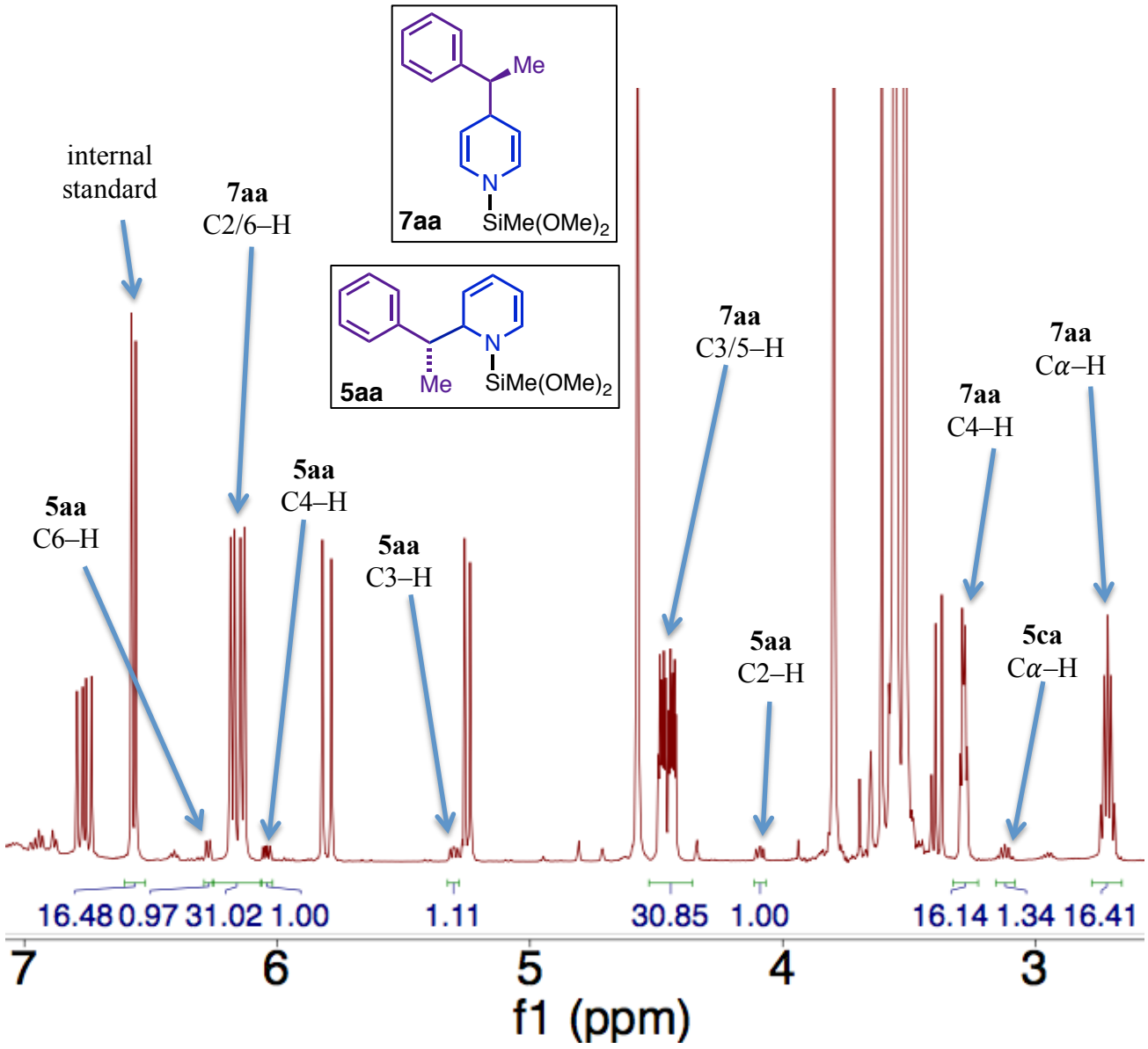

(S)-1-(dimethoxy(methyl)silyl)-4-(1-(o-tolyl)ethyl)-1,4-dihydropyridine (**7ab**)

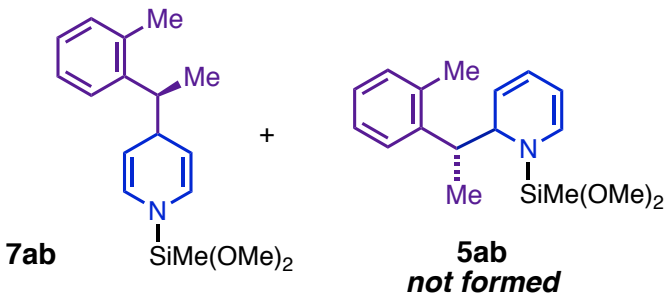

7ab **5ab** ***not formed***

^{1}H NMR (500 MHz, THF-d_8):

7ab

δ 6.22 (dd, *J* = 8.1, 1.1 Hz, 1H; C2/6–H), 6.13 (dd, *J* = 8.1, 1.2 Hz, 1H; C2/6–H), 4.55 (ddd, *J* = 8.2, 3.8, 2.5 Hz, 1H; C3/5–H), 4.41 (ddd, *J* = 8.1, 3.8, 2.5 Hz, 1H; C3/5–H), 3.22 (dt, *J* = 6.3, 3.8 Hz, 1H; C4–H), 3.04 (p, *J* = 6.9 Hz, 1H; C*α*–H), 2.35 (s, 3H; C*ortho*–H), 1.32 (d, *J* = 7.0 Hz, 4H; C*α*–CH_3).

Conversion to **7aa**: 14% (1 h), 23% (2 h), 37% (3.5 h), 60% (7 h), 96% (23.5 h).

(S)-1-(dimethoxy(methyl)silyl)-4-(1-(p-tolyl)ethyl)-1,4-dihydropyridine and *1-(dimethoxy(methyl)silyl)-2-((R)-1-(p-tolyl)ethyl)-1,2-dihydropyridine* (**7ac** + **5ac**)

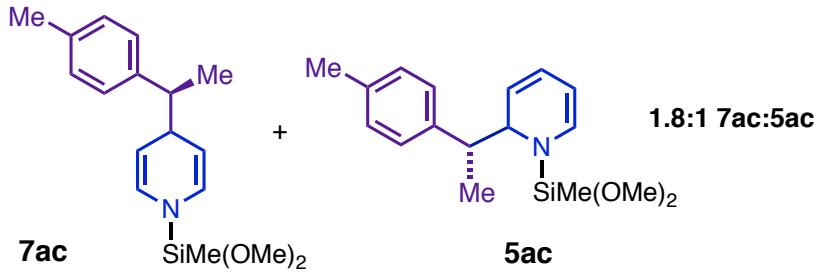

^{1}H NMR (500 MHz, THF-d_8):

7ac

δ 6.14 (d, *J* = 8.1 Hz, 1H; C2/6–H), 6.10 (d, *J* = 8.0 Hz, 1H; C2/6–H), 4.45 (ddd, *J* = 8.1, 3.8, 2.5 Hz, 1H; C3/5–H), 4.40 (ddd, *J* = 8.1, 3.7, 2.5 Hz, 1H; C3/5–H), 2.64 (p, *J* = 6.9 Hz, 1H; C*α*–H), 1.30 (d, *J* = 7.1 Hz, 3H; C*α*–CH_3).

5ac

δ 6.23 (d, *J* = 7.0 Hz, 1H; C6–H), 6.00 (dd, *J* = 9.3, 5.3 Hz, 1H; C4–H), 5.30 – 5.25 (m, 1H; C3–H), 5.22 (ddd, *J* = 6.9, 5.4, 1.3 Hz, 1H; C5–H), 4.06 – 4.01 (m, 1H; C2–H), 3.11 – 3.00 (m, 1H; C*α*–H), 1.27 (d, *J* = 7.1 Hz, 3H; C*α*–CH_3).

Conversion to **7ac**: 6% (3.5 h), 12% (7 h), 29% (24 h).

Conversion to **5ac**: ca. 3% (3.5 h), 4% (7h), 8% (24 h).

(1,4):(1,2) = 1.8:1.

6.1.iii. Dearomatization of 3-phenylpyridine with 3-fluorostyrene.

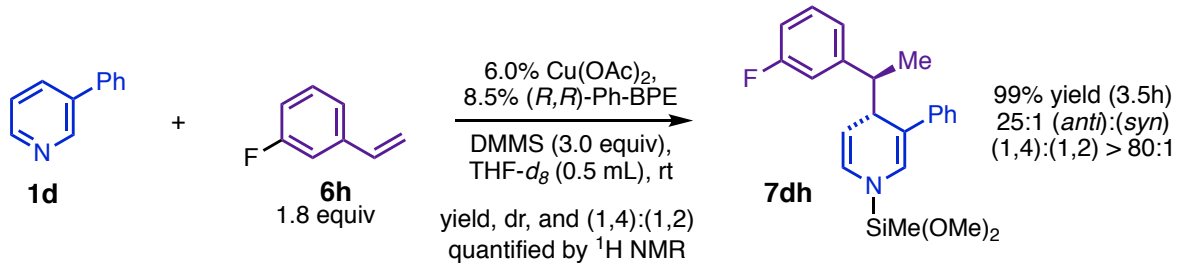

Procedure. The reaction mixture was prepared and analyzed in the manner described in Section 6.1.ii. (above), albeit using a 210 μL aliquot of a heterocycle stock solution prepared from 3-phenylpyridine (93.4 mg, 0.602 mmol), 1,3,5-trimethoxybenzene as an internal standard (32.6 mg, 0.194 mmol), and 300 μL of THF-d_8. The relative stoichiometry values for other reaction components were the same as in section 6.1.ii. $[Het]_0$ for the dearomatization reaction mixture was estimated as 0.50 M.

(S)-1-(dimethoxy(methyl)silyl)-4-((S)-1-(3-fluorophenyl)ethyl)-3-phenyl-1,4-dihydropyridine (**7dh**)

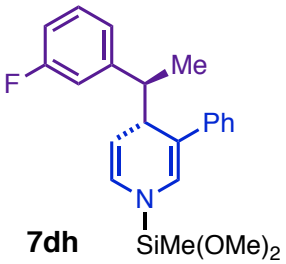

7dh

^{1}H NMR (500 MHz, THF-d_8):

Anti diastereomer
δ 6.33 (s, 1H; C2–H), 6.12 (d, J = 7.9 Hz, 1H; C6–H), 4.83 (dd, J = 7.7, 4.3 Hz, 1H; C5–H), 4.05 (apparent t, J = 4.2 Hz, 1H; C4–H), 2.98 (qd, J = 7.1, 3.3 Hz, 1H; Cα–H), 1.30 – 1.20 (m, 3H; Cα–CH_3).

Syn diastereomer
The C5–H signal of the *syn* diastereomer is partially obscured by the DMMS Si-H satellite peak at δ 4.29 ppm. The integral for this diagnostic can be inferred by subtracting the integral for the other Si–H satellite peak from that of the complex multiplet. The C4–H signal of the syn diastereomer overlaps with the C4–H signal above, and its integral can be estimated by subtracting the integral of the C3–H signal of the anti-diastereomer from the integral of the C4–H signal. Both calculations yield similar values.

Conversion to **7dh**: 99% (3.5 h)

(*anti*):(*syn*) = 25:1 (3.5 h)

(1,4):(1,2) > 80:1. The 1,2-regioisomer was present in exceedingly trace quantities if at all.

6.2.1. In situ ^{1}H-NMR monitoring of the dearomatization of pyridine with 3-vinylfuran. ***(6l)***

(a) Synthesis of *3-vinylfuran*

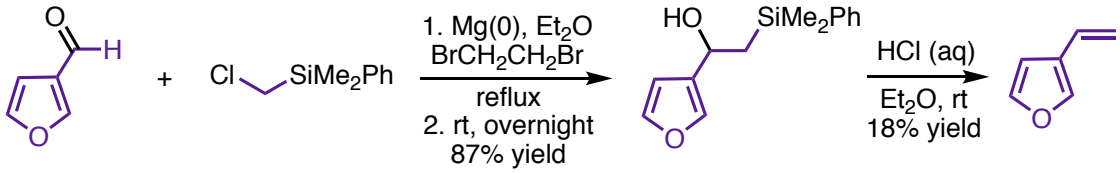

Procedure. Prepared by a modification of literature procedures.[8]

Step One. A 100 mL two-neck round-bottom Schlenk flask was connected to a dual manifold, equipped with a dry PTFE stir-bar, charged with magnesium flakes (1.28 g, 52.7 mmol, 1.32 equiv), and then placed under an N_2 atmosphere and equipped with a dry reflux condenser. Et_2O (25 mL) and (chloromethyl)dimethyl(phenyl)silane (10.1 mL, 56.0 mmol, 1.41 equiv) were injected via the septum, and the mixture was stirred and heated to reflux in an oil bath (bath temperature = 45 °C). A few droplets of 1,2-dibromoethane (ca. 40 μL, *caution: highly carcinogenic*) were added to the reaction mixture. Heating was continued for 90 min, and then the mixture was cooled in an ice-water bath. A solution of 3-furaldehyde (4.20 g, 39.8 mmol) in 12 mL Et_2O was added over the course of 15 min, and the stirred mixture was allowed to warm to rt overnight. On the subsequent

day, the condenser was removed and the dark brown residue present was diluted in Et_2O and quenched by cautious addition of saturated aqueous NH_4Cl (*caution: considerable heat evolution occurs, which can cause uncontrolled boiling of the Et_2O*). The resulting mixture was partitioned between saturated NH_4Cl and Et_2O, and the aqueous layer was back-extracted with Et_2O. The combined organics were dried over $MgSO_4$, filtered, and concentrated *in vacuo* to give the crude β-silyl alcohol as a very viscous brown oil (12.65 g). A 9.9 mg sample of this material was analyzed by ^{1}H NMR in the presence of 18.7 mg 2,6-dimethoxytoluene (NMR internal standard), and it was inferred by comparison of product to standard integrals that the crude sample was ca. 68% β-silyl alcohol by weight.

Step Two. The crude β-silyl alcohol from Step one (11.9 g, 32.8 mmol after correction for purity) was dissolved in 18 mL Et_2O and vigorously stirred in the presence of 22 mL 1.5 M HCl (aq). Reaction progress was periodically monitored by TLC based on lightening of the starting material spot relative to the spot associated with the silanol byproduct. More HCl was periodically added to ensure a reasonable rate of reaction: an 8 mL aliquot of 3.4 M HCl was added after 2 h, and a 6 mL aliquot of 6 M HCl was added 30 min after that. After a total reaction time of 5 h, the organic layer was separated in a separatory funnel, and the HCl layer was extracted 3x with 2 mL aliquots of Et_2O. The combined organics were successively washed with 1 M Na_2CO_3 (2 x 5 mL) and brine (5 mL), and then dried over Na_2SO_4. The supernatant was transferred with a pipet to a 100 mL round-bottom flask, and a few mg of 4-*tert*-butylcatechol were added as a stabilizer. The flask was equipped with a stir bar and a short-path distillation head, and most of the Et_2O was boiled away at atmospheric pressure while the organics were stirred in an oil bath (bath temperature = 45 °C). The collection flask was replaced with a 10 mL RBF containing ca. 1 mg of 4-*tert*-butylcatechol and cooled in a CO_2/^{i}PrOH slurry, and the apparatus was then placed under house vacuum. The receptacle flask was replaced with another 10 mL RBF after collection of ca. 1-2 mL of distillate. The fifth and sixth distillate fractions contained 66 and 88% 3-vinylfuran by weight, respectively, with the balance being Et_2O and minor (2–4 mol% quantities of dimethyl(phenyl)silanol). These fractions were combined (mass = 794 mg) and a 12.1 mg aliquot was added to 13.5 mg 2,6-dimethoxytoleune (internal standard) and analyzed by ^{1}H NMR spectroscopy. Comparison of integrals indicated that the product sample was 69% 3-vinylfuran by mass, giving a corrected yield of 5.8 mmol (18%). ^{1}H NMR (400 MHz, Acetone-d6) δ 7.64 – 7.57 (m, 1H), 7.53 – 7.47 (m, 1H), 6.69 (d, J = 1.9 Hz, 1H), 6.62 (dd, J = 17.7, 10.9 Hz, 1H), 5.52 (dd, J = 17.7, 1.5 Hz, 1H), 5.11 (dd, J = 10.9, 1.5 Hz, 1H).

(b) NMR Experiment

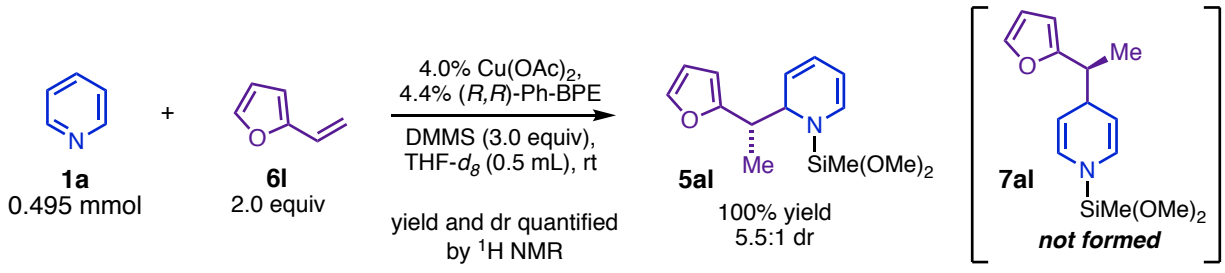

Procedure. Inside a glovebox, an oven-dried one-dram vial was charged with $Cu(OAc)_2$ (3.6 mg, 20 μmol), (*R,R*)-Ph-BPE (11.1 mg, 22 μmol; L_2:Cu = 1.1:1), and the NMR internal standard, 1,3,5-trimethoxybenzene (39.7 mg, 0.236 mmol). The vial was equipped with a small oven-dried PTFE stir-bar and sealed with a PTFE/silicone septum-cap. The solids were dissolved in THF-d_8 (500 μL), and DMMS (180 μL, 1.46 mmol, 2.95 equiv) was added immediately afterward. The resulting

mixture was aged at rt for 15 min, during which time all $Cu(OAc)_2$ dissolved and the color turned orange. Pyridine (40.0 μL, 39.1 mg, 0.495 mmol) and 3-vinylfuran (135 mg of 69 weight% solution; ca. 94 mg 3-vinylfuran delivered = 1.00 mmol = 2.02 equiv) were added in rapid succession and the resulting dearomatization reaction mixture was transferred to an oven-dried medium-wall J-Young NMR tube. A 50 μL aliquot of fresh THF-d_8 was used to complete the transfer, and the NMR tube was sealed with a PTFE piston, removed from the glovebox, and maintained at rt. Proton NMR spectra were recorded (8 scans, d1 = 24s) after 8.5 h, 24 h, and 44 h, and the NMR-yield of **5al** was determined by comparing the integrals of its diagnostic signals to the integral of the internal standard peak; by the 44 h time-point, the yield of **5al** was determined to be 98%. The 1,4-DHP regioisomer was undetectable.

1-(dimethoxy(methyl)silyl)-2-((S)-1-(furan-2-yl)ethyl)-1,2-dihydropyridine (**5al**)

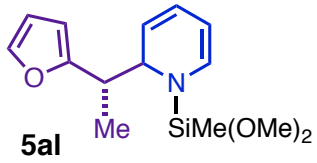

5al

^{1}H NMR (500 MHz, THF-d_8):

Major diastereomer

δ 6.25 (dd, J = 7.0, 1.1 Hz, 1H; C6–H), 5.94 (ddd, J = 9.3, 5.4, 0.8 Hz, 1H; C4–H), 5.15 (ddt, J = 9.4, 5.8 Hz, 1.2 Hz, 1H; C3–H), 5.10 – 5.02 (ddd, J = 6.8, 5.6 Hz, 1.2 Hz, 1H; C5–H; overlap with an olefinic resonance of 3-vinylfuran obscures the known ddd fine structure of this peak, and J's have been estimated from the visible portion of the multiplet), 3.96 (ddd, J = 7.0, 5.8, 0.9 Hz, 1H; C2–H), 2.88 (p, J = 7.1 Hz, 1H; Cα–H), 1.24 (d, J = 7.0 Hz, 3H; Cα–CH_3).

Minor diastereomer

δ 5.87 (ddd, J = 9.3, 5.4, 0.8 Hz, 1H; C4–H), 5.18 (ddd, J = 7.0, 5.4, 1.2 Hz; C5–H), 5.11 (ddt, J = 8.8, 6.2, 1.2 Hz, 1H; C3–H), 3.75 (ddd, J = 9.0, 6.1, 1.2 Hz, 1H; C2–H), 1.27 (d, J = 7.5 Hz, 3H; Cα–CH_3). The C6–H and Cα–H signals of the minor diastereomer are identifiable but partially obscured by the corresponding signals of the major diastereomer.

Conversion to **5al**: 47% (8.5 h), 88% (24 h), 100% (44 h). The 1,4-DHP regioisomer does not form in detectable quantities.

dr = 5.5:1 (44 h)

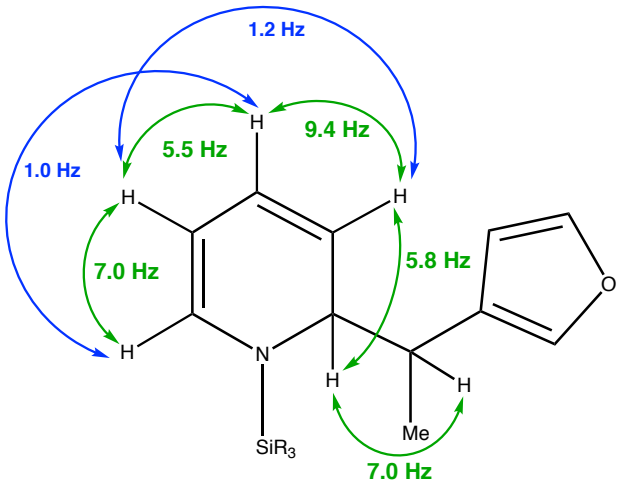

Figure SI-56: Proton NMR coupling-constant network for 1,2-DHP 5al.

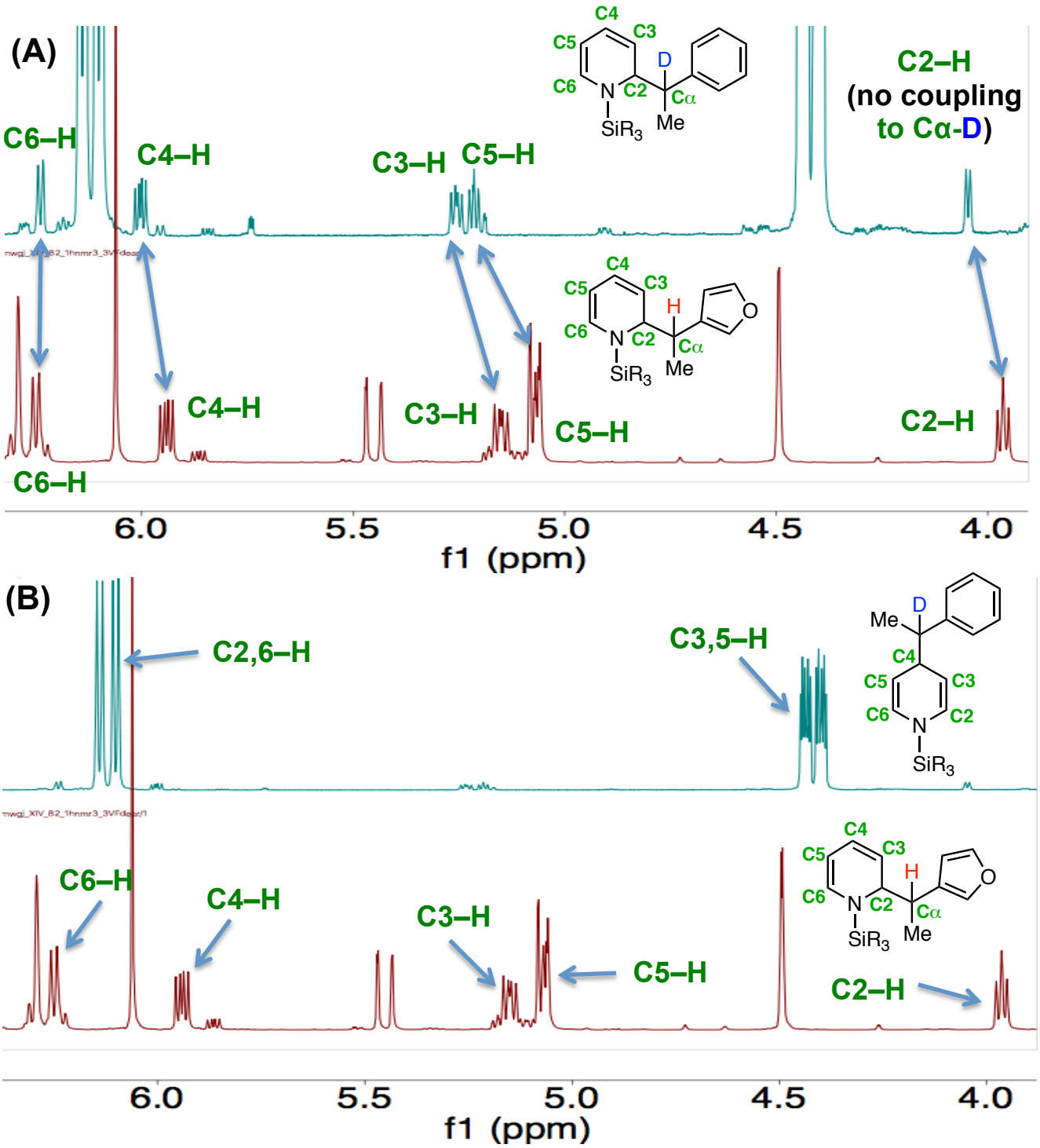

Figure SI-57

(A) Comparison of ^{1}H NMR diagnostics for 5aa and 5al. Note that 5aa is deuterated at C*α* and its C2 resonance is consequently a double rather than an apparent triplet.

(B) Comparison of diagnostic resonances for 1,4-DHP 7aa to those of 5al. There is no 1,4-DHP formed in the reaction of pyridine with 3-vinylfuran.

6.3. NMR analysis of crude 1,4-DHP derived from pyridine and 2-fluorostyrene (6d)

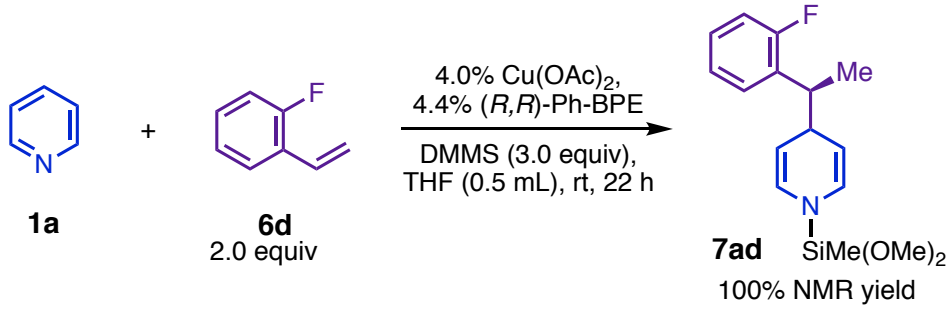

Procedure. The dearomatization of pyridine with 2-fluorostyrene (**6d**) was performed inside a glovebox according to the general procedure in reference 1 with a reaction time of 22 h. The reaction vessel with outfitted with the adapter assembly in Figure SI-7, brought outside the glovebox and stripped of volatiles under high vacuum using a dual manifold. After ca. 30 min of drying under high vacuum, the residue was brought into the glovebox and redissolved in 850 μL of a solution of 33.7 mmol 1,3,5-trimethoxybenzene (internal standard) in C_6D_6. A 100 μL aliquot of this solution was further diluted with C_6D_6 to ca. 600 μL and transferred to an oven-dried J-Young NMR tube, which was subsequently sealed with a PTFE piston. The mixture was analyzed by ^{1}H NMR (8 scans, d1 = 24s), and the conversion to DHP **7ad** was found to be 100% by comparison of the integrals of diagnostic resonances of **7ad** to those of the internal standard peaks.

^{1}H NMR data for **7ad** (500 MHz, C_6D_6). δ 7.21 – 7.10 (m, 1H), 6.88 (dq, J = 6.4, 3.9 Hz, 3H), 6.21 (d, J = 8.0 Hz, 1H; C2/6–H), 6.15 (d, J = 8.0 Hz, 1H; C2/6–H), 4.56 (ddt, J = 14.4, 7.8, 2.9 Hz, 2H; C3/5–H), 3.54 (q, J = 4.3 Hz, 1H; C4–H), 3.23 (d, J = 1.8 Hz, 6H; $Si(OCH_3)_2$), 1.32 (d, J = 7.1 Hz, 3H; Cα–CH3), -0.01 (s, 3H; Si–CH_3). The Cα–H multiplet is visible but partially obscured by the OCH_3 resonance of 1,3,5-trimethoxybenzene.

7. Computational Details

All reported calculations were performed using the ORCA software[9] or Gaussian 03[10]. Images of the 3D structures were rendered using CYLView.[11] The geometry of all reactants and transition states were optimized using the B3LYP functional in the gas phase. In these geometry optimizations, a mixed basis set of SDD[12] for Cu and 6-31G(d) for all other atoms was used. Ground and transition state geometries were validated by vibrational analysis at the same level, showing zero and one imaginary frequencies respectively. Single-point energies were calculated using the BP86[13] hybrid functional on a mixed basis set of SDD for Cu and 6-311+G(d,p) for all other atoms. The D3 dispersion correction with Becke–Johnson damping was applied to these electronic energies.[14] In these energy calculations, the CPCM solvation model[15] with THF as solvent was applied. For benchmark purposes, DLPNO-CCSD(T)[16] calculations as implemented in ORCA were performed on truncated systems using the aug-cc-pVTZ[17] basis set with tight PNO settings and the default corresponding auxiliary basis. The reported Gibbs free energies and enthalpies include zero-point and thermal corrections calculated at 298 K.

Selection of Density Functional

To evaluate the accuracy of various density functionals in the context of the types of reactions and bonding changes in this study, we selected a few representative reactions and performed high-level

ab initio single point calculations using L = PH_3 as a simplified ligand. These geometries were optimized at B3LYP/6-31G(d)-SDD(Cu). Within the functionals evaluated, BP86-D3(BJ) was among the best in terms of approximating the thermochemical parameters. Further, compared to other common functionals, it was much better in approximating the key double-dearomatization barrier. As expected based on our past studies on CuH-catalyzed reactions, inclusion of a suitable dispersion correction method was crucial.[18] Notably, standard functionals like B3LYP, M06, and PBE0 very poorly estimated this transition state energy with or without dispersion correction.

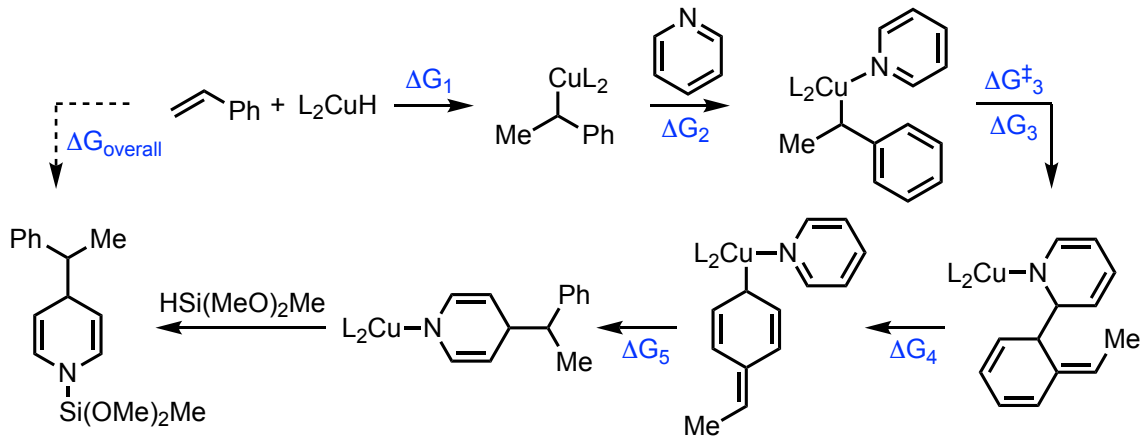

Method/6-311+G(d,p)–SDD(Cu)	Mean Absolute Error vs. DLPNO-CCSD(T)/aug-cc-pVTZ (kcal/mol)	Error in Double-Dearomatization Barrier (kcal/mol)
M06	4.1	+5.9
PBE0	7.4	+11.2
BP86	10.6	+13.3
HF	22.4	+27.8
B3LYP-D3(BJ)	4.6	+6.1
BLYP-D3(BJ)	5.2	+4.9
BMK-D3(BJ)	2.4	+1.5
BP86-D3	3.0	+1.1
BP86-D3(BJ)	2.6	+0.1
M06-D3(BJ)	2.5	+3.8
PBE0-D3(BJ)	2.4	+3.0

Effect of Basis and Solvation Model

The choice of basis set and solvation was evaluated using the double-dearomatization barrier (**[$TS_{14,15}$]aa**) as an indicator, with (*S*,*S*)-Ph-BPE as a ligand. We tested the effect of varying basis set (including all-electron *vs.* effective core potential), solvation model, and choice of solvent. None of these factors had a substantial effect on the calculated barrier. Moreover, the method employed in the manuscript gives an estimate that is neither atypically high nor low within the range obtained.

Method	**[TS$_{14,15}$]aa** (kcal/mol)
Standard: CPCM(THF)/BP86-D3(BJ)/6-311+G(d,p)–SDD(Cu) //B3LYP/6-31G(d)–SDD(Cu)	25.8
PCM instead of CPCM	25.5
SMD instead of CPCM	27.0
Toluene instead of THF	24.8
Pyridine instead of THF	25.7
Diethyl ether instead of THF	25.3
6-31G(d) instead of 6-311+G(d,p)	23.7
6-31G(d,p) instead of 6-311+G(d,p)	23.5
6-31+G instead of 6-311+G(d,p)	22.7
6-31++G instead of 6-311+G(d,p)	22.6
aug-cc-pVDZ instead of 6-311+G(d,p)	23.0
cc-pVTZ instead of 6-311+G(d,p)	26.7
def2SVPP instead of 6-311+G(d,p)	21.8
def2TZV instead of 6-311+G(d,p)	23.4
def2TZVP instead of 6-311+G(d,p)	27.0
def2TZV instead of 6-311+G(d,p) and SDD(Cu)	21.2
def2TZVP instead of 6-311+G(d,p) and SDD(Cu)	26.1
LANL2DZ instead of SDD	24.2
LANL2MB instead of SDD	24.1

Cartesian Coordinates and Calculated Thermodynamic Parameters for Optimized Structures

```
Structure 2aa
Charge: 0
Multiplicity: 1
Imaginary Frequencies: 0
Electronic Energy (B3LYP): -2755.918434
Gibbs Free Energy (B3LYP): -2755.158495
Electronic Energy (BP86+D3(BJ)+CPCM(THF)): -2756.889408
Total Gibbs Free Energy: -2756.129470
Geometry:
 P                 -1.03468500   -1.25874700   -1.20277400
 C                 -0.12387400   -1.70522700   -2.81917200
 C                 -1.18596600   -2.40519900   -3.69090400
 C                 -2.51075900   -1.67015300   -3.46895200
 C                 -2.75709900   -1.59039500   -1.94115800
 H                 -0.88372700   -2.40581600   -4.74522000
 H                 -1.30488400   -3.45368400   -3.39098800
 H                 -3.35146700   -2.17094400   -3.96316000
 H                 -2.45143800   -0.65759800   -3.88741900
 P                  0.87380500   -0.93083600    1.49829000
 C                 -0.03930200   -0.78919000    3.17281500
 C                  0.92470300   -1.37647200    4.22188000
 C                  2.33604800   -0.93025100    3.83334100
 C                  2.55743600   -1.30294300    2.34673800
 H                  0.65016600   -1.04440000    5.23080400
 H                  0.88098500   -2.47307500    4.22349000
 H                  3.10732700   -1.39306800    4.46090300
 H                  2.42937300    0.15531200    3.96140900
```

H	0.08247700	-0.72430200	-3.26544700
H	-3.03225600	-2.59460400	-1.59347500
C	0.46350200	-2.64049900	0.82607100
H	0.38851700	-3.37462500	1.63787100
H	1.33368800	-2.91846800	0.22016800
C	-0.81102500	-2.70960900	-0.04110500
H	-0.07510000	0.29820000	3.31850200
H	2.68367800	-2.39191000	2.28825900
C	-1.46535000	-1.29646800	3.18441300
C	-4.14731800	-2.18029000	3.14502900
C	-2.51323300	-0.41328900	2.86984300
C	-1.79218700	-2.62710000	3.49160900
C	-3.11899100	-3.06491200	3.47343200
C	-3.83786300	-0.85123300	2.84555200
H	-2.28828900	0.62646500	2.64431400
H	-1.01136000	-3.33295800	3.75982900
H	-3.34632200	-4.09841800	3.72316600
H	-4.62770500	-0.14955900	2.59264400
H	-5.17969600	-2.51984800	3.13363700
C	3.76777900	-0.65143700	1.71544400
C	6.07069800	0.53823300	0.59923100
C	3.88985200	0.74517100	1.63120800
C	4.82178600	-1.43685000	1.22883600
C	5.96393900	-0.85084000	0.67686600
C	5.02727300	1.33434600	1.07987900
H	3.08688300	1.37871700	1.99815000
H	4.74909900	-2.52073600	1.28594200
H	6.77144800	-1.48185600	0.31385100
H	5.09944000	2.41775700	1.02867000
H	6.95842100	0.99753800	0.17285100
C	-3.85400700	-0.62958900	-1.53721900
C	-5.95930200	1.11533700	-0.85542900
C	-5.01453100	-1.11032300	-0.91598500
C	-3.76308000	0.74531800	-1.80766100
C	-4.80579200	1.60862000	-1.47122800
C	-6.05995800	-0.24808800	-0.57739200
H	-5.10237600	-2.17238400	-0.69740300
H	-2.86629200	1.14897300	-2.27093400
H	-4.71310500	2.66996200	-1.68484800
H	-6.95232600	-0.64448900	-0.09980000
H	-6.77006900	1.78975600	-0.59368300
C	1.20179100	-2.41147400	-2.63010500
C	3.70910900	-3.64279900	-2.22366500
C	1.33035000	-3.80869900	-2.65273200
C	2.35749000	-1.64409900	-2.40581000
C	3.59662600	-2.25015400	-2.20100700
C	2.57196600	-4.41807100	-2.45331000
H	0.46346700	-4.43588200	-2.83803300
H	2.27928400	-0.55960200	-2.39163000
H	4.47165000	-1.63340400	-2.01861900
H	2.64739200	-5.50213600	-2.48243600
H	4.67438300	-4.11796800	-2.07065300
H	-0.83033600	-3.65435200	-0.59895700
H	-1.69652600	-2.69476700	0.60553900
C	0.81028400	4.21178900	-0.19039300
H	-0.08225800	4.84930500	-0.20190500
C	2.01941700	5.09879900	0.15276100

H	1.84869300	5.62172300	1.09875400
H	2.94024900	4.50970500	0.25965400
H	2.19543700	5.84751900	-0.62804500
C	0.94346900	3.57039500	-1.55903200
C	2.07952500	2.82646900	-1.92061600
C	-0.07957300	3.69664100	-2.51108300
C	2.19244600	2.24498300	-3.18614600
H	2.89298500	2.70253200	-1.21025300
C	0.02499600	3.11633800	-3.77720500
H	-0.96865300	4.26664400	-2.25195100
C	1.16500000	2.38659800	-4.12315300
H	3.09321500	1.69325700	-3.44630400
H	-0.77889900	3.24620400	-4.49851000
H	1.25977900	1.94829100	-5.11369700
Cu	-0.40888900	0.53974000	-0.04235600
N	-0.62378100	2.31736500	0.62108100
C	0.55645100	3.13777800	0.94385600
C	-1.82179300	2.83663500	0.98426300
C	0.40511700	3.77550100	2.30635200
H	1.43401200	2.47448100	0.92906800
C	-1.98503200	3.84563500	1.91145900
H	-2.69269200	2.34122000	0.55392900
C	-0.82824400	4.19676300	2.68834200
H	1.28198400	3.92499100	2.93239900
H	-2.97675700	4.19738200	2.17556800
H	-0.96067800	4.73050400	3.62946600

Structure 7aa
Charge: 0
Multiplicity: 1
Imaginary Frequencies: 0
Electronic Energy (B3LYP): -1118.311518
Gibbs Free Energy (B3LYP): -1118.003026
Electronic Energy (BP86+D3(BJ)+CPCM(THF)): -1118.653399
Total Gibbs Free Energy: -1118.344907
Geometry:

C	-2.228027	1.044110	-0.700908
H	-1.693747	0.550249	-1.522898
C	-2.697881	2.422032	-1.204101
H	-3.446822	2.309254	-1.995485
H	-3.152928	3.011671	-0.398413
H	-1.862121	2.999845	-1.611545
C	-3.411068	0.163364	-0.324524
C	-3.615278	-1.069499	-0.959727
C	-4.327728	0.551273	0.666240
C	-4.696501	-1.887697	-0.624796
H	-2.915678	-1.390787	-1.728173
C	-5.408458	-0.262880	1.006860
H	-4.198514	1.501706	1.178279
C	-5.598754	-1.486987	0.361326
H	-4.832365	-2.837959	-1.135314
H	-6.104560	0.060341	1.776972
H	-6.441725	-2.120445	0.624707
N	1.623018	0.243230	0.346967
C	1.255309	1.567418	0.051896
C	0.583263	-0.579647	0.821202
C	-0.002348	2.028522	0.131153

H	2.080346	2.207991	-0.238110
C	-0.694873	-0.188765	0.927202
H	0.890612	-1.578922	1.117440
C	-1.196432	1.168008	0.483724
H	-0.164191	3.081155	-0.080475
H	-1.416046	-0.898282	1.320945
H	-1.754834	1.641203	1.311587
Si	3.277735	-0.342270	0.337475
C	4.050599	-0.472052	2.033904
H	4.113964	0.511210	2.513443
H	3.448402	-1.120660	2.679554
H	5.059178	-0.898279	1.988648
O	4.048720	0.758792	-0.630477
O	3.291866	-1.883513	-0.262338
C	5.457797	0.850750	-0.784596
H	5.670942	1.704330	-1.434776
H	5.961383	1.012463	0.177669
H	5.870713	-0.053686	-1.249691
C	2.725862	-2.261642	-1.514181
H	2.911867	-3.330191	-1.656067
H	1.644019	-2.083268	-1.529582
H	3.185107	-1.709833	-2.343654

Structure 8
Charge: 0
Multiplicity: 1
Imaginary Frequencies: 0
Electronic Energy (B3LYP): -2197.962326
Gibbs Free Energy (B3LYP): -2197.415915
Electronic Energy (BP86+D3(BJ)+CPCM(THF)): -2198.706941
Total Gibbs Free Energy: -2198.160530
Geometry:

P	0.916236	1.340140	-0.051637
C	0.111480	3.063615	0.135595
C	1.244851	3.993330	0.616024
C	2.530539	3.535018	-0.082248
C	2.678303	2.014584	0.174448
H	1.007066	5.042315	0.400197
H	1.381846	3.912694	1.701656
H	3.414557	4.073025	0.280180
H	2.461182	3.721700	-1.161765
P	-0.916172	-1.340092	-0.051581
C	-0.111092	-3.063383	0.136079
C	-1.244321	-3.993232	0.616595
C	-2.530074	-3.535296	-0.081826
C	-2.678126	-2.014880	0.174684
H	-1.006301	-5.042213	0.401009
H	-1.381446	-3.912403	1.702194
H	-3.413994	-4.073423	0.280665
H	-2.460637	-3.722157	-1.161307
H	-0.116547	3.332467	-0.903340
H	2.920822	1.882327	1.237583
Cu	-0.000554	-0.000309	-1.761989
C	-0.639509	-0.431089	1.569062
H	-0.625281	-1.124006	2.419068
H	-1.519150	0.213130	1.685541
C	0.639312	0.431480	1.569134

H	0.117005	-3.332431	-0.902791
H	-2.920466	-1.882578	1.237849
C	1.193096	-3.065859	0.903597
C	3.665579	-2.961781	2.264333
C	2.381649	-2.741140	0.226189
C	1.272594	-3.344741	2.276390
C	2.496684	-3.295749	2.948939
C	3.603325	-2.683923	0.896150
H	2.344318	-2.524521	-0.839335
H	0.379405	-3.613877	2.832363
H	2.533141	-3.523181	4.011387
H	4.502566	-2.417796	0.347983
H	4.616320	-2.924145	2.789325
C	-3.756403	-1.335063	-0.643776
C	-5.827306	-0.136586	-2.133617
C	-3.618451	-1.127427	-2.025788
C	-4.947125	-0.928808	-0.024591
C	-5.976188	-0.336355	-0.760132
C	-4.644097	-0.533225	-2.761810
H	-2.694144	-1.402489	-2.526842
H	-5.071081	-1.080818	1.045771
H	-6.892576	-0.034012	-0.259247
H	-4.511651	-0.373689	-3.828528
H	-6.624459	0.326292	-2.709351
C	3.756360	1.334595	-0.644176
C	5.826886	0.135871	-2.134344
C	4.947401	0.928809	-0.025294
C	3.617879	1.126339	-2.026039
C	4.643346	0.532017	-2.762221
C	5.976275	0.336232	-0.760998
H	5.071750	1.081267	1.044959
H	2.693323	1.401021	-2.526853
H	4.510495	0.372015	-3.828821
H	6.892915	0.034258	-0.260349
H	6.623894	-0.327104	-2.710199
C	-1.192725	3.066393	0.903073
C	-3.665223	2.962709	2.263806
C	-1.272187	3.345347	2.275861
C	-2.381313	2.741805	0.225676
C	-3.603001	2.684780	0.895642
C	-2.496277	3.296557	2.948406
H	-0.378945	3.614382	2.831805
H	-2.344002	2.525127	-0.839835
H	-4.502275	2.418742	0.347484
H	-2.532716	3.524047	4.010842
H	-4.615966	2.925218	2.788804
H	-0.000583	0.001657	-3.314006
H	0.624930	1.124463	2.419083
H	1.518929	-0.212726	1.685848

Structure 9a
Charge: 0
Multiplicity: 1
Imaginary Frequencies: 0
Electronic Energy (B3LYP): -2507.639557

Gibbs Free Energy (B3LYP): -2506.964385
Electronic Energy (BP86-D3(BJ)/CPCM(THF)): -2508.501757
Total Gibbs Free Energy: -2507.826584
Geometry:

P	0.723225	1.842469	-0.396762
C	-0.206187	3.359260	-1.097980
C	0.826067	4.505238	-1.092719
C	2.182308	3.893658	-1.460043
C	2.421956	2.693410	-0.511161
H	0.528169	5.301378	-1.786109
H	0.898667	4.958784	-0.096409
H	3.001076	4.617876	-1.374826
H	2.169344	3.546964	-2.501494
P	-0.908675	-0.643923	0.974748
C	0.045512	-1.927165	2.029442
C	-1.022728	-2.615693	2.906774
C	-2.310518	-2.700074	2.080902
C	-2.608435	-1.275069	1.555955
H	-0.674031	-3.604227	3.229126
H	-1.218647	-2.032443	3.815208
H	-3.156646	-3.076052	2.668562
H	-2.169202	-3.387940	1.237890
H	-0.377124	3.075314	-2.144098
H	2.619070	3.098829	0.490067
Cu	0.093287	-0.248498	-1.187865
C	-0.795194	0.999527	1.877405
H	-0.789164	0.859019	2.964818
H	-1.720807	1.529882	1.622260
C	0.422611	1.845134	1.456415
H	0.376543	-2.653732	1.278405
H	-2.880641	-0.654066	2.420138
C	1.278390	-1.392093	2.724813
C	3.620859	-0.353471	3.914957
C	2.514406	-1.441700	2.057346
C	1.244964	-0.819832	4.006647
C	2.403445	-0.307717	4.596020
C	3.671397	-0.925196	2.641146
H	2.562663	-1.897011	1.071352
H	0.312497	-0.778439	4.562222
H	2.352006	0.124136	5.592432
H	4.611054	-0.971580	2.097755
H	4.521623	0.043767	4.375379
C	-3.725342	-1.185195	0.539805
C	-5.853261	-1.047456	-1.304841
C	-3.643094	-1.835848	-0.701830
C	-4.890623	-0.465061	0.836860
C	-5.947589	-0.396167	-0.074366
C	-4.696027	-1.767734	-1.613943
H	-2.747298	-2.394542	-0.958236
H	-4.973649	0.043939	1.794877
H	-6.844865	0.161884	0.181726
H	-4.610854	-2.277797	-2.569937
H	-6.673361	-0.997441	-2.016154
C	3.583218	1.802003	-0.896185
C	5.798743	0.212214	-1.611509
C	4.720382	1.741561	-0.078714
C	3.574055	1.047410	-2.080273

C	4.670380	0.260849	-2.434440
C	5.820305	0.955772	-0.430978
H	4.746082	2.318787	0.843128
H	2.695582	1.056744	-2.719576
H	4.639786	-0.318893	-3.353048
H	6.693221	0.928902	0.216394
H	6.651712	-0.401326	-1.888664
C	-1.558212	3.618154	-0.470019
C	-4.109809	3.984456	0.682956
C	-1.745699	4.509314	0.597580
C	-2.679345	2.920597	-0.951654
C	-3.939807	3.095306	-0.381502
C	-3.008854	4.692112	1.166431
H	-0.907547	5.078288	0.988627
H	-2.558275	2.228121	-1.781900
H	-4.784645	2.532246	-0.767161
H	-3.129491	5.393576	1.988067
H	-5.091381	4.128176	1.126441
H	0.320538	2.868105	1.838864
H	1.334360	1.422468	1.895577
C	0.354401	-1.544129	-2.711650
H	1.301123	-1.237022	-3.177341
C	-0.757546	-1.486653	-3.768383
H	-0.664584	-2.280216	-4.531711
H	-1.763697	-1.578749	-3.338951
H	-0.733856	-0.524249	-4.294847
C	0.559095	-2.864334	-2.059938
C	1.809865	-3.197698	-1.480382
C	-0.455272	-3.843857	-1.950050
C	2.017346	-4.398169	-0.806506
H	2.629045	-2.485258	-1.572209
C	-0.249674	-5.046279	-1.267959
H	-1.418349	-3.665826	-2.420715
C	0.983225	-5.335158	-0.680299
H	2.997232	-4.612196	-0.383411
H	-1.059870	-5.771347	-1.211791
H	1.144750	-6.273934	-0.157214

Structure 9l
Charge: 0
Multiplicity: 1
Imaginary Frequencies: 0
Electronic Energy (B3LYP): -2505.409934
Gibbs Free Energy (B3LYP): -2504.764904
Electronic Energy (BP86-D3(BJ)/CPCM(THF)): -2506.276928
Total Gibbs Free Energy: -2505.631899

P	0.550643	1.810130	-0.243440
C	-0.464332	3.303598	-0.869452
C	0.455386	4.525419	-0.678597
C	1.875653	4.075674	-1.036262
C	2.182804	2.795677	-0.219255
H	0.119917	5.368910	-1.294777
H	0.440421	4.864595	0.364849
H	2.622246	4.850866	-0.826778
H	1.938523	3.854199	-2.109406
P	-0.990589	-0.839974	0.874328
C	-0.023476	-2.147531	1.880835

C	-1.087328	-2.897869	2.709147
C	-2.342705	-3.010415	1.837995
C	-2.682564	-1.586616	1.332010
H	-0.711750	-3.879985	3.021925
H	-1.335336	-2.344250	3.623501
H	-3.192960	-3.435427	2.384905
H	-2.148672	-3.670470	0.982726
H	-0.537585	3.112040	-1.947899
H	2.330356	3.096641	0.826128
Cu	0.104495	-0.279081	-1.189289
C	-0.999785	0.730740	1.906006
H	-1.019154	0.503732	2.978706
H	-1.945754	1.228201	1.660751
C	0.179487	1.671573	1.592978
H	0.330926	-2.830858	1.099349
H	-3.043259	-1.008193	2.193028
C	1.191393	-1.619023	2.611683
C	3.496656	-0.586505	3.874405
C	2.429791	-1.591628	1.946848
C	1.136251	-1.128925	3.926245
C	2.276808	-0.619266	4.551777
C	3.568089	-1.077190	2.568168
H	2.500004	-1.980103	0.933291
H	0.201359	-1.150903	4.478921
H	2.209554	-0.251885	5.572830
H	4.510451	-1.062839	2.027761
H	4.383950	-0.192100	4.362691
C	-3.743752	-1.539089	0.253788
C	-5.775012	-1.510642	-1.701929
C	-3.504681	-2.031309	-1.039011
C	-5.017583	-1.031569	0.545377
C	-6.026709	-1.017854	-0.420595
C	-4.508704	-2.016859	-2.007019
H	-2.519808	-2.411467	-1.295876
H	-5.222479	-0.645328	1.541685
H	-7.008597	-0.624560	-0.169196
H	-4.298043	-2.397518	-3.002927
H	-6.556963	-1.500793	-2.456548
C	3.415063	2.041993	-0.671476
C	5.758981	0.716590	-1.507377
C	4.526847	1.940741	0.176289
C	3.496377	1.460977	-1.946923
C	4.656564	0.806913	-2.361706
C	5.689587	1.284939	-0.234909
H	4.482574	2.383155	1.169196
H	2.639865	1.501449	-2.614354
H	4.696820	0.363228	-3.352969
H	6.540615	1.222976	0.438597
H	6.661936	0.206292	-1.831467
C	-1.873439	3.380039	-0.323878
C	-4.517707	3.404185	0.665964
C	-2.223713	4.177544	0.775932
C	-2.879537	2.601527	-0.921994
C	-4.185152	2.607144	-0.432829
C	-3.533121	4.190808	1.264372
H	-1.478781	4.805216	1.255605
H	-2.630614	1.978645	-1.778512

H	-4.938207	1.984951	-0.907487
H	-3.781208	4.822495	2.113598
H	-5.535290	3.415939	1.047063
H	0.001205	2.658938	2.036649
H	1.097557	1.273652	2.041942
C	0.693391	-1.417763	-2.731159
H	1.468442	-0.839331	-3.253910
C	-0.383464	-1.797709	-3.762011
H	0.003390	-2.450414	-4.564826
H	-1.231255	-2.327773	-3.307856
H	-0.798133	-0.901197	-4.239917
C	1.352943	-2.602897	-2.107737
C	2.673043	-2.765432	-1.767781
C	0.725599	-3.836486	-1.671873
O	2.897107	-3.979824	-1.149610
H	3.543612	-2.136296	-1.877696
C	1.695387	-4.611442	-1.111621
H	-0.315629	-4.106657	-1.790419
H	1.697753	-5.600543	-0.676490

Structure 10aa
Charge: 0
Multiplicity: 1
Imaginary Frequencies: 0
Electronic Energy (B3LYP): -2755.924711
Gibbs Free Energy (B3LYP): -2755.165829
Electronic Energy (BP86-D3(BJ)/CPCM(THF)): -2756.880072
Total Gibbs Free Energy: -2756.121190
Geometry:

P	2.177663	0.538992	1.279746
C	2.445696	-0.364183	2.944341
C	3.344111	0.574758	3.776580
C	2.939596	2.014603	3.435347
C	2.981170	2.147027	1.893613
H	3.245534	0.358483	4.847244
H	4.400647	0.433607	3.517218
H	3.603738	2.752283	3.900711
H	1.925159	2.221229	3.800754
P	1.243019	-0.994166	-1.467163
C	1.431487	-0.230490	-3.211298
C	1.361659	-1.422795	-4.188651
C	0.371519	-2.437129	-3.602134
C	0.814134	-2.715455	-2.145172
H	1.067215	-1.086855	-5.190281
H	2.342892	-1.903231	-4.287544
H	0.344179	-3.369356	-4.178353
H	-0.645873	-2.024745	-3.611351
H	1.444320	-0.343447	3.391586
H	4.035123	2.084792	1.590501
C	2.970588	-1.269060	-0.789355
H	3.684636	-1.465063	-1.597959
H	2.900864	-2.181609	-0.184959
C	3.472995	-0.102951	0.083946
H	0.502155	0.341381	-3.323084
H	1.767020	-3.259700	-2.194120
C	2.582261	0.742474	-3.346131
C	4.691650	2.615234	-3.483631

C	2.389700	2.081895	-2.964779
C	3.853747	0.364047	-3.803793
C	4.896375	1.291571	-3.874870
C	3.430857	3.007799	-3.026767
H	1.411224	2.399490	-2.611175
H	4.038853	-0.658063	-4.120861
H	5.869923	0.975681	-4.241001
H	3.253277	4.033313	-2.715688
H	5.503616	3.335152	-3.540397
C	-0.152015	-3.535877	-1.317024
C	-1.933641	-5.133204	0.172943
C	-1.407190	-3.040757	-0.928468
C	0.192358	-4.842919	-0.943143
C	-0.689123	-5.637984	-0.207141
C	-2.288063	-3.831538	-0.190022
H	-1.698300	-2.025641	-1.182101
H	1.160634	-5.244181	-1.235561
H	-0.402915	-6.650905	0.065004
H	-3.249389	-3.422409	0.108204
H	-2.621554	-5.747082	0.748113
C	2.407632	3.432083	1.335462
C	1.400797	5.865955	0.331520
C	3.260614	4.375199	0.744337
C	1.037910	3.729807	1.412945
C	0.539254	4.933689	0.914950
C	2.765119	5.583235	0.248195
H	4.325600	4.162800	0.675470
H	0.346834	3.011906	1.844411
H	-0.526470	5.135289	0.977785
H	3.446539	6.302221	-0.199774
H	1.010914	6.803233	-0.056253
C	2.853045	-1.815050	2.808557
C	3.517275	-4.538077	2.464183
C	4.190926	-2.238118	2.823153
C	1.855004	-2.787833	2.623799
C	2.180169	-4.132620	2.448273
C	4.519152	-3.586042	2.656072
H	4.990236	-1.519262	2.977386
H	0.810572	-2.483929	2.613019
H	1.386824	-4.859000	2.296986
H	5.562593	-3.889838	2.679741
H	3.774655	-5.585854	2.334972
H	4.385437	-0.398875	0.615052
H	3.726761	0.753898	-0.551980
C	-5.653568	0.613198	1.370765
H	-5.951255	1.076731	2.323600
C	-5.138860	-0.796255	1.683230
H	-5.937814	-1.438695	2.071750
H	-4.712164	-1.270189	0.791665
H	-4.338684	-0.740140	2.428371
C	-6.876171	0.642505	0.469114
C	-7.814525	1.678581	0.610051
C	-7.099998	-0.302122	-0.544810
C	-8.928874	1.772610	-0.223395
H	-7.667007	2.420033	1.393095
C	-8.214418	-0.213821	-1.382621
H	-6.399074	-1.119819	-0.681669

C	-9.134929	0.823424	-1.227164
H	-9.639989	2.583730	-0.085087
H	-8.363595	-0.961746	-2.158077
H	-10.004198	0.889491	-1.876583
Cu	0.186545	0.251590	0.172623
N	-1.628496	0.792557	0.414278
C	-2.584866	0.690662	-0.586921
C	-2.114785	1.351628	1.586887
C	-3.887756	1.037719	-0.481711
H	-2.204216	0.320389	-1.538970
C	-3.390522	1.741408	1.808693
H	-1.368588	1.482811	2.370456
C	-4.500802	1.548657	0.801425
H	-4.525607	0.940626	-1.356851
H	-3.640469	2.189440	2.769474
H	-5.011533	2.512297	0.616095

Structure 10ak
Charge: 0
Multiplicity: 1
Imaginary Frequencies: 0
Electronic Energy (B3LYP): -2986.924157
Gibbs Free Energy (B3LYP): -2986.088791
Electronic Energy (BP86-D3(BJ)/CPCM(THF)): -2987.978766
Total Gibbs Free Energy: -2987.1434
Geometry:

P	-2.314911	-0.427406	1.176200
C	-2.067452	-0.188532	3.056425
C	-3.154576	-1.059367	3.719731
C	-3.302866	-2.326014	2.868355
C	-3.527833	-1.874370	1.404416
H	-2.888001	-1.286853	4.758890
H	-4.116217	-0.531806	3.743566
H	-4.134932	-2.955686	3.204513
H	-2.392432	-2.935103	2.934842
P	-1.279003	1.820538	-1.014226
C	-1.969572	1.887058	-2.795669
C	-1.810568	3.355013	-3.237354
C	-0.476056	3.850791	-2.669846
C	-0.469872	3.542837	-1.151976
H	-1.854230	3.441405	-4.330018
H	-2.621975	3.973841	-2.833903
H	-0.324854	4.923125	-2.840560
H	0.356663	3.329736	-3.159269
H	-1.101937	-0.675135	3.239599
H	-4.527600	-1.423011	1.351885
C	-2.731062	2.197376	0.114021
H	-3.442085	2.874592	-0.374580
H	-2.302665	2.735806	0.967805
C	-3.467154	0.938741	0.609554
H	-1.239489	1.292947	-3.360269
H	-1.178407	4.232080	-0.674120
C	-3.320787	1.228497	-2.967217
C	-5.799972	-0.097986	-3.221973
C	-3.383101	-0.166276	-3.133453
C	-4.527100	1.944579	-2.939712
C	-5.754106	1.288003	-3.068346

C	-4.606547	-0.824508	-3.254699
H	-2.460066	-0.741229	-3.163541
H	-4.519245	3.024982	-2.830676
H	-6.674778	1.865778	-3.052599
H	-4.623735	-1.904173	-3.371564
H	-6.754884	-0.606619	-3.323475
C	0.873568	3.708863	-0.474043
C	3.377393	4.119433	0.754653
C	1.985307	2.927048	-0.827062
C	1.040775	4.694802	0.508669
C	2.280321	4.900511	1.119296
C	3.225695	3.131108	-0.221629
H	1.884708	2.142331	-1.572120
H	0.191923	5.312452	0.794659
H	2.387413	5.675808	1.873951
H	4.073620	2.516283	-0.511345
H	4.343923	4.276455	1.225414
C	-3.457274	-2.978988	0.372378
C	-3.389116	-5.073993	-1.511393
C	-4.619102	-3.376128	-0.304410
C	-2.258658	-3.651221	0.087745
C	-2.223238	-4.686409	-0.846287
C	-4.588999	-4.416322	-1.236172
H	-5.558343	-2.867455	-0.097218
H	-1.340325	-3.354347	0.586230
H	-1.280232	-5.181591	-1.060109
H	-5.503653	-4.711809	-1.744055
H	-3.360670	-5.880313	-2.239228
C	-1.940644	1.254430	3.494078
C	-1.619267	3.964963	4.217203
C	-3.031594	2.015162	3.941673
C	-0.683642	1.879728	3.424786
C	-0.522549	3.219536	3.776716
C	-2.871858	3.355817	4.301664
H	-4.015762	1.563694	4.024894
H	0.178009	1.307743	3.087810
H	0.459837	3.677074	3.703880
H	-3.730779	3.921872	4.652947
H	-1.496783	5.007131	4.499394
H	-4.171267	1.206288	1.406581
H	-4.051623	0.503198	-0.209589
C	2.309108	-3.611372	2.686551
H	2.745120	-4.466866	3.204587
C	0.905092	-3.271930	3.094581
H	0.818024	-3.223779	4.190067
H	0.575986	-2.310391	2.686342
H	0.183563	-4.033998	2.762056
C	3.097814	-2.962801	1.793890
C	4.476262	-3.401511	1.609864
C	2.627724	-1.807149	0.925179
C	5.373854	-2.681821	0.900894
H	4.782393	-4.323906	2.100561
C	3.734612	-0.981080	0.361111
H	1.950875	-1.152379	1.492083
C	5.019780	-1.401988	0.284403
H	6.392304	-3.044968	0.789541
H	3.451851	-0.016896	-0.048778

Cu	-0.526130	-0.302588	-0.216939
N	0.994033	-1.219828	-0.942671
C	1.538261	-0.806384	-2.118730
C	1.646746	-2.347209	-0.269858
C	2.467367	-1.499900	-2.854592
H	1.129299	0.127666	-2.507588
C	2.337841	-3.281901	-1.221515
H	0.886759	-2.896067	0.301883
C	2.784711	-2.835230	-2.416512
H	2.818514	-1.113963	-3.805715
H	2.521659	-4.299888	-0.888494
H	3.337408	-3.498708	-3.079835
C	6.067404	-0.583731	-0.374833
C	7.374281	-0.515799	0.140207
C	5.777080	0.154091	-1.538466
C	8.348879	0.274085	-0.470102
H	7.622146	-1.069232	1.042212
C	6.751713	0.945624	-2.146487
H	4.788656	0.065578	-1.982413
C	8.042303	1.012435	-1.615024
H	9.349437	0.316650	-0.046279
H	6.507059	1.498801	-3.050411
H	8.802104	1.626070	-2.092245

Structure 11a
Charge: 0
Multiplicity: 1
Imaginary Frequencies: 0
Electronic Energy (B3LYP): -2507.607562
Gibbs Free Energy (B3LYP): -2506.933761
Electronic Energy (BP86-D3(BJ)/CPCM(THF)): -2508.480937
Total Gibbs Free Energy: -2507.807136
Geometry:

P	1.170180	1.542648	-0.507158
C	0.530746	3.213602	-1.185779
C	1.733701	4.170893	-1.097629
C	2.973433	3.370279	-1.507563
C	3.002736	2.077817	-0.656144
H	1.582322	5.052008	-1.733418
H	1.866635	4.535774	-0.071426
H	3.900020	3.939442	-1.367545
H	2.913386	3.118900	-2.573706
P	-0.808485	-0.586657	1.097079
C	-0.133635	-1.982447	2.218321
C	-1.351875	-2.519039	3.006415
C	-2.602293	-2.316255	2.140445
C	-2.592230	-0.837957	1.687319
H	-1.199198	-3.572699	3.269473
H	-1.479355	-1.972076	3.948376
H	-3.524158	-2.543471	2.688720
H	-2.572934	-2.976065	1.263861
H	0.359163	2.996569	-2.248443
H	3.294110	2.360230	0.363391
Cu	0.099762	-0.491695	-1.012942
C	-0.389836	1.068705	1.864057
H	-0.367723	0.998733	2.957670
H	-1.221149	1.730838	1.593915

C	0.939008	1.657305	1.355736
H	0.143112	-2.741443	1.479393
H	-2.680921	-0.223676	2.594843
C	1.106283	-1.624303	3.006934
C	3.477379	-0.934076	4.382079
C	2.370525	-1.870737	2.443045
C	1.058493	-1.026044	4.276588
C	2.229848	-0.686002	4.957097
C	3.541917	-1.528845	3.119840
H	2.428835	-2.328810	1.458995
H	0.100967	-0.828828	4.750348
H	2.164668	-0.230289	5.941908
H	4.505175	-1.735386	2.660524
H	4.388093	-0.673882	4.914899
C	-3.705243	-0.433821	0.746070
C	-5.863823	0.281632	-0.919447
C	-3.772013	-0.898685	-0.576381
C	-4.734794	0.395358	1.215911
C	-5.807360	0.749659	0.394866
C	-4.842116	-0.542293	-1.398450
H	-2.998383	-1.543822	-0.986248
H	-4.699732	0.763042	2.239645
H	-6.597441	1.387204	0.784158
H	-4.869100	-0.921120	-2.416603
H	-6.698046	0.551702	-1.562017
C	3.961144	1.008453	-1.132639
C	5.781976	-0.972624	-1.981365
C	4.887336	0.449575	-0.240585
C	3.966697	0.555704	-2.461265
C	4.866607	-0.423203	-2.882623
C	5.788801	-0.532153	-0.657482
H	4.902691	0.788035	0.793110
H	3.257732	0.967203	-3.175340
H	4.850967	-0.759238	-3.915930
H	6.499949	-0.947290	0.052158
H	6.483079	-1.734782	-2.309946
C	-0.784610	3.667560	-0.591708
C	-3.280143	4.408039	0.499008
C	-0.867383	4.620167	0.434764
C	-1.980373	3.100671	-1.066034
C	-3.214153	3.459683	-0.525319
C	-2.103598	4.988729	0.972614
H	0.032234	5.093634	0.816112
H	-1.939992	2.361889	-1.863242
H	-4.119835	2.991904	-0.899089
H	-2.142606	5.735323	1.761842
H	-4.240427	4.693549	0.919761
H	1.040337	2.696186	1.693901
H	1.776379	1.093493	1.784620
C	-2.454930	-3.046675	-2.960073
H	-2.796182	-2.318007	-3.694677
C	-3.392423	-4.179959	-2.631881
H	-3.859144	-4.095721	-1.633952
H	-4.215440	-4.223003	-3.354908
H	-2.896905	-5.162304	-2.657778
C	-1.211630	-2.873062	-2.413798
C	-0.328214	-1.752331	-2.783013

C	-0.632109	-3.793043	-1.435390
C	1.052219	-1.791319	-2.465722
H	-0.649547	-1.112296	-3.602832
C	0.676496	-3.707566	-1.031960
H	-1.249146	-4.607000	-1.063906
C	1.565074	-2.706721	-1.532418
H	1.729964	-1.104368	-2.966882
H	1.061828	-4.448560	-0.331531
H	2.623387	-2.720247	-1.294355

Structure 11l
Charge: 0
Multiplicity: 1
Imaginary Frequencies: 0
Electronic Energy (B3LYP): -2505.400672
Gibbs Free Energy (B3LYP): -2504.758374
Electronic Energy (BP86-D3(BJ)/CPCM(THF)): -2506.265256
Total Gibbs Free Energy: -2505.622959
Geometry:

P	-1.077844	1.454201	0.513196
C	-0.275426	2.931746	1.423013
C	-1.425201	3.931676	1.662295
C	-2.681190	3.112234	1.976996
C	-2.849207	2.066025	0.847782
H	-1.171938	4.629627	2.469683
H	-1.609450	4.534222	0.764271
H	-3.577270	3.739297	2.053167
H	-2.565352	2.602334	2.942107
P	0.878285	-0.461446	-1.292187
C	0.130794	-1.734340	-2.502210
C	1.212721	-1.965987	-3.574426
C	2.563099	-1.956634	-2.849668
C	2.634043	-0.656560	-2.009260
H	1.037493	-2.907091	-4.110589
H	1.202022	-1.163526	-4.323251
H	3.410283	-2.009178	-3.544018
H	2.637895	-2.827367	-2.185627
H	-0.006512	2.500327	2.395461
H	-3.152372	2.605262	-0.059516
Cu	-0.281555	-0.669445	0.821107
C	0.399763	1.236027	-1.941102
H	0.320150	1.239659	-3.035148
H	1.237633	1.890357	-1.673172
C	-0.903432	1.786661	-1.326701
H	0.075186	-2.634363	-1.877976
H	2.769082	0.181723	-2.705675
C	-1.274263	-1.412324	-2.959734
C	-3.929553	-0.788138	-3.685764
C	-2.356341	-1.801692	-2.150175
C	-1.551618	-0.714165	-4.144957
C	-2.866567	-0.407139	-4.505599
C	-3.668522	-1.488969	-2.504984
H	-2.158514	-2.353870	-1.234227
H	-0.742388	-0.413784	-4.804387
H	-3.057250	0.127740	-5.432767
H	-4.485251	-1.792366	-1.856095
H	-4.951626	-0.549386	-3.967866

C	3.764884	-0.624069	-1.002500
C	5.932303	-0.589909	0.799440
C	3.757493	-1.435152	0.143817
C	4.875399	0.201764	-1.227087
C	5.952477	0.219340	-0.337602
C	4.830250	-1.415959	1.035415
H	2.907565	-2.079826	0.355182
H	4.898025	0.836770	-2.110438
H	6.805689	0.863487	-0.535845
H	4.797952	-2.045863	1.920258
H	6.766624	-0.577404	1.495829
C	-3.879320	0.992569	1.124659
C	-5.855038	-0.948703	1.647993
C	-5.031106	0.905311	0.330881
C	-3.732848	0.085652	2.186552
C	-4.710334	-0.874606	2.446007
C	-6.012632	-0.054777	0.588259
H	-5.162702	1.598991	-0.496885
H	-2.839485	0.116911	2.804087
H	-4.573695	-1.569968	3.269818
H	-6.899978	-0.099916	-0.038088
H	-6.615651	-1.697735	1.851097
C	0.995745	3.452501	0.788615
C	3.409480	4.314307	-0.395445
C	1.011286	4.522839	-0.118780
C	2.217129	2.828092	1.094341
C	3.410569	3.248425	0.508048
C	2.206310	4.950501	-0.703111
H	0.090422	5.040335	-0.370482
H	2.229667	1.997514	1.796597
H	4.336804	2.737841	0.754126
H	2.193403	5.786517	-1.397841
H	4.337992	4.648721	-0.850286
H	-0.993621	2.859374	-1.537573
H	-1.767253	1.290913	-1.786153
C	0.858205	-2.040445	3.885676
H	0.182919	-1.218977	4.132039
C	1.927657	-2.340328	4.899377
H	1.504798	-2.615753	5.878407
H	2.571008	-3.169872	4.585487
H	2.582131	-1.473411	5.082642
C	0.650779	-2.704912	2.722920
C	-0.442010	-2.434172	1.714614
C	1.410072	-3.829038	2.173132
O	-0.293462	-3.524271	0.693735
H	-1.437572	-2.601014	2.138767
C	0.799627	-4.230513	1.038595
H	2.284459	-4.294275	2.608851
H	1.061989	-5.039055	0.362971

Structure 12a
Charge: 0
Multiplicity: 1
Imaginary Frequencies: 0
Electronic Energy (B3LYP): -2507.610858

Gibbs Free Energy (B3LYP): -2506.936805
Electronic Energy (BP86-D3(BJ)/CPCM(THF)): -2508.476430
Total Gibbs Free Energy: -2507.802377
Geometry:

P	1.444772	0.988097	-1.018727
C	0.907653	2.281885	-2.320376
C	2.222291	2.849085	-2.893785
C	3.218284	1.687567	-2.979833
C	3.262010	1.008394	-1.589098
H	2.049780	3.320938	-3.868832
H	2.632552	3.621835	-2.232006
H	4.220453	2.021306	-3.273475
H	2.887863	0.965593	-3.737623
P	-0.595738	0.198709	1.448961
C	0.010166	-0.724377	3.010087
C	-1.047201	-0.432234	4.094926
C	-2.410008	-0.377458	3.394617
C	-2.280758	0.621835	2.219672
H	-1.014793	-1.193877	4.883492
H	-0.856119	0.535558	4.575283
H	-3.212426	-0.065345	4.073331
H	-2.681098	-1.369192	3.010374
H	0.447301	1.661910	-3.100187
H	3.780406	1.691891	-0.903743
Cu	0.124918	-0.875039	-0.511458
C	0.252361	1.871583	1.437153
H	0.445296	2.226521	2.456827
H	-0.474557	2.557267	0.985898
C	1.561509	1.893092	0.623771
H	-0.100752	-1.775618	2.717643
H	-2.162447	1.623980	2.654227
C	1.466472	-0.497577	3.351365
C	4.215457	-0.097516	3.865396
C	2.445435	-1.286345	2.721986
C	1.896136	0.490798	4.250173
C	3.255810	0.686885	4.506359
C	3.803508	-1.087746	2.969613
H	2.134633	-2.062794	2.026426
H	1.170301	1.110032	4.768963
H	3.562256	1.453826	5.213179
H	4.536496	-1.708115	2.461456
H	5.272219	0.055294	4.067364
C	-3.458770	0.655298	1.269720
C	-5.705944	0.739305	-0.424946
C	-3.748095	-0.415363	0.409707
C	-4.313888	1.766579	1.265471
C	-5.431442	1.809618	0.428670
C	-4.860005	-0.372850	-0.432412
H	-3.102750	-1.289734	0.380116
H	-4.104340	2.605080	1.926813
H	-6.085898	2.677875	0.447018
H	-5.044695	-1.217556	-1.090569
H	-6.573306	0.770856	-1.079394
C	3.973678	-0.326479	-1.551645
C	5.359405	-2.781425	-1.498670
C	5.126015	-0.486422	-0.769851
C	3.525146	-1.422553	-2.305931

C	4.210674	-2.636936	-2.281220
C	5.814990	-1.701486	-0.741770
H	5.490271	0.351331	-0.178999
H	2.623515	-1.332246	-2.906011
H	3.843460	-3.472563	-2.870863
H	6.710130	-1.799684	-0.132796
H	5.892741	-3.727918	-1.480112
C	-0.139082	3.265625	-1.844204
C	-2.157207	5.009687	-0.919427
C	0.184337	4.520825	-1.306121
C	-1.496135	2.906855	-1.914370
C	-2.495310	3.763863	-1.453961
C	-0.814932	5.385027	-0.851312
H	1.220337	4.841125	-1.248185
H	-1.771619	1.941048	-2.331929
H	-3.534147	3.452513	-1.508207
H	-0.539839	6.355581	-0.446270
H	-2.932939	5.683006	-0.564951
H	1.892676	2.927970	0.475143
H	2.352002	1.375082	1.180503
C	-4.203538	-3.770697	-1.770284
H	-4.631715	-3.494970	-2.734572
C	-5.126084	-4.480479	-0.816741
H	-6.150800	-4.092843	-0.895183
H	-5.191629	-5.565323	-1.007841
H	-4.819598	-4.363257	0.229931
C	-2.874608	-3.513232	-1.576726
C	-2.069288	-2.863662	-2.611294
C	-2.124029	-3.891971	-0.376941
C	-0.751286	-2.572165	-2.441895
H	-2.555886	-2.643515	-3.560673
C	-0.808424	-3.581622	-0.216300
H	-2.631555	-4.470530	0.390741
C	-0.041401	-2.800678	-1.181764
H	-0.194059	-2.145894	-3.277381
H	-0.291130	-3.935539	0.677022
H	1.011873	-3.082045	-1.280027

Structure 13aa
Charge: 0
Multiplicity: 1
Imaginary Frequencies: 0
Electronic Energy (B3LYP): -2507.610858
Gibbs Free Energy (B3LYP): -2506.936805
Electronic Energy (BP86-D3(BJ)/CPCM(THF)): -2508.476430
Total Gibbs Free Energy: -2507.802377
Geometry:

P	-0.171670	-1.449472	-1.294967
C	0.768434	-1.464080	-2.972233
C	0.115426	-2.583853	-3.808609
C	-1.380345	-2.582863	-3.493321
C	-1.530883	-2.635466	-1.955348
H	0.314174	-2.434842	-4.877093
H	0.533519	-3.561745	-3.540922
H	-1.902867	-3.427961	-3.957565
H	-1.843131	-1.668970	-3.885961
P	1.463925	-0.291431	1.349853

C	0.791226	-0.707297	3.102579
C	1.989169	-0.555213	4.063511
C	2.876610	0.571111	3.526899
C	3.161407	0.257280	2.040059
H	1.643556	-0.359916	5.086255
H	2.578904	-1.479038	4.099052
H	3.814932	0.661921	4.087095
H	2.359236	1.535568	3.615037
H	0.480863	-0.503686	-3.417579
H	-1.220828	-3.635832	-1.625762
C	1.934711	-1.938371	0.585935
H	2.317358	-2.622390	1.353228
H	2.766069	-1.713573	-0.091801
C	0.796027	-2.619751	-0.193486
H	0.099930	0.121657	3.294727
H	3.793155	-0.640706	2.011295
C	-0.007187	-1.990216	3.198298
C	-1.566299	-4.346097	3.304853
C	-1.388147	-1.960121	2.937161
C	0.572676	-3.228116	3.519803
C	-0.197606	-4.392349	3.573398
C	-2.159009	-3.121702	2.986575
H	-1.856411	-1.013122	2.683952
H	1.633517	-3.294449	3.742086
H	0.276017	-5.336304	3.831174
H	-3.223177	-3.066640	2.774410
H	-2.165140	-5.251815	3.351201
C	3.880329	1.356037	1.290591
C	5.303278	3.405937	-0.026001
C	3.335358	2.643116	1.160908
C	5.149006	1.117632	0.743533
C	5.856502	2.130488	0.091876
C	4.038062	3.657484	0.511018
H	2.347029	2.853054	1.560201
H	5.590198	0.127356	0.833079
H	6.841731	1.921902	-0.317628
H	3.594675	4.645558	0.421042
H	5.850691	4.197531	-0.530414
C	-2.940988	-2.400176	-1.461284
C	-5.612715	-2.063132	-0.612696
C	-3.562261	-3.347377	-0.633838
C	-3.683858	-1.272476	-1.847845
C	-5.006359	-1.108288	-1.432770
C	-4.882902	-3.182712	-0.210612
H	-3.005828	-4.228837	-0.323166
H	-3.225578	-0.505735	-2.466570
H	-5.560686	-0.228612	-1.749380
H	-5.343034	-3.935541	0.424472
H	-6.643418	-1.935923	-0.292948
C	2.280462	-1.489823	-2.882962
C	5.101095	-1.457813	-2.689090
C	3.018109	-2.684860	-2.846967
C	2.992503	-0.279767	-2.830307
C	4.383584	-0.260274	-2.730158
C	4.411522	-2.669446	-2.751662
H	2.510702	-3.643086	-2.903500
H	2.447186	0.659248	-2.866856

```
 H                  4.903021    0.692251   -2.681181
 H                  4.957150   -3.609543   -2.732097
 H                  6.185424   -1.446769   -2.617797
 H                  1.197251   -3.461943   -0.770965
 H                  0.060380   -3.029139    0.508613
 C                 -3.254330    5.004089   -0.787634
 H                 -3.040151    5.858535   -0.146851
 C                 -4.662336    4.877803   -1.304266
 H                 -4.779438    5.215783   -2.348674
 H                 -5.027416    3.839849   -1.274596
 H                 -5.356158    5.479361   -0.704087
 C                 -2.218729    4.168641   -1.107974
 C                 -0.871067    4.374896   -0.585274
 C                 -2.348397    3.027111   -2.011987
 C                  0.150323    3.505837   -0.831068
 H                 -0.691105    5.275361    0.001246
 C                 -1.310284    2.173391   -2.250511
 H                 -3.290058    2.886266   -2.536928
 C                 -0.034877    2.273792   -1.571206
 H                  1.145802    3.730120   -0.451336
 H                 -1.447838    1.369165   -2.975945
 H                  0.838338    1.906348   -2.114653
 Cu                -0.124291    0.635169   -0.151718
 N                 -1.664691    1.330479    1.145517
 C                 -1.380351    2.387729    1.935108
 C                 -2.965888    1.109599    0.858564
 C                 -2.348477    3.237289    2.456218
 H                 -0.327343    2.551185    2.143782
 C                 -3.997349    1.912831    1.329163
 H                 -3.172868    0.252974    0.228411
 C                 -3.685988    3.016200    2.126585
 H                 -2.051578    4.076001    3.078228
 H                 -5.022267    1.685312    1.053472
 H                 -4.466172    3.674193    2.496932

Structure 14aa
Charge: 0
Multiplicity: 1
Imaginary Frequencies: 0
Electronic Energy (B3LYP): -2755.919493
Gibbs Free Energy (B3LYP): -2755.161065
Electronic Energy (BP86-D3(BJ)/CPCM(THF)): -2756.885087
Total Gibbs Free Energy: -2756.126658
Geometry:
 P                 -0.451266   -1.589579   -1.269365
 C                  0.709082   -2.300298   -2.633333
 C                 -0.108620   -3.399809   -3.342219
 C                 -1.562129   -2.932816   -3.400792
 C                 -1.975617   -2.523367   -1.967562
 H                  0.301349   -3.606413   -4.338726
 H                 -0.064006   -4.339696   -2.779224
 H                 -2.233235   -3.709719   -3.786974
 H                 -1.650427   -2.072493   -4.075904
 P                  0.899122   -0.185891    1.410723
 C                 -0.084115   -0.046650    3.071920
 C                  0.941591    0.411925    4.141930
 C                  2.106764    1.121289    3.445635
```

C	2.546884	0.208238	2.281065
H	0.453080	1.052704	4.886120
H	1.334864	-0.454302	4.685903
H	2.942017	1.306817	4.131611
H	1.789764	2.098063	3.056719
H	0.813153	-1.458329	-3.328096
H	-2.069072	-3.439409	-1.369571
C	1.109378	-2.016948	1.069062
H	1.227226	-2.577265	2.002901
H	2.052779	-2.101609	0.518111
C	-0.039273	-2.622011	0.242009
H	-0.766408	0.785764	2.876671
H	2.888863	-0.739040	2.721504
C	-0.928948	-1.242544	3.459078
C	-2.563731	-3.451000	4.141922
C	-2.309757	-1.235766	3.198744
C	-0.390345	-2.383161	4.079772
C	-1.195148	-3.473009	4.415921
C	-3.117816	-2.323699	3.532795
H	-2.756530	-0.360877	2.734941
H	0.669518	-2.425210	4.314708
H	-0.749610	-4.339584	4.897831
H	-4.183823	-2.284485	3.323135
H	-3.190699	-4.297887	4.407443
C	3.671338	0.757994	1.434818
C	5.847457	1.804509	-0.022370
C	3.547124	1.963063	0.725677
C	4.902059	0.087022	1.392994
C	5.982313	0.602572	0.673521
C	4.624874	2.480541	0.006583
H	2.600400	2.495393	0.721977
H	5.017681	-0.847849	1.937365
H	6.928447	0.067031	0.663272
H	4.508406	3.415790	-0.534469
H	6.685490	2.212556	-0.581156
C	-3.289979	-1.778168	-1.899627
C	-5.787024	-0.463348	-1.824887
C	-4.341320	-2.268142	-1.110911
C	-3.511926	-0.606902	-2.644062
C	-4.746527	0.040609	-2.610764
C	-5.578081	-1.618546	-1.070108
H	-4.191950	-3.174770	-0.528376
H	-2.709279	-0.188538	-3.245390
H	-4.893999	0.944419	-3.195804
H	-6.378885	-2.023065	-0.456191
H	-6.750129	0.039610	-1.803723
C	2.101566	-2.694349	-2.180989
C	4.718166	-3.348343	-1.331312
C	2.427223	-3.998966	-1.774709
C	3.121353	-1.727472	-2.157018
C	4.411905	-2.046773	-1.735182
C	3.719929	-4.322570	-1.355584
H	1.675908	-4.782370	-1.791037
H	2.897322	-0.710915	-2.465334
H	5.174050	-1.273318	-1.717885
H	3.944444	-5.342204	-1.052310
H	5.724151	-3.601265	-1.007023

H	0.206397	-3.655444	-0.032351
H	-0.954553	-2.653581	0.845999
C	0.302600	2.059212	-2.117918
H	-0.525778	1.822842	-2.803771
C	1.623945	1.783576	-2.854356
H	1.849600	2.540804	-3.627382
H	2.493670	1.745947	-2.186834
H	1.579378	0.813856	-3.366300
C	0.135169	3.466698	-1.685186
C	-1.130081	4.102390	-1.723931
C	1.209531	4.265559	-1.221765
C	-1.316078	5.417419	-1.303370
H	-1.981245	3.538375	-2.102302
C	1.024705	5.580109	-0.793265
H	2.210737	3.844393	-1.210955
C	-0.241376	6.172354	-0.821949
H	-2.308876	5.860742	-1.359947
H	1.883022	6.153610	-0.446750
H	-0.382695	7.200336	-0.498207
Cu	-0.103073	0.722017	-0.582469
N	-1.911903	1.624169	0.516499
C	-1.675937	2.807350	1.110303
C	-3.178110	1.172511	0.511936
C	-2.669990	3.558831	1.738010
H	-0.651882	3.164298	1.067114
C	-4.237083	1.861040	1.102269
H	-3.343691	0.221703	0.017840
C	-3.977391	3.077565	1.735592
H	-2.415380	4.508528	2.197558
H	-5.238444	1.444069	1.059932
H	-4.777860	3.640051	2.208733

Structure 15aa
Charge: 0
Multiplicity: 1
Imaginary Frequencies: 0
Electronic Energy (B3LYP): -2755.870051
Gibbs Free Energy (B3LYP): -2755.108169
Electronic Energy (BP86-D3(BJ)/CPCM(THF)): -2756.854444
Total Gibbs Free Energy: -2756.092562
Geometry:

P	1.029709	-0.138031	1.344587
C	0.253763	0.825412	2.800157
C	1.422841	1.152073	3.752361
C	2.656230	1.409804	2.878045
C	2.804996	0.188138	1.937411
H	1.175809	2.014069	4.383764
H	1.633358	0.310367	4.424169
H	3.566557	1.545515	3.473961
H	2.517610	2.323186	2.285291
P	-0.822714	-2.039566	-0.608133
C	0.088792	-3.258524	-1.761706
C	-0.878684	-4.444317	-1.936178
C	-2.286794	-3.856392	-2.062762
C	-2.510746	-2.898612	-0.865848
H	-0.602491	-5.049176	-2.808540
H	-0.843970	-5.107309	-1.062608

H	-3.061609	-4.631903	-2.077283
H	-2.374086	-3.302152	-3.005549
H	-0.049618	1.767613	2.328292
H	3.058847	-0.673469	2.570662
C	-0.419619	-2.601420	1.138449
H	-0.345224	-3.695153	1.183450
H	-1.290466	-2.310232	1.738140
C	0.852471	-1.964217	1.728049
H	0.120480	-2.714754	-2.714824
H	-2.648096	-3.516110	0.031005
C	1.516506	-3.561804	-1.360739
C	4.195792	-4.011703	-0.598685
C	2.529977	-2.650109	-1.702948
C	1.875735	-4.709408	-0.638183
C	3.203494	-4.933128	-0.263137
C	3.853716	-2.866149	-1.322306
H	2.274408	-1.755235	-2.266053
H	1.124148	-5.445880	-0.370378
H	3.458993	-5.833296	0.290261
H	4.613222	-2.135938	-1.584897
H	5.227181	-4.184900	-0.303954
C	-3.719218	-1.999288	-1.001154
C	-6.044640	-0.428371	-1.276437
C	-3.874107	-1.128770	-2.091123
C	-4.746730	-2.058782	-0.048927
C	-5.898829	-1.280400	-0.181451
C	-5.026697	-0.355686	-2.230945
H	-3.087372	-1.049675	-2.837161
H	-4.646537	-2.728855	0.802190
H	-6.684587	-1.348530	0.566582
H	-5.128252	0.306503	-3.086289
H	-6.941576	0.174723	-1.386878
C	3.888416	0.323611	0.886139
C	5.992146	0.619007	-0.969119
C	5.151813	-0.235173	1.132725
C	3.697380	1.029750	-0.310195
C	4.737184	1.174143	-1.230153
C	6.196445	-0.087290	0.218604
H	5.319667	-0.790391	2.053583
H	2.728506	1.457681	-0.542823
H	4.552974	1.719728	-2.151675
H	7.167673	-0.525745	0.434052
H	6.802560	0.734513	-1.684107
C	-0.986636	0.179300	3.377281
C	-3.347971	-1.043150	4.331264
C	-0.958567	-0.671811	4.492603
C	-2.225935	0.409263	2.753053
C	-3.392451	-0.196421	3.220356
C	-2.127085	-1.274656	4.966091
H	-0.023177	-0.862747	5.010393
H	-2.271327	1.067772	1.888447
H	-4.334608	-0.004208	2.714371
H	-2.079967	-1.923730	5.836884
H	-4.256068	-1.510480	4.702723
H	0.887504	-2.141449	2.809688
H	1.740147	-2.435445	1.290488
C	-2.710326	3.330160	-0.277737

H	-3.330614	3.089490	0.589447
C	-3.371866	3.107455	-1.604058
H	-4.286431	3.715172	-1.683165
H	-2.724705	3.345774	-2.450357
H	-3.682738	2.060552	-1.712726
C	-1.484965	3.850840	-0.023889
C	-1.106933	4.119156	1.363753
C	-0.456198	4.192316	-1.083688
C	-0.092576	4.962087	1.675556
H	-1.725734	3.691138	2.151663
C	0.416831	5.346576	-0.673095
H	-0.941182	4.412723	-2.039411
C	0.635475	5.653922	0.620713
H	0.136044	5.188596	2.714677
H	0.955258	5.867740	-1.459951
H	1.333453	6.441717	0.895629
Cu	-0.127499	0.144340	-0.693616
N	-0.180209	1.724672	-1.782785
C	-0.574729	1.661118	-3.084557
C	0.542633	2.945460	-1.412314
C	-0.053122	2.435433	-4.095602
H	-1.308054	0.885161	-3.309720
C	1.515943	3.343475	-2.493362
H	1.060408	2.761980	-0.465337
C	1.140810	3.177631	-3.786201
H	-0.403904	2.322486	-5.116178
H	2.452653	3.823444	-2.220629
H	1.775157	3.531199	-4.598431

Structure 15ak
Charge: 0
Multiplicity: 1
Imaginary Frequencies: 0
Electronic Energy (B3LYP): -2986.920868
Gibbs Free Energy (B3LYP): -2986.086942
Electronic Energy (BP86-D3(BJ)/CPCM(THF)): -2987.983142
Total Gibbs Free Energy: -2987.149215
Geometry:

P	2.314911	0.427406	1.176200
C	2.067452	0.188532	3.056425
C	3.154576	1.059367	3.719731
C	3.302866	2.326014	2.868355
C	3.527833	1.874370	1.404416
H	2.888001	1.286853	4.758890
H	4.116217	0.531806	3.743566
H	4.134932	2.955686	3.204513
H	2.392432	2.935103	2.934842
P	1.279003	-1.820538	-1.014226
C	1.969572	-1.887058	-2.795669
C	1.810568	-3.355013	-3.237354
C	0.476056	-3.850791	-2.669846
C	0.469872	-3.542837	-1.151976
H	1.854230	-3.441405	-4.330018
H	2.621975	-3.973841	-2.833903
H	0.324854	-4.923125	-2.840560
H	-0.356663	-3.329736	-3.159269
H	1.101937	0.675135	3.239599

H	4.527600	1.423011	1.351885
C	2.731062	-2.197376	0.114021
H	3.442085	-2.874592	-0.374580
H	2.302665	-2.735806	0.967805
C	3.467154	-0.938741	0.609554
H	1.239489	-1.292947	-3.360269
H	1.178407	-4.232080	-0.674120
C	3.320787	-1.228497	-2.967217
C	5.799972	0.097986	-3.221973
C	3.383101	0.166276	-3.133453
C	4.527100	-1.944579	-2.939712
C	5.754106	-1.288003	-3.068346
C	4.606547	0.824508	-3.254699
H	2.460066	0.741229	-3.163541
H	4.519245	-3.024982	-2.830676
H	6.674778	-1.865778	-3.052599
H	4.623735	1.904173	-3.371564
H	6.754884	0.606619	-3.323475
C	-0.873568	-3.708863	-0.474043
C	-3.377393	-4.119433	0.754653
C	-1.985307	-2.927048	-0.827062
C	-1.040775	-4.694802	0.508669
C	-2.280321	-4.900511	1.119296
C	-3.225695	-3.131108	-0.221629
H	-1.884708	-2.142331	-1.572120
H	-0.191923	-5.312452	0.794659
H	-2.387413	-5.675808	1.873951
H	-4.073620	-2.516283	-0.511345
H	-4.343923	-4.276455	1.225414
C	3.457274	2.978988	0.372378
C	3.389116	5.073993	-1.511393
C	4.619102	3.376128	-0.304410
C	2.258658	3.651221	0.087745
C	2.223238	4.686409	-0.846287
C	4.588999	4.416322	-1.236172
H	5.558343	2.867455	-0.097218
H	1.340325	3.354347	0.586230
H	1.280232	5.181591	-1.060109
H	5.503653	4.711809	-1.744055
H	3.360670	5.880313	-2.239228
C	1.940644	-1.254430	3.494078
C	1.619267	-3.964963	4.217203
C	3.031594	-2.015162	3.941673
C	0.683642	-1.879728	3.424786
C	0.522549	-3.219536	3.776716
C	2.871858	-3.355817	4.301664
H	4.015762	-1.563694	4.024894
H	-0.178009	-1.307743	3.087810
H	-0.459837	-3.677074	3.703880
H	3.730779	-3.921872	4.652947
H	1.496783	-5.007131	4.499394
H	4.171267	-1.206288	1.406581
H	4.051623	-0.503198	-0.209589
C	-2.309108	3.611372	2.686551
H	-2.745120	4.466866	3.204587
C	-0.905092	3.271930	3.094581
H	-0.818024	3.223779	4.190067

H	-0.575986	2.310391	2.686342
H	-0.183563	4.033998	2.762056
C	-3.097814	2.962801	1.793890
C	-4.476262	3.401511	1.609864
C	-2.627724	1.807149	0.925179
C	-5.373854	2.681821	0.900894
H	-4.782393	4.323906	2.100561
C	-3.734612	0.981080	0.361111
H	-1.950875	1.152379	1.492083
C	-5.019780	1.401988	0.284403
H	-6.392304	3.044968	0.789541
H	-3.451851	0.016896	-0.048778
Cu	0.526130	0.302588	-0.216939
N	-0.994033	1.219828	-0.942671
C	-1.538261	0.806384	-2.118730
C	-1.646746	2.347209	-0.269858
C	-2.467367	1.499900	-2.854592
H	-1.129299	-0.127666	-2.507588
C	-2.337841	3.281901	-1.221515
H	-0.886759	2.896067	0.301883
C	-2.784711	2.835230	-2.416512
H	-2.818514	1.113963	-3.805715
H	-2.521659	4.299888	-0.888494
H	-3.337408	3.498708	-3.079835
C	-6.067404	0.583731	-0.374833
C	-7.374281	0.515799	0.140207
C	-5.777080	-0.154091	-1.538466
C	-8.348879	-0.274085	-0.470102
H	-7.622146	1.069232	1.042212
C	-6.751713	-0.945624	-2.146487
H	-4.788656	-0.065578	-1.982413
C	-8.042303	-1.012435	-1.615024
H	-9.349437	-0.316650	-0.046279
H	-6.507059	-1.498801	-3.050411
H	-8.802104	-1.626070	-2.092245

Structure 27aa
Charge: 0
Multiplicity: 1
Imaginary Frequencies: 0
Electronic Energy (B3LYP): -2755.892189
Gibbs Free Energy (B3LYP): -2755.132238
Electronic Energy (BP86-D3(BJ)/CPCM(THF)): -2756.874191
Total Gibbs Free Energy: -2956.114240
Geometry:

P	1.223052	-0.005991	1.469289
C	0.464697	0.111447	3.234805
C	1.650268	0.401209	4.181534
C	2.667053	1.252057	3.416636
C	2.952526	0.530969	2.078766
H	1.301431	0.895723	5.096637
H	2.134861	-0.532303	4.491162
H	3.595509	1.395933	3.982155
H	2.254998	2.251070	3.222667
P	-0.331398	-1.617742	-1.007641
C	0.710782	-2.341960	-2.451323
C	-0.084198	-3.565256	-2.949608

C	-1.566658	-3.199363	-2.892818
C	-1.864834	-2.668379	-1.469879
H	0.235007	-3.849727	-3.959959
H	0.091638	-4.433656	-2.303222
H	-2.214848	-4.052962	-3.124644
H	-1.786977	-2.420208	-3.632346
H	-0.146360	1.019604	3.175876
H	3.494178	-0.395824	2.311607
C	0.303752	-2.535319	0.498729
H	0.575321	-3.567128	0.243131
H	-0.537731	-2.586668	1.199528
C	1.501061	-1.835570	1.170171
H	0.636405	-1.562974	-3.218595
H	-1.847898	-3.523254	-0.781376
C	2.180288	-2.568111	-2.158653
C	4.934974	-2.913706	-1.614838
C	3.094569	-1.514273	-2.329185
C	2.683498	-3.802977	-1.716888
C	4.043693	-3.974127	-1.448470
C	4.452719	-1.680302	-2.058810
H	2.737736	-0.549105	-2.677047
H	2.017818	-4.650831	-1.589095
H	4.405026	-4.943284	-1.113823
H	5.130053	-0.842260	-2.194573
H	5.993536	-3.048821	-1.409522
C	-3.209839	-1.986824	-1.347100
C	-5.772210	-0.820883	-1.182307
C	-3.556713	-0.896609	-2.162423
C	-4.164505	-2.469552	-0.440051
C	-5.433957	-1.892740	-0.354529
C	-4.826515	-0.323930	-2.083579
H	-2.825806	-0.471566	-2.845962
H	-3.913796	-3.312541	0.200529
H	-6.159107	-2.287918	0.352449
H	-5.069397	0.522594	-2.719853
H	-6.761723	-0.375027	-1.125091
C	3.785846	1.328931	1.100020
C	5.406184	2.825318	-0.659675
C	5.044573	0.857613	0.701510
C	3.353611	2.566630	0.597376
C	4.152714	3.307011	-0.273600
C	5.850020	1.597183	-0.168062
H	5.399286	-0.098813	1.079428
H	2.377348	2.954031	0.876262
H	3.790619	4.257743	-0.655161
H	6.825625	1.213481	-0.456260
H	6.028980	3.402704	-1.337495
C	-0.454191	-1.025702	3.629877
C	-2.230336	-3.124402	4.294345
C	0.010094	-2.203952	4.237880
C	-1.832270	-0.920870	3.373507
C	-2.709595	-1.956151	3.697438
C	-0.866413	-3.240680	4.565992
H	1.064359	-2.319597	4.471335
H	-2.218646	-0.016267	2.913171
H	-3.770059	-1.844286	3.487101
H	-0.479498	-4.138939	5.040512

H	-2.912223	-3.929924	4.553337
H	1.751787	-2.350110	2.104996
H	2.380978	-1.895416	0.520125
C	-0.292442	4.432302	-0.902307
H	0.662682	4.457898	-0.378005
C	-1.172845	5.646865	-0.774514
H	-1.431829	6.091006	-1.748745
H	-2.133167	5.448779	-0.263845
H	-0.668947	6.430850	-0.195778
C	-0.534108	3.371245	-1.750284
C	0.383791	2.238303	-1.898388
C	-1.731639	3.286468	-2.569072
C	0.246656	1.368280	-3.012151
H	1.380403	2.346282	-1.470900
C	-1.870229	2.355551	-3.569680
H	-2.505899	4.037121	-2.434224
C	-0.861682	1.389423	-3.844622
H	1.057991	0.672899	-3.217124
H	-2.764415	2.381322	-4.192639
H	-0.952184	0.710061	-4.687979
Cu	-0.218345	0.648780	-0.398116
N	-1.715174	1.665713	0.674721
C	-3.035927	1.395419	0.617586
C	-1.336760	2.810197	1.290649
C	-4.007430	2.210784	1.183631
H	-3.310577	0.481588	0.105120
C	-2.251278	3.684027	1.891176
H	-0.271690	2.988280	1.353234
C	-3.606140	3.388010	1.832980
H	-5.052691	1.928015	1.112279
H	-1.889535	4.583086	2.379951
H	-4.339081	4.049104	2.287498

Structure 27al
Charge: 0
Multiplicity: 1
Imaginary Frequencies: 0
Electronic Energy (B3LYP): -2753.685053
Gibbs Free Energy (B3LYP): -2752.956898
Geometry:

P	0.572999	-0.858729	1.595127
C	-0.468323	-1.154740	3.200688
C	0.513517	-1.743852	4.233923
C	1.876300	-1.087083	4.001506
C	2.211255	-1.256697	2.502817
H	0.144503	-1.589127	5.255779
H	0.619190	-2.826420	4.094637
H	2.661489	-1.532775	4.624037
H	1.831796	-0.021040	4.260538
P	-0.793172	-0.847489	-1.440569
C	0.164382	-1.332008	-3.035142
C	-0.910652	-1.688625	-4.085312
C	-2.144804	-0.823824	-3.810712
C	-2.487460	-0.994302	-2.313416
H	-0.521073	-1.541134	-5.100274
H	-1.198330	-2.744248	-4.007822
H	-2.998543	-1.108539	-4.437887

H	-1.924827	0.229747	-4.027949
H	-0.710886	-0.136773	3.530733
H	2.386261	-2.326609	2.328173
C	-0.819219	-2.388102	-0.375388
H	-0.826067	-3.293909	-0.993012
H	-1.768801	-2.356917	0.171112
C	0.355561	-2.443287	0.613995
H	0.625678	-0.380915	-3.316378
H	-2.809244	-2.034542	-2.168277
C	1.283058	-2.335382	-2.840932
C	3.420136	-4.137095	-2.417436
C	2.583658	-1.868330	-2.578285
C	1.081967	-3.724679	-2.897193
C	2.137515	-4.615548	-2.688905
C	3.637452	-2.758111	-2.365281
H	2.758782	-0.796874	-2.546379
H	0.096469	-4.126425	-3.115584
H	1.954581	-5.685970	-2.743730
H	4.631802	-2.368497	-2.162582
H	4.241705	-4.830658	-2.257705
C	-3.584096	-0.089867	-1.800992
C	-5.684926	1.566907	-0.903506
C	-3.465403	1.308368	-1.836953
C	-4.774363	-0.638601	-1.302199
C	-5.816753	0.178508	-0.858259
C	-4.503123	2.127986	-1.394382
H	-2.547620	1.758651	-2.204788
H	-4.887289	-1.719967	-1.266111
H	-6.732943	-0.271731	-0.483899
H	-4.384315	3.207799	-1.425718
H	-6.493908	2.206498	-0.560530
C	3.436396	-0.504382	2.036083
C	5.762740	0.852054	1.201856
C	4.519619	-1.203235	1.484468
C	3.540797	0.889217	2.160360
C	4.689798	1.561948	1.746497
C	5.673837	-0.534234	1.071542
H	4.458270	-2.284298	1.378422
H	2.706253	1.459455	2.559476
H	4.735284	2.643979	1.828635
H	6.501661	-1.097961	0.648703
H	6.656258	1.377409	0.875679
C	-1.776151	-1.888369	2.995399
C	-4.245851	-3.192205	2.539003
C	-1.902759	-3.278315	3.151764
C	-2.921495	-1.168996	2.611074
C	-4.139287	-1.808460	2.381291
C	-3.122100	-3.921967	2.928043
H	-1.048907	-3.873275	3.460474
H	-2.857611	-0.091607	2.483727
H	-5.001133	-1.222136	2.075319
H	-3.190881	-4.998472	3.062730
H	-5.194044	-3.694232	2.366496
H	0.239527	-3.300846	1.287974
H	1.295453	-2.584184	0.067547
C	2.060888	4.002015	0.183731
H	1.999985	3.504836	1.151636

C	2.197967	5.498941	0.219433
H	3.075226	5.821243	0.801866
H	2.308469	5.927868	-0.782765
H	1.326564	5.987214	0.687321
C	2.010018	3.228900	-0.933261
C	1.904623	1.729830	-0.989668
C	2.015712	3.680361	-2.324359
O	1.960715	1.415793	-2.456025
H	2.800272	1.253159	-0.582264
C	1.988874	2.587127	-3.114646
H	2.051265	4.703647	-2.674598
H	1.980020	2.514414	-4.197981
Cu	0.283174	0.814434	-0.112156
N	-0.984600	2.448780	0.605169
C	-1.071394	3.530193	-0.191303
C	-1.489825	2.553924	1.845194
C	-1.692239	4.717106	0.202253
H	-0.633552	3.428637	-1.178003
C	-2.111904	3.701087	2.330664
H	-1.386832	1.674368	2.472152
C	-2.221783	4.808377	1.486865
H	-1.738617	5.553122	-0.488775
H	-2.503204	3.718935	3.343271
H	-2.704062	5.720684	1.827200

Structure 39
Charge: 0
Multiplicity: 1
Imaginary Frequencies: 0
Electronic Energy (B3LYP): -2760.702901
Geometry:

P	0.766928	1.930471	-1.324312
C	-0.126079	3.068156	-2.594170
C	0.873807	4.189712	-2.929730
C	2.258058	3.540562	-3.005640
C	2.467449	2.735540	-1.699593
H	0.602782	4.697228	-3.864626
H	0.881270	4.953705	-2.141931
H	3.058681	4.278817	-3.136885
H	2.303771	2.866657	-3.870873
P	-0.902142	0.488338	1.498026
C	0.184430	0.165727	2.995424
C	-0.796923	-0.189555	4.148833
C	-2.124418	-0.674123	3.554512
C	-2.509721	0.361358	2.478328
H	-0.344573	-0.938526	4.809262
H	-0.987524	0.695964	4.765819
H	-2.909990	-0.763412	4.314418
H	-2.004167	-1.667266	3.102911
H	-0.208589	2.425452	-3.480969
H	2.654163	3.455285	-0.892383
C	-0.824534	2.306847	1.084952
H	-0.909936	2.882590	2.014159
H	-1.731893	2.505075	0.502061
C	0.421994	2.785154	0.318810
H	0.738238	-0.734145	2.710998
H	-2.635041	1.330609	2.981085

C	1.202311	1.238359	3.325470
C	3.150393	3.202858	3.891875
C	2.554043	1.027384	3.003880
C	0.851169	2.447889	3.949125
C	1.812682	3.420392	4.227694
C	3.515882	2.000602	3.283106
H	2.846201	0.081389	2.553561
H	-0.182123	2.637140	4.229089
H	1.515339	4.347265	4.711794
H	4.556334	1.811863	3.030558
H	3.899860	3.958603	4.111904
C	-3.770504	0.080662	1.688440
C	-6.180591	-0.369453	0.285886
C	-4.018364	-1.152515	1.054047
C	-4.753657	1.076873	1.595752
C	-5.945635	0.858686	0.902432
C	-5.212620	-1.373149	0.366796
H	-3.286494	-1.955702	1.093702
H	-4.585420	2.036316	2.080112
H	-6.691864	1.647576	0.853058
H	-5.384130	-2.334423	-0.110028
H	-7.109776	-0.546724	-0.249012
C	3.629468	1.766751	-1.744395
C	5.843697	0.020312	-1.854335
C	4.711991	1.917059	-0.866127
C	3.672606	0.713570	-2.672717
C	4.767897	-0.147317	-2.731186
C	5.809172	1.053600	-0.917325
H	4.696147	2.722652	-0.135122
H	2.838482	0.561289	-3.353313
H	4.780315	-0.952031	-3.461789
H	6.638122	1.193845	-0.228194
H	6.698368	-0.649186	-1.901543
C	-1.530258	3.467467	-2.197162
C	-4.174199	4.101034	-1.426268
C	-1.845874	4.727906	-1.668094
C	-2.573258	2.534209	-2.340793
C	-3.877251	2.842044	-1.956525
C	-3.154313	5.041920	-1.288551
H	-1.073634	5.483092	-1.558943
H	-2.354540	1.552371	-2.754951
H	-4.660039	2.097193	-2.067770
H	-3.372886	6.028903	-0.888346
H	-5.190857	4.345950	-1.130730
H	0.337940	3.869566	0.169641
H	1.315164	2.620760	0.932618
C	-0.795756	-2.447405	-2.244568
H	0.220742	-2.487337	-2.667838
C	-1.724627	-1.853389	-3.329897
H	-1.754172	-2.485118	-4.235178
H	-2.759680	-1.745022	-2.981949
H	-1.381856	-0.857605	-3.638780
C	-1.189864	-3.838405	-1.868811
C	-0.408966	-4.925083	-2.048459
H	0.587126	-4.823842	-2.478820
Cu	-0.645498	-1.193703	-0.739228
N	2.774368	-2.245452	1.776122

C	2.609232	-3.454047	2.150934
H	2.272594	-3.619240	3.179600
C	4.399906	-3.042153	0.080938
H	5.223102	-2.801981	0.766068
H	4.770904	-2.865485	-0.934402
C	3.977223	-4.513929	0.268664
H	4.831398	-5.098187	0.628505
H	3.684229	-4.950520	-0.692472
C	2.787850	-4.658325	1.260140
H	2.864484	-5.573136	1.857276
H	1.857429	-4.746508	0.679565
C	3.248111	-2.074955	0.394925
H	2.405809	-2.233284	-0.294724
H	3.574208	-1.038340	0.269104
C	-0.884761	-6.290745	-1.609719
H	-0.071042	-7.026697	-1.613726
H	-1.649430	-6.680107	-2.304581
C	-1.513076	-6.169447	-0.208920
H	-0.737293	-5.791028	0.468696
H	-1.828972	-7.145333	0.182963
C	-2.696052	-5.177833	-0.223281
H	-2.763679	-4.688677	0.757135
H	-3.638514	-5.725152	-0.354401
C	-2.596766	-4.094609	-1.343246
H	-3.198286	-4.424068	-2.203481
H	-3.047550	-3.162871	-0.977548

Structure 40
Charge: 0
Multiplicity: 1
Imaginary Frequencies: 0
Electronic Energy (B3LYP): -2760.728289
Geometry:

P	-1.046148	-0.621446	1.480111
C	-0.373206	-0.059125	3.182581
C	-0.853659	-1.124183	4.189486
C	-0.826915	-2.477579	3.468289
C	-1.622493	-2.306375	2.151769
H	-0.225556	-1.120782	5.088697
H	-1.880651	-0.917748	4.515565
H	-1.262360	-3.278920	4.077011
H	0.207428	-2.769470	3.245883
P	-1.450998	1.428192	-1.043360
C	-2.553612	0.972425	-2.545129
C	-2.923182	2.312632	-3.214198
C	-1.719760	3.249476	-3.057653
C	-1.346626	3.260722	-1.556269
H	-3.196718	2.160167	-4.265515
H	-3.790911	2.768177	-2.721318
H	-1.938157	4.265824	-3.406576
H	-0.872304	2.882038	-3.651146
H	0.709700	-0.184911	3.062119
H	-2.675193	-2.160277	2.429342
C	-2.588391	1.551370	0.443993
H	-3.587765	1.894451	0.150502
H	-2.147172	2.331170	1.076664
C	-2.696257	0.237524	1.237363

H	-1.846555	0.457318	-3.206988
H	-2.165590	3.762217	-1.023017
C	-3.671459	0.002092	-2.233800
C	-5.674118	-1.883638	-1.590802
C	-3.401032	-1.377491	-2.246692
C	-4.970183	0.414732	-1.897269
C	-5.961461	-0.518150	-1.582166
C	-4.386335	-2.310685	-1.924863
H	-2.402003	-1.720455	-2.506057
H	-5.223160	1.470861	-1.888827
H	-6.961687	-0.172975	-1.332699
H	-4.143301	-3.369360	-1.932736
H	-6.446575	-2.607807	-1.346166
C	-0.060217	3.982158	-1.218945
C	2.299277	5.410467	-0.633978
C	1.190877	3.507290	-1.643479
C	-0.104120	5.180718	-0.492288
C	1.062666	5.891527	-0.201706
C	2.357779	4.215231	-1.355206
H	1.258116	2.569885	-2.187542
H	-1.064522	5.564456	-0.154237
H	1.002414	6.821753	0.357794
H	3.315536	3.826226	-1.689729
H	3.209889	5.959876	-0.410502
C	-1.552447	-3.480532	1.199680
C	-1.456780	-5.732009	-0.495282
C	-2.677990	-4.298163	1.022312
C	-0.376828	-3.809125	0.506983
C	-0.329404	-4.923476	-0.331002
C	-2.633581	-5.415298	0.185117
H	-3.599267	-4.059249	1.549709
H	0.503450	-3.181481	0.606897
H	0.590811	-5.154497	-0.860993
H	-3.517440	-6.037552	0.068665
H	-1.417808	-6.599490	-1.148712
C	-0.629177	1.397037	3.502968
C	-1.066967	4.146654	3.977661
C	-1.729850	1.832546	4.256695
C	0.251249	2.370219	2.998342
C	0.034749	3.728893	3.226463
C	-1.944515	3.192734	4.494200
H	-2.425079	1.111322	4.676090
H	1.112860	2.055231	2.414068
H	0.726198	4.457701	2.813256
H	-2.800193	3.503948	5.088125
H	-1.235522	5.203980	4.163561
H	-3.187640	0.418055	2.201034
H	-3.314496	-0.479640	0.684132
C	4.613292	-2.544902	1.706367
H	5.487095	-3.073937	2.092324
C	3.295217	-3.050087	2.227856
H	3.353244	-3.226235	3.311193
H	2.480060	-2.342578	2.044690
H	3.007650	-4.008534	1.772009
C	4.832500	-1.513277	0.872979
C	3.732205	-0.671435	0.225581
H	3.005342	-0.403110	1.007693

Cu	0.188277	-0.161421	-0.370552
N	1.740253	-0.612876	-1.332345
C	2.826645	-1.448536	-0.819140
H	2.377977	-2.260284	-0.225216
C	1.904759	-0.255158	-2.729415
H	2.854062	0.287074	-2.920246
H	1.106201	0.440408	-3.018865
C	1.864670	-1.490206	-3.664924
H	2.326765	-1.236883	-4.631177
H	0.821445	-1.764511	-3.870180
C	2.600448	-2.680967	-3.003646
H	3.110115	-3.293692	-3.758267
H	1.873348	-3.336814	-2.506895
C	3.596155	-2.168605	-1.953991
H	4.310128	-1.499343	-2.445461
H	4.182259	-2.991451	-1.527988
C	6.264658	-1.078530	0.593003
H	6.958968	-1.892391	0.836055
H	6.520785	-0.248987	1.272622
C	6.479442	-0.601165	-0.850176
H	6.302624	-1.445535	-1.525809
H	7.527441	-0.308853	-0.992382
C	5.537814	0.576521	-1.208809
H	5.222089	0.488407	-2.255009
H	6.089498	1.523795	-1.143190
C	4.304040	0.670887	-0.280268
H	3.494750	1.224042	-0.766816
H	4.587499	1.258560	0.604176

Structure [TS9,11]a
Charge: 0
Multiplicity: 1
Imaginary Frequencies: 1
Electronic Energy (B3LYP): -2507.603333
Gibbs Free Energy (B3LYP): -2506.928959
Electronic Energy (BP86-D3(BJ)/CPCM(THF)): -2508.475832
Total Gibbs Free Energy: -2507.801458
Geometry:

P	-1.110357	1.436161	-0.519954
C	-0.330258	3.149120	-0.814228
C	-1.452519	3.991130	-1.448603
C	-2.744514	3.639588	-0.702288
C	-2.891862	2.096218	-0.704352
H	-1.221192	5.061923	-1.391557
H	-1.571479	3.743957	-2.511286
H	-3.626676	4.106456	-1.155883
H	-2.686402	4.006156	0.330241
P	0.760749	-1.313288	-0.650151
C	-0.052153	-3.038872	-0.780642
C	1.056139	-3.985187	-1.291071
C	2.386345	-3.487305	-0.713165
C	2.491970	-1.981436	-1.053583
H	0.840773	-5.020785	-1.001230
H	1.115102	-3.965382	-2.386365
H	3.245262	-4.031154	-1.123803
H	2.405231	-3.624269	0.375485
H	-0.173450	3.521133	0.206819

H	-3.210002	1.792935	-1.709991
Cu	-0.237003	-0.053179	1.023801
C	0.362817	-0.364424	-2.216864
H	0.297407	-1.040594	-3.077981
H	1.231235	0.285319	-2.378215
C	-0.917555	0.489209	-2.131947
H	-0.233423	-3.281782	0.273542
H	2.577647	-1.901001	-2.146130
C	-1.383554	-3.054952	-1.498794
C	-3.907896	-2.983759	-2.767485
C	-2.558451	-2.811076	-0.766289
C	-1.504019	-3.269602	-2.880950
C	-2.752036	-3.236241	-3.507955
C	-3.805487	-2.771596	-1.390434
H	-2.489069	-2.648379	0.306431
H	-0.621898	-3.475736	-3.480282
H	-2.818584	-3.412833	-4.578535
H	-4.694722	-2.576502	-0.797305
H	-4.878074	-2.961242	-3.256550
C	3.675170	-1.267413	-0.437660
C	5.954902	-0.030755	0.662101
C	3.758905	-1.020780	0.941023
C	4.749002	-0.881742	-1.253127
C	5.882031	-0.271483	-0.711007
C	4.888499	-0.406927	1.483113
H	2.940679	-1.294571	1.602456
H	4.699706	-1.065965	-2.324542
H	6.705141	0.013438	-1.361626
H	4.928761	-0.221272	2.553075
H	6.834187	0.444314	1.089332
C	-3.892540	1.550968	0.290913
C	-5.799294	0.556713	2.115206
C	-5.006015	0.825488	-0.154590
C	-3.751515	1.769513	1.670752
C	-4.694096	1.278590	2.573841
C	-5.952278	0.331680	0.746843
H	-5.135343	0.647598	-1.220006
H	-2.891775	2.318859	2.045963
H	-4.562420	1.457076	3.637612
H	-6.810781	-0.223241	0.376970
H	-6.533162	0.174528	2.819433
C	1.018196	3.108475	-1.498444
C	3.564560	2.938525	-2.697884
C	1.180689	3.334094	-2.873063
C	2.158370	2.805129	-0.733435
C	3.417155	2.714550	-1.326101
C	2.443707	3.252883	-3.466612
H	0.325216	3.589368	-3.491564
H	2.052492	2.628021	0.335103
H	4.279465	2.461979	-0.716369
H	2.547752	3.440468	-4.532392
H	4.545581	2.873323	-3.160668
H	-0.965684	1.171995	-2.989165
H	-1.797617	-0.162561	-2.186837
C	1.055773	1.572196	3.511488
H	0.268777	2.292921	3.287522
C	2.367895	2.119398	4.007722

H	2.499288	2.033769	5.101971
H	3.234957	1.613305	3.555843
H	2.463076	3.185271	3.766712
C	0.727296	0.233685	3.485375
C	-0.602130	-0.247038	3.064265
C	1.635833	-0.833140	3.905287
C	-0.871152	-1.641471	2.961714
H	-1.450090	0.428755	3.169510
C	1.316110	-2.164544	3.789862
H	2.569068	-0.551342	4.386280
C	0.091179	-2.610689	3.215284
H	-1.887313	-1.940710	2.702894
H	2.033215	-2.905854	4.142442
H	-0.142975	-3.668931	3.148708

Structure [TS10,7]aa
Charge: 0
Multiplicity: 1
Imaginary Frequencies: 1
Electronic Energy (B3LYP): -3316.252846
Gibbs Free Energy (B3LYP): -3315.367427
Electronic Energy (BP86-D3(BJ)/CPCM(THF)): -3317.378159
Total Gibbs Free Energy: -3316.492740
Geometry:

Cu	-0.728217	-0.195590	0.601938
H	6.474347	1.517390	2.279026
H	-0.995792	-0.686775	2.153602
N	1.097965	0.426948	1.864575
C	1.999049	-0.627111	1.634147
C	1.578756	1.682206	1.457927
C	3.151828	-0.528925	0.944861
H	1.692994	-1.578338	2.063879
C	2.705718	1.875615	0.745525
H	0.941446	2.510726	1.742559
C	3.629147	0.758431	0.308375
H	3.764400	-1.419434	0.829021
H	2.963641	2.893680	0.458830
H	3.592704	0.658304	-0.794506
C	5.419795	1.280805	2.097877
H	5.164461	0.385491	2.674946
H	4.808614	2.099859	2.489962
C	5.144360	1.090572	0.602255
H	5.322703	2.057532	0.108388
C	6.061743	0.081606	-0.075565
C	6.346074	0.220959	-1.444253
C	6.620479	-1.014913	0.597762
C	7.150464	-0.698024	-2.117700
H	5.934418	1.070364	-1.986278
C	7.427447	-1.938874	-0.071612
H	6.433116	-1.149619	1.658712
C	7.695603	-1.786226	-1.432169
H	7.358503	-0.559906	-3.175981
H	7.850191	-2.777614	0.476152
H	8.327246	-2.502188	-1.951553
P	-0.443358	-1.350763	-1.358114
P	-2.504090	1.031973	-0.301692
C	-2.042567	-1.008433	-2.276034

H	-1.920925	-1.205915	-3.348389
H	-2.757112	-1.744425	-1.888556
C	-2.599045	0.414345	-2.070608
H	-2.006433	1.129216	-2.653211
H	-3.628474	0.463168	-2.446320
C	-0.200018	-3.209932	-1.712533
H	-0.940851	-3.453953	-2.485482
C	0.973215	-0.831833	-2.527711
H	1.798629	-0.639846	-1.831471
C	1.325976	-2.101988	-3.327840
H	0.628759	-2.243876	-4.162756
H	2.331554	-2.022605	-3.758168
C	1.199859	-3.289640	-2.368759
H	1.326349	-4.251386	-2.879779
H	1.978568	-3.230025	-1.598532
C	-4.141709	0.513390	0.538274
C	-5.104213	1.702945	0.349221
H	-5.578955	1.668697	-0.639229
H	-5.910629	1.671348	1.092179
C	-3.078090	2.840418	-0.524386
H	-3.481820	2.888338	-1.544602
C	-4.269015	2.981555	0.454439
H	-4.851962	3.879558	0.217054
H	-3.891846	3.103747	1.477529
H	-3.857130	0.480258	1.596947
C	-2.033566	3.924972	-0.381626
C	-1.864458	4.870974	-1.402298
C	-1.261439	4.052385	0.783911
C	-0.954465	5.922154	-1.266711
H	-2.455471	4.786916	-2.311945
C	-0.353198	5.102957	0.920563
H	-1.351593	3.313126	1.576198
C	-0.195871	6.042772	-0.101671
H	-0.844070	6.647262	-2.069193
H	0.236222	5.186124	1.830307
H	0.511218	6.860523	0.009878
C	-4.649358	-0.861164	0.157672
C	-4.176139	-1.984586	0.857628
C	-5.564532	-1.072570	-0.885687
C	-4.594614	-3.272315	0.522698
H	-3.461517	-1.843967	1.664770
C	-5.988507	-2.361236	-1.220226
H	-5.965649	-0.229976	-1.441162
C	-5.504238	-3.466799	-0.519967
H	-4.204745	-4.121845	1.075968
H	-6.703797	-2.497156	-2.027581
H	-5.837691	-4.468347	-0.778548
C	0.715874	0.441372	-3.305693
C	0.979207	1.680841	-2.696292
C	0.199861	0.443492	-4.610863
C	0.726608	2.879327	-3.363924
H	1.377192	1.706896	-1.683988
C	-0.048248	1.643252	-5.283068
H	-0.003927	-0.493221	-5.120957
C	0.210840	2.865787	-4.662468
H	0.928143	3.822422	-2.864210
H	-0.441124	1.618005	-6.296452

H	0.018699	3.798137	-5.186804
C	-0.410964	-4.151470	-0.548060
C	-1.423288	-5.119480	-0.601054
C	0.412295	-4.113927	0.588341
C	-1.610783	-6.024659	0.446260
H	-2.070376	-5.167534	-1.474194
C	0.228522	-5.015799	1.635936
H	1.200275	-3.369426	0.655129
C	-0.784990	-5.975611	1.569759
H	-2.398263	-6.771099	0.379011
H	0.877582	-4.968425	2.506426
H	-0.926620	-6.678728	2.385997
O	-0.969285	1.669097	3.214638
C	-1.402357	2.341421	4.387938
O	1.053330	0.389904	4.540134
C	2.199977	1.207913	4.530717
C	-1.090543	-1.040027	4.471756
H	-0.581458	2.495689	5.099241
H	-2.199171	1.785133	4.901026
H	-1.800794	3.319329	4.092508
H	2.949666	0.855764	3.812578
H	2.646051	1.183100	5.533519
H	1.967150	2.256189	4.289389
H	-0.999320	-0.804387	5.537657
H	-0.698354	-2.053688	4.315080
H	-2.149565	-1.063375	4.183419
Si	-0.146886	0.191184	3.339519

Structure [TS11,12]a
Charge: 0
Multiplicity: 1
Imaginary Frequencies: 1
Electronic Energy (B3LYP): -2507.607469
Gibbs Free Energy (B3LYP): -2506.931047
Electronic Energy (BP86-D3(BJ)/CPCM(THF)): -2508.480582
Total Gibbs Free Energy: -2507.804160
Geometry:

P	1.163186	1.547004	-0.501317
C	0.513505	3.213807	-1.179335
C	1.710623	4.178414	-1.090777
C	2.955077	3.385688	-1.501463
C	2.992759	2.092847	-0.650848
H	1.553516	5.058874	-1.726063
H	1.841456	4.543602	-0.064435
H	3.878222	3.960348	-1.361214
H	2.896318	3.134701	-2.567748
P	-0.815107	-0.580997	1.101379
C	-0.138584	-1.977036	2.220314
C	-1.353527	-2.503812	3.019398
C	-2.606251	-2.308591	2.155244
C	-2.599066	-0.833909	1.689557
H	-1.201151	-3.554846	3.293049
H	-1.476931	-1.946413	3.955810
H	-3.526765	-2.532081	2.707326
H	-2.578400	-2.975235	1.283842
H	0.343564	2.995893	-2.242062
H	3.281855	2.376777	0.368916

Cu	0.081985	-0.481860	-1.018536
C	-0.395233	1.072602	1.871769
H	-0.371630	1.001173	2.965275
H	-1.226199	1.735937	1.603663
C	0.933383	1.660734	1.362146
H	0.127179	-2.740313	1.481511
H	-2.693829	-0.211982	2.591167
C	1.110250	-1.623158	2.996609
C	3.497387	-0.940137	4.347098
C	2.367764	-1.871447	2.418577
C	1.077277	-1.027110	4.267725
C	2.256685	-0.690584	4.936033
C	3.547061	-1.532976	3.083235
H	2.414342	-2.327690	1.432989
H	0.125421	-0.828968	4.752390
H	2.203128	-0.236552	5.922327
H	4.504769	-1.740407	2.612884
H	4.414327	-0.682640	4.870485
C	-3.710571	-0.443554	0.740232
C	-5.866500	0.244530	-0.940217
C	-3.763489	-0.911049	-0.581958
C	-4.752606	0.374247	1.202223
C	-5.823965	0.714864	0.373771
C	-4.832205	-0.568078	-1.411573
H	-2.979242	-1.547048	-0.985872
H	-4.728151	0.744059	2.225497
H	-6.623822	1.343822	0.757009
H	-4.847825	-0.947719	-2.429650
H	-6.699523	0.504202	-1.588582
C	3.959454	1.030781	-1.127334
C	5.798064	-0.933820	-1.975927
C	4.887276	0.476615	-0.233989
C	3.972287	0.581604	-2.457112
C	4.881170	-0.389054	-2.878391
C	5.797471	-0.497015	-0.650812
H	4.897097	0.812454	0.800624
H	3.262178	0.989127	-3.172329
H	4.871224	-0.722324	-3.912665
H	6.509704	-0.908532	0.059844
H	6.506089	-1.689550	-2.304502
C	-0.804765	3.660246	-0.585843
C	-3.305189	4.386529	0.503193
C	-0.893083	4.607883	0.444780
C	-1.997470	3.091391	-1.065343
C	-3.233672	3.443286	-0.525461
C	-2.131730	4.969355	0.981846
H	0.003997	5.082869	0.830224
H	-1.952764	2.356830	-1.866232
H	-4.136910	2.974061	-0.903337
H	-2.175091	5.712102	1.774464
H	-4.267344	4.666521	0.923366
H	1.035954	2.699324	1.700871
H	1.770938	1.096066	1.789625
C	-2.413386	-3.034986	-2.969011
H	-2.735091	-2.295037	-3.701744
C	-3.377552	-4.151754	-2.664086
H	-3.963137	-3.995859	-1.739857

```
 H                 -4.107909   -4.264091   -3.474800
 H                 -2.876396   -5.123926   -2.554029
 C                 -1.178028   -2.875140   -2.401724
 C                 -0.279101   -1.758319   -2.753488
 C                 -0.619459   -3.800302   -1.415004
 C                  1.102779   -1.825880   -2.432643
 H                 -0.579934   -1.121373   -3.583879
 C                  0.690745   -3.741917   -1.012675
 H                 -1.252370   -4.600295   -1.039915
 C                  1.599901   -2.761201   -1.516353
 H                  1.791034   -1.140174   -2.921069
 H                  1.060157   -4.489497   -0.310638
 H                  2.656240   -2.789934   -1.270234

Structure [TS13,10]aa
Charge: 0
Multiplicity: 1
Imaginary Frequencies: 1
Electronic Energy (B3LYP): -2755.887826
Gibbs Free Energy (B3LYP): -2755.125849
Electronic Energy (BP86-D3(BJ)/CPCM(THF)): -2756.875025
Total Gibbs Free Energy: -2756.113048
Geometry:
 P                 -0.196756   -1.601619   -1.202746
 C                  0.766754   -1.706721   -2.860288
 C                  0.075803   -2.825570   -3.669792
 C                 -1.419277   -2.776183   -3.349641
 C                 -1.562181   -2.790620   -1.809535
 H                  0.275469   -2.703978   -4.741309
 H                  0.467319   -3.808823   -3.383018
 H                 -1.965404   -3.618110   -3.791245
 H                 -1.862576   -1.859325   -3.758534
 P                  1.442620   -0.264943    1.369435
 C                  0.733304   -0.522799    3.130902
 C                  1.935179   -0.389752    4.088168
 C                  2.868030    0.677313    3.509102
 C                  3.147033    0.294483    2.036132
 H                  1.598108   -0.139901    5.101708
 H                  2.484266   -1.336670    4.159311
 H                  3.807939    0.755676    4.068534
 H                  2.387202    1.663029    3.555021
 H                  0.526031   -0.752328   -3.343580
 H                 -1.252614   -3.784426   -1.459347
 C                  1.874609   -1.982135    0.747573
 H                  2.222585   -2.615667    1.572728
 H                  2.723629   -1.837512    0.069739
 C                  0.730485   -2.694978    0.002669
 H                  0.097978    0.360780    3.263271
 H                  3.770766   -0.609279    2.043208
 C                 -0.152103   -1.741205    3.293572
 C                 -1.868119   -3.972924    3.519527
 C                 -1.518008   -1.639449    2.975095
 C                  0.332531   -2.982663    3.734416
 C                 -0.516690   -4.086802    3.847385
 C                 -2.365620   -2.742072    3.083058
 H                 -1.907463   -0.686734    2.625498
 H                  1.377539   -3.098137    4.006463
```

H	-0.118210	-5.035470	4.198440
H	-3.415259	-2.636995	2.823302
H	-2.528418	-4.831304	3.611431
C	3.870710	1.355722	1.237612
C	5.302728	3.339325	-0.168324
C	3.322462	2.632244	1.034136
C	5.146205	1.093760	0.717662
C	5.858082	2.073600	0.021562
C	4.030720	3.613921	0.340882
H	2.328704	2.860757	1.409905
H	5.589646	0.111396	0.864860
H	6.848626	1.847542	-0.365230
H	3.586392	4.595175	0.196739
H	5.853747	4.105729	-0.706519
C	-2.967086	-2.536514	-1.310984
C	-5.631876	-2.162337	-0.466662
C	-3.623495	-3.508249	-0.542417
C	-3.669196	-1.367037	-1.642942
C	-4.988781	-1.183587	-1.228591
C	-4.942704	-3.325501	-0.121752
H	-3.097184	-4.422115	-0.275624
H	-3.179693	-0.585008	-2.217273
H	-5.512451	-0.270232	-1.497932
H	-5.431691	-4.096044	0.468784
H	-6.659669	-2.017758	-0.145246
C	2.274801	-1.791877	-2.742526
C	5.089111	-1.871367	-2.487507
C	2.956730	-3.013726	-2.618873
C	3.039113	-0.613126	-2.746144
C	4.427578	-0.648201	-2.615879
C	4.347064	-3.053420	-2.493560
H	2.407291	-3.950237	-2.627977
H	2.539654	0.346171	-2.853004
H	4.988210	0.281945	-2.612224
H	4.849418	-4.013350	-2.405118
H	6.171079	-1.903598	-2.392145
H	1.118663	-3.587164	-0.503768
H	-0.025885	-3.032139	0.720940
C	-2.849354	5.053468	-0.599680
H	-2.415249	5.917850	-0.096706
C	-4.266424	5.234941	-1.082172
H	-4.329693	5.704222	-2.078079
H	-4.803458	4.278584	-1.151859
H	-4.834996	5.872534	-0.393320
C	-1.930111	4.188945	-1.234929
C	-0.533291	4.244680	-0.920089
C	-2.333097	3.126005	-2.109790
C	0.348479	3.262411	-1.326648
H	-0.169796	5.088385	-0.337259
C	-1.446117	2.144862	-2.510410
H	-3.359502	3.091160	-2.462681
C	-0.105063	2.141819	-2.060434
H	1.402799	3.339676	-1.071841
H	-1.787342	1.356710	-3.181525
H	0.614152	1.451659	-2.492649
Cu	-0.347822	0.420394	-0.122630
N	-1.628485	1.479777	0.995003

C	-1.151803	2.576227	1.662086
C	-2.962792	1.520530	0.683799
C	-1.885250	3.707485	1.915221
H	-0.120271	2.500877	2.001300
C	-3.768123	2.611154	0.898086
H	-3.368935	0.604652	0.266690
C	-3.187957	3.840145	1.343777
H	-1.429271	4.530590	2.458720
H	-4.823298	2.550689	0.648098
H	-3.838582	4.639736	1.684084

Structure Eq-[TS14,15]aa
Charge: 0
Multiplicity: 1
Imaginary Frequencies: 1
Electronic Energy (B3LYP): -2755.869246
Gibbs Free Energy (B3LYP): -2755.106027
Electronic Energy (BP86-D3(BJ)/CPCM(THF)): -2756.847902
Total Gibbs Free Energy: -2756.084683
Geometry:

P	-0.903592	-1.741460	-0.874722
C	0.017478	-2.839442	-2.138791
C	-0.987237	-3.951188	-2.497370
C	-2.364779	-3.293733	-2.614417
C	-2.610966	-2.471898	-1.324957
H	-0.692050	-4.461707	-3.422311
H	-1.020888	-4.712674	-1.708308
H	-3.164936	-4.029820	-2.755028
H	-2.385488	-2.632287	-3.489225
P	0.935592	-0.188365	1.444164
C	0.021059	0.565620	2.954784
C	1.110107	0.845747	4.017557
C	2.432149	1.115788	3.291508
C	2.637438	-0.045523	2.291891
H	0.810850	1.685524	4.656223
H	1.240858	-0.021595	4.675813
H	3.278869	1.182285	3.985382
H	2.385254	2.069983	2.750243
H	0.118411	-2.187979	-3.016067
H	-2.838992	-3.177991	-0.516289
C	0.685735	-2.047267	1.502601
H	0.681069	-2.410005	2.537060
H	1.574053	-2.465805	1.015793
C	-0.585075	-2.544448	0.788275
H	-0.327307	1.524368	2.555340
H	2.762739	-0.964692	2.881296
C	-1.201304	-0.193321	3.428902
C	-3.525439	-1.587084	4.233438
C	-2.473431	0.196515	2.974760
C	-1.122539	-1.290865	4.302594
C	-2.270124	-1.980519	4.700383
C	-3.620891	-0.492652	3.370602
H	-2.559664	1.048142	2.305802
H	-0.159429	-1.611813	4.690048
H	-2.180779	-2.823091	5.381701
H	-4.591267	-0.165804	3.006039
H	-4.418948	-2.120391	4.547478

C	3.842055	0.098931	1.389178
C	6.161208	0.392149	-0.190500
C	3.912423	1.084999	0.392423
C	4.952744	-0.737667	1.573658
C	6.103478	-0.594080	0.795729
C	5.059365	1.228845	-0.388570
H	3.066941	1.743488	0.214140
H	4.917350	-1.507718	2.341521
H	6.953525	-1.250845	0.963366
H	5.087055	2.001136	-1.152143
H	7.055702	0.510559	-0.796519
C	-3.749189	-1.479495	-1.415765
C	-5.921832	0.310162	-1.591001
C	-4.801296	-1.530069	-0.490648
C	-3.803157	-0.508827	-2.428733
C	-4.878451	0.374885	-2.518096
C	-5.877862	-0.644269	-0.574281
H	-4.778403	-2.273547	0.303054
H	-2.994492	-0.434022	-3.151390
H	-4.897838	1.119672	-3.309065
H	-6.683172	-0.704975	0.153120
H	-6.758327	0.999951	-1.660231
C	1.409367	-3.262673	-1.718566
C	4.026797	-3.947813	-0.912876
C	1.688063	-4.525152	-1.174080
C	2.473434	-2.355562	-1.859884
C	3.765995	-2.687769	-1.457877
C	2.984614	-4.864816	-0.777533
H	0.897734	-5.261118	-1.063768
H	2.280539	-1.372433	-2.281762
H	4.565155	-1.959999	-1.561224
H	3.176141	-5.851784	-0.364068
H	5.033560	-4.210987	-0.600388
H	-0.550136	-3.636222	0.682160
H	-1.465579	-2.304691	1.396092
C	-0.053335	1.870274	-2.844590
H	-1.135742	1.956508	-2.792082
C	0.467592	0.851682	-3.831098
H	0.564302	1.278469	-4.842113
H	1.451540	0.450094	-3.563846
H	-0.220805	0.002701	-3.914194
C	0.685411	2.854933	-2.240987
C	0.025673	3.894179	-1.369490
C	2.128565	2.942349	-2.408342
C	0.838102	5.124636	-1.171534
H	-0.971434	4.148407	-1.747211
C	2.831224	4.039861	-2.023808
H	2.644126	2.129827	-2.912704
C	2.163051	5.178506	-1.427099
H	0.333523	5.975538	-0.721303
H	3.902981	4.091386	-2.204416
H	2.737723	6.075367	-1.208663
Cu	-0.479671	0.433118	-0.509288
N	-1.256968	2.136904	-0.010546
C	-0.367535	3.265207	0.149101
C	-2.584507	2.414326	-0.073766
C	-0.951532	4.332594	1.020041

```
 H                  0.597971    2.912143    0.534694
 C                 -3.151168    3.600675    0.337796
 H                 -3.217351    1.593029   -0.404314
 C                 -2.294430    4.528606    1.020119
 H                 -0.278844    4.985510    1.570458
 H                 -4.226477    3.738817    0.300604
 H                 -2.732677    5.347675    1.588661

Structure Ax-[TS14,15]aa
Charge: 0
Multiplicity: 1
Imaginary Frequencies: 1
Electronic Energy (B3LYP): -2755.870185
Gibbs Free Energy (B3LYP): -2755.106970
Electronic Energy (BP86-D3(BJ)/CPCM(THF)): -2756.851791
Total Gibbs Free Energy: -2756.088577
Geometry:
 P                  0.486032   -1.209828    1.261399
 C                 -0.242732   -1.126243    3.031981
 C                  0.713407   -1.956714    3.916173
 C                  2.129976   -1.785636    3.358919
 C                  2.066127   -2.103233    1.847334
 H                  0.638207   -1.642234    4.964167
 H                  0.446568   -3.019862    3.883582
 H                  2.851440   -2.444121    3.856886
 H                  2.476131   -0.755633    3.510650
 P                 -1.613590   -0.549993   -1.245733
 C                 -1.040399   -1.001955   -3.017260
 C                 -2.328944   -1.304946   -3.806244
 C                 -3.394784   -0.315055   -3.330436
 C                 -3.449737   -0.398522   -1.786373
 H                 -2.149772   -1.234095   -4.886217
 H                 -2.678451   -2.325635   -3.606907
 H                 -4.381600   -0.527981   -3.758877
 H                 -3.125816    0.702198   -3.642241
 H                 -0.106071   -0.071318    3.296349
 H                  1.834118   -3.172450    1.748167
 C                 -1.702119   -2.184634   -0.325025
 H                 -2.028375   -2.987613   -0.997853
 H                 -2.493291   -2.047178    0.421362
 C                 -0.397140   -2.601895    0.375751
 H                 -0.638986   -0.051043   -3.388434
 H                 -3.904279   -1.362872   -1.524596
 C                  0.077458   -2.020600   -3.092520
 C                  2.221489   -3.853659   -3.190303
 C                  1.407701   -1.585356   -2.956733
 C                 -0.154512   -3.391464   -3.283997
 C                  0.907171   -4.299099   -3.333731
 C                  2.467334   -2.490980   -3.001344
 H                  1.607902   -0.527980   -2.800395
 H                 -1.166818   -3.763877   -3.410078
 H                  0.702384   -5.355170   -3.491537
 H                  3.484575   -2.129891   -2.882577
 H                  3.046882   -4.559479   -3.231995
 C                 -4.264422    0.692450   -1.128350
 C                 -5.873755    2.698608    0.033373
 C                 -3.964643    2.052001   -1.309161
```

C	-5.382766	0.360931	-0.350018
C	-6.181495	1.351435	0.226229
C	-4.760412	3.044447	-0.736663
H	-3.097410	2.340913	-1.897339
H	-5.634082	-0.686456	-0.198372
H	-7.047786	1.068127	0.818847
H	-4.507436	4.089962	-0.890685
H	-6.494233	3.472535	0.476905
C	3.342283	-1.832143	1.082558
C	5.776178	-1.397414	-0.271536
C	3.991477	-2.879491	0.414125
C	3.934360	-0.559795	1.061068
C	5.138231	-0.344854	0.390127
C	5.198383	-2.667581	-0.256358
H	3.550132	-3.873868	0.422117
H	3.456803	0.272287	1.570143
H	5.573997	0.650556	0.386592
H	5.686654	-3.496887	-0.762055
H	6.715662	-1.228618	-0.791076
C	-1.721366	-1.433298	3.138094
C	-4.500557	-1.926697	3.273488
C	-2.216045	-2.730645	3.347749
C	-2.652235	-0.389241	3.004726
C	-4.024827	-0.629614	3.067405
C	-3.589683	-2.974526	3.415916
H	-1.530726	-3.564214	3.469164
H	-2.293453	0.624539	2.845061
H	-4.719216	0.197507	2.951803
H	-3.945891	-3.987456	3.585505
H	-5.568844	-2.117587	3.330051
H	-0.596431	-3.430895	1.065952
H	0.323456	-2.963591	-0.367126
C	-0.127423	2.864402	1.523107
H	-0.576640	2.332449	2.364648
C	-1.095747	3.659162	0.686292
H	-1.392894	4.581416	1.213365
H	-0.684897	3.952292	-0.282709
H	-2.015203	3.095469	0.498215
C	1.238210	3.005794	1.556153
C	1.987841	2.449372	2.670164
C	2.034627	3.665175	0.476289
C	3.294064	2.760849	2.889782
H	1.444564	1.843721	3.394954
C	3.362422	4.155258	0.907865
H	1.470095	4.432322	-0.058094
C	3.988792	3.674718	2.008414
H	3.808907	2.372042	3.765758
H	3.876260	4.849727	0.247554
H	4.997835	3.991526	2.260760
Cu	0.223263	0.601693	-0.075412
N	1.089364	1.911476	-1.233819
C	0.418402	2.534324	-2.237151
C	2.326261	2.513585	-0.817715
C	0.950602	3.492912	-3.067528
H	-0.599570	2.179546	-2.401320
C	3.050998	3.210585	-1.914812
H	2.950459	1.773347	-0.314837

C	2.357798	3.747529	-2.950066
H	0.358776	3.919758	-3.870413
H	4.125500	3.344383	-1.820299
H	2.868986	4.319771	-3.722396

Structure [TS15,10]ak
Charge: 0
Multiplicity: 1
Imaginary Frequencies: 1
Electronic Energy (B3LYP): -2755.870185
Gibbs Free Energy (B3LYP): -2755.106970
Electronic Energy (BP86-D3(BJ)/CPCM(THF)): -2756.851791
Total Gibbs Free Energy: -2756.088577
Geometry:

P	0.291168	1.427355	1.485609
C	1.506637	0.754536	2.794991
C	1.167197	1.524442	4.090581
C	-0.347955	1.745407	4.114052
C	-0.748947	2.379097	2.759677
H	1.515245	0.962789	4.965391
H	1.673275	2.497384	4.111411
H	-0.660797	2.391014	4.943096
H	-0.861314	0.784619	4.242072
P	1.241101	0.984344	-1.688611
C	0.220904	1.865051	-3.050434
C	1.164242	2.000999	-4.264192
C	2.067451	0.764237	-4.287123
C	2.697728	0.630903	-2.880767
H	0.587719	2.109362	-5.191058
H	1.791462	2.896335	-4.172454
H	2.849512	0.835402	-5.052699
H	1.474930	-0.130493	-4.517854
H	1.175148	-0.280673	2.932513
H	-0.358574	3.405560	2.744276
C	2.011580	2.335432	-0.633210
H	2.280390	3.204474	-1.245986
H	2.947125	1.899887	-0.263256
C	1.154580	2.804396	0.559618
H	-0.536380	1.109578	-3.294160
H	3.400243	1.465491	-2.753137
C	-0.511865	3.111346	-2.600785
C	-1.925205	5.378121	-1.681533
C	-1.817985	2.994244	-2.093565
C	0.065343	4.390615	-2.646622
C	-0.633806	5.512223	-2.193396
C	-2.515318	4.112519	-1.635281
H	-2.287678	2.014535	-2.056895
H	1.065577	4.525122	-3.048310
H	-0.166966	6.492673	-2.246838
H	-3.520754	3.991307	-1.241984
H	-2.469442	6.251338	-1.331578
C	3.453330	-0.658100	-2.644359
C	4.914538	-3.044929	-2.280004
C	2.814371	-1.908159	-2.680468
C	4.836790	-0.630626	-2.420044
C	5.563491	-1.810307	-2.241444
C	3.534968	-3.088272	-2.499997

H	1.741881	-1.959112	-2.847483
H	5.352283	0.326803	-2.388983
H	6.637003	-1.762078	-2.076694
H	3.017894	-4.043753	-2.532870
H	5.476388	-3.965044	-2.143558
C	-2.238514	2.436203	2.502096
C	-5.025118	2.591610	2.104144
C	-2.873032	3.673456	2.326144
C	-3.026099	1.274100	2.470478
C	-4.405251	1.350853	2.275614
C	-4.253566	3.753748	2.128711
H	-2.280235	4.585378	2.348770
H	-2.558509	0.299796	2.585415
H	-4.994644	0.438240	2.252632
H	-4.723683	4.725199	1.999132
H	-6.099468	2.649615	1.952361
C	2.961436	0.722500	2.378078
C	5.651477	0.594663	1.531503
C	3.823795	1.817742	2.546457
C	3.479661	-0.441600	1.786946
C	4.807151	-0.505185	1.363022
C	5.155188	1.754270	2.129121
H	3.464962	2.729765	3.014686
H	2.834569	-1.308475	1.668555
H	5.178235	-1.413528	0.897677
H	5.804748	2.613511	2.275989
H	6.687531	0.545929	1.207236
H	1.768974	3.400647	1.245381
H	0.345218	3.451848	0.201356
C	-3.603629	-4.222547	-2.163326
H	-3.112006	-4.465406	-3.100104
C	-5.090748	-4.457079	-2.112593
H	-5.355730	-5.388050	-1.589118
H	-5.610413	-3.636487	-1.599082
H	-5.509436	-4.529491	-3.122564
C	-2.823933	-3.891161	-1.093673
C	-1.405369	-3.463615	-1.308478
C	-3.339186	-3.759798	0.249894
C	-0.566067	-3.423196	-0.101975
H	-0.918808	-4.020591	-2.117748
C	-2.529514	-3.515804	1.316585
H	-4.395924	-3.948225	0.420111
C	-1.091656	-3.372977	1.159627
H	0.508916	-3.323204	-0.244375
H	-2.950934	-3.511355	2.318015
Cu	-0.530804	0.087598	-0.091649
N	-1.860097	-0.846026	-1.106709
C	-1.449649	-1.864597	-2.050450
C	-3.186074	-0.595753	-1.020460
C	-2.320271	-1.973021	-3.226151
H	-0.393735	-1.723928	-2.303094
C	-4.134272	-1.069644	-1.905089
H	-3.478630	0.077233	-0.216415
C	-3.662621	-1.767590	-3.059272
H	-1.929245	-2.428491	-4.133243
H	-5.182949	-0.827371	-1.773198
H	-4.351741	-1.975455	-3.876330

C	-0.233325	-3.239362	2.364770
C	-0.699720	-2.591811	3.525839
C	1.071008	-3.771166	2.403257
C	0.100580	-2.470701	4.663708
H	-1.701456	-2.171848	3.534200
C	1.875079	-3.643489	3.535453
H	1.443818	-4.318580	1.542507
C	1.396400	-2.991428	4.675318
H	-0.293602	-1.970790	5.545716
H	2.873930	-4.073081	3.534586
H	2.018663	-2.903743	5.561836

[TS15,13]aa
Charge: 0
Multiplicity: 1
Imaginary Frequencies: 1
Electronic Energy (B3LYP): -2755.865911
Gibbs Free Energy (B3LYP): -2755.104243
Electronic Energy (BP86-D3(BJ)/CPCM(THF)): -2756.851447
Total Gibbs Free Energy: -2756.089779
Geometry:

P	-0.417484	-1.746249	-1.060608
C	0.580217	-2.271779	-2.610731
C	-0.230393	-3.416636	-3.253325
C	-1.713160	-3.087266	-3.068153
C	-1.938433	-2.782591	-1.567669
H	0.040176	-3.536728	-4.309442
H	-0.013653	-4.371044	-2.758398
H	-2.364152	-3.907852	-3.392027
H	-1.982478	-2.210385	-3.670744
P	1.250517	-0.272414	1.412542
C	0.340306	-0.118434	3.092840
C	1.443669	0.054450	4.158762
C	2.593634	0.837379	3.520117
C	2.953745	0.123198	2.197261
H	1.044812	0.557982	5.047858
H	1.821425	-0.920787	4.488979
H	3.470517	0.895858	4.176197
H	2.277056	1.868495	3.317841
H	0.489998	-1.396935	-3.266624
H	-1.835147	-3.728679	-1.019864
C	1.451300	-2.111416	1.090064
H	1.642880	-2.653965	2.023816
H	2.355162	-2.195724	0.475144
C	0.261995	-2.761645	0.358601
H	-0.184493	0.837852	2.982446
H	3.395316	-0.848711	2.455621
C	-0.706741	-1.178485	3.365654
C	-2.712048	-3.122317	3.795080
C	-2.035178	-0.949406	2.967405
C	-0.408197	-2.399751	3.991805
C	-1.399401	-3.360941	4.204853
C	-3.025657	-1.909675	3.176172
H	-2.286592	-0.009482	2.484163
H	0.602625	-2.609125	4.329720
H	-1.142797	-4.295408	4.697817
H	-4.042802	-1.706868	2.852686

H	-3.483476	-3.868886	3.964886
C	3.935677	0.864206	1.318210
C	5.825576	2.237114	-0.267573
C	3.702208	2.183339	0.895684
C	5.134242	0.250237	0.928262
C	6.071985	0.927145	0.144607
C	4.634820	2.862493	0.111804
H	2.780768	2.684773	1.179639
H	5.337991	-0.769730	1.246688
H	6.997506	0.430834	-0.136540
H	4.430922	3.882690	-0.202542
H	6.553617	2.768256	-0.874670
C	-3.299357	-2.203285	-1.251610
C	-5.891971	-1.222205	-0.737178
C	-4.190129	-2.914285	-0.435048
C	-3.728969	-0.985060	-1.800961
C	-5.012709	-0.500550	-1.548448
C	-5.475007	-2.430882	-0.178208
H	-3.875523	-3.860262	0.000334
H	-3.051668	-0.397245	-2.414916
H	-5.320790	0.448359	-1.978826
H	-6.149526	-3.002426	0.454248
H	-6.891173	-0.843060	-0.540976
C	2.056489	-2.521167	-2.384556
C	4.821915	-2.899207	-1.942495
C	2.569246	-3.784495	-2.048366
C	2.963936	-1.455046	-2.502104
C	4.328851	-1.636915	-2.280532
C	3.936168	-3.971771	-1.830827
H	1.905173	-4.639254	-1.963007
H	2.594854	-0.468364	-2.770785
H	5.003396	-0.790453	-2.368892
H	4.307315	-4.961768	-1.578230
H	5.885446	-3.046695	-1.775424
H	0.540667	-3.765647	0.015171
H	-0.578955	-2.877553	1.052160
C	-1.612297	5.526597	-1.617678
H	-2.503285	5.754384	-2.204922
C	-1.034284	6.692618	-0.868475
H	-1.700974	7.040729	-0.066896
H	-0.068554	6.462798	-0.407144
H	-0.883539	7.551353	-1.540601
C	-1.129168	4.257491	-1.706021
C	-0.001266	3.715868	-0.892700
C	-1.747253	3.311015	-2.628762
C	0.730553	2.610209	-1.490694
H	0.651147	4.484197	-0.474499
C	-1.164497	2.127705	-2.950645
H	-2.668124	3.616945	-3.122186
C	0.127308	1.764772	-2.391062
H	1.742847	2.404166	-1.151317
H	-1.626930	1.469633	-3.683983
H	0.692383	0.957231	-2.850668
Cu	-0.319216	0.406386	-0.360236
N	-1.402029	1.835135	0.485894
C	-0.700903	3.048256	0.721167
C	-2.752698	1.876655	0.467261

C	-1.460214	4.117103	1.374551
H	0.275957	2.854062	1.180654
C	-3.514395	2.956959	0.865223
H	-3.237676	0.952721	0.162276
C	-2.825377	4.090093	1.380137
H	-0.913400	4.957371	1.795450
H	-4.597552	2.900725	0.854518
H	-3.385524	4.912284	1.822182

[TS27,2]aa
Electronic Energy (B3LYP): -2755.892296
Gibbs Free Energy (B3LYP): -2755.129332
Electronic Energy (BP86-D3(BJ)/CPCM(THF)): -2756.876226
Total Gibbs Free Energy: -2756.113262
Geometry:

P	1.346718	1.097829	-1.067551
C	0.744885	2.436358	-2.303835
C	2.028842	2.993529	-2.949284
C	2.985192	1.814508	-3.149880
C	3.116312	1.086382	-1.789383
H	1.802410	3.509568	-3.890705
H	2.508485	3.727464	-2.289696
H	3.970145	2.134732	-3.510070
H	2.580641	1.125380	-3.902720
P	-0.311046	0.319466	1.723952
C	0.693900	-0.383249	3.202444
C	-0.139725	-0.054693	4.459446
C	-1.616275	-0.165756	4.077972
C	-1.828537	0.706434	2.819708
H	0.127364	-0.728749	5.282592
H	0.059082	0.966546	4.806945
H	-2.280318	0.162705	4.886501
H	-1.865760	-1.210696	3.858352
H	0.213392	1.858728	-3.068615
H	3.715969	1.724125	-1.127150
C	0.391809	2.037836	1.458690
H	0.659167	2.496552	2.418487
H	-0.420223	2.634428	1.027462
C	1.614103	2.053623	0.521947
H	0.638796	-1.463553	3.031331
H	-1.698144	1.754705	3.119766
C	2.158623	0.003284	3.247834
C	4.909082	0.666745	3.259128
C	3.099740	-0.780064	2.557249
C	2.631952	1.123329	3.951111
C	3.989894	1.451355	3.956828
C	4.456034	-0.454139	2.559361
H	2.756482	-1.652920	2.011448
H	1.943916	1.748189	4.512226
H	4.327908	2.321461	4.514118
H	5.156100	-1.080207	2.012929
H	5.965750	0.920703	3.267880
C	-3.194181	0.575279	2.183112
C	-5.798961	0.378496	1.116930
C	-3.755868	-0.676362	1.883973
C	-3.958735	1.723080	1.926937
C	-5.246886	1.629369	1.396206

C	-5.046950	-0.772724	1.362440
H	-3.178629	-1.582994	2.045122
H	-3.542801	2.702258	2.154424
H	-5.821762	2.533724	1.212947
H	-5.463175	-1.752808	1.143649
H	-6.804842	0.300510	0.713197
C	3.780282	-0.271304	-1.867805
C	5.081433	-2.766942	-2.056614
C	5.030080	-0.479924	-1.268147
C	3.192827	-1.339896	-2.563687
C	3.834923	-2.574505	-2.658302
C	5.677387	-1.714410	-1.360990
H	5.502281	0.335196	-0.724283
H	2.217738	-1.210610	-3.026552
H	3.358263	-3.388539	-3.197694
H	6.648428	-1.850661	-0.891597
H	5.580715	-3.729230	-2.128853
C	-0.242547	3.433383	-1.732212
C	-2.149623	5.211184	-0.644796
C	0.131311	4.712396	-1.292685
C	-1.595956	3.066461	-1.622194
C	-2.537761	3.941761	-1.082368
C	-0.812450	5.592520	-0.755670
H	1.162429	5.041448	-1.378330
H	-1.906612	2.079397	-1.954009
H	-3.575265	3.628360	-1.005135
H	-0.497995	6.580544	-0.428982
H	-2.882923	5.897769	-0.230062
H	1.900933	3.089817	0.304377
H	2.466576	1.577533	1.018204
C	-2.312529	-3.586539	-1.366528
H	-1.957802	-3.558924	-2.394331
C	-3.655881	-4.235024	-1.154362
H	-3.596959	-5.321618	-0.970295
H	-4.203384	-3.808993	-0.298408
H	-4.292121	-4.098312	-2.036992
C	-1.331272	-3.515211	-0.367047
C	0.007151	-3.035076	-0.645403
C	-1.572622	-3.891080	1.002297
C	1.032493	-3.145681	0.313232
H	0.287013	-2.874608	-1.684522
C	-0.553505	-3.952765	1.934967
H	-2.563666	-4.238375	1.282447
C	0.775421	-3.608266	1.603552
H	2.048275	-2.895918	0.011806
H	-0.776653	-4.316817	2.937326
H	1.576516	-3.727817	2.327760
Cu	-0.230904	-0.618622	-0.417601
N	-1.596289	-0.714242	-1.929812
C	-2.837290	-1.248550	-1.700802
C	-1.211920	-0.599110	-3.224523
C	-3.791523	-1.345463	-2.751622
H	-3.172567	-1.229738	-0.673710
C	-2.041010	-0.818515	-4.306566
H	-0.182747	-0.283742	-3.378764
C	-3.393786	-1.157825	-4.053937
H	-4.814338	-1.613764	-2.505915

H	-1.669300	-0.676789	-5.316379
H	-4.098915	-1.260599	-4.874739

[TS27,2]al
Charge: 0
Multiplicity: 1
Imaginary Frequencies: 1
Electronic Energy (B3LYP): -2753.674956
Gibbs Free Energy (B3LYP): -2752.941791
Electronic Energy (BP86-D3(BJ)/CPCM(THF)): -2754.655538
Total Gibbs Free Energy: -2753.922372
Geometry:

P	0.755178	-0.585149	1.702978
C	-0.204724	-0.635788	3.364777
C	0.777638	-1.260103	4.371783
C	2.150291	-0.642477	4.093791
C	2.447425	-0.794955	2.580698
H	0.448823	-1.088193	5.404633
H	0.837925	-2.346825	4.231962
H	2.944407	-1.109945	4.688223
H	2.136741	0.420389	4.365360
P	-0.716937	-1.106378	-1.235484
C	0.229408	-1.809275	-2.756539
C	-0.852765	-2.146680	-3.813689
C	-2.086252	-1.273144	-3.554037
C	-2.408105	-1.404803	-2.048398
H	-0.453576	-2.006114	-4.825475
H	-1.149953	-3.198833	-3.737668
H	-2.943762	-1.583286	-4.163234
H	-1.878076	-0.223569	-3.801571
H	-0.314949	0.423880	3.630609
H	2.741453	-1.836175	2.398691
C	-0.696613	-2.435107	0.080261
H	-0.717442	-3.432760	-0.373014
H	-1.629772	-2.307943	0.640657
C	0.510334	-2.319856	1.026687
H	0.787663	-0.937016	-3.102670
H	-2.646571	-2.461493	-1.861217
C	1.238917	-2.898963	-2.454940
C	3.180111	-4.866771	-1.856483
C	2.582311	-2.548286	-2.229406
C	0.893115	-4.258047	-2.372843
C	1.851188	-5.230578	-2.078144
C	3.540231	-3.519531	-1.933792
H	2.868981	-1.501784	-2.283102
H	-0.132238	-4.572302	-2.547159
H	1.555819	-6.275550	-2.026312
H	4.572813	-3.220518	-1.771074
H	3.926252	-5.624386	-1.632018
C	-3.572097	-0.572593	-1.560150
C	-5.799214	0.938873	-0.719918
C	-3.500903	0.825307	-1.472493
C	-4.779690	-1.198100	-1.216776
C	-5.885964	-0.452155	-0.804867
C	-4.600242	1.574334	-1.053028
H	-2.572339	1.330719	-1.713994
H	-4.855103	-2.281981	-1.276288

H	-6.813410	-0.958985	-0.549867
H	-4.510152	2.654465	-0.975081
H	-6.656686	1.522704	-0.395522
C	3.553730	0.101078	2.067947
C	5.653234	1.739222	1.135903
C	4.676394	-0.453234	1.437817
C	3.501733	1.496338	2.219758
C	4.539837	2.307074	1.761081
C	5.716817	0.355189	0.974285
H	4.736686	-1.532022	1.310180
H	2.636402	1.958118	2.688922
H	4.475365	3.384637	1.886203
H	6.576656	-0.098965	0.488709
H	6.460243	2.371469	0.776166
C	-1.593801	-1.230383	3.272377
C	-4.201435	-2.282482	3.014804
C	-1.890766	-2.533610	3.698670
C	-2.635382	-0.461351	2.722924
C	-3.922241	-0.980648	2.589786
C	-3.182146	-3.053538	3.573055
H	-1.118456	-3.152503	4.144857
H	-2.432215	0.551979	2.386255
H	-4.702440	-0.369407	2.145836
H	-3.387887	-4.064081	3.917189
H	-5.204600	-2.688364	2.915460
H	0.414651	-3.045577	1.843846
H	1.430275	-2.563524	0.482024
C	0.983269	4.081509	-1.214076
H	1.250618	4.191351	-0.163558
C	0.851948	5.386147	-1.963749
H	1.820965	5.878072	-2.138704
H	0.378893	5.252316	-2.946057
H	0.230287	6.091450	-1.398708
C	1.481918	2.930565	-1.856189
C	1.893521	1.695168	-1.244589
C	1.544418	2.694246	-3.283122
O	2.375314	0.844355	-2.303200
H	2.595187	1.672368	-0.415678
C	2.090755	1.464647	-3.463071
H	1.267018	3.382719	-4.069393
H	2.326751	0.910998	-4.363792
Cu	0.192286	0.796374	-0.205886
N	-0.801197	2.507527	0.289897
C	-1.016902	3.443356	-0.711689
C	-0.900043	2.947359	1.563203
C	-1.743070	4.646899	-0.399470
H	-1.158100	3.014140	-1.700307
C	-1.387011	4.188145	1.933193
H	-0.614219	2.227247	2.326234
C	-1.878046	5.036650	0.909070
H	-2.124074	5.257210	-1.212946
H	-1.473829	4.451656	2.982279
H	-2.381858	5.966858	1.162224

8. References

1. Gribble, M. W. Jr.; Guo, S.; Buchwald, S. L. *J. Am. Chem. Soc.* **2018**, *140*, 5057-5060.
2. Dhayalan, V.; Gadekar, S. C.; Alassad, Z.; Milo, A. *Nat. Chem.* **2019**, 11, 543-551.
3. Blackmond, D. G. *Angew. Chem. Int. Ed.* **2005**, *44*, 4302-4320. (b) Blackmond, D. G. *J. Am. Chem. Soc.* **2015**, *137*, 10852-10866.
4. For more information of hazard classifications specific to eye injury, see: United Nations. Serious Eye Damage/Eye Irritation. *Globally Harmonized System of Classification and Labeling of Chemicals (GHS), Third Revised Edition*, New York and Geneva, 2009, pp 133-144. available at: http://www.unece.org/fileadmin/DAM/trans/danger/publi/ghs/ghs_rev03/English/03e_part3.pdf (accessed October 13, 2017).
5. "Prudent Practices in the Laboratory [electronic resource]: Handling and Management of Chemical Hazards / Committee on Prudent Practices in the Laboratory: An Update." Board on Chemical Sciences and Technology, Division of Earth and Life Studies, National Research Council of the National Academies. Washington, D.C.: National Academies Press, 2011.
6. Helfferich, F. G. *Kinetics of Multistep Reactions, 2nd Edition;* Green, N. J. B., Ed.; Comprehensive Chemical Kinetics 40; Elsevier: Amsterdam, 2004, pp 227-239.
7. Bandar, J. S.; Pirnot, M. T.; Buchwald, S. L. *J. Am. Chem. Soc.* **2015**, *137*, 14812-14818.
8. Waser, J.; Gaspar, B.; Nambu, H.; Carreira, E. M. *J. Am. Chem. Soc.* **2006**, *128*, 11693-11712. (b) Tanaka, R.; Nakano, K.; Nozaki, K. *J. Org. Chem.* **2007**, *72*, 8671-8676.
9. Neese, F. The ORCA Program System. *WIREs Comput. Mol. Sci.* **2012**, *2*, 73.
10. Frisch, M. J. *et al*., Gaussian 03, Revision C.02. Gaussian, Inc., Wallingford CT (**2010**).
11. Legault, C. Y. CYLView, 1.0b. University of Sherbrooke, Quebec, Canada (**2009**).
12. Dolg, M.; Wedig, U.; Stoll, H.; Preuss, H. *J. Chem. Phys.* **1987**, *86*, 866.
13. (a) Becke, A. D. *Phys. Rev. A* **1988**, *38*, 3098. (b) Perdew, J. P. *Phys. Rev. B* **1986**, *33*, 8822.
14. (a) Grimme, S.; Antony, J.; Ehrlich, S.; Krieg, S. *J. Chem. Phys.* **2010**, *132*, 154104. (b) Grimme, S.; Ehrlich, S. Goerigk, L. *J. Comp. Chem.* **2011**, *32*, 1456.
15. (a) Barone, V.; Cossi, M. *J. Phys. Chem. A* **1998**, *102*, 1995. (b) Cossi, M.; Riga, N.; Scalmani, G.; Barone, V. *J. Comp. Chem.* **2003**, *24*, 669.
16. (a) Riplinger, C.; Neese, F. *J. Chem. Phys.* **2013**, *138*, 034106. (b) Riplinger, C.; Sandhoefer, B.; Hansen, A.; Neese, F. *J. Chem. Phys.* **2013**, *139*, 134101.
17. (a) Kendall, R. A.; Dunning, Jr., T. H.; Harrison, R. J. *J. Chem. Phys.* **1992**, *96*, 6796. (b) Woon, D. E.; Dunning, Jr., T. H., *J. Chem. Phys.* **1993**, *98*, 1358. (c) *J. Chem. Phys.* **2005**, *123*, 064107.
18. Lu, G.; Liu, R. Y.; Yang, Y.; Fang, C.; Lambrecht, D. S.; Buchwald, S. L.; Liu, P. *J. Am. Chem. Soc.* **2017**, *139*, 16548-16555.

9. Spectral Attachments.

9.1. NMR Spectra of crude 7ad

^{1}H NMR (500 MHz, Benzene-d6) δ 7.19 – 7.10 (m, 1H), 6.87 (apparent dq, J = 6.4, 3.9 Hz, 3H), 6.20 (d, J = 8.0 Hz, 1H), 6.15 (d, J = 8.0 Hz, 1H), 4.55 (apparent ddt, J = 14.4, 7.8, 2.9 Hz, 2H), 3.53 (q, J = 4.3 Hz, 1H), 3.24 – 3.20 (m, 5H), 1.31 (d, J = 7.2 Hz, 3H), -0.02 (s, 3H). The benzylic C–H resonance is obscured by the methoxy resonance of the internal standard (1,3,5-trimethoxybenzene)

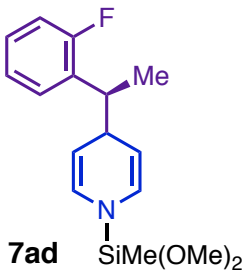

7ad

9.2. Chiral SFC Chromatograms.

All analyses were performed on a Daicel CHIRALCEL OD-H column (4.6 x 250 mm, 5 μM particle size) using $scCO_2$ containing 6% of a 0.1% (v/v) solution of diethylamine in MeOH; fr = 2.5 mL/min, column temperature = 40 °C, quantitation wavelength = 261 nm.

(a) Analysis of racemic **41dh**

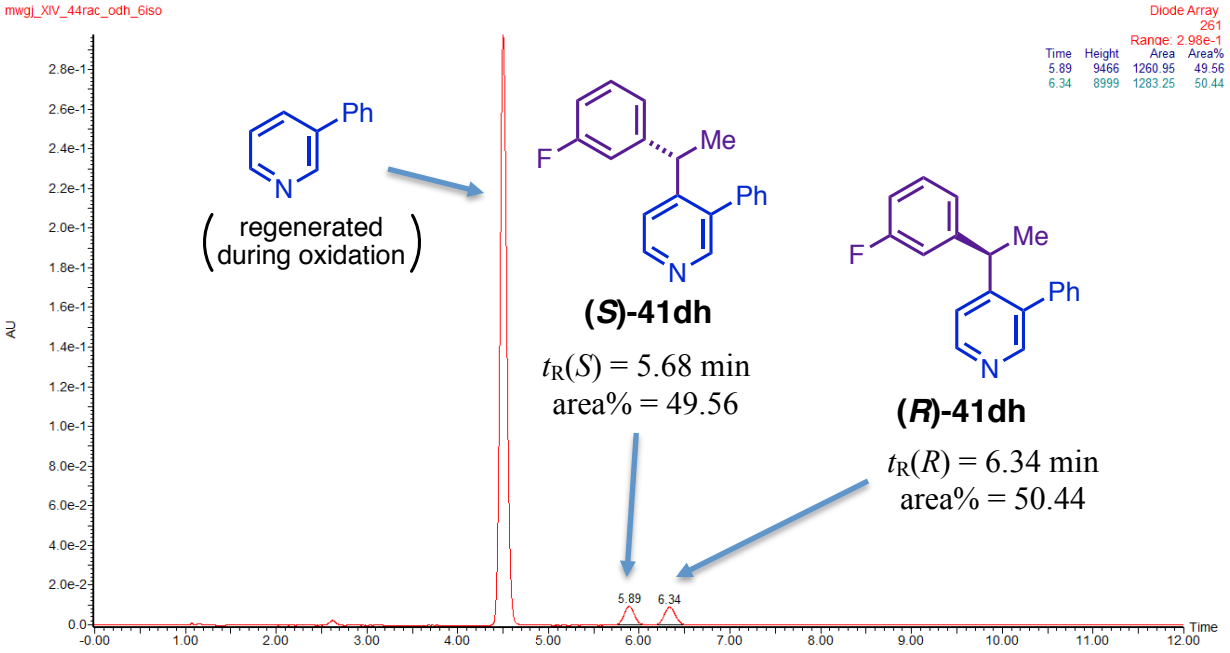

(b) Analysis of **41dh** obtained from reaction mixture **A** in section 5.2.iii.

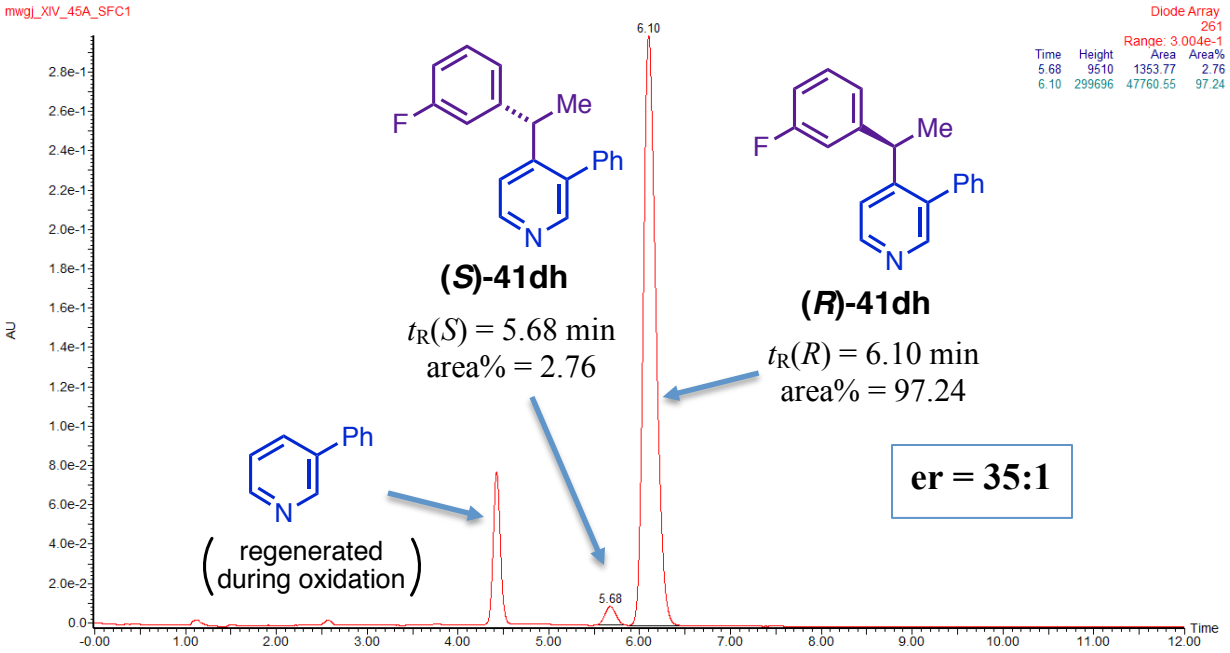

(c) Analysis of **41dh** obtained from reaction mixture **B** in section 5.2.iii.

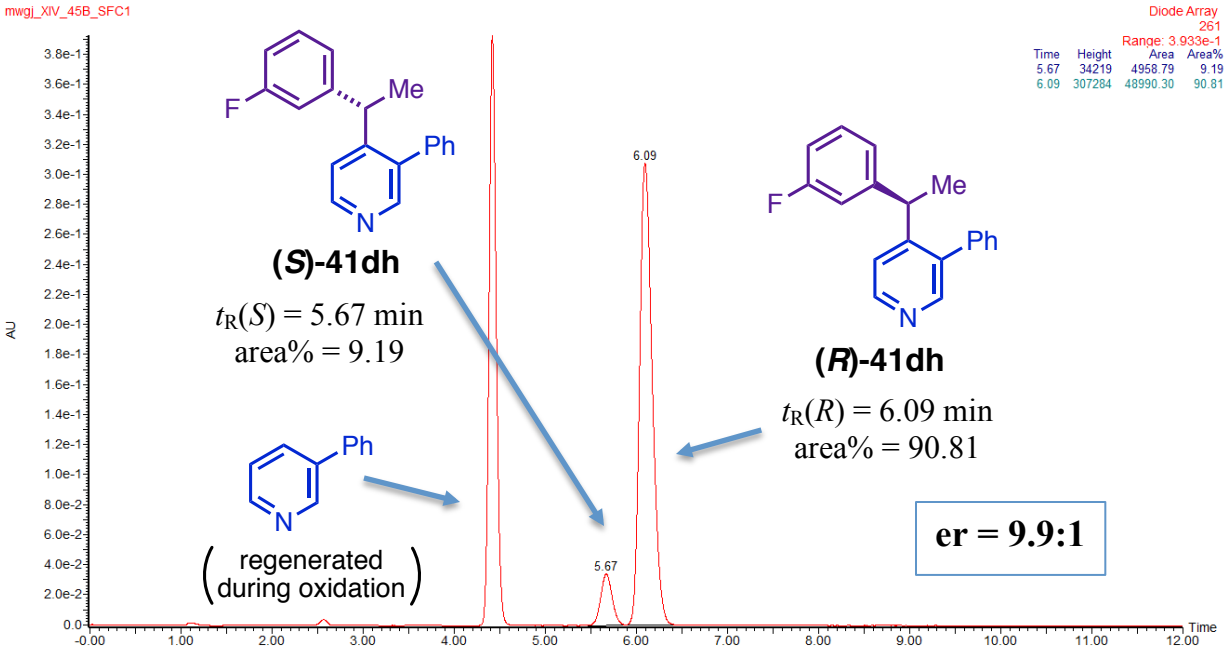

(d) Analysis of **41dh** obtained from reaction mixture **C** in section 5.2.iii.